

**Non-destructive detection of counterfeit and
substandard medicines using X-ray diffraction**

Chiaki Caroline Emily Crews

University College London

April 2018

A thesis submitted for the degree of Doctor of Philosophy

I, Chiaki Crews, confirm that the work presented in this thesis is my own. Where information has been derived from other sources, I confirm that this has been indicated in the thesis.

Chiaki C E Crews

Abstract

The prevalence of counterfeit and substandard medicines has been growing rapidly over the past decade, and fast, non-destructive techniques for their detection are urgently needed to counter this trend. In this thesis, both energy-dispersive X-ray diffraction (EDXRD) and pixelated diffraction ("*PixD*") combined with chemometric methods were assessed for their effectiveness in detecting poor-quality medicines within their packaging.

Firstly, a series of caffeine, paracetamol and cellulose mixtures of known concentrations were pressed into tablets. EDXRD spectra of each tablet were collected both with and without packaging. Principal component analysis (PCA) and partial least-squares regression (PLSR) were used to study the data and construct calibration models for quantitative analysis. The concentration prediction errors for the packaged data were found to be very similar to those obtained in the unpackaged case, and were also on a par with reported values in the literature using higher-resolution angular-dispersive X-ray diffraction (ADXRD).

Following this, soft independent modelling by class analogy (SIMCA) classification was used to compare EDXRD spectra from a test set of over-the-counter (OTC) medicines containing various combinations of active pharmaceutical ingredients (APIs) against PCA models constructed using spectra collected for paracetamol and ibuprofen samples. The test samples were selected to emulate different levels of difficulty in authenticating medicines correctly, ranging from completely different APIs (easy) to those with a small quantity of additional API (difficult). This classification study found that the sensitivity and specificity were optimal at data acquisition times on the order of 75~150s, and regardless of whether layers of blister and card packaging surrounded the tablet in question.

This experiment was repeated on a novel, compact system incorporating a pixelated detector, which was found to reduce the required data acquisition times for optimal classification by a factor of five.

Table of Contents

CHAPTER 1: INTRODUCTION & BACKGROUND	14
1.1 COUNTERFEIT AND SUBSTANDARD MEDICINES.....	14
1.1.1 <i>Background and definitions</i>	14
1.1.2 <i>Prevalence</i>	17
1.1.3 <i>Impacts and contributing factors</i>	20
1.2 COUNTERMEASURES.....	22
1.2.1 <i>Social countermeasures</i>	22
1.2.2 <i>Technological countermeasures</i>	29
1.3 X-RAY DIFFRACTION	44
1.3.1 <i>Background</i>	44
1.3.2 <i>Applications of ADXRD</i>	48
1.3.3 <i>Applications of EDXRD</i>	52
1.4 SCOPE OF THIS PHD THESIS	55
CHAPTER 2: EQUIPMENT AND METHODS	56
2.1 EDXRD SYSTEM.....	56
2.1.1 <i>Setup A</i>	57
2.1.2 <i>Setup B</i>	60
2.2 MINIPiXD SYSTEM.....	64
2.2.1 <i>HEXITEC detector</i>	65
2.2.2 <i>X-ray source</i>	67
2.2.3 <i>Sample positioning</i>	68
2.2.4 <i>Sample imaging</i>	69
2.3 CHEMOMETRICS	69
2.3.1 <i>Principal components analysis (PCA)</i>	69
2.3.2 <i>Partial Least-squares Regression (PLSR)</i>	71
2.3.3 <i>Soft Independent Modelling of Class Analogy (SIMCA)</i>	72
2.3.4 <i>Pre-processing</i>	73
CHAPTER 3: CONTROLLED MIXTURE TESTS	75
3.1 BACKGROUND.....	75
3.2 METHODOLOGY	77
3.2.1 <i>Sample preparation</i>	77
3.2.2 <i>Sample scanning</i>	79
3.3 RESULTS AND DISCUSSION	80

3.3.1	<i>Exploratory data analysis</i>	80
3.3.2	<i>Model Calibration</i>	87
3.3.3	<i>Predictions</i>	96
3.4	SUMMARY	97
CHAPTER 4: INTACT FORMULATIONS TESTS.....		98
4.1	BACKGROUND	98
4.2	METHODOLOGY	99
4.2.1	<i>Sample collection</i>	99
4.2.2	<i>Sample scanning</i>	99
4.2.3	<i>Chemometrics</i>	100
4.3	RESULTS AND DISCUSSION	100
4.3.1	<i>Exploratory analysis and PCA model development</i>	100
4.3.2	<i>SIMCA classification</i>	112
4.4	SUMMARY	120
CHAPTER 5: <i>MINIPIXD</i> TESTS.....		121
5.1	BACKGROUND	121
5.2	METHODOLOGY	121
5.2.1	<i>Sample collection</i>	121
5.2.2	<i>Sample scanning & data analysis</i>	122
5.3	RESULTS AND DISCUSSION	123
5.3.1	<i>Exploratory analysis and PCA model development</i>	123
5.3.2	<i>SIMCA classification</i>	130
5.4	SUMMARY	137
CHAPTER 6: CONCLUSIONS AND FUTURE WORK.....		138
6.1	CONCLUSIONS	138
6.1.1	<i>Controlled mixture tests</i>	138
6.1.2	<i>Intact formulation tests</i>	139
6.1.3	<i>miniPixD tests</i>	139
6.2	FUTURE WORK.....	140
6.2.1	<i>Sampling medicines</i>	140
6.2.2	<i>Instrumentation</i>	141
6.2.3	<i>Data analysis methods</i>	143
6.2.4	<i>Implementation</i>	144
CHAPTER 7: APPENDIX		148

List of Tables

TABLE 1.1 EXAMPLES OF CASES INVOLVING COUNTERFEIT OR SUBSTANDARD MEDICINES	17
TABLE 3.1 STUDIES ON ADXRD (REFLECTION GEOMETRY) AND PLSR; PRE-PROCESSING FOR BEST RESULT SHOWN; FULL CROSS-VALIDATION USED IN ALL CASES	76
TABLE 3.2 PERCENTAGES OF EACH MATERIAL USED IN SAMPLES	78
TABLE 3.3 RESULTS OF PLSR: RMSECV FROM TRAINING SET / RMSEP FROM TEST SET (WHERE APPLICABLE); 'SHORT' SPECTRUM RESULTS IN ITALICS IN EACH CASE; AND NUMBER OF PLS-FACTORS USED IN PARENTHESES. ALL MODELS MEAN-CENTRED.	89
TABLE 3.4 PREDICTION RESULTS FOR UNPACKAGED TABLETS	96
TABLE 6.1 UPDATE TO COMMENTS FOR "POWDER X-RAY DIFFRACTION" EXTRACTED FROM KOVACS <i>ET AL.</i> 'S TABLE COMPARING TECHNOLOGIES FOR DETECTING COUNTERFEIT AND SUBSTANDARD DRUGS [157]	145
TABLE 7.1 DETAILS OF PARACETAMOL SAMPLES	150
TABLE 7.2 DETAILS OF IBUPROFEN SAMPLES	151
TABLE 7.3 DETAILS OF 'OTC-OTHER' SAMPLES	152

List of Figures

FIGURE 1.1 MAP OF TRADE ROUTES OF COUNTERFEIT MEDICINES [17].....	15
FIGURE 1.2 CITATION REPORT FOR WEB OF SCIENCE SEARCH (TOPIC: (COUNTERFEIT OR FAKE OR FALSIFIED OR SUBSTANDARD) AND (PHARMACEUTICAL OR MEDICINE OR DRUG)), 1997-2017	18
FIGURE 1.3 (L) AWARENESS-RAISING CAMPAIGN POSTER, CAMBODIA [31]; (R) FDA CAMPAIGN, USA [115]	27
FIGURE 1.4 PROPOSED SCHEME OF WHERE COUNTERFEIT SAMPLES WERE PRODUCED AND DISTRIBUTED [116]	27
FIGURE 1.5 (LEFT) TRACK-AND-TRACE SYSTEM TO BE ROLLED OUT WITHIN THE EU [140]; (RIGHT) NATIONAL VARIATIONS IN BARCODES USED FOR SERIALISATION [141]	31
FIGURE 1.6 CAN YOU TELL WHICH ARE COUNTERFEIT? (ANSWER – THE RIGHT-HAND COLUMN) [149].....	32
FIGURE 1.7 TO USE A PAD: APPLY CRUSHED TABLET AND STAND CARD UPRIGHT IN WATER FOR 3 MINUTES [172]	37
FIGURE 1.8 IMAGES OF VIAGRA (COUNTERFEIT AND AUTHENTIC) SUBJECT TO NIR WAVELENGTHS: (A) 1000NM, (B) 1500NM, (C) 2000NM, AND (D) 2500NM [195]	41
FIGURE 1.9 THE DIFFERENCE BETWEEN CONVENTIONAL AND SORS RAMAN SPECTROSCOPY [193]	42
FIGURE 1.10 TWO TYPES OF CRYSTALLOGRAPHIC PLANE WITHIN THE SAME CRYSTAL LATTICE (ADAPTED FROM [212]).....	44
FIGURE 1.11 SCATTERED X-RAYS SHOWING CONSTRUCTIVE AND DESTRUCTIVE INTERFERENCE.....	45
FIGURE 1.12 CONES OF DIFFRACTION FROM TWO TYPES OF CRYSTALLOGRAPHIC PLANE EXPOSED BY CRYSTALLITES IN A POWDER SAMPLE [221].....	45
FIGURE 1.13 DIAGRAM OF A TYPICAL REFLECTION ADXRD SETUP [225].....	46
FIGURE 1.14 DIAGRAM OF AN EDXRD SETUP (ADAPTED FROM [229])	47
FIGURE 1.15 ARRANGEMENT OF PARACETAMOL MOLECULES IN POLYMORPHS (A) FORM I AND (B) FORM II [237]; THEIR RESPECTIVE ADXRD PROFILES (GENERATED USING MERCURY V.3.9 [238] AND CSD-HXACAN18 & COTZAN [239])	49
FIGURE 1.16 (L) VIAGRA TABLETS – ONLY TOP LEFT TABLET IS GENUINE; (R) DIFFRACTION PATTERN FOR COUNTERFEIT TABLET B (IN BLUE) COMPARED TO THE GENUINE VIAGRA PATTERN (IN GREY) [240]	50
FIGURE 1.17 GEOMETRY OF THE <i>CHEMIN</i> INSTRUMENT; 24.0MM X 23.3MM ACTIVE AREA OF DETECTOR [243]....	50
FIGURE 1.18 WHY CHEMOMETRIC METHODS ARE USED IN CHEMICAL ANALYSIS [259].....	52
FIGURE 1.19 (A) XT250 SYSTEM GEOMETRY, WHERE $2\theta = 2.562^\circ$ [272]; AND (B) GEOMETRY OF PORTABLE EDXRD SYSTEM BY CUEVAS <i>ET AL.</i> , WITH (1) X-RAY TUBE, (2) DETECTOR, (3) SAMPLE, (4 & 5) COLLIMATORS, AND (6) LASER POINTER SHOWN [270].....	53
FIGURE 1.20 ILLUSTRATION OF HOW A CONE OF DIFFRACTION (AT A PARTICULAR X-RAY ENERGY) FROM THE SAMPLE IMPINGES UPON THE HEXITEC DETECTOR [273].....	53
FIGURE 2.1 SCHEMATIC OF EDXRD SYSTEM VIEWED FROM ABOVE, WITH ZOOMED DETAIL OF ANGLES.....	56
FIGURE 2.2 AM-241 SPECTRUM; X-AXIS ENERGIES ARE RESULT OF CALIBRATION USING LABELLED PEAKS.....	57
FIGURE 2.3 STEP-SCANNING POSITIONS USED IN SETUP A.....	58
FIGURE 2.4 SIDE VIEW OF “PACKAGED” SAMPLE HOLDER SETUP.....	58
FIGURE 2.5 MEASURED X-RAY TUBE SPECTRUM AT 60KV; ZOOMED PORTION HIGHLIGHTING SHAPE OF SPECTRUM AT ENERGIES ABOVE TUNGSTEN CHARACTERISTIC PEAKS	59

FIGURE 2.6 RESULT OF THE PILL MAPPING PROCEDURE.....	61
FIGURE 2.7 RASTER SCAN TRAJECTORIES USED IN SETUP B; \diamond MARKS CENTRAL “START” POSITION	62
FIGURE 2.8 COMPARISON OF XRD INTENSITIES FOR CAPLETS CONTAINING GROOVE (I.E. “THIN” SECTION).....	62
FIGURE 2.9 TOP VIEW OF BLISTER PLUS CARD PACKAGING SETUP	63
FIGURE 2.10 EFFECT OF CHANGING L_1 DISTANCE ON UNPACKAGED HEDEX (1) SPECTRA (300S, NO RASTER)	63
FIGURE 2.10 (A) SCATTERING ANGLES FOR EACH PIXEL ARE COMBINED WITH (B) ENERGY SPECTRUM MEASURED BY EACH PIXEL TO CONVERT INTO (C) MOMENTUM TRANSFER SPACE; RESULTING IN (D) SUMMED SPECTRUM FROM ALL PIXELS [273].....	64
FIGURE 2.11 SCHEMATIC OF <i>MINIPixD</i> VIEWED FROM ABOVE, SHOWING KEY COMPONENTS [276]	65
FIGURE 2.12 ANGULAR RANGE COVERED BY THE HEXITEC IN <i>MINIPixD</i> ; SHOWING EXCLUDED PIXELS	66
FIGURE 2.13 SYSTEM STABILITY TEST OVER 1000 MINUTES.....	68
FIGURE 2.14 SCHEMATIC OF PCA TRANSFORMATION (ADAPTED FROM [280])	70
FIGURE 2.15 SCHEMATIC OF THE SIMCA METHOD FROM SIRVEN ET AL. [282] SHOWING PCA MODELS FOR SPECTRA OF 3 SAMPLE CLASSES (VISUALISED IN A 3-WAVELENGTH SPACE); \blacksquare IS AN UNKNOWN SPECTRUM TO BE CLASSIFIED.....	72
FIGURE 3.1 ADXRD SPECTRA OF SOME COMMONLY USED EXCIPIENTS (DATA COLLECTED BY AUTHOR)	77
FIGURE 3.2 MIXTURE DESIGN SHOWING AMOUNTS OF EACH CHEMICAL IN EACH SAMPLE.....	79
FIGURE 3.3 EXAMPLES OF TRIPPLICATE SCANS EXHIBITING PREFERRED ORIENTATION: SAMPLE 2 (A) WITHOUT AND (B) WITH STEP-SCANNING; SAMPLE 11 (C) WITHOUT AND (D) WITH STEP-SCANNING.....	80
FIGURE 3.4 CALCULATED PERCENTAGE TRANSMISSION FOR PURE MATERIALS IN PRESSED TABLET FORM.....	81
FIGURE 3.5 EDXRD PROFILES FROM COMBINATIONS OF PURE MATERIAL SPECTRA COMPARED TO EXPERIMENTAL DATA	82
FIGURE 3.6 CALCULATED % TRANSMISSION FOR PACKAGING MATERIALS.....	83
FIGURE 3.7 PC1 VS PC2 SCORES FROM PCA ON TRIPPLICATE RAW SPECTRA OF UNPACKAGED SAMPLES	84
FIGURE 3.8 PC1 VS PC2 SCORES FROM PCA ON MEAN RAW SPECTRA OF UNPACKAGED SAMPLES	84
FIGURE 3.9 LOADINGS PLOTS FOR PCs 1-3 FROM PCA ON MEAN RAW SPECTRA OF UNPACKAGED SAMPLES, COMPARED TO REFERENCE SPECTRA.....	85
FIGURE 3.10 EXAMPLES OF PC LOADINGS THAT CONTAINED PEAKS MATCHING PREFERRED ORIENTATION EFFECTS	86
FIGURE 3.11 COMPARISON BETWEEN EDXRD SPECTRA FOR EXAMPLES OF UNPACKAGED AND PACKAGED SAMPLES	87
FIGURE 3.12 PC1 VS PC2 SCORES FROM PCA ON MEAN RAW SPECTRA OF PACKAGED SAMPLES	87
FIGURE 3.13 DIAGNOSTIC PLOTS OF Y-RESIDUALS VS PREDICTED Y FOR RAW, “LONG” SPECTRA OF TRAINING SET ONLY	90
FIGURE 3.14 PREDICTED VS NOMINAL CONCENTRATIONS OF CAFFEINE FOR UNPACKAGED SAMPLES; CROSS VALIDATION (\times) AND TEST SET (\triangle) RESULTS; DASHED LINE DENOTES WHERE $Y = X$	92
FIGURE 3.15 PREDICTED VS NOMINAL CONCENTRATIONS OF PARACETAMOL FOR UNPACKAGED SAMPLES; CROSS VALIDATION (\times) AND TEST SET (\triangle) RESULTS; DASHED LINE DENOTES WHERE $Y = X$	92
FIGURE 3.16 PREDICTED VS NOMINAL CONCENTRATIONS OF CELLULOSE FOR UNPACKAGED SAMPLES; CROSS VALIDATION (\times) AND TEST SET (\triangle) RESULTS; DASHED LINE DENOTES WHERE $Y = X$	93

FIGURE 3.17 PREDICTED VS NOMINAL CONCENTRATIONS OF CAFFEINE FOR PACKAGED SAMPLES; DASHED LINE DENOTES WHERE $Y = X$	94
FIGURE 3.18 PREDICTED VS NOMINAL CONCENTRATIONS OF PARACETAMOL FOR PACKAGED SAMPLES; DASHED LINE DENOTES WHERE $Y = X$	95
FIGURE 3.19 PREDICTED VS NOMINAL CONCENTRATIONS OF CELLULOSE FOR PACKAGED SAMPLES; DASHED LINE DENOTES WHERE $Y = X$	95
FIGURE 4.2 TRIPPLICATE SPECTRA COLLECTED FOR UNPACKAGED ALEXANDER’S PARACETAMOL (2) (A & B) AND HEDEX (1) (C & D) FOR 600S AND 5S ACQUISITIONS RESPECTIVELY.....	101
FIGURE 4.3 PC2 VS PC1 SCORES FROM PCA ON SPECTRA FROM 600S SCANS OF UNPACKAGED PARACETAMOL.....	103
FIGURE 4.4 PC1 LOADINGS FROM PCA ON SPECTRA FROM 600S SCANS OF UNPACKAGED PARACETAMOL.....	103
FIGURE 4.5 PC2 VS PC1 SCORES FROM PCA ON SPECTRA FROM 5S SCANS OF UNPACKAGED PARACETAMOL.....	104
FIGURE 4.6 PC1 LOADINGS FROM PCA ON SPECTRA FROM 5S SCANS OF UNPACKAGED PARACETAMOL.....	104
FIGURE 4.7 BOOTS PARACETAMOL (4) SPECTRA WITH DIFFERENT PACKAGING LEVELS, PLUS BACKGROUND SPECTRA (600S).....	105
FIGURE 4.8 PC2 VS PC1 SCORES FROM PCA ON SPECTRA FROM 600S SCANS OF BLISTER-PACKAGED PARACETAMOL	106
FIGURE 4.9 PC1 LOADINGS FROM PCA ON SPECTRA FROM 600S SCANS OF BLISTER-PACKAGED PARACETAMOL ...	106
FIGURE 4.10 PC2 VS PC1 SCORES PC1 LOADINGS FROM PCA ON SPECTRA FROM 600S SCANS OF “BLISCARD” PARACETAMOL.....	107
FIGURE 4.11 PC1 LOADINGS FROM PCA ON SPECTRA FROM 600S SCANS OF “BLISCARD” PARACETAMOL.....	107
FIGURE 4.12 EDXRD SPECTRA FROM IBUPROFEN MANUFACTURERS INCLUDED IN THIS STUDY.....	108
FIGURE 4.13 PC2 VS PC1 SCORES FROM PCA ON SPECTRA FROM 600S SCANS OF UNPACKAGED IBUPROFEN.....	110
FIGURE 4.14 PCs 1-3 LOADINGS FROM PCA ON SPECTRA FROM 600S SCANS OF UNPACKAGED IBUPROFEN.....	110
FIGURE 4.15 PC2 VS PC1 SCORES FROM PCA ON SPECTRA FROM 600S SCANS OF ALL UNPACKAGED SAMPLES.....	111
FIGURE 4.16 PC1 LOADINGS FROM PCA ON SPECTRA FROM 600S SCANS OF ALL UNPACKAGED SAMPLES.....	112
FIGURE 4.17 SENSITIVITY RESULTS FROM SIMCA TESTS ON PARACETAMOL MODELS.....	113
FIGURE 4.18 SPECIFICITY RESULTS FROM SIMCA TESTS ON PARACETAMOL MODELS.....	113
FIGURE 4.19 SPECTRA FROM BOOTS PARACETAMOL TABLETS WITH AND WITHOUT CODEINE (UNPACKAGED, 600S SCANS) COMPARED TO REFERENCE SPECTRA.....	115
FIGURE 4.20 SPECIFICITY RESULTS FROM SIMCA TESTS ON IBUPROFEN MODELS.....	116
FIGURE 4.21 SPECTRA FROM BOOTS IBUPROFEN CAPLETS WITH AND WITHOUT CODEINE (UNPACKAGED, 600S SCANS) COMPARED TO REFERENCE SPECTRA.....	117
FIGURE 4.22 RESULTS FROM SIMCA TESTS ON CP PHARMACEUTICALS MODEL.....	118
FIGURE 4.23 RESULTS FROM SIMCA TESTS FOR MANUFACTURER-SPECIFIC AUTHENTICATION.....	118
FIGURE 5.1 ALEXANDER’S PARACETAMOL (1) SPECTRA WITH DIFFERENT PACKAGING LEVELS, PLUS BACKGROUNDS (60s).....	123
FIGURE 5.2 BACKGROUND-SUBTRACTED UNPACKAGED SPECTRA FROM ALEXANDER’S PARACETAMOL (1) FOR ALL ACQUISITION TIMES USED.....	124
FIGURE 5.3 PC2 VS PC1 SCORES FROM PCA ON SPECTRA FROM 60S SCANS OF UNPACKAGED PARACETAMOL.....	125
FIGURE 5.4 PC1 LOADINGS FROM PCA ON SPECTRA FROM 60S SCANS OF UNPACKAGED PARACETAMOL.....	125

FIGURE 5.5 PC2 VS PC1 SCORES FROM PCA ON SPECTRA FROM 1S SCANS OF UNPACKAGED PARACETAMOL.....	126
FIGURE 5.6 PC1 LOADINGS FROM PCA ON SPECTRA FROM 1S SCANS OF UNPACKAGED PARACETAMOL.....	126
FIGURE 5.7 PC1 LOADINGS PLOT FROM PCA ON SPECTRA FROM 60S SCANS OF UNPACKAGED GALPHARM PARACETAMOL SAMPLES	127
FIGURE 5.8 PC2 VS PC1 SCORES (TOP) AND PCs 1-3 SCORES (BOTTOM) FROM PCA ON SPECTRA FROM 60S SCANS OF UNPACKAGED IBUPROFEN.....	128
FIGURE 5.9 PCs 1-3 LOADINGS FROM PCA ON SPECTRA FROM 60S SCANS OF UNPACKAGED IBUPROFEN	129
FIGURE 5.10 PC1 LOADINGS FROM PCA ON SPECTRA FROM 1S SCANS OF UNPACKAGED IBUPROFEN	129
FIGURE 5.11 SPECIFICITY RESULTS FROM SIMCA TESTS ON PARACETAMOL MODELS	131
FIGURE 5.12 H_i VS S_i PLOTS FOR UNPACKAGED (A) 60S & (B) 1S SCANS (PARACETAMOL TEST 1)	132
FIGURE 5.13 SPECIFICITY RESULTS FROM SIMCA TESTS ON GALPHARM PARACETAMOL MODEL.....	133
FIGURE 5.14 SPECIFICITY RESULTS FROM SIMCA TESTS ON IBUPROFEN MODELS.....	135
FIGURE 5.15 H_i VS S_i PLOT FOR BLISTER-PACKAGED 1S SCANS (IBUPROFEN TEST 1)	136
FIGURE 5.16 SPECIFICITY RESULTS FROM SIMCA TESTS ON CP PHARMACEUTICALS IBUPROFEN MODEL.....	136
FIGURE 6.1 IMAGES OF COUNTERFEIT VIAGRA SAMPLE TAKEN USING <i>miniPixD</i> : (A) UNPACKAGED, (B) IN BLISTER ONLY, (C) IN BLISTER AND CARD PACKET, AND (D) WITH PATIENT INFORMATION LEAFLET	142
FIGURE 6.2 CLASSIFICATION OF MEDICAL PRODUCTS TO BE USED BY THE WHO GLOBAL SURVEILLANCE AND MONITORING SYSTEM AND THE MEMBER STATE MECHANISM [REF].....	147

List of publications

Crews, C., Kenny, P.S., O'Flynn, D. and Speller, R.D., 2018. Multivariate calibration of energy-dispersive X-ray diffraction data for predicting the composition of pharmaceutical tablets in packaging. *Journal of Pharmaceutical and Biomedical Analysis*, 151, p.186-193.

Moss, R.M., Amin, A.S., **Crews, C.**, Purdie, C.A., Jordan, L.B., Iacoviello, F., Evans, A., Speller, R.D. and Vinnicombe, S.J., 2017. Correlation of X-ray diffraction signatures of breast tissue and their histopathological classification. *Scientific Reports*, 7, p.12998.

Moss, R., **Crews, C.**, Wilson, M. and Speller, R., 2017. miniPixD: a compact sample analysis system which combines X-ray imaging and diffraction. *Journal of Instrumentation*, 12(02), p.P02001.

O'Flynn, D., **Crews, C.**, Drakos, I., Christodoulou, C., Wilson, M.D., Veale, M.C., Seller, P. and Speller, R.D., 2016. Materials identification using a small-scale pixellated x-ray diffraction system. *Journal of Physics D: Applied Physics*, 49(17), p.175304.

Crews, C.C., O'Flynn, D., Sidebottom, A. and Speller, R.D., 2015, June. Quantitative energy-dispersive x-ray diffraction for identification of counterfeit medicines: a preliminary study. In *Next-Generation Spectroscopic Technologies VIII* (Vol. 9482, p.94820D). International Society for Optics and Photonics.

I dedicate this thesis to my grandparents

袴田國子、袴田義一

(Kuniko Hakamada & Yoshikazu Hakamada)

Audrey Florence Crews & Charles Gordon Crews

Chapter 1: Introduction & Background

1.1 Counterfeit and Substandard Medicines

1.1.1 Background and definitions

Counterfeiting is a vast and complex problem – it affects an incredibly wide range of products that can be copied and sold for profit. Many are familiar with the counterfeiting of luxury branded goods, DVDs and computer software, but are less familiar with the illicit trade in other goods ranging from counterfeit lighters [1], toys [2], food (olive oil and basmati rice have been counterfeited [3]), and even automotive and aeroplane parts [2]. Recently, the Organization for Economic Cooperation and Development (OECD) estimated that the trade in counterfeit goods worldwide was now worth half a trillion US dollars [4], and in 2011, The International Chamber of Commerce (ICC) estimated that counterfeit products resulted in 3,000 deaths and costed governments and consumers €14.5 billion a year within the G20 nations [5].

Medicines and medical devices have also been targeted by counterfeiters, which is particularly alarming. The late Dora Akunyili, former head of Nigeria’s Food and Drug regulation agency (NAFDAC) argued that:

“Drug counterfeiting quite frankly is one of the greatest atrocities of our time, it is mass murder, it is a form of terrorism against public health as well as an act of economic sabotage. It violates the right to life of innocent victims.” [6]

Organised crime groups are known to be capitalising on this trade, in what is thought to be a shift away from the illicit drugs trade [7]. It has also been linked to the financing of terrorist activities, along with the wider trade in counterfeit goods [8]. Several reports on the link between counterfeit medicines and organised crime have been published in recent years [9,10], and the UN Office on Drugs and Crime (UNODC) launched an anti-counterfeiting campaign (dubbed “Don’t Buy Into Organized Crime”) in January 2014, which covers counterfeit medicines [11]. Estimates of the size of the counterfeit medicines market range from US\$ 70 billion to US\$ 200 billion [12]; the World Economic Forum presented an estimate of US\$ 200 billion in 2011 (compared to US\$ 280 billion for the illicit trade in marijuana, cocaine, opium and heroin combined) [13].

India and China were found to be the source of counterfeit medicines in many cases [14,15], and a report by the United Nations Interregional Crime and Justice Research Institute (UNICRI) contained a section dedicated to “China and India as Exporters and Consumers of Counterfeit Medicines” [9]. In a Royal United Services Institute for Defence and Security Studies (RUSI) report, all the UK-based operations to combat counterfeit medicines cited China as the, or one of the source(s) of counterfeit drugs [16]. Figure 1.1 illustrates the significant role that India and China play, compared to other countries.

Figure 1.1 Map of trade routes of counterfeit medicines [17]

Counterfeit medicines can take several forms. They may have no active pharmaceutical ingredient (API), the API in the incorrect dose (some in fact have too much API [18,19]), or mixed with another API [17,20]. There are many instances where the wrong API is used, which not only results in treatment failure, but adds the risk of potentially life-threatening allergic reactions (such as in the cases of counterfeit Tamiflu containing penicillin [21], or antimalarials containing sulphadoxine [22]). All the above may be manufactured with the incorrect excipients*, once again raising the issue of allergic reactions; plus they may contain toxic substances and other contaminants as a result of being manufactured in unsanitary conditions [23]. Lastly, even those which contain the correct API in the correct dose – so-called “professional” counterfeits, which pose less of a public health risk [20] – may dissolve at the incorrect rate if formulated with the wrong excipients, thus increasing or decreasing the bioavailability of the API and making them unsafe [14].

* Excipients are the various ingredients in a pharmaceutical formulation (for example: fillers, binders, colourings and flavourings) other than the API.

However, there is currently no international consensus on a definition of “counterfeit medicines”. Intellectual property (IP) issues have been blamed for disagreements over any suggested definitions, due to mix-ups with generic medicines [24]. For example, in 2008 and 2009, Dutch customs officials seized generic HIV and cancer medicines in transit from India, as they infringed European IP laws and were hence deemed to be counterfeit [14]. Confusion abounds – in a recent research article the authors grouped counterfeit and generic versions of a drug together, and attempted to distinguish these from the “genuine” (i.e. branded) drugs using an analytical technique (Raman spectroscopy). They unsurprisingly found that the generic and branded drugs were very similar and difficult to discriminate [25].

Another source of confusion is the different but related problem of substandard medicines. These are “genuine medicines produced by manufacturers authorized by the national medicines regulatory authority (NMRA) which do not meet quality specifications set for them by national standards”, according to the World Health Organisation (WHO) in 2009 [26]. Thus, these may contain contaminants or amounts of API that are outside the tolerance boundaries set by the pharmacopoeia, for example. There have been various calls to further highlight the issue of substandard medicines, which can be overshadowed by excessive focus on the counterfeit kind [27–30]. Notably, a recent report on the findings of the artemisinin combination therapy (ACT) consortium’s drug quality programme found that counterfeits were found in only two of the six malaria-endemic countries studied (and constituted <8% of samples in these cases), whereas substandard versions of these antimalarials were found in all six (6.0 - 37% of samples collected in each) [30]. Medicines that contain no API, contain unapproved chemicals, or chemicals that mimic the effects of the correct API, can be strongly indicative of deliberate counterfeiting [15], as are medicines in fake packaging [31], but in general it is difficult to determine the intention of the manufacturer with certainty [23,32], so many researchers do not make the distinction with substandards [33]. Though the difference between the two may be important when determining effective countermeasures [31], it is arguably not as important when considering the impacts on patients’ health [27,34].

For the purposes of this thesis, the definition given above for substandard medicines, and the following definition of counterfeit medicines (from the WHO in 2009) will be used:

“A counterfeit medicine is one which is deliberately and fraudulently mislabelled with respect to identity and/or source. Counterfeiting can apply to both branded and generic products, and counterfeit products may include products with the correct ingredients or with the wrong ingredients, without active ingredients, with insufficient active ingredients or with fake packaging” [26];

although the issue of medicines (whether authentic or counterfeit) in fake packaging will *not* be considered here. Note that the term “falsified” is nowadays preferred over “counterfeit”, and since January 2016, the WHO favours the rather vague term “Substandard, Spurious, Falsely labelled, Falsified and Counterfeit (SSFFC) medicines” as a temporary measure until an agreement is reached on definitions [35]. “Counterfeit” is used in this thesis for simplicity and due to the greater familiarity and wider usage of this term.

1.1.2 Prevalence

Counterfeit and substandard medicines are not a novel problem – awareness of the issue was evident at a meeting arranged by the WHO in 1985 [36]. In 1988, a World Health Assembly (WHA) resolution requested that the WHO “initiate programmes for the prevention and detection of the export, import and smuggling of falsely labelled, spurious, counterfeited or substandard pharmaceutical preparations”; in 1994, another resolution requested that it “assist member states in their efforts aimed at combating counterfeit drugs” [37]. Yet, many cases have been reported over the years, a very small selection of which are shown in Table 1.1, which demonstrates the breadth of countries and drug type that have been and continue to be affected.

Year	Incident	Country	Ref
1995	Substandard kala-azar (visceral leishmaniasis) treatment results in deaths	India	[38]
2001	20,000 counterfeit painkillers containing boric acid and lead paint seized	Colombia	[2]
2003	130,000 counterfeit Panadol (paracetamol) tablets seized	China	[39]
2003	FDA recalls 18 million counterfeit Lipitor (cholesterol-lowering) tablets	USA	[40]
2005	Case study of death caused by counterfeit artesunate (antimalarial) containing incorrect API	Myanmar (Burma)	[41]
2007	MHRA recalls counterfeit Zyprexa (antipsychotic), Plavix (heart disease drug), and Casodex (prostate cancer drug)	UK	[42]
2008	Counterfeit Viagra results in reports of one death and 11 hospitalisations	China	[43]
2009	Counterfeit diabetes drugs containing excessive amount of glibenclamide kills two patients	China	[44]
2011	Counterfeit Zidolam-N (HIV/AIDS treatment) accidentally distributed by Médecins Sans Frontières (MSF)	Kenya	[45]
2012	Contaminated heart medicine causes 120 deaths and hundreds of adverse reactions	Pakistan	[46]
2013	150,000 counterfeit Postinor-2 (emergency contraceptive) tablets containing no API seized	Nigeria	[47]
2014	Diazepam (anti-anxiety drug) containing wrong API haloperidol (antipsychotic) found to be cause of hundreds of adverse reactions	DRC	[48]
2016	Counterfeit painkiller Norco (paracetamol and hydrocodone) containing other dangerous APIs results in several deaths	USA	[49]

Table 1.1 Examples of cases involving counterfeit or substandard medicines

Figure 1.2 Citation report for Web of Science search (TOPIC: (counterfeit OR fake OR falsified OR substandard) AND (pharmaceutical OR medicine OR drug)), 1997-2017

Until recently, much of the literature on counterfeit medicines came from the grey literature and the media [50,51]. However, as Figure 1.2 illustrates, there appears to be a clear rise in academic research output in this area over the past decade. Accurately measuring the prevalence of counterfeit and substandard medicines is nevertheless still a challenge, resulting in a limited body of empirical research on the problem. This is in part due to the lack of differentiation between the different types of poor-quality medicines. There are also logistical obstacles to having truly randomised sampling for such studies, such as the lack of lists of vendors – including unregulated markets – for the sampling frame, and the need for ‘mystery shoppers’ to avoid bias from sellers [26], rendering such investigations prohibitively expensive for some [21]. Others have encountered difficulties in acquiring samples of genuine medicines from legitimate manufacturers to be used as references [21,52]. A 2013 editorial in *The Lancet* commented on this lack of rigorous research and robust data to give true estimates of the problem, and mentioned that governments and pharmaceutical companies have been known to withhold information on the matter [46].

To this end, in 2009 Newton *et al.* proposed a format for carrying out statistically valid field surveys, including a checklist of guidelines on what to cover when reporting the information (the Medicine Quality Assessment Reporting Guidelines (MEDQUARG)), in an attempt to standardise the procedure [32]. The checklist has been used in a literature review to score study methodology, but very few scored highly [33], and only 15.4% (6/39) of the publications logged on the Worldwide Antimalarial Resistance Network (WWARN) Antimalarial Quality Surveyor since the MEDQUARG publication stated that they followed the guidelines [53]. This indicates that many researchers do not appear to have taken the recommendations on board, possibly

due to a lack of awareness or because they were not able to due to certain constraints. Some would argue that the quality of such information should not affect decision-making, as the problem needs to be tackled regardless. However, better evidence of prevalence is hoped to help mobilise governments to commit resources and take action [54].

In more economically developed countries, the main products targeted by counterfeiters tend to be “lifestyle” medicines, such as erectile dysfunction or slimming pills [17]. These are commonly sold by illegal online pharmacies, without the need for a prescription [55] – hence attracting customers who may wish to hide the fact that they are purchasing such medications. There are also those who turn to online pharmacies simply to try to save money, or because it is more convenient [55,56]. Consumers may not know where they are really buying medicines from – for example, many “Canadian” online pharmacies targeting patients in the USA are not in fact based in Canada [57]. The rapid increase in the number of illegal online pharmacies in recent years is a source of concern, and a 2009 survey of general practitioners in the UK found that 25% had treated a patient who had suffered from an adverse effect from medication purchased online [12].

Incidents of counterfeit and substandard medicines entering the legitimate supply chain tend to be relatively uncommon due to strong regulatory frameworks in these countries. In the UK, the Medicines and Healthcare Products Regulatory Agency (MHRA) detected 14 cases of counterfeit medicines entering the supply chain between 2004-2011 (the last incident being in 2007), of which nine were only detected and recalled after reaching patients [58]. A review of MHRA drug alerts between 2001-2011 found 182 incidents of substandard medicines (excluding reports of packaging defects) in this period; this figure includes medical products such as vaccines and inhalers. The USA has seen worrying cases of deaths caused by poor-quality drugs over the past several years [59], and according to the Food and Drug Administration (FDA), the top five brands associated with the ten highest-volume incidents of counterfeit or diverted medicines were: Zyprexa (antipsychotic), Viagra (erectile dysfunction), Lipitor (statin), Zoloft (antidepressant), and Risperdal (antipsychotic) [60].

In less economically developed countries, the prevalence of poor-quality medicines for malaria, tuberculosis and HIV/AIDS are key areas of concern [17,51], although a large proportion of studies focus on antimalarials only [29]. It is important to note that, in reality, *all* therapeutic categories of medicine have been affected [29,61]. Medicines for neglected tropical diseases may be particularly vulnerable [27] – for example, in 2012, a sample of a kala-azar treatments collected in Bangladesh were found to contain no API [62,63], which is alarming considering the history of deaths caused by poor-quality medication for this illness (see Table 1.1).

There are a few studies that have made more reliable assessments of incidence levels using random sampling. A study published in 2001 surveyed 27 drug types (including antimalarials and antibiotics) collected in randomly selected registered pharmacies in Lagos and Abuja, Nigeria, and found that 48% failed quality testing [18]. A 2009 study of antimalarials in south-eastern Nigeria found that 37% contained no or insufficient API [64]. In 2005, 12.2% of various antimalarials sampled in Tanzania were found to be of poor quality [65]; a 2010 study found that 12.1% of artemisinin combination therapies (ACTs) – the current first-line defence against malaria – in Tanzania failed quality tests [66]. A recent random-sampling study by Antignac *et al.* found that 16.3% of cardiovascular drugs in sub-Saharan Africa were of poor quality [67].

In southeast Asia, a random survey of artesunate quality in Lao PDR in 2003 found that 88% of outlets sold counterfeit versions of the drug, which either contained none of the correct API, or sub-therapeutic amounts of other antimalarial APIs that had been withdrawn from the market due to ineffectiveness [22]. A follow-up survey carried out in 2012 found that the proportion of poor-quality antimalarials had decreased, but still stood at 25% [68]. Another survey of antimalarial drug quality in Cambodia (from private health outlets only), carried out at the end of 2010, found 31.3% to be substandard, but none were deemed to be counterfeit [69]. A random survey of five different drug types (including antibiotics) collected in 2010 in Cambodia found that 15% of samples had the incorrect quantity of API [70].

A review article focusing on prevalence studies – only 15 out of 44 which were deemed to be of good methodological quality – found that the median prevalence of poor quality drugs in Africa and Asia was 28.5%, and that the percentage of poor-quality medicines sold by unlicensed outlets was significantly higher (50%) than for licenced outlets (24%) [33].

1.1.3 Impacts and contributing factors

The impacts of counterfeit and substandard medicines are wide-ranging, and include [31,71–73]:

- Increased morbidity (number of people with disease) and mortality (number of deaths), as demonstrated by some of the cases in Table 1.1; for example, a recent study estimated that 3.75% of under-five deaths in Sub-Saharan Africa were caused by poor-quality antimalarials [74];
- Adverse effects from incorrect APIs, toxic ingredients and other contaminants (including pathogens [75]) introduced into medicines produced by illegal manufacturers – or by licenced manufacturers which fail to meet GMP standards;

- Drug resistance caused by medicines containing sub-therapeutic amounts of API (more likely in substandard than counterfeit medicines [23]), potentially rendering first-line defences against diseases ineffective; concerns were raised in a letter to The Lancet back in 1995 [76], and repeated in more recent years by various parties [26,77–81];
- Loss of confidence by patients and healthcare workers in healthcare systems and drug manufacturers if high rates of poor-quality medicines are present;
- Economic impact on patients who waste money on ineffective drugs, and on costs of continued treatment, transport, hospital stays, and lost earnings;
- Economic impact on healthcare systems dealing with patients taking such medicines;
- Lost income (in the case of counterfeits) and brand damage for manufacturers of the genuine product

The literature suggests several factors that have promoted the growth in the trade of counterfeit medicines, including [17,82]:

- **Profit** – there is always a high demand for medicines, and large profits can be made; according to Pfizer, it is more profitable to produce and sell 1kg of counterfeit Viagra than 1kg of heroin [9]; the high cost of genuine drugs has been suggested as being the main reason that consumers are compelled to seek cheaper drugs [17,83]; although it may equally be due to demand exceeding supply [23];
- **Complex supply chains** – supply chains are far more complex in developing countries compared to developed countries, and the use of wholesalers facilitates the introduction of counterfeits into legitimate distribution routes [26,84]; medicines are particularly vulnerable as they are small and light, hence easy to transport [85];
- **The Internet** – a useful distribution channel that is very hard to police; online pharmacies use marketing tactics to lure in customers effectively [86];
- **Technological advances** – make it easier to imitate packaging and ingredients in counterfeits; for example, a hologram used on an antimalarial product was counterfeited in 14 different ways over nine years, with each iteration becoming increasingly sophisticated [87].
- **Inadequate disincentives** – penalties are less severe than for the illicit drugs trade, and when the counterfeiters' money is not seized, they can re-start their counterfeiting operation [12]; countries that *do* have harsher penalties also need to support enforcement efforts;

- **Corruption** – of customs officials, regulatory authorities, and manufacturers [88]; some of the latter work a “third shift” to use equipment to produce knock-off versions of their products to sell on [14,15];

In addition to the above, factors that have facilitated the proliferation of substandard as well as counterfeit medicines include:

- **Weak regulation and enforcement** – NMRAs in countries that lack infrastructure struggle to carry out spot checks on pharmacies and on products, ensure that supply chains are secure, and ensure that healthcare providers procure medicines from trusted sources; US FDA and European authorities have been criticized for infrequent inspections of drug manufacturers in China [89]; in India, medicines regulation is down to local authorities in each of 35 states, which has resulted in uneven standards and is accused of being ineffective [14]; in Africa, the majority of countries’ NMRAs lack resources and are not legally mandated to perform critical regulatory functions [90];
- **Lack of awareness** – amongst the public (for example, a survey in Laos found that 80–96% of consumers were not aware of poor-quality drugs [91]), but also health officials, policy-makers, doctors, pharmacists, and other stakeholders, meaning poor-quality medicines may not be considered to be the reason for treatment failure [26];
- **Lack of will and reputational repercussions** – pharmaceutical companies may not act due to fears of damaging their reputation, and governments may wish to avoid causing panic [92]; the USA and EU were first (in 2011-2012) to legally require the pharmaceutical industry to inform their relevant NMRA of drug counterfeiting incidents [93];

1.2 Countermeasures

1.2.1 Social countermeasures

In this section, current and proposed social countermeasures for preventing the scourge of counterfeit and substandard medicines will be discussed (drawn from various sources [30,31,73,82,94,95]).

1.2.1.1 Regulation and inspection

Regulation is hugely important for the medicines supply chain, because as Newton *et al.* remarked: “there is little point in determining the most efficacious drugs if the quality of the drug supply is not monitored and maintained” [31]. In the UK, the MHRA works with the

Royal Pharmaceutical Society of Great Britain (RPSGB) to carry out targeted spot checks of medicines in the UK market [96]. Yet there are still countries which lack – or lacked until recently – a functioning NMRA. For example in Pakistan, the NMRA was only re-established in 2012 after two years of unregulated pharmaceutical industry activity was held partly responsible for numerous deaths that year (see Table 1.1); although commentators had doubts about the effectiveness of this newly-established agency due to a lack of funds [97]. Similarly, the WHO’s Regional Committee for Africa stated that between 2005 and 2015, the percentage of member states with NMRAs increased from 87% to 96%, where the majority were unable to function effectively due to a lack of resources – but aimed to have a functional NMRA in all member states by 2025 [90].

Regulatory implementation by NMRAs should include the proper registration of drugs, licensing of pharmacies, monitoring of the supply chain, investigation of any issues and possibly prosecution. It is also vital to remove drugs that are no longer effective from the market, such as older-generation antimalarials [31]. A recent literature review found that drug registration and WHO-prequalification* appear to be effective countermeasures, but “licensing of drug outlets alone appeared to be ineffective in reducing the prevalence of counterfeit and substandard drugs”, possibly due to a lack of inspections [98].

Enforcing good manufacturing practice (GMP) amongst manufacturers is also key to eradicating poor-quality medicines. The United States Agency for International Development (USAID) and the US Pharmacopeial Convention (USP) have run a joint initiative to improve quality assurance (QA) and quality control (QC) systems in over 35 developing countries since 1992 – re-launched in 2009 as “Promoting the Quality of Medicines (PQM)” [99]. A review of four pre- and post-intervention studies for PQM found that there was a significant increase in the quality of medicines in all cases [98]. Countries that are not involved in such schemes could possibly raise some funds required for effective regulation by increasing the costs of drug registration, which are currently very low in developing countries [73] – alternatively, the “twinning” of NMRAs between developing and developed countries to provide financial assistance has been suggested [31].

The accreditation of online pharmacies is also important to assist consumers in choosing safe sources of medications. The Verified Internet Pharmacy Practice Site (VIPPS) accreditation logo is used in the USA and Canada [100] to verify if a site is genuine; a similar system using the

* A WHO service that assesses the quality, safety and efficacy of medicinal products, used by international procurement agencies to guide medicines purchasing decisions.

“EU common logo” exists in EU member states [101]. Awareness-raising, discussed below, is also necessary for such measures to be effective. Some NMRAs have staff members who monitor and take down fake online pharmacies, freezing their assets where possible*.

1.2.1.2 *Legislation and enforcement*

A common argument in the literature is the need for legislation to clearly identify counterfeiting as a crime. This can admittedly be problematic due to the multinational scope – the Council of Europe’s “*Convention on counterfeiting of medical products and similar crimes involving threats to public health*”, otherwise known as the MEDICRIME Convention, is the first attempt to set up a legal framework that facilitates international cooperation on this matter [102]. However, its wording has faced criticism [103,104] and it has currently only been ratified by 11 countries, so more work is needed to discuss and raise awareness [105]. Legislation against substandard medicines could also be considered, as although the issue can be addressed by good regulation, the repeated accidental production of poor-quality drugs may be deemed to be irresponsible enough to be treated as a criminal act, as the consequences to the consumer are equally serious as for counterfeits [15,27]. One practitioner has produced a “*Model Law on Medicine Crime*”, available for use free of charge by any governments wishing to implement it, which covers both counterfeit and substandard medicines as well as special provisions for Internet sales [106].

Penalties for counterfeiting should arguably be as severe as for illicit drugs production and distribution, with police and customs authorities required to treat cases with the same gravity [31]. In the UK, there is a maximum sentence of 8 years for introducing counterfeit medicines into the supply chain†. Another source stated that sentences are normally two years in the UK, but it can be easier to deter criminals by confiscating all their assets (the MHRA have the power to do this); prosecuting criminals on the grounds of trademark offences can result in longer, 10- to 14-year sentences, and pharmaceutical companies are often willing to cooperate to achieve this ‡. The Chinese government has also amended its laws to strengthen penalties for counterfeiting medicines, which can now be a maximum of life imprisonment or even the death penalty [26].

Legislation is in itself not sufficient to deter counterfeiters, as enforcement is also essential. One important actor in this regard is Interpol, which leads a number of operations to tackle pharmaceutical crime, focusing on various different areas of the world (e.g. Operation Storm in

* Presented at the MHRA’s “Law Enforcement Officers Open Day”, 2014.

† Presented by Michael Deats (WHO) at the Joint Pharmaceutical Analysis Group’s “Combating Counterfeit Medicines” symposium, 2014.

‡ Presented by Gift Minta (MHRA) at UCL Security and Crime Science Seminar, 2013.

southeast Asia, and Operation Giboia in southern Africa) or the Internet (Operation Pangea) [107]. Most large pharmaceutical companies have in-house security departments which work with local and international law enforcement agencies to collect the information required for prosecution [26]. But enforcement can be problematic, particularly as it involves a large range of “disparate agencies with limited budgets and competing priorities” [26]. Resources for enforcement purposes may be limited even in more economically developed countries, due to a lack of political will to act on this matter [108].

1.2.1.3 *Surveillance*

The WHO operates a Global Surveillance and Monitoring System for SSFFC medical products, which was launched in 2013. Regulatory personnel in 113 member states have received training (as of early 2016) on how to report suspected products, with more training planned in the future. The WHO guarantees a response within 72 hours (24 hours in an emergency, i.e. if adverse events or deaths have been reported), where they request further information and may provide technical assistance to the relevant NMRA in order to confirm the report. They may then take action such as issuing a medical product Rapid Alert in instances where there is a significant threat posed, or other member states may be affected. The data collected is also collated and analysed to generate statistics that may support evidence-based policy-making for the prevention, detection and response to such medicines [109].

On the other hand, the Pharmaceutical Security Institute (PSI) logs cases of counterfeit (not substandard) medicines – presumably only those reported by its members from the pharmaceutical industry – in its Counterfeit Incident System. This data is aggregated to provide snapshots of the counterfeit situation, but there are numerous criticisms of the current state in which this is run: notably, the detailed data is proprietary to PSI members; there are inconsistencies in the information provided for each incident; and a disproportionate number of incidents are logged by countries that have better regulatory systems, giving a skewed view of the problem, which is not as helpful to policy-makers [110].

In the UK, the MHRA has had an anti-counterfeiting strategy, now called the “Falsified Medical Products Strategy”, since 2007, which it launched in conjunction with a 24-hour hotline specifically for reporting counterfeit medicines [111]. This runs alongside the Yellow Card Scheme – an online form for reporting counterfeit medicines, “defective” (poor-quality) medicines, adverse incidents or unexpected side effects. Both these reporting mechanisms are open to use by members of the public as well as healthcare professionals, unlike the aforementioned two surveillance mechanisms.

1.2.1.4 Awareness-raising

Raising awareness of the risks posed by poor-quality medicines is important for all stakeholders. Patients in particular need this information in order to make informed decisions about medicines purchases. In 2006, researchers found evidence that TV and radio campaigns about the dangers of counterfeit medicines were effective in changing purchasing behaviours, to avoid illicit drug markets, amongst the general public in Benin [98]. In Cambodia, where many counterfeit antimalarials have imitation holograms on their packaging, an awareness-raising campaign involving radio, TV and poster warnings (see Figure 1.3 (left)) was reportedly beneficial [31]. Even where effective regulation may not be possible, awareness-raising could help protect consumers [112], although it does have its limitations, such as literacy rates of the population, and the inability to spread the message to remote areas [108]. It is also important to ensure that any campaigns do not go so far as to make patients fear *all* medicines [26].

Targeting consumers susceptible to purchase from fake online pharmacies is also important. In 2009, the MHRA, RPSGB, Pfizer, The Patients' Association and Heart UK ran a short clip shown on TV and in cinemas as part of its "Get Real, Get a Prescription" campaign, warning against purchasing prescription-only medicines online [113]. The European Alliance for Access to Safe Medicines (EAASM) also targeted online shoppers by running a seemingly genuine online pharmacy, and using common advertising tactics to direct traffic to their site. Once there, customers who attempted to purchase medicines were instead presented with safety messages and links to legitimate pharmacy sites. The site received 182,000 unique visitors in the two-month campaign period [114].

Informing medical professionals is also key, as they may not suspect poor-quality medicines in cases of treatment failure in patients. An advice leaflet issued by the RPSGB in 2009 contains "Guidance for Pharmacists and Dispensing Doctors" on the matter, including when to suspect that a medicine is counterfeit, and how to contact the MHRA if so [96]. In 2014, the US FDA started a campaign dubbed "Know Your Source", consisting of a series of leaflets such as the one shown in Figure 1.3, encouraging healthcare professionals to check the credentials of wholesalers and raising awareness of poor-quality products. In addition, there have been instances where wholesalers were conned into buying counterfeit medicines unintentionally, attracted by the lower prices offered by the seller [9] – so raising awareness in these sectors is also required.



Figure 1.3 (L) Awareness-raising campaign poster, Cambodia [31]; (R) FDA campaign, USA [115]

1.2.1.5 Cooperation and exchange of information

Cooperation at national and international levels is important due to the trans-national nature of both the legitimate and illegitimate medical supply chains. Figure 1.4 illustrates how a recent forensic analysis of counterfeit versions of a certain product, from multiple seizures, pointed to the involvement of numerous countries spanning several continents. Such information could lead to better intelligence-led interventions [116], but would require collaboration and information-sharing between multiple actors such as: NMRAs, police forces, customs officials, the judiciary, pharmaceutical manufacturers, distributors, and healthcare professionals.

Figure 1.4 Proposed scheme of where counterfeit samples were produced and distributed [116]

This is not straightforward – a case in point being the International Medical Products Anti-Counterfeiting Taskforce (IMPACT), established by the WHO in 2006 and endorsed by representatives from 57 NMRAs, and twelve international associations of patients, healthcare professionals, pharmaceutical manufacturers and wholesalers [117]. This initiative suffered from suspicions by generics manufacturers, NGOs and various governments due to the possible conflation with IP issues [118,119], and although IMPACT has attempted to rebut such concerns [117], the WHO eventually detached itself from IMPACT in 2010 [120]. As previously touched

on in section 1.1.1, this disagreement surrounding the definition of counterfeit medicines is an issue that needs to be addressed urgently for progress to be made [89,120].

Nevertheless, there are examples of successful collaborations, such as the operation detailed in Newton *et al.*'s 2008 paper, where police officers, criminal analysts, chemists, palynologists (to study pollen grain contaminants) and healthcare professionals, as well as Interpol and the Western Pacific WHO Regional Office worked together to provide the evidence required for the Chinese authorities to dismantle a counterfeiting operation [121]. In Nigeria, the NAFDAC has taken a proactive approach to tackling importation of counterfeit and substandard medicines by working directly with the Chinese and Indian governments since 2009, and this has led to convictions of counterfeiters in both China and India [108]. There is also the PQM program (see section 1.2.1.1), which requires the ongoing cooperation between NMRAs, healthcare professionals and governments [98].

Interpol's Operation Pangea is a huge international collective effort targeting illegal online pharmacies specifically, and has run for an annual "week of action" since 2008. The number of participating countries has grown from 10 to 115 in 2015, and NMRAs, customs officials, police forces, pharmaceutical companies, postal services, internet service providers (ISPs), domain names registrars, and payment providers (PayPal, MasterCard, and Visa), have all joined forces to take down thousands of websites each year, seizing millions of counterfeit and illicit medicines, and arresting hundreds of perpetrators [107].

1.2.1.6 *Improving access to affordable medicines*

Some practitioners have argued that measures must be taken to reduce the cost of medicines, thereby decreasing the likelihood that sellers and consumers will look to purchase cheaper versions from unregulated sources, thereby exposing themselves to counterfeit or substandard medicines [31,122,123]. Governments may be able to intervene by reducing taxes, and encouraging domestic manufacturing and distribution of good-quality, affordable generics where possible [33].

However, others have noted that cheap medicines are still targeted by counterfeiters – possibly due to economies of scale, but also because counterfeiters will always be able to bypass additional production costs incurred by those running a legitimate operation (R&D, employee, and licencing costs) [7,23,24]. There is also evidence to suggest that consumers perceive free or cheap generic medicines distributed by public health authorities as being of poorer quality than more expensive branded goods that they can buy elsewhere, which would undermine efforts to reduce drug costs [124].

1.2.2 Technological countermeasures

The countermeasures described above are predominantly societal initiatives recommended to or implemented by governments and international organisations. In addition to these measures, there are many technological solutions that are being or have the potential to be applied to tackle the problem. These can be divided into three broad areas: product protection technologies, track-and-trace technologies, and analytical techniques; the former two focus on tackling counterfeit medicines, whereas the latter provides opportunities to detect all types of poor-quality pharmaceuticals.

1.2.2.1 *Product protection technologies*

Due to the increase in incidence of counterfeit medicines, the WHO recommended in 2002 that “the design of the packaging must therefore contribute to preventing tampering with, or the counterfeiting of, certain medicinal products” [125]. There exists a wide range of product protection technologies on the market, commonly divided into: *overt* features (those which are visible to anyone); *covert* features (necessitating a simple instrument to detect); and *forensic* features (highly secretive with details divulged on “need to know” basis only) [126].

Overt features include tamper-evident packaging, which is mandated by the US FDA for over-the-counter (OTC) medicines since 1983 (Federal Regulation 211.132) [127], and by the EU as of 2016 (Commission Delegated Regulation 2016/161) [128]. However, tamper-evident methods have been shown to be easily defeated [129,130], so their usefulness is debatable. Another widely-used feature is the hologram, but this has had its effectiveness reduced over time due to their manufacturing equipment being widely available, making counterfeit versions widespread [131].

Another overt technique is the use of scratch-off codes on medicines packaging (such as on the blister pack), which is then sent by SMS for verification. There are various providers of this technology, and it is popular in India and several African countries [17]. An advantage is that public health authorities can be alerted to any incidents of counterfeit medicines in the supply chain when a code fails. Concerns with this approach are that its effectiveness relies on consumers owning mobile phones and having connectivity, and that it inherently relies on the end user to carry out the verification. Moreover, because this is a “one-use” feature, it cannot be used for verification by middle men in the supply chain [108].

Covert methods that are widely used include invisible inks that fluoresce under UV light. Each one can be designed to emit a particular range of wavelengths, and so can be used in combination to create UV-visible images which are difficult to replicate [131]. A related but less

widespread method is the use of infrared “upconverting” phosphor inks, which can convert light from cheap infrared lasers to visible light for authentication purposes [132,133].

So-called “forensic” features include biological, chemical and physical taggants. Biological taggants normally involve the use of DNA fragments of a specific sequence that are incorporated into a label or security ink on the packaging, and are detected by the addition of the complementary DNA strand with a fluorescent probe that only activates when there is a match. This technique is cheap, durable, and can be screened in the field, but does require strict secrecy and specific equipment which may not be available to practitioners [126,133,134].

Chemical taggants include pH-sensitive materials, or other chemicals that require more sophisticated equipment than covert methods for authentication; physical taggants may be specially designed particles of different colour combinations that are only visible with the use of a microscope, for example [126].

One of the main disadvantages of all product protection technologies is the set-up and running costs involved in introducing an extra step in the manufacturing process [135]. Many also have the potential to be easily replicated and disseminated by counterfeiters, so features need to be changed regularly (on the order of every 12-18 months, according to one source [136]) because there is no way of knowing with certainty if and when a certain product protection feature has been defeated [137]. In addition, the implementation of such features requires constant awareness of what to look for amongst all those implicated in the supply chain, which may be unrealistic [134,136]. Also, it is important to note that authenticating the *packaging* is not the same as authenticating the *medicine* itself [108]. Moreover, all the above techniques become redundant if a product is repackaged (legally) at any stage in the supply chain [136,137] – indeed, this creates the additional problem that discarded genuine packaging may be sold on to counterfeiters [9,137,138].

1.2.2.2 *Track-and-trace*

The purpose of track-and-trace is to enable a user to determine the current and past movements of a certain product – at any point in a distribution chain – based on a unique product identifier. The application to medicines authentication within the pharmaceutical supply chain has been discussed for many years, as it is thought that “a mandatory track-and-trace system for drugs is the best way to monitor the chain of custody and protect patients from unsafe drugs” [26]. But it has proven difficult for agreements to be reached between NMRAs in terms of which technology to use, and how best to implement it [59]. The current two main competing

technologies for this application are radio-frequency identification (RFID) tags and 2-D matrix barcodes [139].

The main drawback of RFID technology comes down to its cost, but even if it were to become more affordable, it is unclear whether it would be practical to implement in the less economically developed countries that are most affected by poor-quality drugs [26]. One researcher noted that although the cost per RFID tag has decreased over the years, the added cost of computer systems and readers is often overlooked, and can be significant in comparison to the cost of living in such countries [108]. RFID was ultimately not chosen in the EU; possibly due to responses to a consultation, where stakeholders stated that RFID would not be more effective at securing the supply chain than 2-D matrix barcodes, and that its costs (estimated to be five times greater) could therefore not be justified [140]. IMPACT had already stated in their 2008 brochure that their “consensus is that full implementation of RFID can only be envisaged in a distant future; as a consequence, the most realistic alternative to enable tracking and tracing medical products along the supply chain is the use of two-dimensional bar codes” [94].

Thus, the European Commission published a delegated act on 9th February 2016 containing details of a point-of-dispensing verification system (as opposed to full track-and-trace) using 2-D matrix barcodes that is to be implemented by all manufacturers within the EU by 9th February 2019 [128]. The system is due to function as depicted in Figure 1.5 (L), with barcodes uploaded to a database by the manufacturer, verification taking place prior to being handed to the patient, and with all other verification by intermediaries being on a voluntary basis.

Figure 1.5 (left) Track-and-trace system to be rolled out within the EU [140]; (right) national variations in barcodes used for serialisation [141]

Similar systems using 2-D barcodes have been implemented in Brazil in 2009, and in Turkey in 2011 [26]. The USA passed a pharmaceutical track-and-trace bill in 2013, which was due to take effect in 2017 [141] but has since been postponed [142]. China and India were also in the process of rolling out track-and-trace type systems, but timings appear to be uncertain [14,143]. In

addition to this, different countries have adopted different types of serialisation methods [141] (see Figure 1.5 (R)) which may add to the confusion where supply chains cross over.

1.2.2.3 Analytical Methods

As mentioned above, counterfeiters tend to be adept at altering their products in order to overcome countermeasures used by manufacturers. This process of continual move and countermove can be thought of as an “arms race” where those striving to fight the offenders need to be dynamic in their response [108,144]. Some counterfeiters have honed their production methods to make their products pass visual inspection, right down to the pill or capsule level (for example, see Figure 1.6), so there is a growing requirement for chemical analyses to test their composition for the purposes of authentication [9,31,56,130,145–148]. Presumably, even in cases where the packaging or pills have *not* been perfectly copied, scouring them visually to find errors may be more time-consuming than the use of a rapid analytical method. Chemical analysis methods have the added advantage that they may also be capable of detecting substandard medicines.

Figure 1.6 Can you tell which are counterfeit? (Answer – the right-hand column) [149]

Analytical methods range from simple chemico-physical tests to more sophisticated techniques; some of which are likely to be useable in the field, and others which require more high-tech laboratories. The choice of technology will depend on a range of factors, such as the cost, scalability, training required, regulatory implications and specific country needs – so there will

be no one universally applicable technology [94,148]. Timing and throughput is important for fieldwork, or in cases where large quantities of suspect medicines are seized, so there is a demand for fast methods that require minimal sample preparation [87]. Compromises may need to be made however between the amount of information required for decision-making, the speed of analysis, and the resources available [56,148].

Unfortunately, there is a lack of evaluation studies for both non- and technological countermeasures, meaning there is a very little evidence to support any interventions currently being employed or considered [21,23,72,98]. Cost-benefit analyses are also noticeably lacking. It is therefore difficult to compare detection capabilities of the various analytical techniques, as there are very few critical comparisons between technologies in peer-reviewed journals, and most journal articles describe tests carried out on different sample sets of medicines, prepared differently, and with different data analysis methods. Regardless, it is thought that “an understanding of the technological landscape, the range and gaps in available technologies, and the likely improvements in the near future is essential” for discussing the use of technologies in the developing world for counterfeit and substandard medicines detection [26]. Improving access to such analytical chemistry facilities and training will be important for creating a sustainable solution [21].

Note that the remainder of this section does not constitute an exhaustive list of analytical technologies for this application, as there are myriad options, but the most commonly considered techniques are covered here.

1.2.2.3.1 Bulk property methods

Measuring properties such as the weight, density, refractive index and pH of medicines, and comparing these to genuine samples, is possible with cheap, simple and rugged devices [31,145]. Refractometry, for example, has been shown to be fast and field-adaptable as a method, and has been trialled for assessing antimalarial quality [150]. Measurement of the colour of tablets and/or packaging using colorimetry – looking at the reflectance visible spectra in this case – could also be useful, as it is more objective than making a judgment by eye. However, a study found that genuine packaging for certain products varied in colour between batches, making it difficult for comparisons to be made [151]. These methods tend to lack specificity and do not give much information [17].

Dissolution testing is often overlooked as a bulk property method, but is an important means to assess medicines quality [31], as it is affected by various aspects such as particle sizes and

manufacturing methods [56]. The downsides are that it is destructive, time-consuming, and has been known to have problems with inconsistencies depending on operating procedures [152].

1.2.2.3.2 Colorimetric analysis

Colorimetric methods also include the use of a reagent that reacts with the compound of interest to produce a coloured substance, which is then analysed via its absorption (or transmission) spectrum. A well-known example in the case of medicines quality testing is the use of Fast Red TR (FRTR) dye, which will turn yellow when added to a solution made up from artesunate tablets (an antimalarial) *if* the correct API is present [31]. Quantitative measurements may then be made as a function of absorbance, based on a prior calibration.

Advantages include the fact that the method is simple to use without much training, is cheap, uses non-flammable, non-toxic solvents, and is field-adaptable [31,148,153]. It does however require a small amount of the tablet to be dissolved, so is a destructive method [148], and takes 10mins to carry out [154]. The reagents may also be difficult to source in certain locations [155]. Counterfeiters have also been known to specifically add other APIs or impurities to their products which contain the same functional groups that react with the FRTR dye in order to pass the test [87,153]. Although the FRTR dye test has been used successfully in the past in countries such as Laos and Ghana, in recent years, the method has become somewhat obsolete, due to the replacement of the old antimalarial therapies with ACTs [155].

1.2.2.3.3 Counterfeit Detection Device 3 (CD-3)

The CD-3 device was developed by the US FDA, and functions by imaging a sample (pill or packaging) whilst illuminating it with a selection of light-emitting diodes (LEDs) covering the UV to IR range. This is then visually compared to an image taken for an authentic sample, which may be stored in a library [155,156]. It is hand-held, battery-operated, relatively cheap (around US\$ 1000), easy to use with very little training, and can scan through blister packaging [155–158]. It is thus suitable for use in a variety of places including borders and international mail centres, as well as remote parts of the world [157].

An evaluation study found that it had a sensitivity (true positive rate, i.e. the proportion flagged as authentic out of the total number of authentic) of 100% and specificity (true negative rate) of 98.4% when tested on 203 samples of counterfeit and genuine antimalarials collected in Laos [156]. A more recent evaluation of the device, tested on 84 samples of antimalarials collected in Ghana, resulted in a sensitivity of 100% and specificity of 64% [159]. It therefore appears to have a tendency to incorrectly categorise genuine products as substandard or

counterfeit. It also suffers from user-dependent results, due to the decision-making being based on visual comparisons with a library image [159].

1.2.2.3.4 Microfluidics chip

A microfluidics chip contains small channels where liquids on the micro-litre scale are injected and mixed in a controlled manner, and then can be imaged or tested for fluorescence depending on the application [26]. Such “lab-on-a-chip” methods have been widely hailed as having the potential to be used in medical diagnostic tests in challenging settings [160]. The technology has also recently been developed into a device called PharmaCheck to test for counterfeit and substandard medicines; different “probes” for testing a few types of antibiotic and antimalarial have been made so far [161]. It is expected to be light, small (shoebox-sized), battery- or solar-powered, cheap, and easy to use [26,162].

A downside is that it requires dissolution of the sample, and the solution used needs to be made up freshly daily to avoid variations. Furthermore, the fluorescent probe used for quantitative analysis needs to be specific to the drug type being tested, so the technique is not applicable to a wide range of medicines [162].

1.2.2.3.5 Chromatography

There are numerous chromatographic methods, which separate out mixtures by passing a “mobile” phase (a gas or liquid containing the mixture of interest) through a “stationary” phase, the latter affecting the speed at which the different components in the former travel. All are destructive forms of analysis, as they require the dissolution of the medicine being tested. A review by Deconinck *et al.* covers many sub-types of chromatography for this application in more depth [163]; here we will focus on those that are most prominent in the literature.

A. High performance liquid chromatography (HPLC)

HPLC is the widely accepted “gold standard” technique for drug quality analysis, and is used for monographs in pharmacopoeias. It can be combined with UV-vis spectroscopy or mass spectrometry to further confirm the identity of substances [26]. The instrumentation requires a laboratory with trained chemists for its use, and is large, expensive, needs an electricity supply, and consumables (solvents and reagents) [23,26,153]. Analysis times are slow [21,31], and the results provide information on quantities of APIs and impurities, but not excipients [148]. Even where HPLC facilities have been set up in certain countries for the purpose of medicines quality testing, there have been reports of difficulties obtaining the necessary solvents – for example, in South America, where restrictions are placed on sales of certain chemicals to stifle the illicit drug trade [87]. A simplified and rugged HPLC setup, utilising readily-available chemicals, is

currently under development, and looks promising for use as one level below this “gold standard” [164].

B. Thin-layer chromatography (TLC)

TLC is a simple form of chromatography, normally requiring a small, microscope-slide sized glass plate coated in an adsorbent material (the stationary phase), onto which the test liquid is applied before immersing one end into the mobile phase, which travels up through the plate. The method is fairly quick, does not require as much training as for more complex chromatographic methods [21,31,148], and is good for field use in resource-poor settings, as most solvents are cheap and widely available [26]. However, the fact that consumables are required can be a downside – and they can be toxic and flammable [31]. Also, only grossly substandard or counterfeit medicines (with very low proportion of, or no API, or with the wrong API) are detected [21]. It also appears that reproducibility of results is a problem when users of different levels of expertise use this method [153]. A recent study overcame some issues with user variability by utilising a mobile phone camera positioned on a custom-made box that contained the TLC plate under a UV light source. The smartphone could then be used for analysis by image processing, thus identifying the differences between samples with different APIs [165].

1.2.2.3.6 Combined methods

A. The Global Pharma Health Fund (GPHF) Minilab

The Minilab is a portable toolkit containing all the labware, reagents, and standards for comparison required for a technician to conduct simple disintegration testing, TLC, and colorimetry on suspect medicines. It is relatively cheap, only requires access to running water for its use, and the reagents are non-hazardous and widely available. It does require some training to use, but it has proven to be very popular, with 500 Minilabs in 80 countries reportedly in use [26].

Worryingly, a WHO survey of antimalarial quality found that the Minilab disintegration test “failed to identify 85.0% of samples proven to be non-compliant with specifications”; and the TLC test also failed to identify 58.5% of such samples [154]. Similarly, a study of antimalarials collected in Afghanistan compared Minilab test results to those from a bioanalytical laboratory, and found discrepancies in disintegration tests [166]. A comparison of Minilab TLC results from substandard antibiotics compared to HPLC also concluded that there was a huge underestimation of the number of substandard drugs using TLC [167]. These studies suggested that although the Minilab has its uses in resource-poor settings, it was important to note its

limitations, as it only seemed able to detect grossly substandard medicines [154,166,167]. The Tanzanian Food and Drugs Authority, which piloted the Minilab, had raised this issue in the past [23], but others still see this as a first line of defence, and results have been quoted in various publications on drug quality [168,169]. However, a recent evaluation study found it to identify counterfeit and substandard drugs with 100% sensitivity and specificity [159].

B. Paper test cards

An alternative simple field method is the paper test card: a combination of TLC and colorimetry. These are destructive methods, requiring pills to be dissolved or crushed, but are simple to use, and very cheap. Ioset and Kaur produced a paper test for artemisinin derivatives (ARTs), an antimalarial, which could detect these with high specificity (true negative rate), as it did not react with other types of antimalarial, nor antiretroviral drugs, antibiotics, and other common drugs. However, it took 40 minutes to develop the cards, and required the use of reagents [170]. Another test card prototype for artesunate (another antimalarial) used small circular filter papers pre-treated with various reagents. As for the previous case, pills needed to be dissolved then pipetted onto the pads, but the colour change only took five minutes to develop [171].

Figure 1.7 To use a PAD: apply crushed tablet and stand card upright in water for 3 minutes [172]

The Paper Analytical Device (PAD) for antimalarials, antibiotics and tuberculosis medicines, on the other hand, does not require any other kit. Tablets are rubbed across the card directly, which is dipped into water that travels up lanes containing different reagents that create colour changes; the analysis time takes less than 10 minutes (see Figure 1.7). The resulting “colour bar codes” are then compared to a digital library of standards created with authentic medicines, and images can be uploaded via mobile phones and stored on a database with a QR code identifier (printed onto each PAD). The technique is sensitive to different excipients, however, so different brands may produce very distinct results, which need to be included in the database for comparisons. It is also important to note that this method is only useful for very poor quality medicines [172,173].

1.2.2.3.7 Capillary electrophoresis (CE)

CE requires a small amount of sample to be dissolved in a specific solvent, and its component ions are then separated by applying a voltage across a capillary containing the resulting solution. The ions move at different rates based on electrophoretic mobility, and this is detected by UV/Vis absorbance spectrophotometry within the capillary itself. A study showing the use of CE for testing the quality of an ACT demonstrated how the method is cheap, easy to use, requires only very small volumes of solutions, and that the equipment is long-lasting [163,174]. Marini *et al.* have built a portable CE module as a prototype for the quantification of API in antimalarials, which takes 20 minutes on average for analysis; the method does require a certain amount of training due to the different methods required for each drug type [175]. One such unit was installed at the National University of Rwanda in 2015 [176].

1.2.2.3.8 Ion-mobility spectrometry (IMS)

In an ion-mobility spectrometer, the analyte is introduced in the gaseous phase and is ionised before being driven by an electric field through a “drift tube”; the time taken for different ions to reach the detector is dependent on factors such as the mass, charge, size and shape of each. It is essentially a separation technique, and the spectrum provides a fingerprint of the original mixture, which can be compared to known mixtures on a database [56,177].

IMS has been extensively developed and applied to narcotics and explosives detection, but has yet to be applied to the problem of poor-quality medicines specifically [21], even though it has been suggested as a cheaper, portable, and more rapid option for pharmaceutical quality control (QC) compared to HPLC [178]. Another advantage is its low limit of detection; for example, it was found to be capable of detecting the presence or absence of API in a cancer drug when it only constituted 1.0 weight% of a tablet [177]. However, it requires a few cleaning cycles to remove all traces of the analyte after each use [179], and is a destructive method.

1.2.2.3.9 Mass spectrometry (MS)

MS also involves the ionisation of materials, but at higher energies, resulting in fragmentation. The fragments are accelerated by an electric field and deflected by a magnetic field (the amount of deflection depends on the mass and charge of the fragment) before being detected. The mass spectra of mixtures of chemicals can be very complex, so it is often coupled to a separation technique such as liquid chromatography [148]. Used in this way, MS is a highly sensitive technique, and provides information on both APIs and excipients [23,148]. It is capable of differentiating between very similar APIs, which may appear to be the same using other analytical methods; and are also sensitive to the isotope ratios of various elements present,

providing forensic information which can link poor-quality drugs back to a common manufacturing site [26,117,158,180] – as seen in Newton *et al.*'s investigation into counterfeit antimalarials in southeast Asia [121].

However, not only is this method destructive, but the equipment is large, expensive, requires running electricity, and requires extensive training to use [26,148,158]. It is also time-consuming, with limited sample throughput when using traditional methods [145,148,158]. Recent developments have made the process much more rapid (in the region of 15 to 30s) by using ambient ionization techniques such as direct analysis in real time (DART) and desorption electrospray ionisation (DESI), which do not require prior sample preparation [21,23,56,148]. DESI MS also allows spatially resolved measurements to be made [21,148].

1.2.2.3.10 FTIR, NIR, Raman spectroscopy

Spectroscopic techniques use the interaction between electromagnetic radiation of particular wavelengths and a material to provide information on the latter. Their applications to counterfeit and substandard medicines have been extensively studied. The advantages of these methods is that they do not require any consumables such as chemical solvents, and hand-held versions of the instruments that do not require mains electricity have been developed [153,158], with their compactness and portability being particularly advantageous for field use [21,148]. They also only require a very short analysis time [148,153], and relatively little training is required to make simple comparisons to a spectral database [21,23,148,158].

Nevertheless, the high capital cost of equipment is a limiting factor that has impeded wider distribution [21,148,153,181]. Moreover, the radiation used tends to have a short penetration depth, so although these methods are “non-destructive” in the sense that they do not always require crushing or dissolution of tablets, they may only interrogate their surface or coating layer [148]. A study comparing FTIR, NIR and Raman spectroscopy found that using combinations of the methods may be optimal [182]; another comparison found Raman to be superior to NIR for field work due to portability and cost [155]. Ultimately, the choice will depend on a range of factors, but comparisons to other field-based methods such as the GPHF Minilab tend to agree that the spectroscopic hand-held readers outperform the former in most respects except cost [153,181].

A. Fourier-transform infrared (FTIR) spectroscopy

This technique produces an absorption spectrum from mid-infrared radiation transmitted through the sample; peaks in absorption occur at frequencies that coincide with specific bond stretching and bending modes, providing information on the presence of certain chemical

functional groups. Commonly, an attenuated total reflectance (ATR) attachment is used so that a sample can be scanned directly, so long as it is in contact with the probe, without any further sample preparation needed – but due to the radiation's very short penetration depth, it is not possible to make measurements through blister packaging [148]. In fact, pills are often crushed or milled in order to obtain the best results [183,184].

B. Near infrared (NIR) spectroscopy

NIR spectroscopy probes the absorption spectrum of materials in the 800 - 2500nm range [23]. Absorption bands tend to be broad and hence overlap in this range, so statistical methods are applied to extract useful information [185]. Advantages of this technique are that it is very sensitive to even small differences in concentration, with reports of anything from 1 to 0.04weight% differences being detected [186,187]. The method also requires no sample preparation [148,188], as the radiation is more penetrating than mid-infrared [21] and can go through glass [185]. The hand-held NIR instrument Phazir-RX (Thermo Scientific) has been compared favourably to the Minilab for in-field measurements [181], and preliminary tests of a novel hand-held device, SCiO (Consumer Physics), have proven to be equally promising [189,190].

However, NIR radiation does not consistently penetrate packaging [21], so multiple scans are often required to be sure of the result, which counteracts the advantage of the high speed of scanning [181]. There are also reports of problems with its sensitivity to the moisture content of drugs as this changes the spectra, and the extent of the change depends on the product as well as the humidity of the conditions it was stored in [191].

C. NIR hyperspectral imaging

NIR spectroscopy combined with imaging results in a 3-dimensional data cube of spectral information for each pixel [192], which is useful for visualising the surface distribution of chemicals in a tablet [21,148]. Good contact with samples is required, so tablets need to be removed from packaging [193], and scans take a few minutes [192,194]. However, a recent study found that using longer wavelengths enabled the analysis of tablet composition at increased depths (see Figure 1.8) and was less sensitive to edges and curvature [195]. Lopes *et al.* imaged authentic and counterfeit versions of GSK products, plus pressed tablets of some pure reference materials, and found that it was possible to use a linear combination of the latter to roughly quantify the amounts of API present in each pixel of the tablets (with errors on the order of 10weight%), thus identifying the counterfeits. However, tablet coatings needed to be removed, and the flattest part of tablets needed to be scanned (avoiding curvature and

debossing) for optimal results [196]. Similar studies have been carried out on aspirin [192] and Viagra tablets also [197].

Figure 1.8 Images of Viagra (counterfeit and authentic) subject to NIR wavelengths: (a) 1000nm, (b) 1500nm, (c) 2000nm, and (d) 2500nm [195]

D. Raman spectroscopy

In Raman spectroscopy, monochromatic light (commonly 785nm) from a laser source is transmitted through the sample, and the scattered light produces a spectrum of peaks that is used to identify the material. The technique is convenient in that it can scan through blister packaging, and so does not require sample preparation [21,56,148,198], plus it is not as sensitive to environmental factors as NIR spectroscopy. The resulting spectra contain more information than NIR in terms of number and sharpness of peaks [198]. Nigeria's NAFDAC was an early adopter of the TruScan (Thermo Scientific) handheld Raman spectrometer for quick spot checks of medicines; the device can be operated by inserting a pill directly into the reader, but also comes with an attachment for scanning through blisters [108]. A recent study demonstrated that TruScan correctly identified 72/73 authentic samples, and all 11 counterfeit or substandard samples tested [159].

Yet, even though the laser light can penetrate through plastic, it still suffers from a lack of penetration depth, so there is a risk that only the tablet surface is probed [21]; in addition, the small laser spot size (0.2 - 2.5mm diameter) means that only a small area is sampled [191]. Although APIs are often strong Raman scatterers, excipients tend not to be, so poor-quality medicines with incorrect excipients may not be detected – but as the latter are more NIR-active, it has been suggested that these two techniques could be used to complement one another [199]. Similarly to NIR, Raman can be sensitive to the curvature of surfaces, so is best applied to scan a flat portion of a tablet [200]. An additional consideration is that the presence of lasers in such equipment can create more obstacles when dealing with customs officials [181].



Figure 1.9 The difference between conventional and SORS Raman spectroscopy [193]

The key issue that was repeatedly encountered with Raman spectroscopy was how background fluorescence from certain APIs masked the Raman scatter [21,148,181,201]. When the TruScan was evaluated by the United States Pharmacopeial Convention (USP), they concluded that it may not be suitable for detecting poor-quality medicines with slight variations in API content for this reason [202]. This issue could be resolved through the use of two (or more) wavelengths to probe the samples [203], but would require further development in the miniaturisation of lasers in order to incorporate these into portable readers [21].

An alternative is to use spatially offset Raman spectroscopy (SORS), as depicted in Figure 1.9. In this geometry, the Raman scatter is collected away from any interfering signals from fluorescence from the tablet or packaging (at the point where the beam is incident) [200]. It is therefore possible to subtract the background spectrum from the packaging – although spectra can suffer from distortions when using certain offsets [193]. SORS technology has been extensively developed at the Science and Technology Facilities Council's (STFC) Rutherford Appleton Laboratory (RAL), and a commercial hand-held reader is now available [204].

1.2.2.3.11 Nuclear magnetic resonance (NMR) spectroscopy

NMR spectroscopy analyses how certain nuclei (hydrogen-1 and carbon-13 are commonly studied in organic compounds) interact with radio frequency radiation whilst subjected to a variable magnetic field. The sample is usually dissolved in a deuterated solvent within a thin glass tube. The technique provides detailed chemical information without the need for a standard for comparison [21,26,148]. Although it has traditionally been overlooked for quality control purposes, pharmaceutical companies are starting to use this method more often [205].

Nevertheless, the equipment is bulky, expensive, and needs laboratory conditions (stable temperatures, running electricity) and a highly trained technician to operate; and analyses are time-consuming [26,148]. It is also inherently insensitive to chemicals present in low

concentrations [206]. Because all compounds in a mixture (including APIs, excipients, and any impurities) that contain the nucleus being interrogated will contribute to the spectrum, this can be difficult to interpret, so a separation technique may need to be applied first. However, newer NMR techniques that are able to separate the signals from different components are being more widely implemented [56,148,205]. Other advances include the development of low-field, cryogen-free, benchtop NMR instrumentation that has been used to test “lifestyle” medicines purchased online, detecting those that were adulterated [206].

1.2.2.3.12 Nuclear Quadrupole Resonance (NQR)

NQR is related to NMR, and uses radio frequency radiation to obtain qualitative and quantitative information on chemical mixtures such as medicines – without the need for consumables nor involving any sample preparation [158,207]. As it does not require an external magnetic field, the instrumentation is far more compact than that for NMR, and can be made at a cost of less than US\$ 250 [208]. The European CONPHIRMER consortium utilised this technology to develop a portable device for medicines quality testing in a truly non-destructive fashion – i.e. without the removal of packaging [209]. It was tested on counterfeit antimalarials, showing that quantitative analysis was possible based on the difference in the signal compared to that of a genuine sample; the result was supported by HPLC analysis [210]. It was also found to be sensitive to the slight differences between the same product made by different manufacturers [210]. It can be used to analyse a whole packet, or multiple packets, of a medicine at the same time [211].

Although the method relies on nuclear quadrupole resonance from nuclei with spin quantum number $I > 1$ [207], this is not an issue for the best part of APIs found in medicines, as roughly 50% of elemental isotopes fulfil this criterion [211] (aspirin being a notable exception that is “NQR-silent” [208]). As with many other methods, spectra from genuine products are required for comparison and authentication [208,211]. Downsides of this technique are the relatively long acquisition times [158], and the risk of noise from surrounding sources of interference [207].

1.2.2.3.13 X-ray diffraction (XRD)

XRD is frequently overlooked for this application, as it is traditionally considered as being too complex, with large instruments that are not useful for fieldwork [145]. It is however the focus of this thesis; thus, the method is discussed in greater depth in the following section.

1.3 X-ray Diffraction

1.3.1 Background

Figure 1.10 Two types of crystallographic plane within the same crystal lattice (adapted from [212])

Crystalline materials are composed of ordered arrays of atoms or molecules, which can be thought of as a “unit cell” of a fixed arrangement of atoms or molecules that is repeated in all three dimensions. As Figure 1.10 illustrates, different crystallographic planes are formed by this regular arrangement of atoms or molecules. Each set of parallel planes has a fixed inter-planar distance (d) between them, and different types of plane have different values of d .

If X-rays of the same energy scatter coherently (Rayleigh scatter) from atoms or molecules in adjacent crystallographic planes, they can interfere constructively or destructively depending on their phase relationship, as shown in Figure 1.11. It can be predicted that constructive interference will occur whenever the angle between the plane and incident or scattered X-ray (θ) and the inter-planar distance (d) is such that this results in the second X-ray travelling an integer number of wavelengths ($n\lambda$) further than the first X-ray, such that they remain in phase. This relationship, termed Bragg’s Law, can be calculated using trigonometry resulting in the following equation:

$$n\lambda = 2d \sin\theta \quad (1)$$

The phenomenon of constructive interference of coherently scattered X-rays of a particular energy, at specific angles, is called *X-ray diffraction (XRD)*. The resulting pattern of peaks in intensity is unique to each material (except in very rare cases [213]), and so can be taken to be a “fingerprint”. Bragg’s Law is applied to extract d values for each type of crystallographic plane present in a material, which can in turn be used to elucidate further information about the structure. Thus, XRD is an analytical tool for structural characterisation of materials. It does not provide a direct measure of a material’s chemical composition [214]; however, the information generated by XRD can be used to identify the material, and hence, its chemical composition.

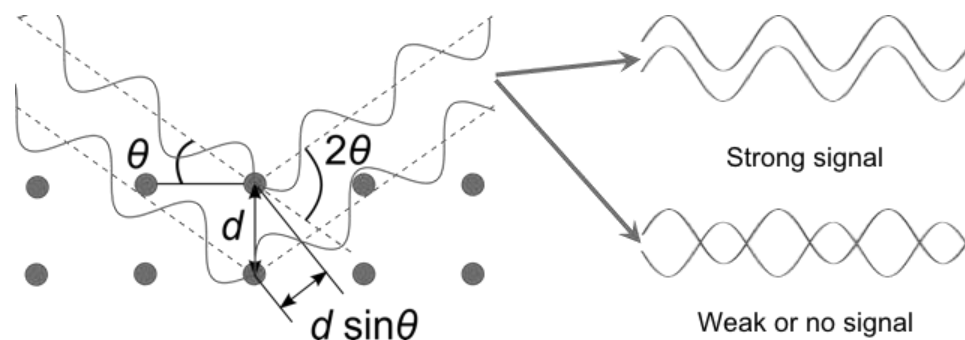


Figure 1.11 Scattered X-rays showing constructive and destructive interference

A lot of materials we call powders are in fact polycrystalline. It is assumed that, statistically, all possible orientations of crystals are represented equally in a powder, and therefore all crystallographic planes are “visible” to an incident X-ray beam. Consequently, cones of diffraction at the scattering angles corresponding to each type of plane are formed as shown in Figure 1.12. However, some crystals have shapes (e.g. needle-like, or plate-like [215]) that result in a tendency for them to align in a particular orientation, and this can be exacerbated if they are pressed into sample plates during the sample preparation process [212,216] or compacted into tablets [217]. This causes some crystal planes to be over-represented whilst others are under-represented in the observed diffraction pattern, and is termed the *preferred orientation effect*. This artefact is known to hamper efforts to identify or quantify materials by XRD [218–220], so methods of reducing its influence are often introduced into experimental setups – as described in the sections below.

Figure 1.12 Cones of diffraction from two types of crystallographic plane exposed by crystallites in a powder sample [221]

It is worth mentioning that even in powders of amorphous solids, i.e. those which lack long-range order, there exists some short-range order due to the preference for molecules to pack in a certain way, making some interatomic distances more common than others. This normally results in one or two broad diffraction peaks [218]. Interest in XRD of amorphous materials has grown in recent years – since 2010, the International Centre for Diffraction Data (ICDD) has

been producing reference patterns of amorphous organic materials, including pharmaceutical excipients [222]. Amorphous APIs also exist, but are not commonly used due to problems with their lower stability and tendency to convert into their most stable crystalline form [223,224].

There are two methods by which Bragg's Law (equation (1)) is interpreted for use in XRD experiments: angular-dispersive XRD (ADXRD) and energy-dispersive XRD (EDXRD).

1.3.1.1 Angular-dispersive XRD

In ADXRD, monochromatic X-rays – usually copper (Cu) K_{α} (8.04keV) from a filtered Cu X-ray source – are directed at the sample, and diffracted X-rays are detected for a range of 2θ angles. In this way, whenever the detector intersects a cone of diffraction such as those illustrated in Figure 1.12, a peak in intensity is observed. Organic materials such as the APIs of pharmaceutical medicines tend to have larger d -spacings than inorganic materials, meaning their diffraction peaks are concentrated at low 2θ when these relatively low-energy X-rays are used.

Figure 1.13 Diagram of a typical reflection ADXRD setup [225]

Figure 1.13 shows an example of ADXRD in reflection (Bragg-Brentano) geometry – the most common setup used [226]. Here, the flat-plate sample holder and detector are tilted to cover a range of θ and 2θ , respectively. Samples are also spun during data acquisition to reduce the effects of preferred orientation. Transmission (Debye-Scherrer) geometry may also be used, where samples can be placed inside capillary tubes for analysis. This is beneficial when the sample size is limited, or if it is air-sensitive as the capillary can be sealed. Another advantage is that preferred orientation effects may be reduced in this geometry [227].

ADXRD provides high-resolution XRD spectra, and the ICDD states that the technique can be expected to identify mixture components down to 5weight% [222], although another source indicated a <1weight% detection limit was possible if problems associated with sample preparation, such as preferred orientation, were overcome [228].

Figure 1.14 Diagram of an EDXRD setup (adapted from [229])

In EDXRD, the scattering angle 2θ is fixed, and a range of X-ray energies (e.g. the continuous spectrum from an X-ray tube) is used. An example of a typical setup is shown in Figure 1.14. An energy-resolving detector is used to collect data on both the intensity and energies of the diffracted X-rays, resulting in an EDXRD spectrum. Commonly, the energy axis is converted into a unit called *momentum transfer* (x), which incorporates information on both the angle and energy, making it non-system-dependent. This is useful for making comparisons between EDXRD systems set up at different fixed angles, and for comparisons between ADXRD and EDXRD. For the purposes of this calculation, the Bragg equation is rearranged as follows:

$$\left(\frac{1}{2d}\right) x = \frac{1}{\lambda} \sin \theta \quad (2)$$

$$\therefore x = \frac{E}{hc} \sin \theta \quad (3)$$

To calculate x in nm^{-1} using E in keV, this equation is simplified to:

$$x = E \times 0.805 \times \sin \theta \quad (4)$$

where 0.805 is a constant incorporating $\frac{1}{hc}$, the conversion of units of energy (E) from J to keV, and of momentum transfer (x) from m^{-1} to nm^{-1} . Thus, for a fixed angle, larger d -spacings (i.e. smaller x) in pharmaceutical compounds will result in peaks at relatively lower energies. This can be taken into account in system design by choosing a low angle such that the diffraction peaks of interest fall at higher energies, so long as these are within the range of the X-ray energies provided by the X-ray source spectrum.

The quality of EDXRD spectra is limited by the energy resolution $\left(\frac{\Delta E}{E}\right)$ of the detector, although this may be overshadowed by the loss of angular resolution $\left(\frac{\Delta \theta}{\theta}\right)$ due to the range of angles accepted through the scatter collimator (rather than specifically at the nominal angle). The latter is a result of a compromise made in order to detect sufficient diffracted X-rays in an acceptable time scale, but results in significantly broader, overlapping peaks compared to ADXRD.

1.3.1.3 Other X-ray interactions

X-rays at the energies of interest can also interact with matter by photoelectric absorption or incoherent (Compton) scatter. The former occurs when an incident X-ray photon transfers all of its energy to an electron, which is subsequently ejected. The latter occurs when an X-ray interacts with a loosely-bound electron, imparting some of its energy as well as changing its direction of travel, thus contributing to background scatter. This is in contrast to coherent scattering discussed above, which result when an X-ray interacts with a tightly-bound electron, with no transfer of energy, but a change in its direction of travel.

Together, photoelectric absorption and scatter cause the *attenuation* of X-rays. This attenuation effect is energy-dependent, and relates to the mass attenuation coefficients (μ/ρ) of the chemicals that make up the attenuating material. This information is available online in databases run by the National Institute of Standards and Technology (NIST) [230,231]. The mass attenuation coefficient is multiplied by the density of the material (ρ) to find the linear attenuation coefficient (μ). This in turn is used to calculate the proportion of transmitted X-rays (I/I_0) after passing through thickness x of the material, using the Beer-Lambert equation:

$$I/I_0 = \exp(-\mu(E)x) \quad (5)$$

1.3.2 Applications of ADXRD

1.3.2.1 Materials identification

ADXRD is widely used by chemists and material scientists for the characterisation of novel compounds, or for identification purposes – for example, to confirm that the product of a reaction is as expected. Powder ADXRD is also the gold-standard technique within the pharmaceutical industry for investigating polymorphism – the different crystal structures formed when molecules of a certain chemical are arranged in different ways – an example of which is given in Figure 1.15. It is well-established that the formation of particular polymorphs can be influenced by manufacturing processes [198,213,232], and their differing properties (such as dissolution rate) mean that identification is crucial for quality assurance, as well as for IP reasons [226,233,234]. Aside from pharmaceutical compounds, other organic materials have been analysed with ADXRD – for example, tissue samples (to discriminate between healthy tissue and tumours) [235], and illicit drugs with cutting agents [236].

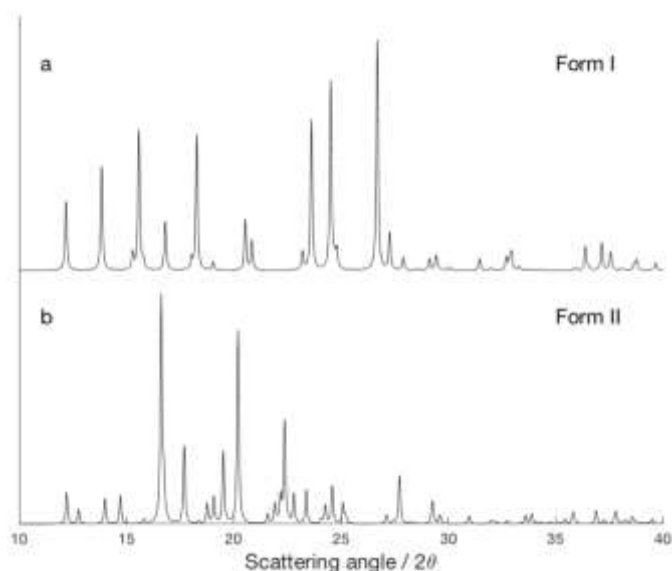


Figure 1.15 Arrangement of paracetamol molecules in polymorphs (a) form I and (b) form II [237]; their respective ADXRD profiles (generated using Mercury v.3.9 [238] and CSD-HXACAN18 & COTZAN [239])

Despite strong evidence to demonstrate that ADXRD is a reliable means of identifying different materials, few researchers have applied it hitherto to the detection of poor-quality medicines. It was cited in a review of analytical methods used for detecting counterfeit medicines, where the authors commented that ADXRD has the advantages of requiring minimal sample preparation (compared to methods such as chromatography), and providing information on excipients as well as APIs – but incorrectly stated that it could only be used to identify a few APIs [148]. Moreover, in one study, ADXRD was applied to the study of excipient composition for a forensic investigation into the source of counterfeit antimalarials, finding that this differed substantially between counterfeits and the authentic medicine [121].

Dégardin *et al.* reported in 2013 that “further fast analytical tools have been recently investigated for counterfeit detection and may offer new avenues, like X-ray powder diffraction” [17]. In the research communication that they referred to, ADXRD in reflection geometry was used on whole Viagra tablets – genuine samples from Pfizer, and counterfeit samples seized by police and customs authorities. It was found that the diffraction patterns could be reliably discriminated visually to identify counterfeit samples, as shown in Figure 1.16 [240]. However, due to the relatively low X-ray energies used in ADXRD, the tablets were removed from their packaging to avoid attenuation effects during this experiment. Furthermore, differences in spectra were observed when the tablet coatings were removed, as the X-rays could only probe the surface of samples. This raises the possibility that poor-quality medicines with the correct coating could still pass ADXRD inspection, highlighting a drawback of this technique.

Figure 1.16 (L) Viagra tablets – only top left tablet is genuine; (R) Diffraction pattern for counterfeit tablet b (in blue) compared to the genuine Viagra pattern (in grey) [240]

A disadvantage of traditional ADXRD equipment is its large size, due to its moving parts. A possible solution is to use a large-area pixellated detector that collects diffraction intensities at a range of angles whilst remaining in a fixed position. One such example of this is found in the portable, battery-operated ADXRD instrument, *Terra* – the commercial adaptation of the *CheMin* instrument which was launched to Mars on board the Curiosity rover in 2011 [241]. Figure 1.17 shows the setup used in *CheMin*, and *Terra* is presumably similar in design. Diffraction patterns are collected on an area summed circumferentially at incremental radii (from the central through-beam) to produce a plot of intensity vs scattering angle. A novel sample holder was designed to shake the sample powder during analysis such that random orientations of crystallites are exposed to the beam [242]. This instrument is, however, limited to the study of samples prepared by being ground up before being placed into the thin sample holder [243]. Nevertheless, it has been reported as being used for in-field studies of counterfeit pharmaceuticals [158,244]. As far as the author is aware, the results in the public domain are limited to a conference presentation [245] that demonstrated how diffraction patterns were significantly different in grossly counterfeit versions of Viagra and antimalarials, as well as the application to successfully identifying excipients within both authentic and counterfeit drugs.

Figure 1.17 Geometry of the *CheMin* instrument; 24.0mm x 23.3mm active area of detector [243]

1.3.2.2 *Materials quantitation*

Traditionally, ADXRD has been used for basic quantitation of a material within a mixture by comparing the area of a diffraction peak to its reference intensity ratio (RIR) from a database (as seen in the *CheMin* presentation [245]), by incorporating an internal standard. The method is thus unsuitable for non-destructive analysis, as it requires sample preparation [215,246].

Another option is to create a calibration line between peak(s) in mixtures of known concentrations, and use this to quantify the amount of a substance in an unknown mixture by regressing its peak area(s) [247].

However, these methods become more challenging in complex mixtures where many peaks overlap, are broader, or where multiple constituents need to be quantified [198,233,246,248]. In these cases, whole-pattern fitting methods are favoured, as they are less likely to be influenced by errors introduced during the sample preparation process (including preferred orientation effects). This approach improves the accuracy since it takes account of changes across the full spectral range rather than a selected peak or two [198,215]. Rietveld refinement is a widely-used whole-pattern fitting method for quantitative analysis [227], but requires databases of crystal structures to use, and is limited to crystalline materials [246].

Thus, the application of multivariate statistical methods to spectra (which contain hundreds, or even thousands, of variables; hence “multivariate”) – a field dubbed *chemometrics* – is of growing interest in the pharmaceutical sector. The use of chemometrics can permit faster, cheaper, and potentially non-destructive analyses to quantify sample properties that would otherwise require time-consuming, expensive or destructive testing (Figure 1.18). Chemometric methods for calibration and quantitation from ADXRD data have been shown to give superior results when compared to the univariate method (using selected peak heights or areas) [248–251]. These methods also extend beyond quantitative analysis and can be used for pattern recognition and classification of spectral datasets. The chemometric methods that were employed in this thesis are described in more detail in Chapter 2.

Spectroscopic techniques (Raman, NIR, FTIR) combined with chemometrics have been widely reported for the analysis of poor-quality medicines (e.g. [188,191,252,253]). A recent review with a specific focus on chemometrics applied to the identification of counterfeit medicines covered a range of chromatographic methods, spectroscopic methods, and NMR [254]. Remarkably, the literature on chemometrics applied to ADXRD spectra of pharmaceutical mixtures [214,215,233,246,249,251,255–258] (discussed further in Chapter 3) makes no mention of the poor-quality medicines problem. In addition, it was noted in a “round robin” of quantitative

analysis methods (by the International Union of Crystallography's Commission on Powder Diffraction) that the XRD community was reluctant to study pharmaceutical compounds in general [227].

Figure 1.18 Why chemometric methods are used in chemical analysis [259]

1.3.3 Applications of EDXRD

EDXRD can be applied to material characterisation studies in the same way as ADXRD, but in addition is the preferred method for probing materials subjected to high pressures (in diamond anvil cells), and in-situ mechanistic studies [260]. The latter two usually require synchrotron X-ray sources, rather than laboratory-based X-ray sources, due to the far superior X-ray flux that significantly reduces data acquisition times and allows for stricter collimation and hence better resolution spectra [261]. As with ADXRD, most research in this area is focused on inorganic materials analysis, but there are a few studies describing EDXRD to study and identify, quantify or classify organic materials such as biological tissues [262–264], explosives [265], illicit drugs [266,267], and even sugar [268].

The advantages of EDXRD over ADXRD are that the absence of moving parts allows for more compact instrumentation designs, that data collection is more rapid, and that the higher-energy X-rays used in EDXRD will penetrate further into samples [269–271]. The latter point allows for the non-destructive analysis of relatively thick samples as well as analysis through packaging. Notably, X-rays can probe through thin foil (such as those used in blister packaging), unlike the other through-package methods of NQR and Raman spectroscopy described above – an aspect that is discussed further in subsequent chapters of this thesis.

EDXRD has reportedly been applied to the non-destructive authentication of pharmaceuticals via the dedicated XT250 system designed by XStream Systems [272]. This utilises an air-cooled X-ray source (operated at 10 - 80kV, with corresponding currents of 4.0 - 0.5mA) and a

cadmium telluride (CdTe) detector. Its confocal design with circular-slit collimators allows control over the position that is interrogated within a sample (Figure 1.19A). The system then compares EDXRD fingerprints of unknown samples against a database of known drugs, using an on-board “material recognition software engine”. The authors state that samples take <5min to authenticate – “often in as little as 30s” – and with accuracies >98% [272]. However, no further journal publications other than the cited article published in 2009 could be found.

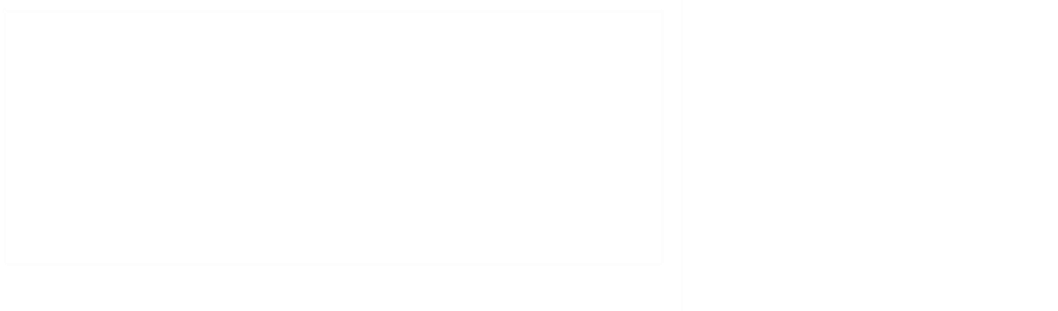


Figure 1.19 (A) XT250 system geometry, where $2\theta = 2.562^\circ$ [272]; and (B) geometry of portable EDXRD system by Cuevas *et al.*, with (1) X-ray tube, (2) detector, (3) sample, (4 & 5) collimators, and (6) laser pointer shown [270]

More recently, a compact EDXRD system was developed and described in an article by Cuevas *et al.* [270]. This was designed specifically for use in cultural heritage applications; thus, the system was constructed in reflection geometry, to allow single-sided interrogation of archaeological artefacts (Figure 1.19B). A small Moxtek X-ray source (operated at 10 - 50kV and 0.2mA) and a silicon drift detector were employed for this purpose; in addition, motorised stages, a range of collimator sizes, and a laser pointer were used to adjust the measurement position and even allow for ADXRD data to be collected [270]. Note that the EDXRD measurements reported here were taken at relatively large scattering angles (15 - 20°) due to the small *d*-spacings in the inorganic materials that were examined.

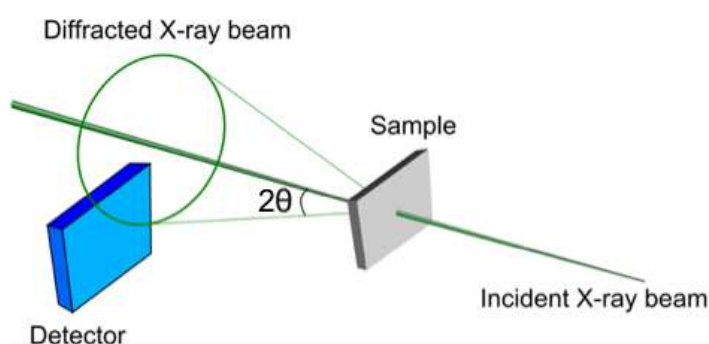


Figure 1.20 Illustration of how a cone of diffraction (at a particular X-ray energy) from the sample impinges upon the HEXITEC detector. © SISSA Medialab Srl. Reproduced by permission of IOP Publishing. All rights reserved [273]

Another method of combining aspects of ADXRD and EDXRD has been demonstrated by the use of a pixelated, energy-resolving detector – HEXITEC [274] – developed by the STFC and tested by the Radiation Physics group at UCL. This was positioned such that it intersected cones of diffraction from a sample, as shown in Figure 1.20; by knowing the diffraction angles at each pixel of the detector, the energy spectra for all 6400 pixels could be converted into momentum transfer space and summed. The setup, dubbed “*PixD*” (pixelated diffraction), was found to produce spectra that contained sufficient information to classify drugs and explosive materials after acquisition times on the order of seconds, using chemometric methods [273]. The footprint of this system was further reduced by replacing the large laboratory X-ray source with a compact, air-cooled Amptek Mini-X [275]. A related system – named “*miniPixD*” – has more recently been developed, combining the *PixD* concept with X-ray imaging capabilities to provide image-guided X-ray diffraction (IGXRD). Here, contents of a sample of interest can be imaged before selecting a position to take a diffraction measurement [276]. This instrument has already been successfully applied to the identification of different tissue types in excised breast tissue samples [277]. Both *PixD* and *miniPixD* have been shown to produce good quality XRD spectra in preliminary measurements on pharmaceuticals within their blister packaging [275,276]. Hence, this potential application was explored further in this thesis.

1.4 Scope of this PhD thesis

The aim of this project was to evaluate the effectiveness of XRD for the non-destructive, through-packaging identification of counterfeit and substandard medicines. The EDXRD and *miniPixD* instrumentation and chemometric methods that were used are described in the following chapter of this thesis – and as far as the author is aware, the experiments that follow are the first studies to combine the two for pharmaceutical analysis.

Chapter 3 presents an experiment in which a series of ternary mixtures pressed into tablets were used to test the suitability of EDXRD spectra for calibration and quantitative analysis.

In Chapter 4, EDXRD analyses of solid pharmaceutical dosage forms – “the most common form of counterfeit or diverted products” according to the FDA [60] – were performed, both with and without packaging. A chemometric method was applied to test its ability to sort the spectra, collected at a range of acquisition times, into known API classes.

Chapter 5 describes how XRD data acquisition times were reduced by studying the samples using the *miniPixD*, thereby demonstrating the potential of this compact instrument for practical application.

This last point is an important consideration for all anti-counterfeiting technologies. Portable, user-friendly devices would clearly be of great use for both drug regulators and medical practitioners, particularly in remote areas in the developing world, where the infrastructure to build laboratories for pharmaceutical quality analysis does not exist. The need for modern “state of the art” technologies in the field, instead of simple testing kits such as the Minilab, was recently highlighted by reports that the latter suffer from problems with reproducibility and biased, user-dependent results [153].

Chapter 2: Equipment and Methods

2.1 EDXRD system

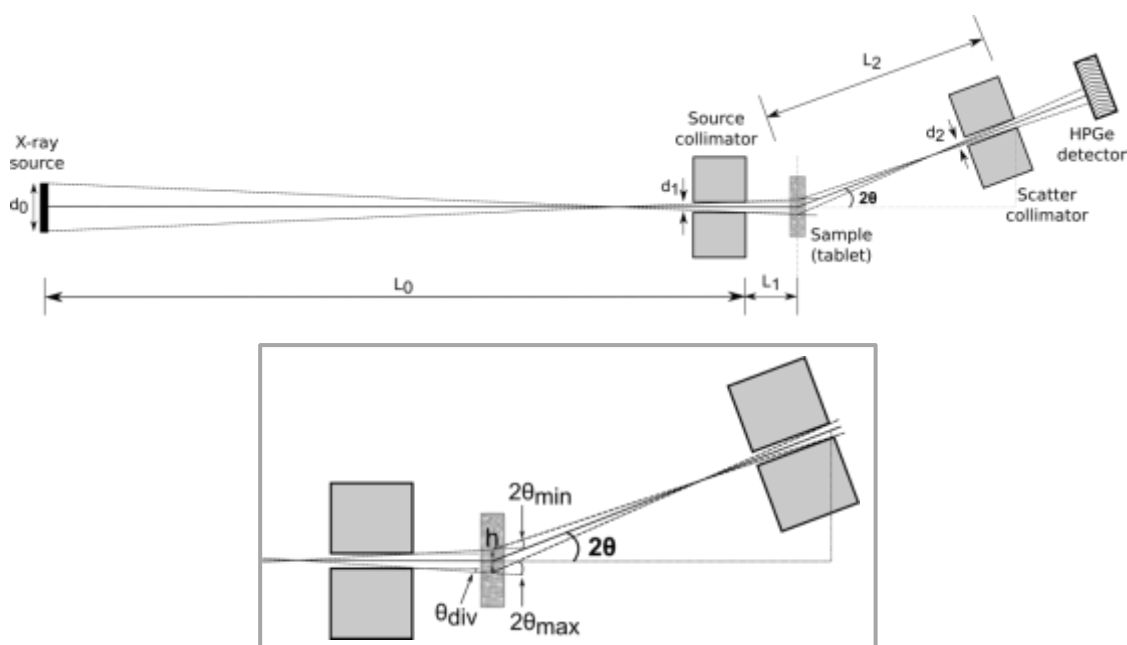


Figure 2.1 Schematic of EDXRD system viewed from above, with zoomed detail of angles

Figure 2.1 shows the experimental setup used in the first two EDXRD studies (Chapters 3 and 4). The X-ray source was a water-cooled X-ray tube (MXR-160, Comet) with a tungsten target (with 3mm-diameter focal spot (d_0)) and beryllium window, operated by an AGO Installations system (MG/01/160/320, Philips). The X-ray tube was covered by a lead-lined casing with a 5mm-diameter exit window. Two 2cm-thick brass pinhole collimators were positioned before and after the sample, with the source collimator being 1.1mm (d_1) in diameter, and the scatter collimator 1.0mm (d_2). The sample stage was affixed to a set of horizontal and vertical motorised linear stages (M-IMS300PP, Newport) such that the sample could be moved in the plane perpendicular to the beam direction from outside the laboratory.

A high-purity germanium (HPGe) detector (GLP-36360/13-P, EG&G Ortec) held at 77K (using an Ortec X-COOLER-II controlled by a CryoSecure unit), was linked to an Ortec DSPEC jr 2.0 unit, which contained the high voltage control (set to a 1kV bias voltage), amplifier, and multi-

channel analyser (MCA)* used to assign each detected photon's energy to one of 512 channels. Maestro-32 software (v.6.06, Ortec) was used to control the data acquisition parameters. The detector was calibrated using the 14.0, 17.7, and 59.6keV characteristic peaks in a spectrum collected from an americium-241 radioactive source – shown in Figure 2.2. Its energy resolution was calculated to be 0.54keV at 59.6keV (using the FWHM), i.e. $\frac{\Delta E}{E} = 0.9\%$.

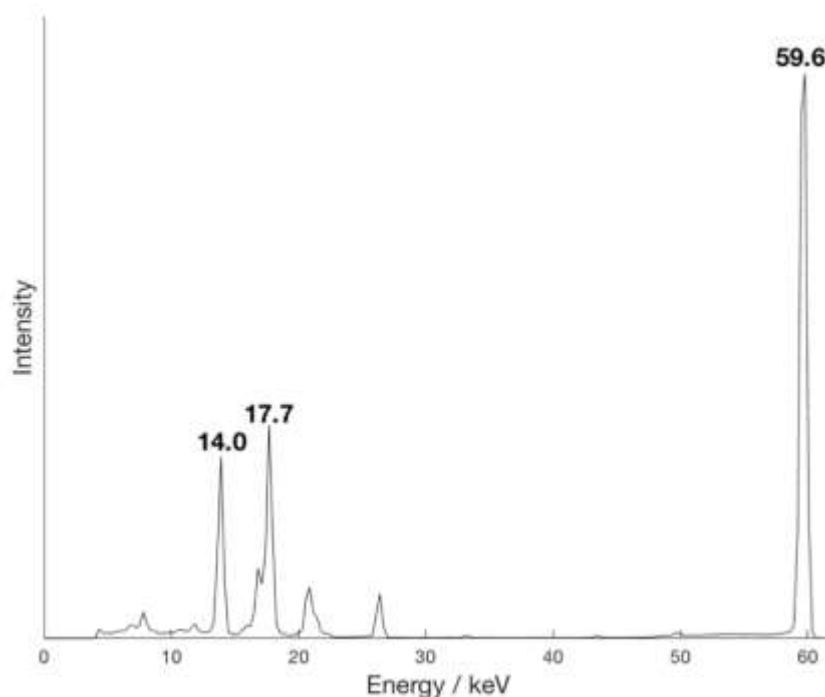


Figure 2.2 Am-241 spectrum; x-axis energies are result of calibration using labelled peaks

2.1.1 Setup A

For the experiments described in Chapter 3 – where unpackaged and “packaged” tablets of known compositions were studied – the EDXRD system was set up such that distance L_0 was 220mm, and samples were positioned such that they were centred at 17mm (L_1) from the source collimator and 57mm (L_2) from the scatter collimator.

The sample position was controlled by a Newport XPS-Q8 controller linked to a computer via an Ethernet cable, using the Newport GUI accessed via a web browser to make simple movements to specified positions. After initial tests, certain samples were step-scanned in 30 positions repeatedly, according to the schematic shown in Figure 2.3. These scanning positions were chosen such that the incident X-rays avoided the edges of sample 1 (pure caffeine), identified by finding stage positions at which the diffraction intensity was significantly reduced.

* MCA: analyses a series of voltage pulses, and sorts them into a histogram or “spectrum” of number of events versus pulse-height which relates to energy.

For the packaged sample scans, pieces of card, foil and plastic taken from Sainsbury's paracetamol packaging were cut to size and fashioned into a sample holder such that the tablets would have foil and card on one side, and plastic and card on the other as shown in Figure 2.4.

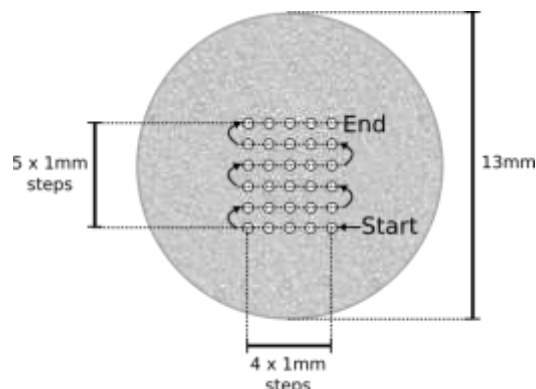


Figure 2.3 Step-scanning positions used in Setup A

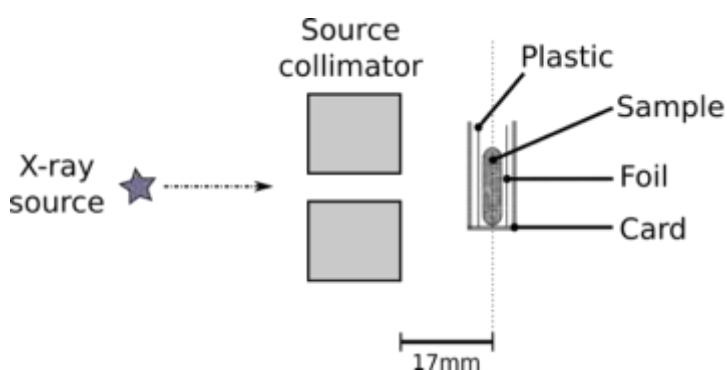


Figure 2.4 Side view of "packaged" sample holder setup

The nominal scattering angle (2θ in Figure 2.1) for Setup A was found to be 6.3° , as determined by comparing the spectrum collected from a caffeine sample on the system to a caffeine reference spectrum. The range of diffraction angles accepted by the scatter collimator was calculated using trigonometry:

$$2\theta_{min} = \tan^{-1} \left[\frac{L_2 \sin 2\theta - \frac{d_2}{2} \cos 2\theta - \frac{h}{2}}{L_2 \cos 2\theta + \frac{d_2}{2} \sin 2\theta} \right] - \theta_{div} \quad (6)$$

$$2\theta_{max} = \tan^{-1} \left[\frac{L_2 \sin 2\theta + \frac{d_2}{2} \cos 2\theta + \frac{h}{2}}{L_2 \cos 2\theta - \frac{d_2}{2} \sin 2\theta} \right] + \theta_{div} \quad (7)$$

where θ_{div} , the divergence angle, was calculated from:

$$\theta_{div} = \tan^{-1} \left[\frac{\frac{d_0}{2} + \frac{d_1}{2}}{L_0} \right] \quad (8)$$

and h , the beam width at the sample, was:

$$h = d_1 + 2L_1 \tan \theta_{div} \quad (9)$$

h was found to be 1.4mm, and the $2\theta_{\max} - 2\theta_{\min}$ acceptance angle range came to 3.5° , or an angular resolution ($\frac{\Delta 2\theta}{2\theta}$) of 55%. This was relatively large, but the diffracted X-rays were not equally likely to be collected from all scatter angles in this range in reality, due to a Gaussian-like distribution of angular acceptance weighted heavily in the centre, as described by Luggar *et al.* [278]. Indeed, by finding the FWHM of sample 1's caffeine diffraction peak at 15.1keV (0.67nm^{-1}), the angular resolution was calculated to be 22%. This was over 24 times greater than the calculated detector energy resolution, highlighting how the angular resolution is the limiting factor of this EDXRD setup when it comes to elucidating diffraction peaks.

The X-ray source was operated at a peak voltage of 60kV. The tube spectrum at this energy was measured directly using a $50\mu\text{m}$ pinhole collimator and the HPGc detector, with the lowest possible X-ray tube current setting (approx. 0.2mA on the analogue dial), and is shown in Figure 2.5. This spectrum translated to momentum transfer values of 0.17 to 2.6nm^{-1} , suitably covering the region where diffraction peaks of organic chemicals of interest tend to fall. Note that the tube spectrum also included the characteristic L-lines from the tungsten anode at 8.37, 9.82, and 11.3keV. During data acquisition, the current was kept at a moderate level of 2mA to avoid deterioration of the X-ray tube filament.

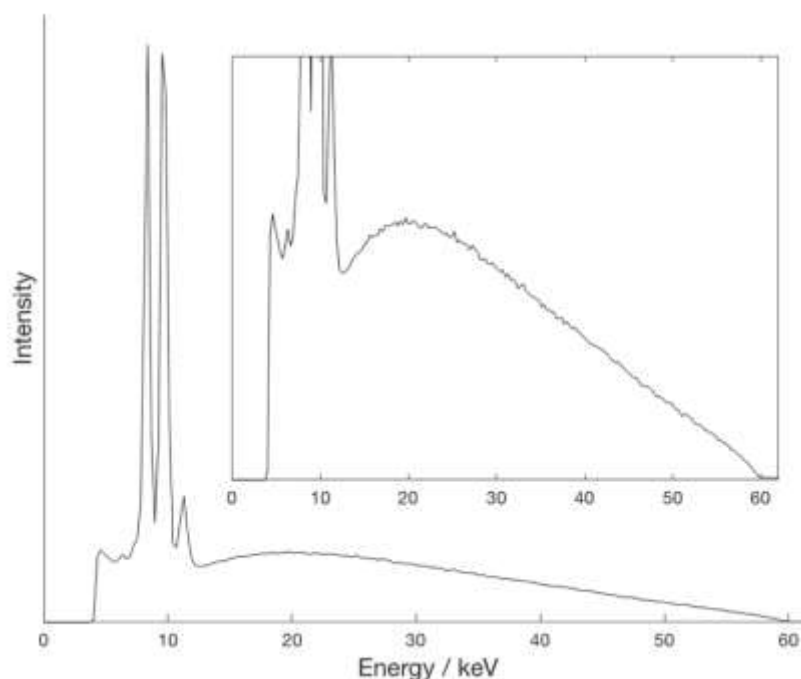


Figure 2.5 Measured X-ray tube spectrum at 60kV; zoomed portion highlighting shape of spectrum at energies above tungsten characteristic peaks

2.1.2 Setup B

2.1.2.1 EDXRD system assembly

The EDXRD setup was dismantled then reassembled to create “Setup B” (for Chapter 4 experiments) using the following procedure. Initially, the exit window on the X-ray tube casing was adjusted such that the X-ray beam was directed parallel to the surface of the optical bench, as well as being parallel to the edge of the bench. This was determined by using a flat panel detector (PaxScan, Varian Medical Systems Inc.) to image the beam at increasing distances from the source. Fine metal wires were affixed onto the panel in a crosshair to mark the correct position at which the beam should fall.

Following this, the source collimator (without pinhole insert) – mounted on a rotation stage attached to a set of vertical and horizontal translation stages – was positioned such that L_0 was maintained at 220mm. The stage positions were adjusted manually whilst imaging the X-ray beam until this was centred correctly. The pinhole insert was then replaced, and rotated slightly until the through-beam was once again circular and centred correctly. This process was repeated after the addition of the scatter collimator (also affixed to rotation and translation stages), which was initially positioned in line with the source collimator.

After alignment, a caffeine sample (sample 1 from Chapter 3) was positioned such that it was centred at 20mm (L_1) from the source collimator. The scatter collimator was rotated to roughly 6° and translated perpendicular to the X-ray beam (and parallel to the bench surface) until the laser spot from a laser beam pointed back through the pinhole was visible on the caffeine sample surface. The HPGe detector was then positioned to detect any diffracted X-rays from the sample, and spectra were acquired for 120s (with the tube operated at 60kV, 2mA) with the scatter collimator translated along a series of positions in 0.2mm steps. The position yielding the maximum summed total counts of diffracted X-rays was identified; L_2 was 100mm and the nominal scattering angle (2θ) was found to be 5.9° using the same method as above.

The slight reduction in scattering angle meant that diffraction peaks were shifted to a higher energy (but would not change in terms of momentum transfer), such that lower energy diffraction peaks were less likely to be affected by attenuation. This change also shifted the characteristic L-lines from tungsten to lower momentum transfer values (as their energies are not angle-dependent) which made them less likely to overlap with diffraction peaks. However, in doing so, a previously masked background peak – a lead L_β line, from the lead shielding surrounding the system – appeared at 12.6keV.

The modifications to distances L_1 and L_2 in this new setup improved the angular resolution of the system from 55% to 42%. The downside to this was the reduction in count rate as a result of the scatter collimator, and hence HPGe detector, being further from the sample. Therefore, the tube voltage used was increased to 80kV (still at 2mA) to boost the count rate, resulting in the inclusion of characteristic K-lines from tungsten at 58.0, 59.3 and 67.2keV in the X-ray tube spectrum – high enough energies as to not interfere with diffraction peaks.

In addition to the above changes, the controller for the Newport stages was changed from a XPS-Q8 to a ESP301 system (with USB link) during the course of this experiment. Raster scan trajectories (as opposed to step-scanning) were scripted in LabVIEW (v.12.0, National Instruments) for the former, and in Matlab (R2014b, MathWorks) for the latter. Data collection for all the different acquisition times was automated by utilising the scripted “.job” file feature in Maestro (v.6.06, Ortec).

2.1.2.2 *Sample scanning*

In order to find the best coordinates for raster scanning, a Nurofen Migraine Pain caplet was first “imaged” by summing all counts from 10-second acquisitions at various stage positions (Figure 2.6). The raster scan positions were chosen such that the X-ray beam would cover the most uniform, central part of the pill face. This sample was chosen as it was one of the smaller caplets, and this scanning region would therefore fit in all other caplets. This same procedure was used to map out a trajectory for tablets, using Pro Plus (the smallest tablets used). The stages were moved to a central “start” position (2mm higher in tablets than caplets, due to their circular shape) and a series of movements were made relative to this according to the trajectories shown in Figure 2.7. This raster scan was repeated throughout all acquisitions.

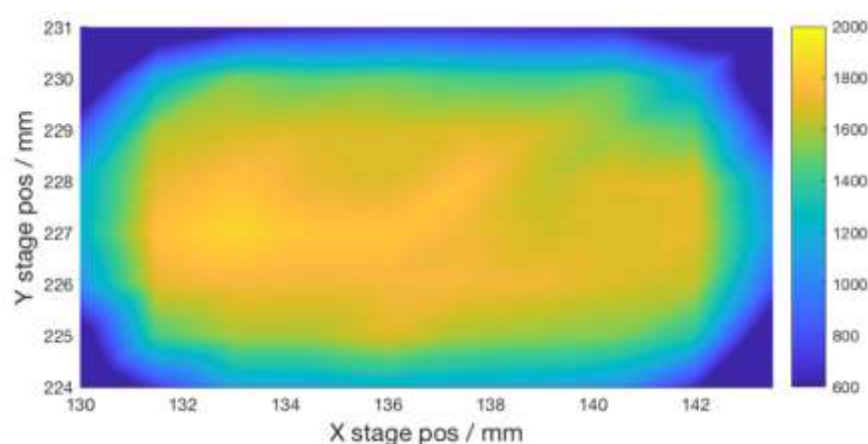


Figure 2.6 Result of the pill mapping procedure

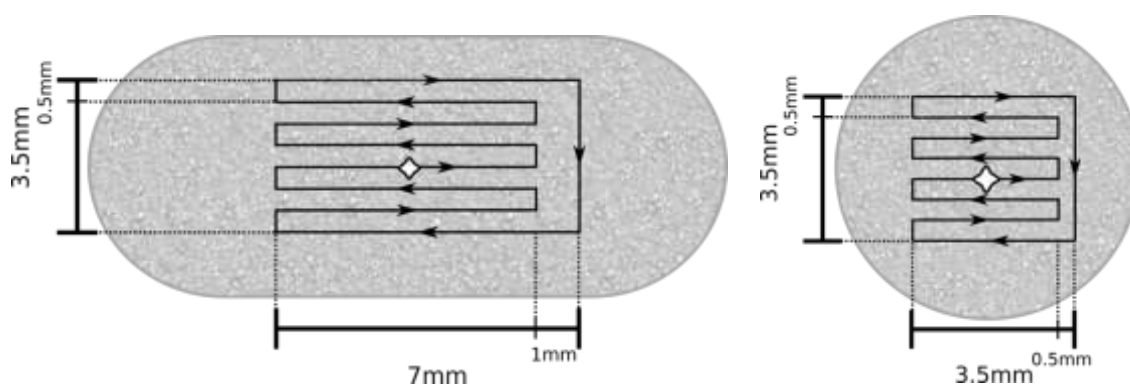


Figure 2.7 Raster scan trajectories used in Setup B; \diamond marks central “start” position

Some paracetamol- and aspirin-containing caplets had a groove down the middle to facilitate splitting them in half. To see what effect this had on count rate, an Anadin Extra caplet was scanned for 600s both along its groove (“thin” scan), and in the thickest part of the caplet (“thick” scan) for comparison (Figure 2.8). The groove was located using the same mapping method as above. The mean percentage reduction in counts was 9.6% in the “thin” region, but only 1.5% in the part of the spectra that excluded the tungsten characteristic peaks. This was within the error range from Poissonian counting (e.g. $\pm 2\%$ for the peak at 1.27nm^{-1} with ~ 2500 counts). Moreover, during a raster scan the X-ray beam would pass through this grooved region for a minority of the acquisition time, so this feature was not expected to have a significant effect.

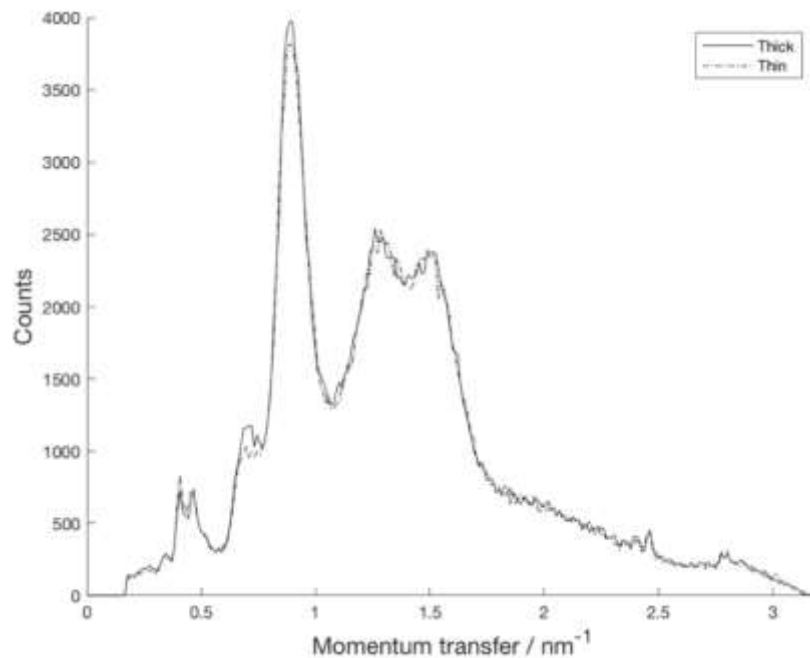


Figure 2.8 Comparison of XRD intensities for caplets containing groove (i.e. “thin” section)

For the blister-packaged sample scans, a single blister was cut out from a blister sheet and positioned upright on the sample stage. The only exceptions were the two soluble samples (Solpadeine Headache Soluble and Boots Paracetamol Extra Soluble) which had their tablets

packaged individually within plastic-lined paper. For these, one packet from each was sliced open on one end, such that the tablet could stand upright on its side whilst still being within this packaging. When collecting the data for blister- *and* card-packaged samples, a ring of card taken from a purchased packet of paracetamol was used to surround each blister (with L_1 maintained at 20mm) as shown in Figure 2.9.

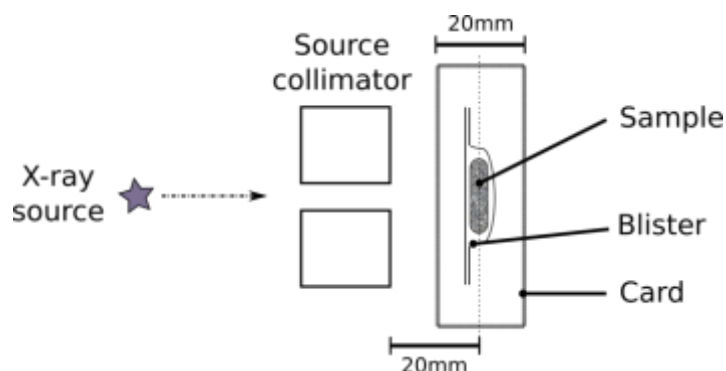


Figure 2.9 Top view of blister plus card packaging setup

The distance L_1 needed to be maintained in order to collect diffracted X-rays at the nominal scattering angle. An increase in L_1 resulted in peaks shifting to lower momentum transfer values, as the scattering angle that the data were collected at was greater than the nominal value of 5.9° ; and vice versa for smaller L_1 (see Figure 2.10) – due to the detector collimator being wide enough to accept a range of angles. The effect was greater on peaks at higher momentum transfer due to the curved shape of the X-ray tube spectrum (as in Figure 2.5) resulting in greater differences in the numbers of incoming X-ray photons in the higher E region.

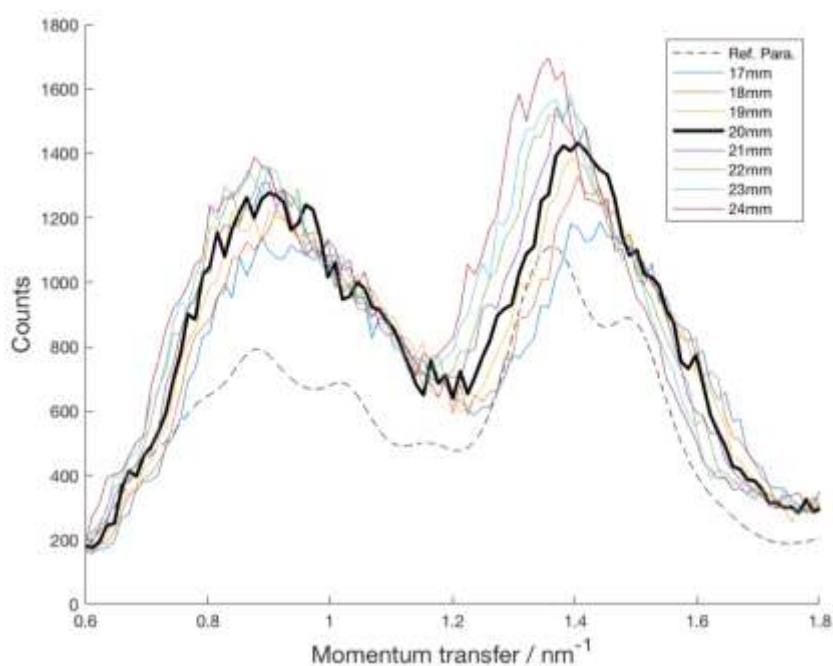


Figure 2.10 Effect of changing L_1 distance on unpackaged Hedex (1) spectra (300s, no raster)

2.2 miniPixD system

In Chapter 5, a selection of pharmaceuticals were studied using the aforementioned *miniPixD* system [276]. The key novelty of this method was the use of the pixelated, energy-resolving HEXITEC detector [274], with 80 x 80 pixels of CdTe of 250 μ m pitch – i.e. with an area of 20mm x 20mm. The use of a CdTe detector instead of a HPCe detector, although lower in energy resolution (with measured FWHM of 1.6keV at the 59.6keV peak for the former [276], compared to 0.54keV for the latter), avoided the necessity to cool the system to liquid nitrogen temperatures. This in turn allowed the system to be built such that it was more compact than traditional EDXRD systems. As discussed in section 1.3.3, by knowing the geometry of the system and calculating the diffraction angle at each pixel of the detector, the energy spectra for all 6400 pixels could be converted into momentum transfer space and summed – as illustrated in Figure 2.11 – allowing XRD spectra to be collected on the order of seconds. The overall *miniPixD* setup is illustrated in Figure 2.12, and each component along with any tests that were carried out prior to the experiment in Chapter 5 are described below.

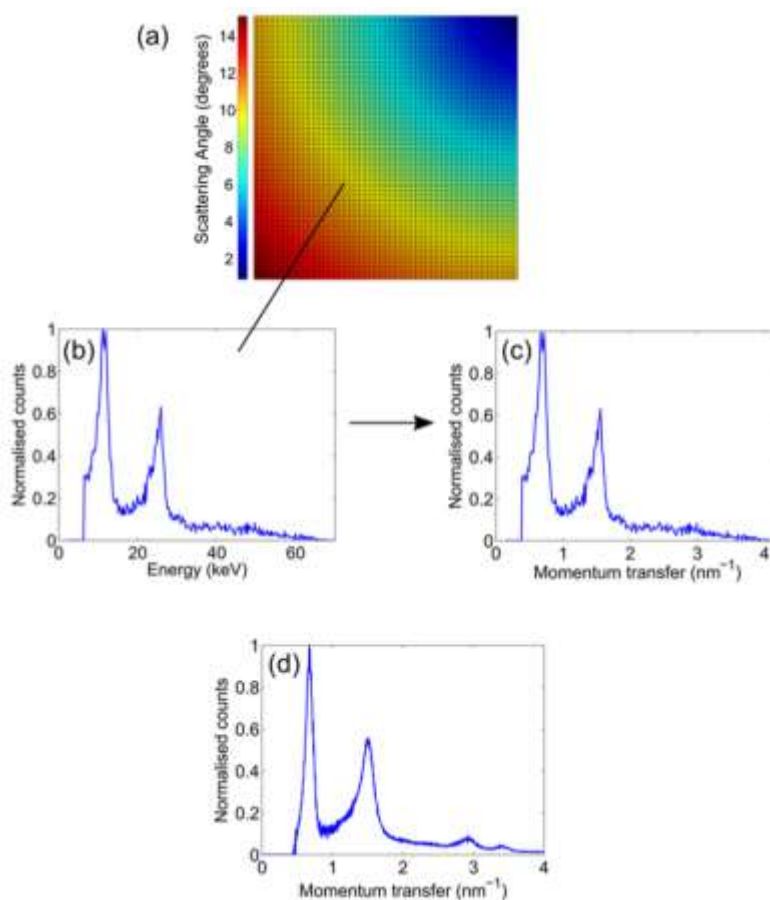


Figure 2.11 (a) Scattering angles for each pixel are combined with (b) energy spectrum measured by each pixel to convert into (c) momentum transfer space; resulting in (d) summed spectrum from all pixels. © SISSA Medialab Srl. Reproduced by permission of IOP Publishing. All rights reserved [273]

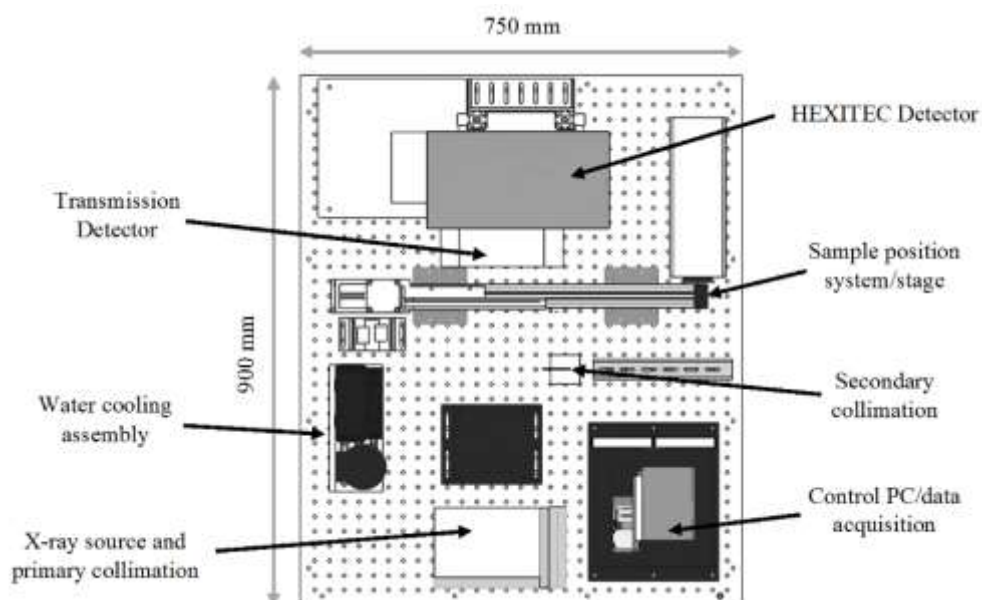


Figure 2.12 Schematic of *miniPixD* viewed from above, showing key components [276]

2.2.1 HEXITEC detector

The HEXITEC detector and data acquisition parameters were controlled using the 2Easy software provided. The detector crystal was Peltier-cooled to 12°C during measurements, and was also subjected to a bias voltage of -475V provided by a Kiethley HV power supply (2410 1100V SourceMeter). The bias was refreshed every 60s to prevent polarisation of the detector, which is known to reduce detector performance over prolonged periods [279]; the data acquisition was automatically halted during the bias refresh periods.

Data was collected overnight from an americium-241 source positioned on the front of the detector casing for the purposes of calibrating the individual detector pixels. The three major peaks (as seen in Figure 2.2) were identified in the raw ADU* spectra for each pixel, and linear fit coefficients were calculated for the ADU to energy conversion using a Matlab (R2015a, MathWorks) script†. This script also identified any defective pixels with spectra that did not have exactly three identified peaks, of which there were 192 out of 6400, i.e. 3%. These pixels, along with their four neighbours, were excluded from data analysis due to the unreliability of their collected data. The energy axes for the remaining pixels – initially in 400 bins in the range of 0 to 4000ADU– were thus converted into 400 x 0.25keV energy bins in the range of 0 to 100keV; a low energy threshold of 5keV (or 199ADU) was also applied to eliminate detector noise [277].

* ADU = analog-to-digital unit.

† Provided by Dr Robert Moss; private communication.

In order to calculate the diffraction angle at each pixel, it was first necessary to determine the position of the X-ray beam centre (positioned just off one corner of the detector) and the sample-detector distance. The diffraction data from a caffeine sample (sample 1 from Table 3.2; scanned for 1 hour), positioned on the sample stage where the pharmaceutical samples were later scanned, was used for this purpose. The resulting diffraction image was plotted in Matlab for energies windowed such that one of the caffeine diffraction rings intersecting the detector was visible, and the beam centre was determined by fitting a circle through this ring. The beam centre was thus found to lie at 1.4mm below and 1.2mm to the left of the bottom left corner. The sample-detector distance was then established by adjusting an initial starting value (based on a rough measurement to the estimated position of the detector crystal within the casing) in the HEXITEC data processing script* until the resulting caffeine XRD spectrum had its major peaks at the correct momentum transfer values (0.67 and 1.47nm^{-1}). The sample-detector distance was thus found to be 138mm.

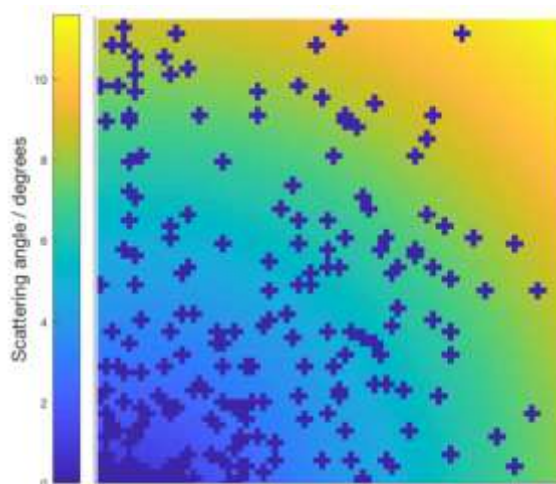


Figure 2.13 Angular range covered by the HEXITEC in *miniPixD*; showing excluded pixels

Using the above values, the pixels were calculated to cover an angular range between 0.6° and 11.6° – as illustrated in Figure 2.13. These parameters were saved into the HEXITEC data processing script that was then used for all data collected on the *miniPixD*. This code carried out the conversion of each energy spectrum to momentum transfer space (using equation (4)), and summed counts across all pixels. Since some scattering angles and therefore momentum transfer values were represented more than others, a correction was also included to account for this [276].

* Developed by Dr Daniel O'Flynn and Dr Robert Moss.

Despite the difference in detector energy resolution, when the FWHM of peaks from caffeine profiles collected using the earlier EDXRD setup B were compared to those acquired using *miniPixD*, the latter were found to offer marginally better spectral resolution [276].

2.2.2 X-ray source

A SenTek 9001 X-ray tube with tungsten target and 0.2mm diameter focal spot, filtered by a 120 μ m Be window, had been chosen for this system due to its compact size (longest dimension 20cm) and weight (8kg). Both this X-ray source and the on-board PC were cooled by a water-based coolant which was circulated through the components by a pump, and cooled by a radiator and PC fans (the “water cooling assembly” in Figure 2.12). In order to use the source for IGXRD, the primary collimator (2mm-thick lead) positioned 37mm from the X-ray source focal spot had both a 1mm \times 20mm slot for imaging, and a 0.6mm pinhole for diffraction. The pencil beam resulting from the latter was further collimated by a 0.6mm pinhole in 2mm-thick lead, positioned 235mm from the primary collimator (“secondary collimation” in Figure 2.12), such that the incident beam diameter at the sample was approx. 1mm [277]. There was no detector-side collimation in this system.

Initially, data were acquired using the X-ray source at its maximum operating voltage and current of 80kV and 2.0mA respectively. However, the source was found to suffer from occasional power cut-outs when monitored over longer periods of time. There was no indication that the source was overheating, but in order to reduce the suspected strain on the *miniPixD* power supply, the tube was operated at 72kV and 0.7mA instead.

Furthermore, measurements on pharmaceutical tablets highlighted the issue that a large amount of background scatter was masking diffraction features in the collected spectra. This was found to be caused by the X-rays emerging from the larger slot collimator beside the pinhole collimator on the X-ray source. Therefore, the slot was covered with lead throughout the diffraction experiments. It was not removed at any point because tests showed that, in the current setup, it was not possible to replace the lead cover reproducibly such that the background was constant. In addition to this, 2 \times 0.5mm-thick sheets of aluminium were positioned immediately prior to the secondary collimation of the beam to cut the number of low-energy photons reaching the detector – effectively reducing a large background peak at the low momentum transfer end of the resulting XRD spectra.

Despite these modifications being made, problems with the reproducibility of data collected for the same sample on different days – and over long periods on the same day – became apparent. The system stability was consequently tested by leaving the X-ray source and detector switched

on for approx. 17 hours, with the collected data divided into 100 x 10-minute snapshots. The energy spectrum from each snapshot was subtracted from that of the final ten minutes (presumed to be once the system had stabilised), and the *absolute* differences in counts for each energy bin were summed and plotted (see Figure 2.14). These absolute differences did not fall below ~4000 counts in total due to the baseline noise level in the spectra. Figure 2.14 suggested that approx. 4 hours of waiting time was required for the system to reach levels of greater stability after switching on. Thus, by introducing this waiting time prior to data collection, the reproducibility of spectra was much improved.

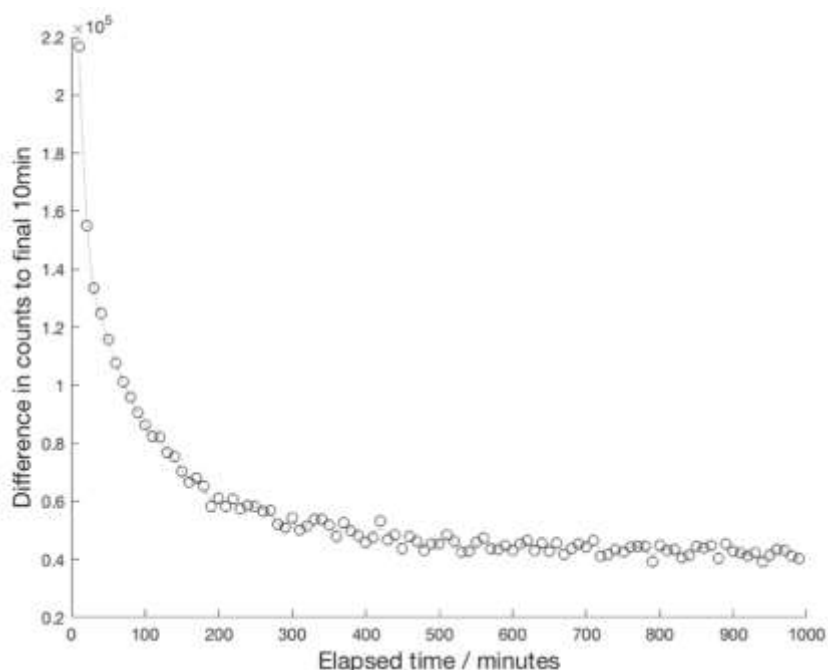


Figure 2.14 System stability test over 1000 minutes

2.2.3 Sample positioning

Samples were moved remotely by controlling the set of linear stages in the plane perpendicular to the X-ray beam via Matlab (R2015a, MathWorks). A raster-scanning Matlab script* was used to repeatedly move the sample in a 3mm x 3mm or 6mm x 3mm raster (with 0.5mm increments between rows), depending on pill shape. A central starting position for both caplet and tablet raster scans was determined by firstly using a sheet of X-ray fluorescent Lanex positioned on the sample stage to image the X-ray beam position, and overlaying this image onto a real-time image of the pill (captured by webcam from inside the radiation laboratory) as it was moved.

* Provided by Dr Robert Moss; private communication.

2.2.4 Sample imaging

Lastly, a linear detector array (gadolinium oxysulfide scintillator) on board the *miniPixD* could be used for transmission imaging. This was performed with the X-ray source set at the same operating parameters as for diffraction. A graphical user interface (GUI) had been made to allow users to image a sample and pick a point of interest, for it to position the sample appropriately for a diffraction measurement to be made. The 2Easy software for the HEXITEC was then used for data acquisition. Note that the lead cover introduced in section 2.2.2 (to reduce background scatter) was removed prior to imaging.

2.3 Chemometrics

2.3.1 Principal components analysis (PCA)

Chemometric methods were introduced in section 1.3.2.2 as being useful for the purposes of analysing large datasets of spectra to extract useful information. Within such studies, PCA is often performed for exploratory data analysis and unsupervised pattern recognition (i.e. without prior knowledge of classes). PCA effectively summarises the data by re-plotting it onto an alternative set of axes – the principal components (PCs) – using linear combinations of the original spectral variables. The first PC describes the direction of maximum variance, with each subsequent PC describing as much of the residual variance as possible whilst being orthogonal to all others, until all variation is described. This process is illustrated by a simple case in Figure 2.15, noting that although only three variable axes are shown in the left-hand plot, there would be many more in the case of a spectrum, where each wavelength or energy contributes an additional orthogonal axis. There can be as many PCs as $(N-1)$, where N is the number of samples, but because the amount of information contained in each decreases as higher PCs start to explain noise rather than the pattern(s) of interest (if any), it is useful to select the number of PCs that best describes the data whilst leaving out any background contributions.

If we take the matrix of all spectra for the samples (\mathbf{X}) this decomposition can be described mathematically by the following equation:

$$\mathbf{X} = \mathbf{TP}^T + \mathbf{E} \quad (10)$$

where \mathbf{T} is called the scores matrix and \mathbf{P} is the corresponding loading matrix; \mathbf{TP}^T is the summarised version of \mathbf{X} . The residuals not described by the model of the chosen number of PCs are contained in matrix \mathbf{E} (i.e. the background and noise).

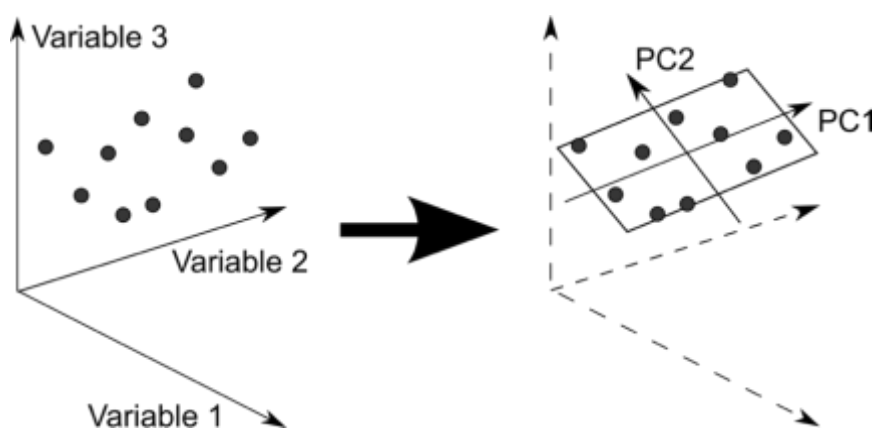


Figure 2.15 Schematic of PCA transformation (adapted from [280])

The scores matrix is composed of vectors which designate the positions of each sample along a particular PC, and by plotting these scores for two or three PCs, the similarities and/or differences between samples can be visualised. The loadings describe how much each variable from the original coordinate system contributes to each PC, if at all – they can be thought of as the transformation matrix between the original variable space and PC-space. The greater in magnitude the loading of an original spectral variable for a particular PC, the more it contributes to determining the score of a sample on this PC. Therefore, interpretations of what real-world phenomena the PCs correspond to can be attempted by plotting the loadings for a particular PC against spectral variables. The largest loadings, corresponding to the most important diagnostic variables, in such a plot may help indicate the presence of a certain material in a mixture.

The decision as to *how many* PCs to retain for modelling the system is made by considering various factors, the most important of which are [281]:

- the plot of percentage explained variance vs number of PCs used, which increases with each additional PC, providing a measure of the overall modelling error, and is used to find at what point PCs no longer contribute significantly to describing the variance in the data;
- the plot of residuals vs variable number, showing how much of a particular measurement variable is *not* explained by a given number of PCs – should be random noise once enough PCs have been applied to describe features of interest;
- the loadings plot for any given PC, which is used to determine if the features described by the PC are worth retaining for the purposes of the experiment.

In Chapters 3 to 5 of this thesis, PCA models were calculated using both The Unscrambler software (v.9.5, CAMO) and Matlab (R2017b, MathWorks, using the inbuilt *pca* function), which gave the same results.

2.3.2 Partial Least-squares Regression (PLSR)

PLSR is another method of data reduction which can be applied to large spectral datasets in combination with known response variables, such as concentrations. A calibration model is built such that the PLS-factors – analogous to PCs – account for the maximum covariance between the concentration matrix \mathbf{Y} and spectral variables \mathbf{X} , to find \mathbf{B} , the matrix of regression coefficients for each PLS-factor:

$$\mathbf{Y} = \mathbf{XB} + \mathbf{F} \quad (11)$$

where \mathbf{F} is the y-residuals matrix, describing any variation in concentrations not explained by the number of PLS-factors used in the model.

All calibration models must be validated to assess the suitability of data pre-treatments (if any), as well as for choosing the optimum number of PLS-factors to retain for the model for use in future predictions. A common method called full cross-validation (or “leave-one-out” validation) was used in this thesis; the model is calibrated repeatedly whilst leaving out one sample spectrum, until all n training set samples have been left out in turn. The differences in the predicted y (\hat{y}) and actual y for this “left-out” sample, i.e. the y-residuals ($\hat{y}_i - y_i$), are used to calculate the residual y -variance, i.e. the concentration variance:

$$residual\ y\ variance = \frac{\sum(\hat{y}_i - y_i)^2}{n-1} \quad (12)$$

and the root mean-square error of cross validation (RMSECV) is calculated from its square root:

$$RMSECV = \sqrt{\frac{\sum_{i=1}^n (\hat{y}_i - y_i)^2}{n-1}} \quad (13)$$

The points where both the RMSECV and residual concentration variances vs number of PLS-factors stopped decreasing sharply were used to help identify the optimal number of PLS-factors for predicting the concentration of each mixture component. To avoid the risk of over-fitting the data, the smaller number of PLS-factors was preferred where this point was not clearly defined. In addition, m test set samples were used to assess the PLSR models’ prediction performance by calculating root mean-square errors of prediction (RMSEP):

$$RMSEP = \sqrt{\frac{\sum_{i=1}^m (\hat{y}_i - y_i)^2}{m}} \quad (14)$$

Diagnostic plots suggested by Beebe *et al.* [281] were used to check the samples for outliers. In the plot of studentised concentration residuals* vs sample leverage†, samples with studentised residuals greater than ± 2.5 and leverages greater than three times the average would normally warrant further attention. The plot of concentration residuals vs predicted concentrations was also used to check whether the residuals were not concentration-dependent (the ideal case is when the points vary randomly about a line of zero slope and zero intercept).

In Chapter 3 of this thesis, PLSR calibration models were constructed and validated using the “regression” function of The Unscrambler software.

2.3.3 Soft Independent Modelling of Class Analogy (SIMCA)

SIMCA is a popular classification method based on PCA models constructed for each class, with their optimum number of PCs determined in advance. Each PCA model should be constructed from a training set of samples to cover the expected variability within classes in present and future samples – or updated to maintain this information. The concept of SIMCA is illustrated in Figure 2.16 – the classification of a sample of unknown composition is based on the closeness of its spectrum to one or more PCA models included; it is possible for it to be unclassified, or classified as one or multiple classes. In Chapters 4 and 5 of this thesis, SIMCA classifications were performed using The Unscrambler’s “classify” function, after first creating relevant PCA models in the same program.

Figure 2.16 Schematic of the SIMCA method from Sirven et al. [282] showing PCA models for spectra of 3 sample classes (visualised in a 3-wavelength space); ■ is an unknown spectrum to be classified

* Studentised residuals have been divided by the concentration standard deviation and $\sqrt{1 - H_i}$ and are in units of standard deviations from the mean, such that they can be compared on a common scale.

† Leverage (H_i) is a measure of how different a sample is from the others in the dataset, and thus a measure of its influence on a model.

In The Unscrambler, samples are recognised as belonging to a particular class if they fall within model-dependent limits for both the sample-to-model distance (S_i) (orthogonal distance from the sample to the class as defined by its PCs) and the sample leverage (H_i)[†] [283]. The former threshold is calculated as follows:

$$S_{max} = S_0 \sqrt{F_{crit}(1, I_{cal})} \quad (15)$$

where I_{cal} is the number of samples used in the training set for the PCA model; F_{crit} is the critical value of the F-distribution for a given significance level and for the degrees of freedom in parentheses; and S_0 is the average distance within the model:

$$S_0 = \sqrt{total\ residual\ x\ variance(a)} \quad (16)$$

where a is the number of PCs used in the model. The leverage limit is calculated using:

$$H_{max} = 3 \times \frac{a+1}{I_{cal}} \quad (17)$$

A S_i vs H_i plot for all test samples that includes the S_{max} and H_{max} limits can thus be used to see where the samples lie relative to these thresholds, and visualise the classification process. The significance level was initially set to 5% – what is normally used in statistics [283] – meaning there was a 5% chance that a sample would fall outside the class when it belonged to it (a false negative), and 95% of samples which truly belonged would fall within the class. In later experiments, classification results using the more restrictive 10% significance level were also recorded, as this decreased F_{crit} and hence S_{max} .

SIMCA classifications were validated using both a “positive” test set (the “authentic” samples left out from the training set used for the PCA model), and a set of “negative” control samples (the “poor-quality medicine” analogues). The results were compiled such that the *sensitivity* (ratio of true positive classifications to the number of positive test samples), and *specificity* (ratio of true negative classifications to the number of all negative control samples) of each SIMCA classification could be compared. Note that these were the definitions used in this particular thesis – other authors occasionally use the reverse meanings of “positive” and “negative” in the context of medicines authentication [159].

2.3.4 Pre-processing

For the most part, the analyses contained in this thesis focus on the use of raw XRD data for plotting, and mean-centred data when using chemometric methods. Mean-centring is commonly applied as standard and thus does not always appear to be clearly stated when used in the literature. It is calculated by subtracting the average value for each variable within the

calibration set from its corresponding variable. In addition to this, some further data pre-treatments were performed to test their effect on the results of PLSR (in Chapter 3), and are described below.

Multiplicative scatter correction (MSC) is a transformation that is applied to remove multiplicative (i.e. amplification of counts) and/or additive (i.e. offset of counts) scatter effects caused by different particle sizes, path lengths, and background effects. It was originally designed for light-based systems such as NIR spectra, but has been found to improve results when applied to other analytical techniques [281]. Initially, the number of counts for each variable for each sample may be plotted against the mean number of counts for that variable to provide a diagnostic plot – different gradients or offsets for different samples are indicative of multiplicative scatter effects. If required, a regression is fitted to these data such that the slope accounts for the common amplification, and the y -intercept for the common offset. This correction is then applied to the full spectra, and any test set spectra, prior to chemometric analysis [283,284]. Standard normal variate (SNV) is a related and commonly used method where individual spectra are mean-centred and scaled by the standard deviation of values of all variables for the spectrum. It is similar to MSC in that it is also applied to remove scatter effects, but may be favoured over MSC as it performs this transformation using data from individual spectra instead of the entire dataset – and thus does not require re-calculating with the addition of further samples [285].

A first-order derivative pre-treatment was also trialled, as this has been known to correct for baseline drift in spectra [286]. Savitzky-Golay derivatives were calculated in The Unscrambler; this performs a least-squares fit of a polynomial at each point in the spectrum to smooth the data before taking the derivative of the fitted polynomial. The window used for smoothing needs to be chosen carefully such that it is not too narrow (and not removing noise) nor too wide (and removing features of interest). A downside with this type of pre-processing is that it can be difficult to relate the results of PCA or PLSR analysis on these data back to the original data.

Chapter 3: Controlled Mixture Tests

3.1 Background

Firstly, the question of whether laboratory-based EDXRD systems were inherently able to detect changes in quantities of chemicals commonly found in pharmaceuticals needed to be addressed. This was a concern as EDXRD spectra collected from these systems suffer from a loss of resolution compared to ADXRD data, as mentioned in section 1.3.1.2.. PLSR was therefore applied to test whether EDXRD spectra from calibration mixtures of known concentrations could be used to quantify the contents of unknown samples from their spectra.

There are numerous examples of spectroscopic techniques being combined with PLSR in this way for the quantitative analysis of pharmaceutical mixtures. Raman in particular is a popular method due to its ability to detect polymorphism and to probe consolidated mixtures [25,198,287–289]. One such study looked at ternary mixtures of paracetamol, starch and sucrose, covering a range of concentrations between 0 and 80weight%. Their Raman spectra were acquired through blister packaging to construct a PLSR model, resulting in a RMSECV of 1.4weight%. The authors reported the potential application to counterfeit medicines detection, amongst others [289].

A summary of publications that combine ADXRD with PLSR on pharmaceutical mixtures is presented in Table 3.1. It is noteworthy that none of the study authors mentioned the potential application of this method to the problem of counterfeit and substandard medicines, but were instead interested in areas such as quality control of raw chemicals, or comparisons to other analytical techniques. A few of the studies cited in Table 3.1 also compared PLSR to univariate quantification methods; for example, Croker *et al.* found a significant improvement when using the former (RMSEP of 1.81 vs 6.71weight%) [251]. This was attributed to the use of the full spectrum as opposed to individual peaks that suffered from preferred orientation effects.

As far as the author is aware, there are no previous studies on the non-destructive quantitative analysis of pharmaceutical mixtures using EDXRD spectra combined with chemometric methods.

Materials	Pre-processing	PLS-factors	RMSECV (weight%)	Aims and observations	Ref
Carbamazepine (CBZ) anhydrate and dihydrate	MSC	2	2.93	Quantification of anhydrate after exposure to water. Compared to Raman: RMSECV = 1.06%	[255]
Famotidine forms A and B	Scaled, smoothed, and 1 st derivative	2	1.450	Quantification for potential industrial applications; model excluded one peak with large intensity variations. Compared to Raman: RMSECV = 1.560, but using three bands of spectra	[215]
Piracetam forms II and III	None	1	2.17	Simple quantification; model excluded peak with large intensity variations. Raman and NIR gave better results (1.06% and 1.11% respectively) but using MSC and 2 nd derivative pre-processing	[251]
Crystalline and amorphous tacrolimus formulations	None	2	1.092 / 1.20	Quantification for potential use in monitoring conversion of amorphous API to crystalline form in formulations (to assess shelf life)	[256] / [257]
Crystalline and amorphous diltiazem hydrochloride formulations	None	3	3.85 (segmented CV)	Quantification for potential use in monitoring conversion of amorphous API to crystalline form in formulations (to assess shelf life)	[249]
Ranitidine HCl forms I, II and amorphous	MSC, and not mean-centred	4	4.6 - 6.5	Quantification for quality control. Compared to Raman: RMSECV = 2.3% - 4.4% with SNV and mean-centring, using 3 PLS-factors	[233]
CBZ forms I and III, saccharin, and CBZ-saccharin co-crystal	Area-normalised then smoothed	3	1.0 - 3.7	Quantification for potential use in manufacturing quality control. Compared to FTIR: RMSECV = 0.5% - 7.0% with SNV and smoothing	[258]
Theophylline (API), lactose, mic. cellulose, starch	None	1 (API) or 3	3.71 - 7.15	Quantification in intact pharmaceutical samples; tablets pressed with range of pressures with minimal change in results	[246]
Aspirin, paracetamol, ibuprofen, caffeine	SNV	3	4.3 - 7.1	Quantification using fused data from ADXRD & FTIR; fused data was very similar, and FTIR-only gave RMSECV = 10.0% - 13.7% (using parts of spectra)	[214]

Table 3.1 Studies on ADXRD (reflection geometry) and PLSR; mean-centring presumed and full-cross validation used unless otherwise stated

3.2 Methodology

3.2.1 Sample preparation

Paracetamol (Acetaminophen BioXtra, $\geq 99.0\%$; Sigma Aldrich), caffeine (ReagentPlus®; Sigma Aldrich), and microcrystalline cellulose (average particle size $50\mu\text{m}$; Acros Organics) were all used as received. The former two are common APIs, and the latter, a common excipient used as a dilutant. The paracetamol was confirmed to be polymorph form I, as used in solid oral dosage forms. Microcrystalline cellulose has an XRD pattern that is representative of other common excipients in terms of its peak broadness and momentum transfer range, as shown in Figure 3.1.

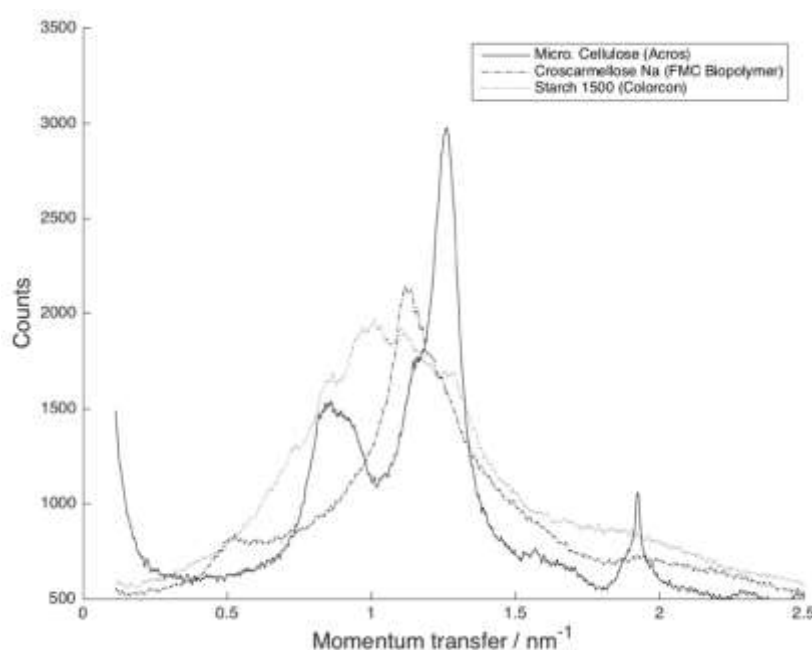


Figure 3.1 ADXRD spectra of some commonly used excipients (data collected by author)

These three chemicals were weighed and combined in the ratios shown in Table 3.2 to make up 1.00g of each mixture. This calibration mixture design, shown by the filled triangles in Figure 3.2, was created using the design wizard in The Unscrambler (v.9.5, CAMO). A test set of samples T1-T6 was also made, in a similar fashion to what has been reported in other studies [215,251], and taking into account Esbensen *et al.*'s recommendation that the test set should be at least 25% the size of the training set [283].

Each sample mixture was ground with an agate mortar and pestle for three minutes to mix thoroughly and to reduce particle sizes – with the aim to decrease preferred orientation effects [215]. More vigorous mixing techniques such as milling were avoided to prevent potential polymorph phase transitions [215,222,233,251]. Sieving was also avoided as the paracetamol

powder exhibited a build-up of electrostatic charge when ground, making it difficult to handle; this additional step also risked introducing artefacts resulting from selecting particles of a certain size [246,290].

400mg of each mixture was transferred to a 13mm-diameter die and pressed into tablets using an automated Speca Press. A 1-ton load (equivalent to 67.0MPa; used by Moore *et al.* [246]) was applied, with a dwell time of two seconds before the pressure was released. The compacted tablets were then extracted carefully from the die.

Sample	Caff	Para	Mic. cell.
1	100	0.00	0.00
2	80.0	20.0	0.00
3	80.0	0.00	20.0
4	60.0	40.0	0.00
5	60.0	20.0	20.0
6	60.0	0.00	40.0
7	40.0	60.0	0.00
8	40.0	40.0	20.0
9	40.0	20.0	40.0
10	40.0	0.00	60.0
11	20.0	80.0	0.00
12	20.0	60.0	20.0
13	20.0	40.0	40.0
14	20.0	20.0	60.0
15	20.0	0.00	80.0
16	0.00	100	0.00
17	0.00	80.0	20.0
18	0.00	60.0	40.0
19	0.00	40.0	60.0
20	0.00	20.0	80.0
21	0.00	0.00	100
Cent	33.3	33.3	33.3
T1	80.0	10.0	10.0
T2	10.0	80.0	80.0
T3	10.0	10.0	80.0
T4	53.3	23.3	23.3
T5	23.3	53.3	23.3
T6	23.3	23.3	53.3

Table 3.2 Percentages of each material used in samples

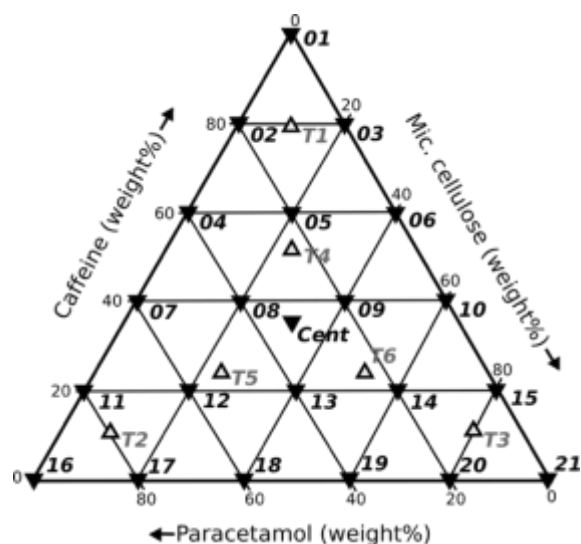


Figure 3.2 Mixture design showing amounts of each chemical in each sample

Over-the-counter (OTC) medicines were also purchased for testing: Boots Paracetamol Extra tablets (65mg caffeine, 500mg paracetamol, 5.75mm thick), Panadol Extra Advance tablets (65mg caffeine, 500mg paracetamol, 5.75mm thick), and Bayer's Pro Plus tablets (50mg caffeine, 3.07mm thick). A tablet from each was removed from their blister packs, and the Boots and Panadol tablets were sliced to reduce their thickness to approximately 3mm before analysis, making them more comparable to the pressed tablets' and Pro Plus tablet's thicknesses.

3.2.2 Sample scanning

All samples were scanned in triplicate, with a different part or side of the tablet scanned each time, in the EDXRD setup A described in section 2.1.1. In the initial scans, a preferred orientation effect was evident in all samples containing paracetamol, with some peaks showing large variations in intensity between scans. Rotating the sample was not an option in this experimental setup, nor would it be suitable for the ultimate goal of scanning whole tablets in packaging. Others have overcome this issue by either shaking samples or by scanning at different points to smooth out discrepancies [242,291]. In this instance, a set of translation stages was added and used to scan all paracetamol-containing tablets in 30 positions for 10s/step (see section 2.1.1). This step-scanning procedure was also used for paracetamol-containing tablets in the "packaging" configuration, as well as the test set of tablets, which all contained paracetamol. The OTC medicines were scanned in a fixed position for 300s.

3.3 Results and Discussion

3.3.1 Exploratory data analysis

3.3.1.1 Preferred orientation effect

The collected spectra were initially processed and plotted using Matlab (R2017b, MathWorks). The spectra for samples 2 and 11 in Figure 3.3 demonstrate how there was a great improvement in the repeatability of data acquired whilst step-scanning, although preferred orientation was still evident in samples with a high paracetamol content (e.g. sample 11 was 80% paracetamol). Otherwise, the raw spectra did not reveal any unusual features upon initial inspection.

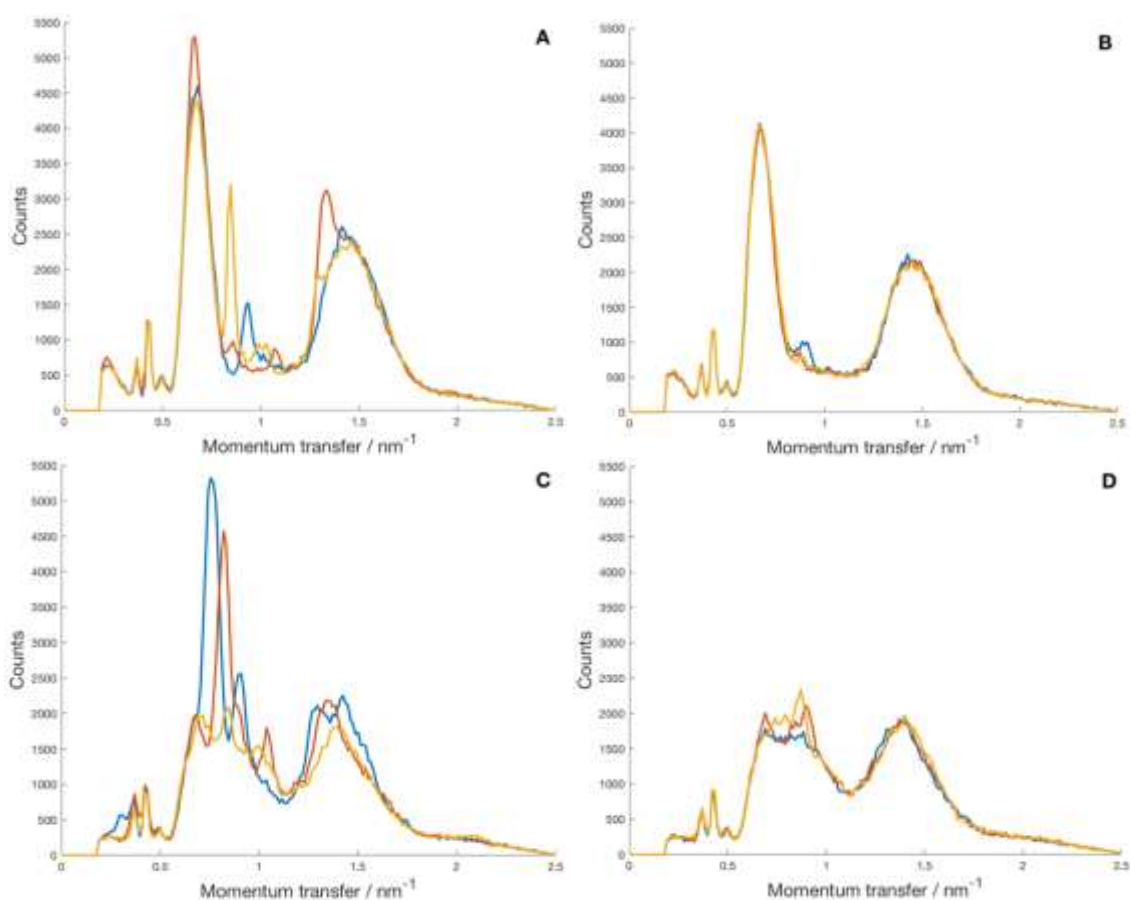


Figure 3.3 Examples of triplicate scans exhibiting preferred orientation: sample 2 (A) without and (B) with step-scanning; sample 11 (C) without and (D) with step-scanning

3.3.1.2 Attenuation effects

Tables of mass attenuation coefficients (μ/ρ) for energies up to 60keV were obtained by inputting the formulae of the three chemicals of interest into the FFAST database available on the NIST website [230]. The densities (ρ) of caffeine, paracetamol and microcrystalline cellulose were calculated to be 1.23, 1.26, and 1.46gcm⁻³ respectively from measured volumes and masses

of samples 1, 16 and 21 (i.e. the pure materials). It was noted that these values matched reported densities of these materials, so it could be assumed that the powders had been compacted sufficiently without leaving voids in the tablets. The linear attenuation coefficients (μ) could then be calculated, and along with the measured tablet thicknesses (x), were used to calculate the percentage of X-rays transmitted through a sample using the Beer-Lambert equation (equation (5) in section 1.3.1.3). The resulting plot in Figure 3.4 reveals that for all three of these organic materials, X-ray transmission reaches >99% for incident X-ray energies >12keV (0.53nm^{-1} in this system). It warrants mentioning here that the Cu K_{α} X-rays (8.04keV) commonly used in ADXRD would suffer much more from attenuation if used in transmission mode for tablets of this thickness. The characteristic lines from the tungsten X-ray source, as well as a weak caffeine diffraction peak, fell in this $<0.53\text{nm}^{-1}$ region of the spectra. Therefore, a comparison was made between the effect of both omitting and including this region – dubbed “short” and “long” spectra, respectively – in the PLSR analyses below.

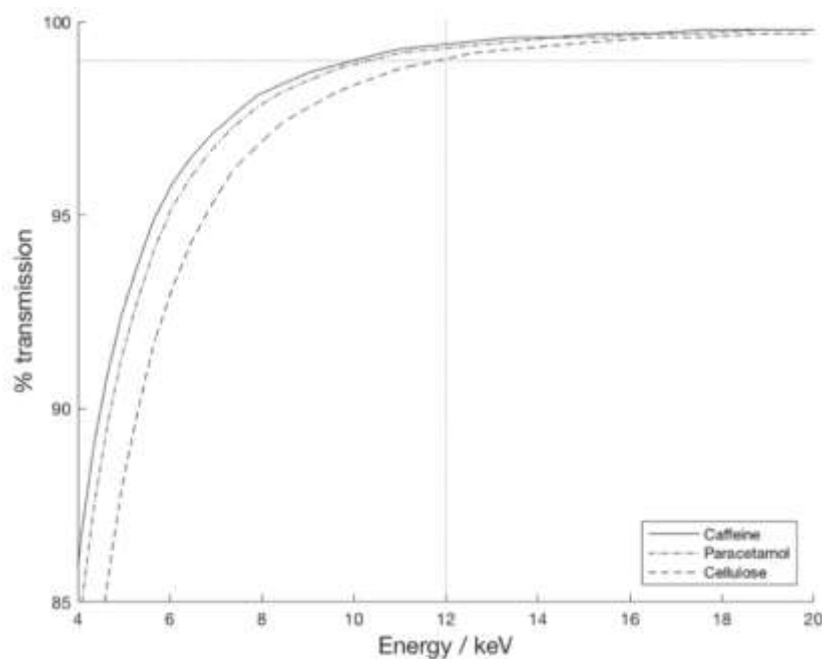


Figure 3.4 Calculated percentage transmission for pure materials in pressed tablet form

It was expected that much of the self-attenuation effect on diffracted X-rays could be discounted, and this was tested by comparing the spectra collected experimentally from the mixtures to those calculated from combinations of pure material spectra in their corresponding ratios. For example, $(0.6 \times \text{sample 1 spectrum}) + (0.2 \times \text{sample 16 spectrum}) + (0.2 \times \text{sample 21 spectrum})$ should correspond to the sample 5 spectrum if this assumption was valid. Indeed, the resulting plots in Figure 3.5 demonstrated that any variations in attenuation caused by the different amounts of each chemical in the actual mixtures were small enough that this did not noticeably

affect the spectra; it was a preferred orientation peak that produced a more significant difference between the calculated and experimental spectrum in the case of sample 11.

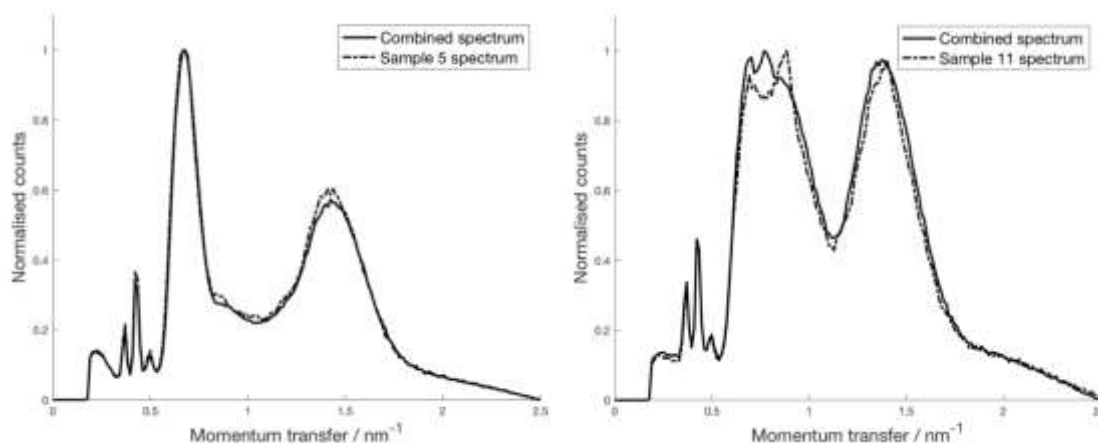


Figure 3.5 EDXRD profiles from combinations of pure material spectra compared to experimental data

The aluminium and plastic (normally PVC [292]) used in blister packaging, plus the card (i.e. cellulose) of outer packaging also contributed to the attenuation of X-rays. Furthermore, the plastic and card contributed weak, broad diffraction peaks in the 0.6 - 1.6nm⁻¹ range. On the other hand, diffraction peaks from metals fall at higher momentum transfer values due to their significantly smaller *d*-spacings; the aluminium diffraction peaks occurring >2.1nm⁻¹ would therefore not have affected the diffraction peaks of interest.

The linear attenuation coefficients of the packaging materials were calculated assuming the card contained cellulose only. The nominal densities of Al and PVC were 2.70 and 1.40gcm⁻³ respectively [293]. For card, a range of densities (min. 0.35, max. 0.9gcm⁻³) were used as a rough guide, based on the quoted grammage of “cereal carton clay-coated recycled board” in [294]. The Al foil thickness was presumed to be 0.03mm (a mid-range thickness [211]), and measured thicknesses for PVC (0.25mm) and card (0.76mm total – as there was card on both faces of the tablets) were used to calculate the percentage X-ray transmissions plotted in Figure 3.6. Here, >99% of X-rays were found to be transmitted when incident X-ray energies were greater than 11keV (i.e. 0.49nm⁻¹) – bearing in mind that the values used were based on estimates. Overall, the packaging would have primarily attenuated peaks at lower energies only.

On a separate note, spectral corrections to account for the X-ray tube spectrum shape (shown in Figure 2.5) were not applied here, as a simple multiplication of all spectra would be discounted by the chemometric methods used.

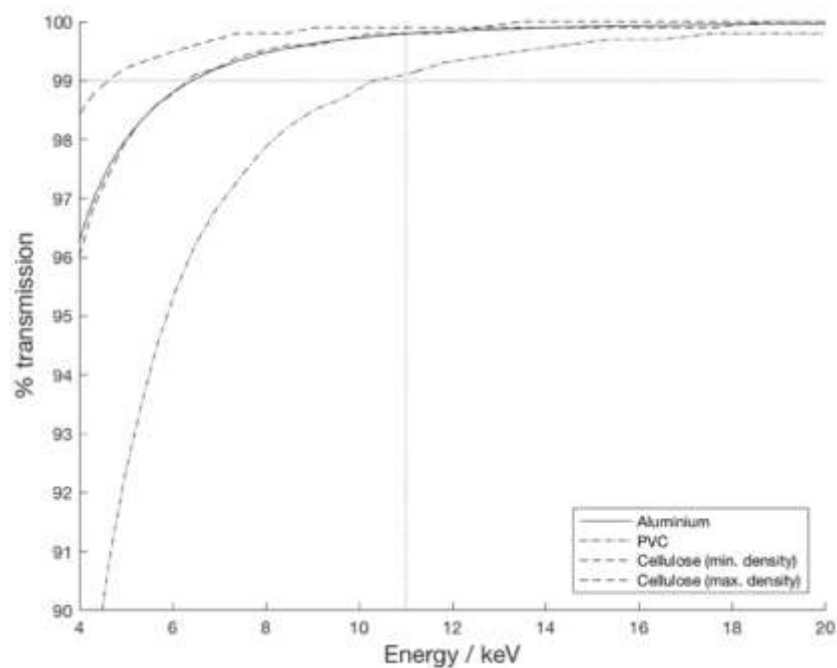


Figure 3.6 Calculated % transmission for packaging materials

3.3.1.3 Unpackaged samples

The raw spectra collected for unpackaged samples were exported into The Unscrambler software, and PCA was initially carried out on all mean-centred, “long” spectra for the triplicate scans of the 22 samples in the training set. The scores plot for PC1 (describing 92% of the variance) against PC2 (5.6% variance) in Figure 3.7 demonstrated how this unsupervised technique clearly separated the sample spectra into their correct positions in the mixture design (compare to Figure 3.2). The points corresponding to repeat scans shown here were found to be far more closely grouped than in earlier results prior to the introduction of step-scanning.

Interestingly, samples 11 and 17 – both containing 80weight% of paracetamol – still showed a greater variation between repeat scans compared to other samples in Figure 3.7, whereas the pure paracetamol (sample 16) spectra were closely matched. A possible explanation for this is that introducing 20weight% of caffeine or cellulose to the mixture – with particles of different shapes and sizes – encouraged the paracetamol crystals to align in certain directions, exacerbating the preferred orientation effect in these mixtures. It was not thought to be caused by a reduction in the homogeneity of mixtures, as the general shape of the repeat spectra were closely matched. Samples 12 and 18 also displayed a similar behaviour.

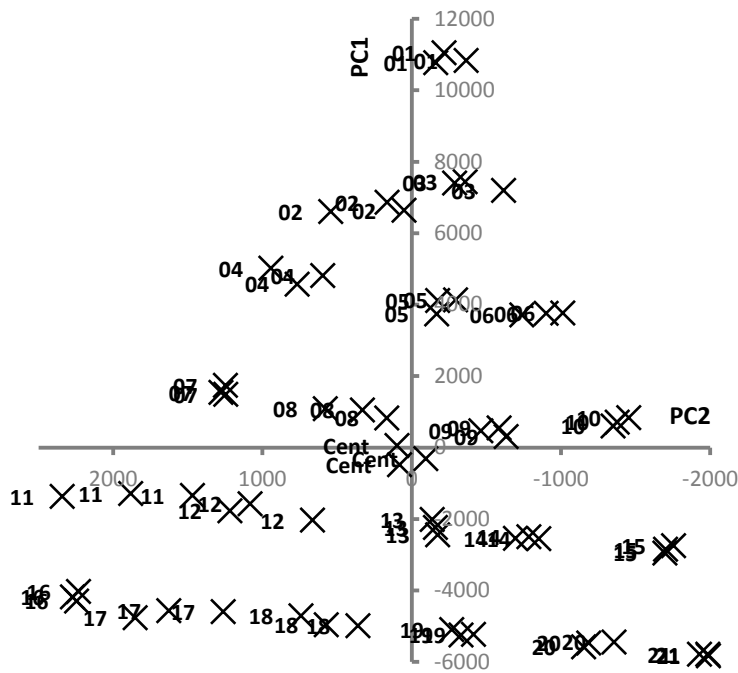


Figure 3.7 PC1 vs PC2 scores from PCA on triplicate raw spectra of unpackaged samples

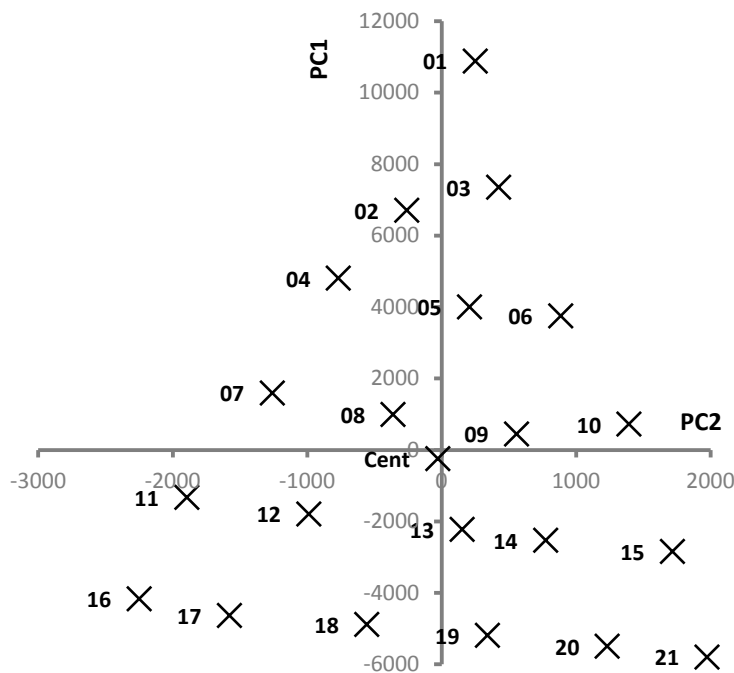


Figure 3.8 PC1 vs PC2 scores from PCA on mean raw spectra of unpackaged samples

The mean spectrum for each sample was calculated, and PCA was repeated, resulting in the PC1 vs PC2 scores plot shown in Figure 3.8. The explained variances for PCs 1, 2 and 3 were 93%, 5.6% and 0.47% respectively. The caffeine composition dominated the variation between spectra in PC1, which can be explained by the strong diffraction peaks of caffeine that very distinctly confirm its presence in a mixture. The link between PCs and mixture composition was

made clearer by plotting the loadings of the PCs and comparing these to reference spectra (generated using Mercury v.3.9 [238] and CSD-NIWFEE05 (caffeine), HXACAN18 (paracetamol) and JINROO05 (cellulose) [239]), as shown in Figure 3.9. The peaks seen in the PC1 loadings closely match the positions of caffeine diffraction peaks. Similarly, the PC2 loadings appeared to pick out the paracetamol peaks from the remaining variation in the spectra. Although PC3 had a very low percentage of explained variance, its loadings appeared to describe the remaining contribution to the variation between spectra from microcrystalline cellulose.

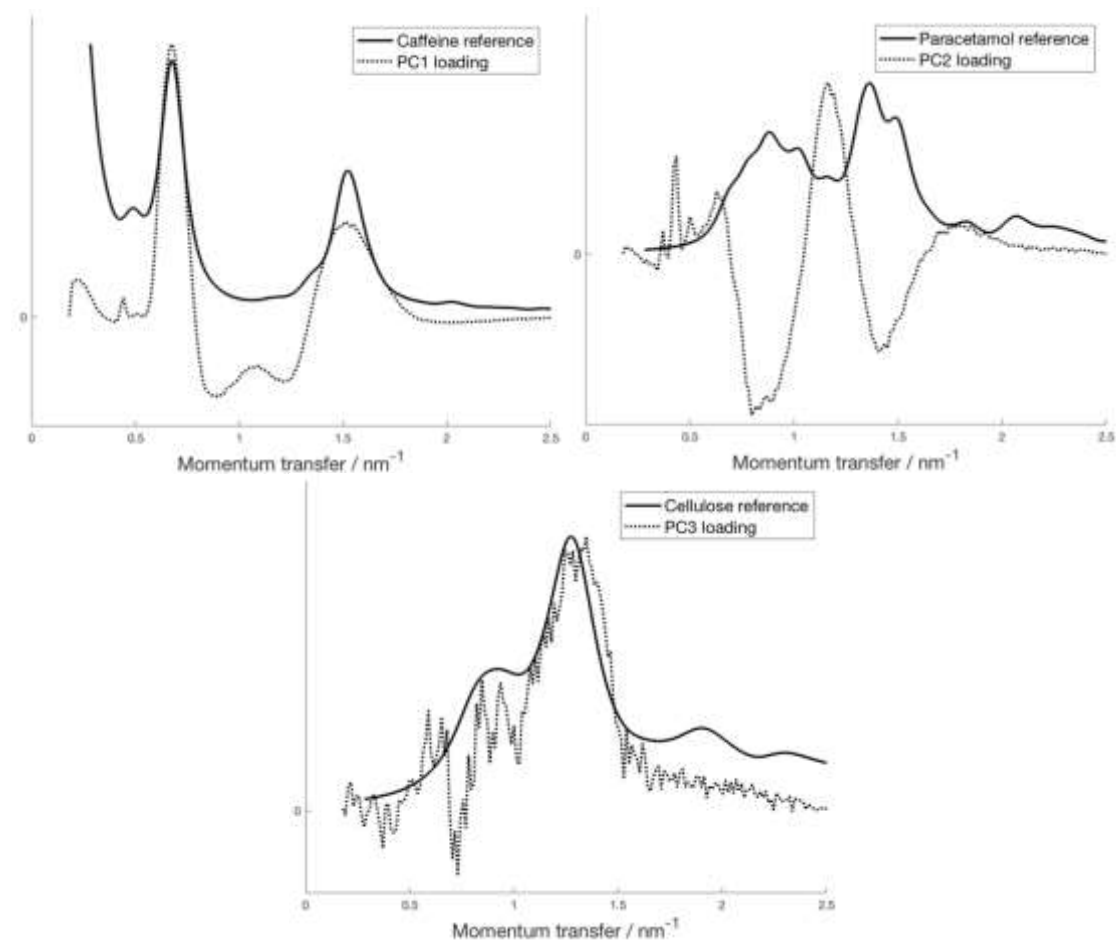


Figure 3.9 Loadings plots for PCs 1-3 from PCA on mean raw spectra of unpackaged samples, compared to reference spectra

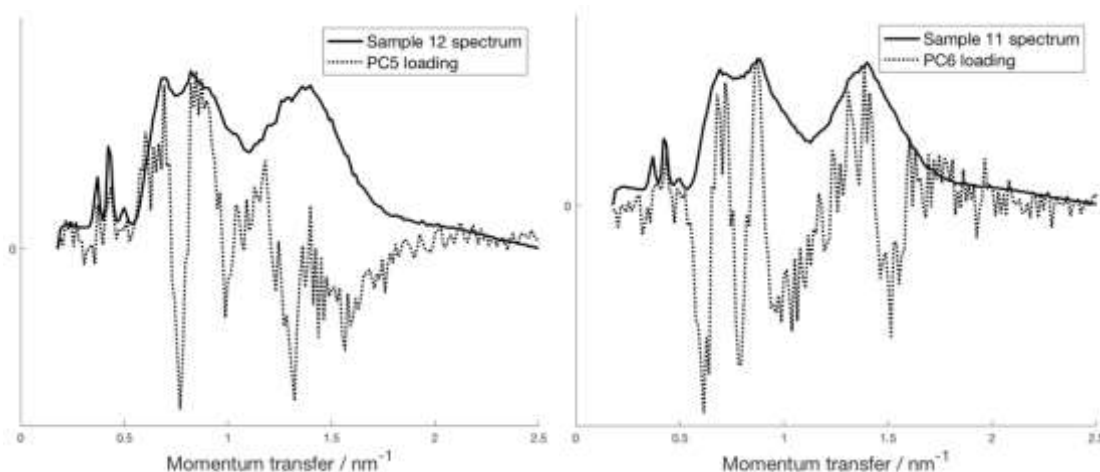


Figure 3.10 Examples of PC loadings that contained peaks matching preferred orientation effects

Some of the higher PCs' loading plots showed evidence of the preferred orientation exhibited by certain samples containing paracetamol. For example, PC5 (N.B. only 0.10% explained variance) has some peaks in its loading plot that match the position of some of the "peakiness" in sample 12's spectrum (60weight% paracetamol); PC6 (0.06% explained variance) did the same for sample 11 (80weight% paracetamol), as shown in Figure 3.10. This meant that by selecting only the lower number of PCs (or PLS-factors) in PCA (or PLS) to model the mixtures, classification and regression could be carried out without being influenced by these preferred orientation effects.

3.3.1.4 Packaged samples

The overall effect of the introduction of packaging can be observed by comparing the unpackaged and packaged spectra of any sample, as shown in Figure 3.11. There was a drop in intensity at the lower momentum transfer range (particularly noticeable in the tungsten L-lines) due to greater attenuation of lower energy X-rays. There was also a visible rise in counts at higher momentum transfer values due to the additional scatter. This interplay between additional attenuation effects as well as additional scatter meant that a simple subtraction of the unpackaged from the packaged spectra would not result in the "package-only" spectrum.

The same PCA treatment as above was carried out using the mean raw spectra for all packaged samples, giving the scores plot shown in Figure 3.12. The explained variances for the first three PCs were 90%, 8.1% and 0.74% respectively. The loading plots for these three PCs were found to be very similar to those for the unpackaged samples, indicating that the presence of packaging had not obscured the diffraction features of interest in the spectra.

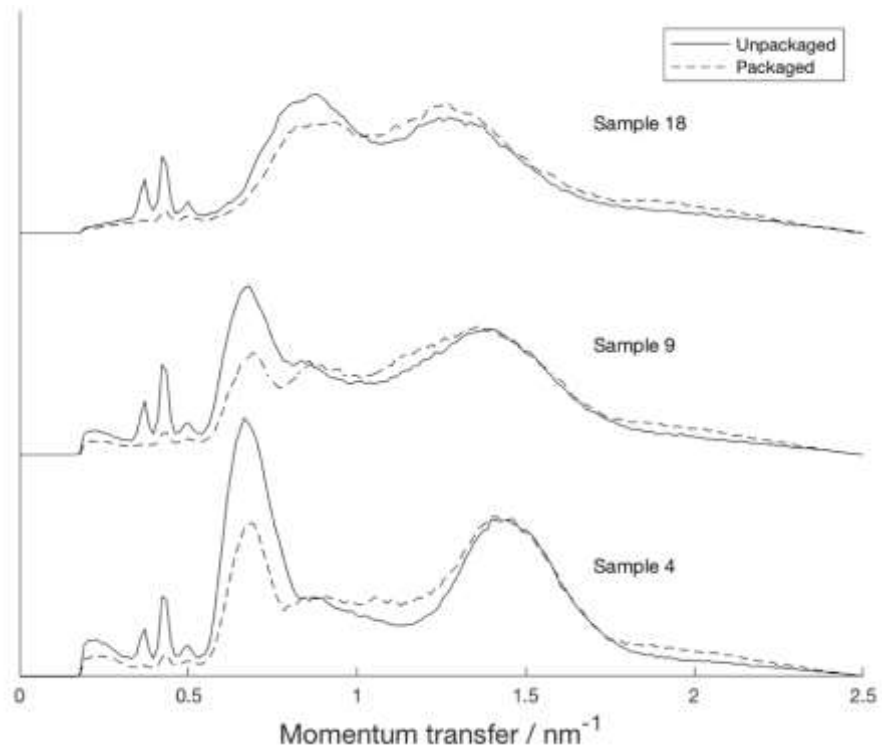


Figure 3.11 Comparison between EDXRD spectra for examples of unpackaged and packaged samples

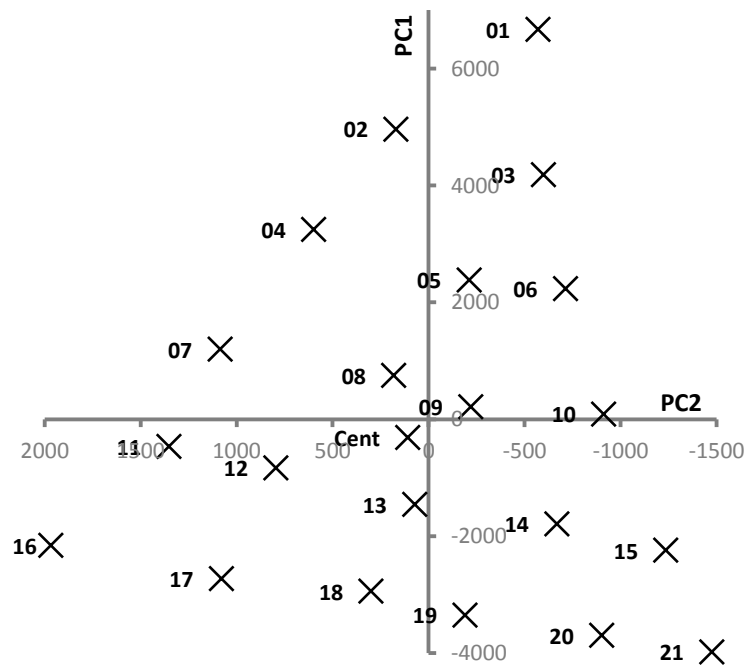


Figure 3.12 PC1 vs PC2 scores from PCA on mean raw spectra of packaged samples

3.3.2 Model Calibration

3.3.2.1 Unpackaged

PLSR was used for model calibration using the mean spectra for the 22 samples in the training set, plus the nominal concentrations of mixture components as Y-variables. Both “short” and

“long” spectral regions were studied, as discussed above. The former corresponded to 12.2 - 40.3keV, or 0.538 - 1.78nm⁻¹; the latter encompassed the full range of the X-ray tube spectrum i.e. 4.02 - 56.6keV, or 0.178 - 2.50nm⁻¹.

The models were validated using both full cross validation and test set validation. The optimum number of PLS-factors was then chosen by taking into consideration the diagnostics that were presented in section 2.3.2, and the corresponding RMSECVs and RMSEPs are presented in Table 3.3. MSC and SNV were also applied as pre-processing methods to assess their effect. The results of taking the 1st derivative of the spectra, using Savitsky-Golay smoothing with an 11-point window size and a 1st order polynomial fit, are also presented; the 2nd derivative of the spectra were found to give significantly worse results.

During the course of this analysis, it became apparent that in many cases the RMSEP was better than RMSECV, which can be explained by the fact that the test set that was used was in a region of the mixture design that was well described by the calibration model. Swapping samples between test set and training set caused some variation in results, but even when using samples 1, 2, 3, 11, 15, 16, 17, 20, and 21 (at the three extremities of the mixture space) as a test set and the remainder as a training set, the results were very similar (for raw, “long” spectra, RMSECV / RMSEP for caffeine: 1.60 / 2.33; paracetamol: 2.63 / 3.55; microcrystalline cellulose: 2.10 / 3.83), demonstrating the robustness of the model.

Diagnostic tools (described previously in section 2.3.2) were also applied to check for sample outliers in the PLSR model built from the raw, “long” spectra. Although samples 2 and 14 had studentised concentration residuals that were slightly higher than recommended (for caffeine and for microcrystalline cellulose, respectively) none of the sample leverages were over the suggested limit of three times the average, thus none of the samples were considered outliers.

The overall model was checked by plotting concentration residuals (predicted minus measured) against predicted concentrations; these should be randomly distributed about zero. In Figure 3.13 a fanning effect was observed in the case of caffeine, where higher predicted concentrations resulted in less accurate predictions. In particular, the sample 2 concentration was noticeably overpredicted, whereas sample 1 was underpredicted. This effect was not improved significantly by the addition of more PLS-factors to the model describing caffeine concentration. The plots for paracetamol and microcrystalline cellulose displayed a better distribution of residuals.

RMSECV / RMSEP (weight%)	Raw	MSC	SNV	1st derivative
Unpackaged				
Caffeine	2.00 / 1.82 (2)	3.88 / 1.89 (3)	2.57 / 1.19 (3)	2.34 / 1.95 (1)
	<i>1.99 / 1.77 (2)</i>	<i>3.68 / 1.92 (3)</i>	<i>2.54 / 1.23 (3)</i>	<i>2.34 / 1.96 (1)</i>
Paracetamol	2.41 / 3.36 (2)	4.22 / 1.88 (3)	3.66 / 3.05 (2)	2.26 / 1.80 (2)
	<i>2.58 / 3.87 (2)</i>	<i>4.47 / 2.05 (3)</i>	<i>3.78 / 2.99 (2)</i>	<i>2.39 / 1.98 (2)</i>
Mic. cellulose	1.78 / 2.44 (3)	5.54 / 2.40 (2)	4.00 / 2.73 (2)	1.85 / 2.89 (2)
	<i>1.97 / 2.78 (3)</i>	<i>5.85 / 2.43 (2)</i>	<i>4.47 / 2.74 (2)</i>	<i>1.87 / 3.05 (2)</i>
Packaged				
Caffeine	2.04 (2)	1.47 (2)	1.94 (2)	1.84 (3)
	<i>2.03 (2)</i>	<i>1.46 (2)</i>	<i>1.94 (2)</i>	<i>1.84 (3)</i>
Paracetamol	2.88 (3)	3.52 (2)	3.13 (3)	2.59 (3)
	<i>2.89 (3)</i>	<i>3.51 (2)</i>	<i>3.10 (3)</i>	<i>2.58 (3)</i>
Mic. cellulose	2.20 (3)	2.71 (2)	2.10 (3)	2.92 (2)
	<i>2.26 (3)</i>	<i>2.69 (2)</i>	<i>2.11 (3)</i>	<i>2.92 (2)</i>

Table 3.3 Results of PLSR: RMSECV from training set / RMSEP from test set (where applicable); “short” spectrum results in italics in each case; and number of PLS-factors used in parentheses. All models mean-centred.

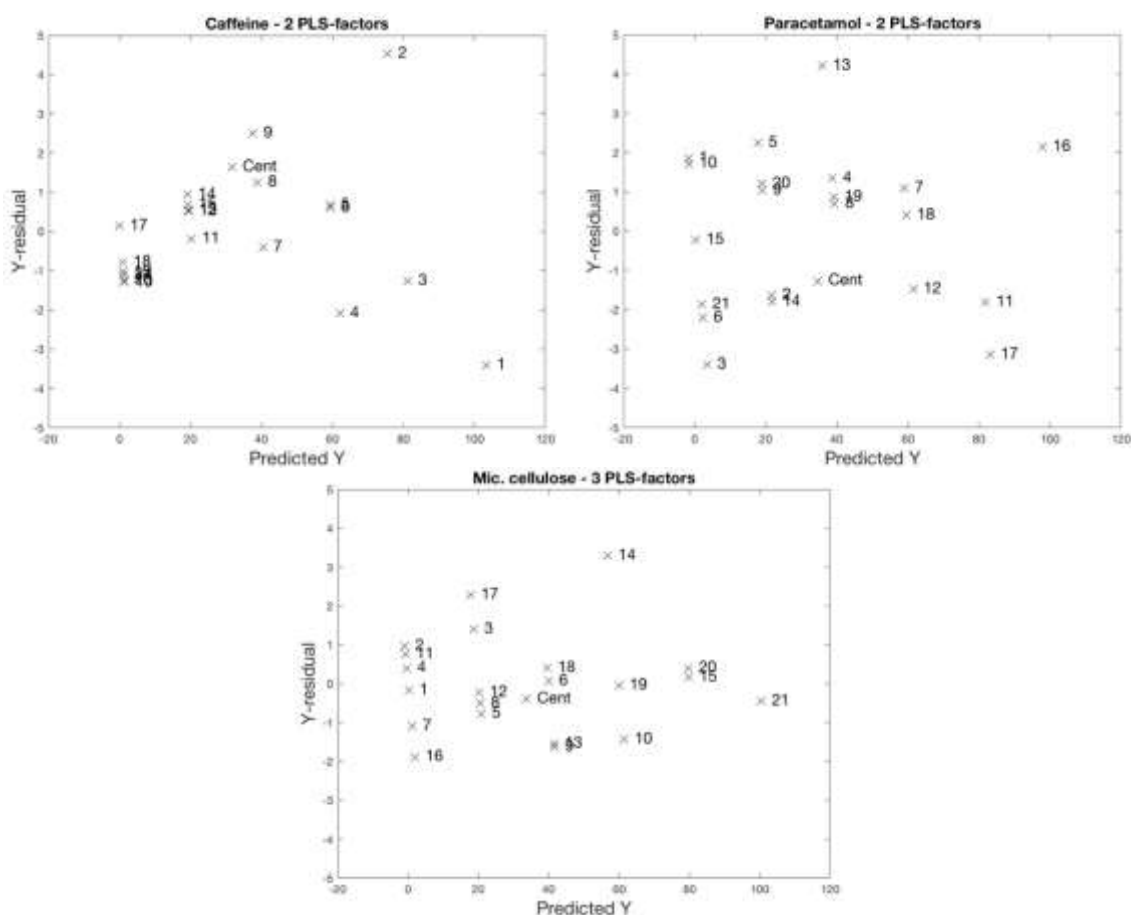


Figure 3.13 Diagnostic plots of Y-residuals vs predicted Y for raw, “long” spectra of training set only

The difference between using the full spectrum or excluding the region containing the characteristic L-lines was found to be marginal, with the “short” spectra giving slightly worse results overall. This seemed to suggest that there was some information contained within this missing part of the spectra that made the model a better predictor when using the “long” spectra, even though attenuation corrections for each individual sample had not been made in this lower-energy region.

A calibration model was also constructed using the spectra in the region greater than 18.8keV (0.83nm^{-1}) only, in an attempt to avoid the influence of the strong caffeine peak whilst leaving the 1.47nm^{-1} peak to model caffeine concentration. However, the results deteriorated significantly, presumably due to the loss of important spectral information including that from overlapping parts of the paracetamol spectra, so this procedure was not pursued further.

The application of MSC and SNV as pre-processing methods did not improve the model, as can be seen from the similar or raised RMSEs in Table 3.3. For MSC, the diagnostic plot of spectral value versus mean spectral value did not show any strong tendencies for different slopes or offsets between samples, which indicated that it was probably not needed. In fact, this

treatment resulted in the need for an additional PLS-factor to best describe the data. In the case of SNV, oddly the caffeine was best described by the use of 3 PLS-factors – the loadings plot showed that this 3rd factor contained additional information on the caffeine spectrum.

The 1st derivative of the spectra gave the best improvement, with similar RMSEs achieved using fewer PLS-factors than for the raw data. This type of pre-treatment has been found to be advantageous by correcting for baseline drift across profiles [283,286]. However, it has the disadvantages of requiring a careful choice of the number of points to use for smoothing (which would vary with different spectra containing sharper or broader peaks), as well as making model interpretation more difficult.

In the absence of any significant improvement to the model performance from using pre-treatments, the use of raw data was preferred. The predicted concentrations from cross-validation and test set validation for the “long” spectra were plotted against nominal concentrations for caffeine (Figure 3.14), paracetamol (Figure 3.15) and microcrystalline cellulose (Figure 3.16). These plots showed that there was a strong positive correlation in all cases. The paracetamol concentration predictions in Figure 3.15 were slightly more spread in the lower concentration range, as expected by the slight variations in spectra from preferred orientation that were not included in the calibration model. The RMSECV and RMSEP values in Table 3.3 thus follow from this by showing that the largest errors were for paracetamol; the caffeine and cellulose values exhibited smaller errors. Note that the nominal concentration values are likely to differ from the actual concentrations due to errors introduced when measuring the powders and due to possible inhomogeneity in the mixture; in a similar experiment by Moore *et al.*, the cumulative error in preparing such tablets was estimated to be 2 to 3%, therefore these results are statistically acceptable [246].

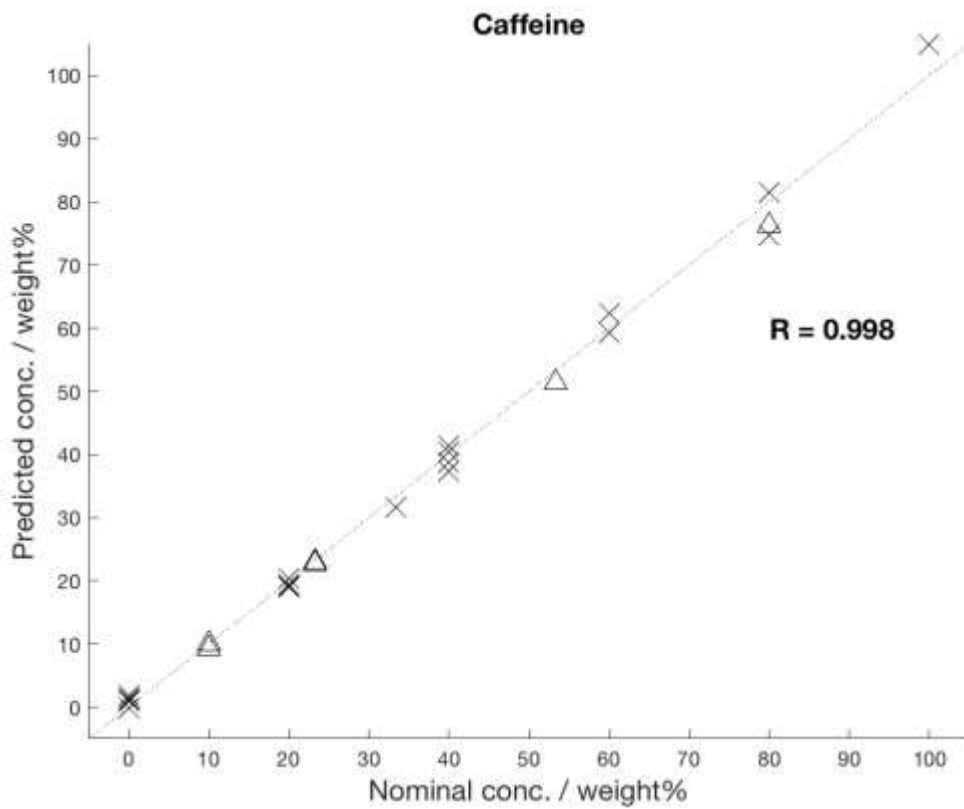


Figure 3.14 Predicted vs nominal concentrations of caffeine for unpackaged samples; cross validation (x) and test set (Δ) results; dashed line denotes where $y = x$

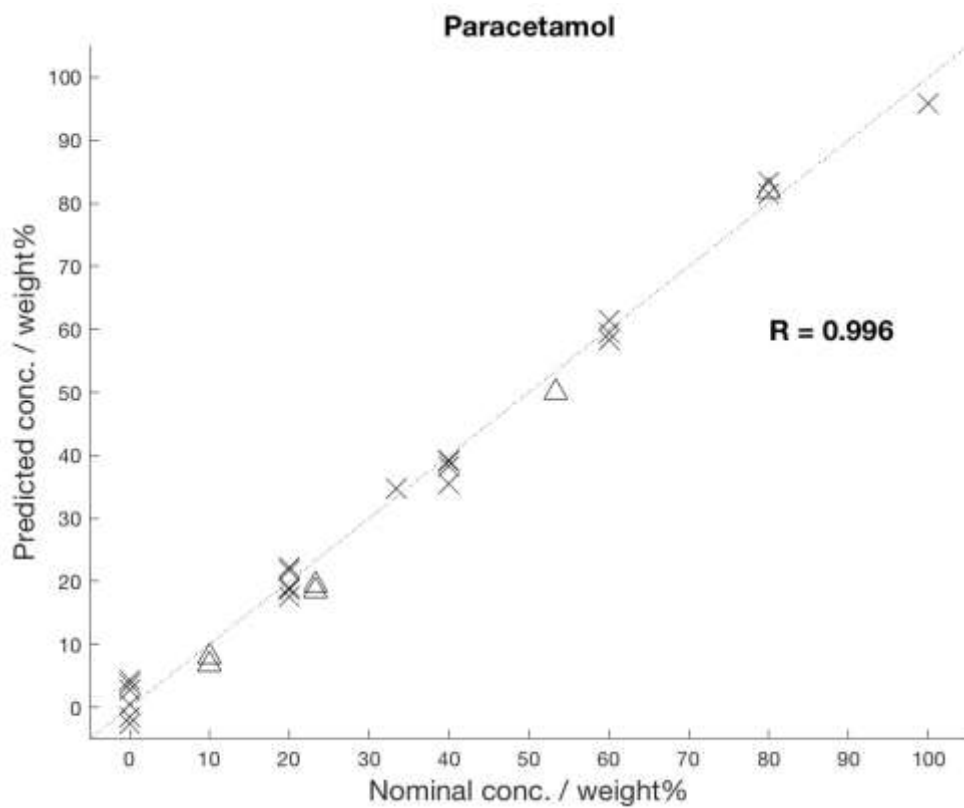


Figure 3.15 Predicted vs nominal concentrations of paracetamol for unpackaged samples; cross validation (x) and test set (Δ) results; dashed line denotes where $y = x$

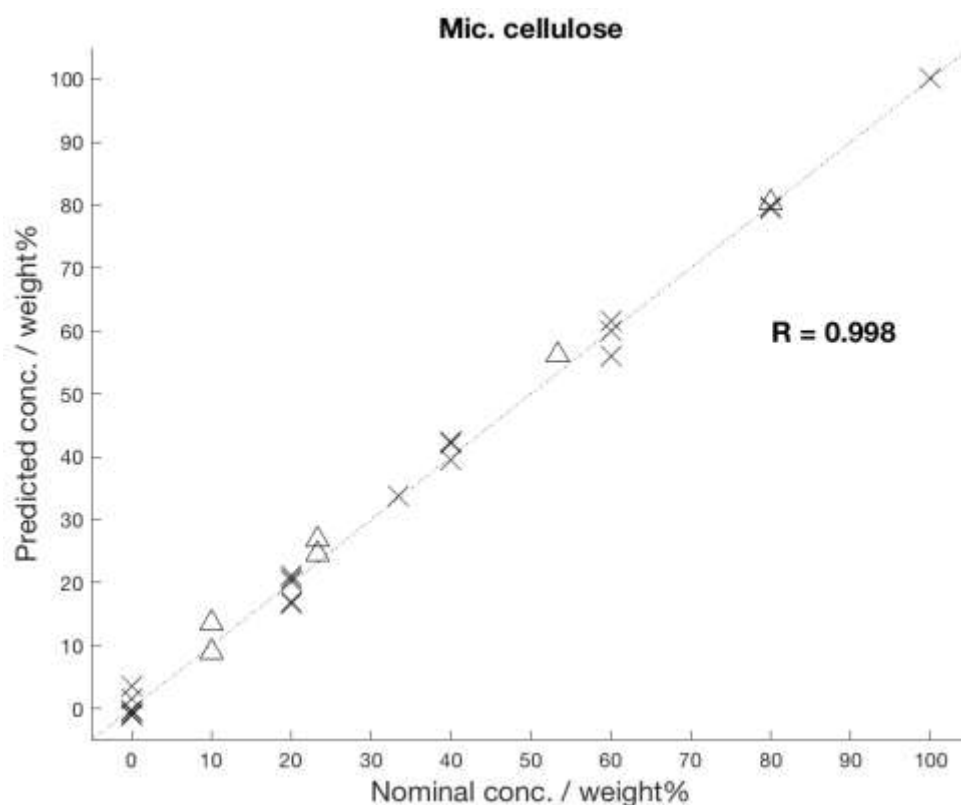


Figure 3.16 Predicted vs nominal concentrations of cellulose for unpackaged samples; cross validation (x) and test set (Δ) results; dashed line denotes where $y = x$

3.3.2.2 Packaged

The same methods that were used for the unpackaged dataset were applied to the mean spectra for the packaged samples, with the resulting RMSECVs also presented in Table 3.3. The predicted concentrations from cross-validation for the raw, “long” spectra were plotted against nominal concentrations for caffeine (Figure 3.17), paracetamol (Figure 3.18) and microcrystalline cellulose (Figure 3.19). Once again, these plots demonstrated that there was a strong correlation between the two and that the model was performing well. Unfortunately, due to an accidental loss of alignment in the EDXRD system prior to collecting data for all packaged test samples, there are no RMSEP values.

RMSECVs for the PLSR model based on raw, “long” spectra were in general higher for the packaged dataset than for the unpackaged case. There was a 20% and 24% increase on the RMSECV values for paracetamol and microcrystalline cellulose respectively, but only a 2% increase for caffeine. It is possible that some of the potential change in prediction error for caffeine was mitigated by the greater effect of attenuation on its main peak (which had previously adversely affected the “unpackaged” model as seen in Figure 3.13). A higher PLS-factor that described the effect of packaging could not be identified; as others have noted, it is

possible that the interference caused by this additional component was not isolated in one factor but could be present in a variety of PLS-factors, thus influencing the predictive ability of the model [289].

The same diagnostic tools were applied to this model and once again there were no noticeable outlier samples. The concentration residual vs predicted concentrations plot for caffeine no longer displayed a strong “fanning” effect as seen previously – likely to be an effect of the attenuation of the caffeine peak. Instead, the centroid sample stood out as having the greatest concentration residual, but as it did not have a high leverage it was not considered to be problematic.

The same pre-processing methods as above were trialled here, and the results have been included in Table 3.3. The effect of MSC was more promising than for the unpackaged dataset, but in general the three methods used gave a mixed response in terms of improving the RMSECVs for one or two of the constituent chemicals whilst adversely affecting the other(s). Furthermore, the difference between using the “long” and “short” spectra was marginal, due to the attenuation of features at low energies by the packaging, thereby reducing their influence.

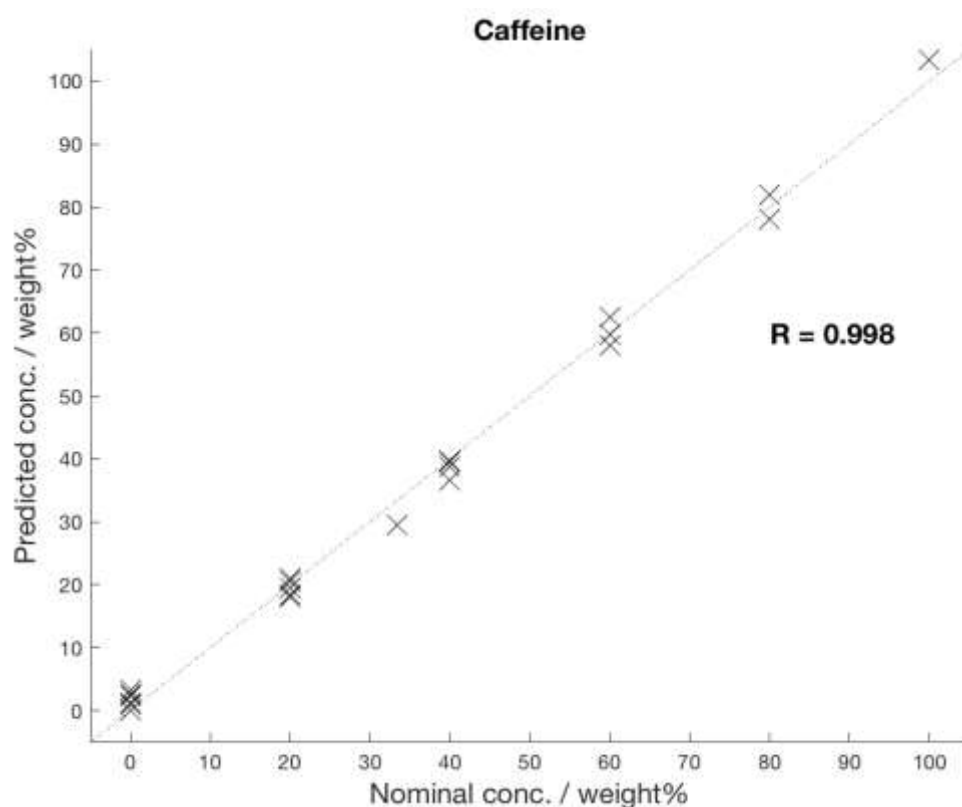


Figure 3.17 Predicted vs nominal concentrations of caffeine for packaged samples; dashed line denotes where $y = x$

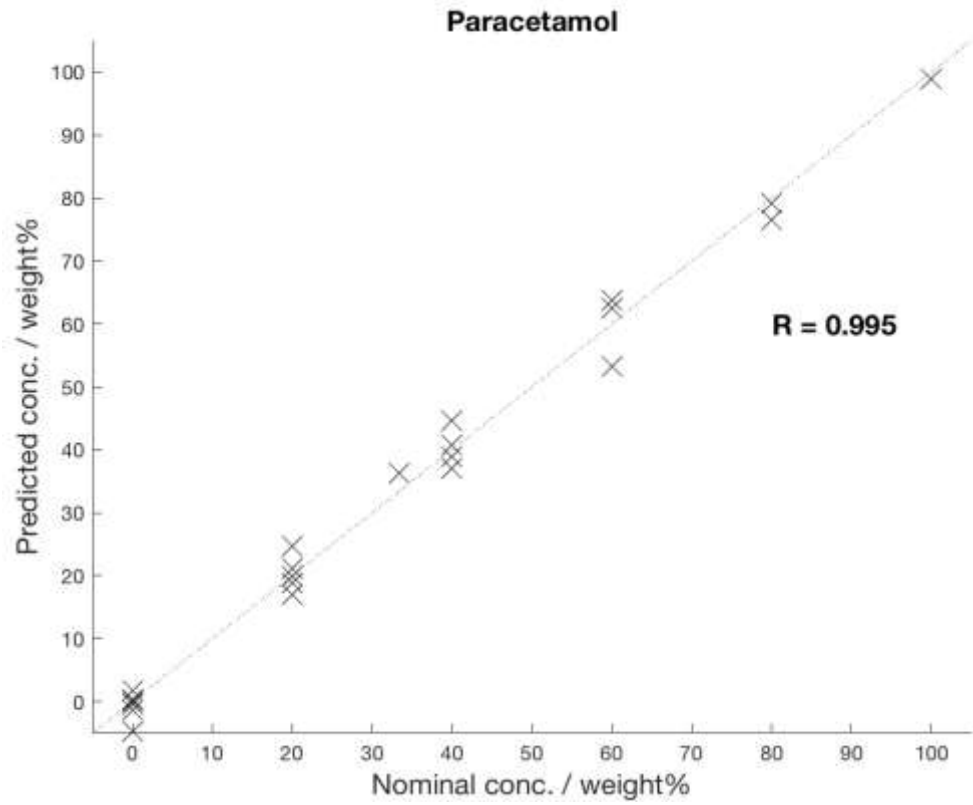


Figure 3.18 Predicted vs nominal concentrations of paracetamol for packaged samples; dashed line denotes where $y = x$

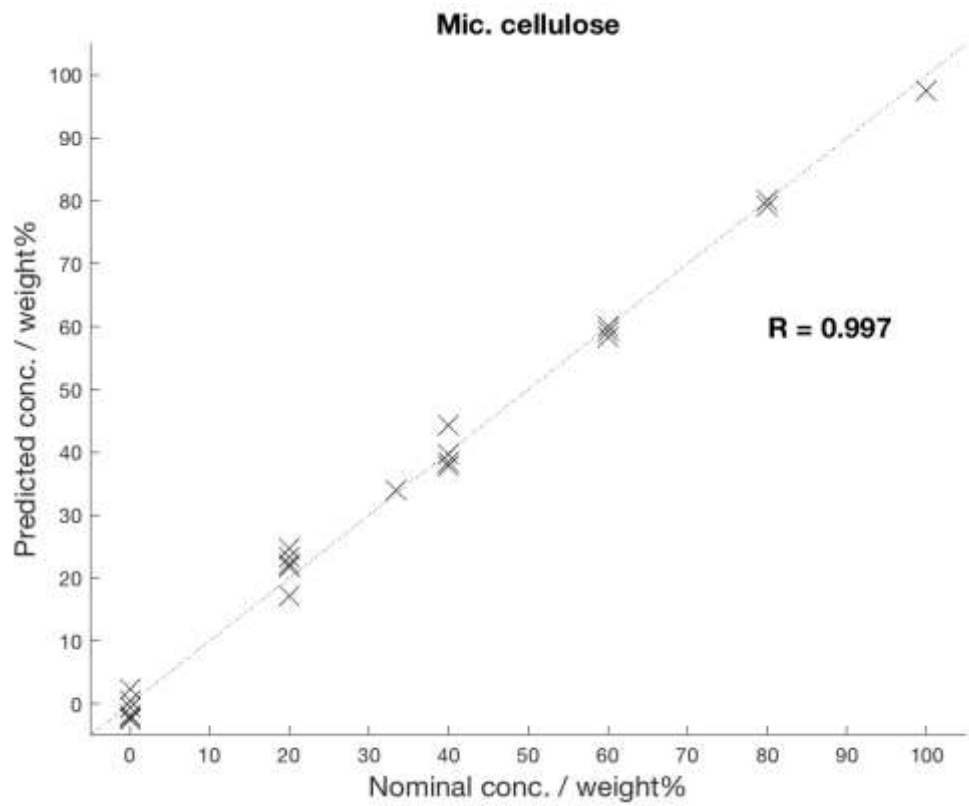


Figure 3.19 Predicted vs nominal concentrations of cellulose for packaged samples; dashed line denotes where $y = x$

3.3.3 Predictions

Additional concentration predictions were made in The Unscrambler using spectra from samples of OTC medicines that contained one or both of the APIs used in the calibration above. Note that this experiment was only carried out on unpackaged tablets.

Nominal API concentrations (in weight%) were calculated from the stated API mass divided by the measured tablet mass. The nominal concentration errors were calculated using the error when weighing tablets, and information from the British Pharmacopoeia monograph for “paracetamol and caffeine tablets”, which allows for the actual amount of API to be $\pm 5\%$ of the stated amount – although it was not known whether it was likely to vary to this extent in practice. Similar information for caffeine-only tablets could not be found, so it was presumed that variation in API percentage would be of the same range. Deviations of predictions are computed by the software, and can be thought of as a 95% confidence interval around the predicted value [295].

Sample	Nominal (weight%)			Predicted (weight%)		
	Caff	Para	M. cell	Caff	Para	M. cell
Panadol Extra Advance	8.6 \pm 0.4	66 \pm 3	-	7.2 \pm 9.5	71 \pm 12	-
Boots Paracetamol Extra	10.0 \pm 0.5	78 \pm 4	-	7.7 \pm 8.7	77 \pm 11	-
Pro Plus	31.3 \pm 1.6	-	-	41 \pm 13	-	-

Table 3.4 Prediction results for unpackaged tablets

The resulting predictions presented in Table 3.4 were generally close to the nominal concentrations, although technically they are considered to be outliers as their large prediction deviations reveal their different composition compared to the mixtures used for model calibration. None of the samples used contained microcrystalline cellulose, and they all contained a variety of other excipients, so prediction results were not expected to be accurate – yet, this still demonstrated some predictive ability even outside the mixture types for which the model had been made.

3.4 Summary

The above work describes a preliminary study on ternary mixtures using EDXRD, which is not commonly used for analysis of pharmaceutical powders. The use of PLSR on raw spectra resulted in predictive abilities on a par with those reported in the literature for other analytical techniques, which was very promising. More specifically, the RMSECV values (2.1weight% on average) were better than those quoted in a study presenting the quantitative analysis of ternary mixtures by ADXRD and PLSR (5.5weight% on average) [233]. This was despite the EDXRD spectra used here being of far lower resolution, and without requiring data pre-treatments. This result was then successfully replicated for tablets *inside* packaging, although the prediction errors were increased slightly.

In the context of the detection of poor-quality medicines, it should be noted that the use of PLSR analysis will be limited, as it is not feasible to create calibration models for the vast number of possible combinations of pharmaceutical materials in order to predict exact concentrations of constituents in a suspect tablet. Rather, classification methods providing a pass/fail type response based on a library of spectra from known, genuine medicines is expected to carry more potential in this area – and is the route commonly used in conjunction with other analytical methods as seen in section 1.2.2.3.. Therefore, this approach was taken for the remainder of this thesis.

Chapter 4: Intact Formulations Tests

4.1 Background

The experiment described in the previous chapter showed the potential for EDXRD to be used in a non-destructive manner to assess poor-quality solid pharmaceutical formulations. However, it became apparent that it would not be realistic to build calibration models for all possible pharmaceutical API/excipient combinations for accurate quantitation. More importantly, quantitation would not be required for a preliminary fast-screening test in the field, as other analytical methods (such as HPLC) would be far more effective for this purpose. Therefore, a pass/fail classification method was investigated next.

There are many examples in the literature of the use of classification methods applied to spectroscopic and chromatographic data from pharmaceuticals (e.g. [52,183,188,253]). The only case where classification was applied to ADXRD data was in a short communication by Komsta and Maurin [296]. They analysed a range of OTC medicines (after removing their coatings and grinding them) and used a method called PLS-Discriminant Analysis (PLS-DA) to categorise them on the basis of the presence or absence of paracetamol. Their preliminary results showed that neither visual inspection nor simple correlation would have identified the paracetamol peaks, but that no samples were misclassified when using PLS-DA. They concluded by suggesting that this novel area of research was worth investigating further.

In the present study, SIMCA (see section 2.3.3) was chosen as the classification method because it allows for further sample classes to be added independently to the existing set of PCA models, such that the “library” of drug types may be kept up to date [297]. To this end, PCA models encompassing expected variations of spectra from the drug class(es) of interest must first be constructed. For example, Scafì *et al.* previously used NIR spectra from at least ten different batches of aspirin that were acquired in local pharmacies [186]. Rodionova *et al.* used several batches of amlodipine (a medicine to treat hypertension) from seven different manufacturers, each containing 5mg of API and similar excipients. A selection of drugs containing completely different APIs (to emulate grossly substandard products) as well as drugs containing the same API combined with other APIs (to emulate poor-quality drugs that are more challenging to detect) were purchased for testing against the model developed [52]. Similarly, in Said *et al.*'s study, a selection of paracetamol tablets were purchased and then compared to test samples

that included additional APIs, or had a different API [188]. In this way, they demonstrated how a combination of NIR spectra and SIMCA could be used to check whether intact formulations were of good or poor quality, *without* any quantitative determination of API nor excipient concentrations. A similar approach was chosen for the purposes of the work described below.

4.2 Methodology

4.2.1 Sample collection

OTC painkillers were chosen for this study due to their low cost, wide availability, range of manufacturers, and range of APIs plus combinations of APIs used. 23 packets of tablets or caplets (elongated tablets, more similar in shape to capsules) containing 500mg paracetamol as the sole API were purchased in various pharmacies and supermarkets, encompassing six different manufacturing sources. Purchases were made over a period of several months in order to sample a range of batch numbers (between two to eight per manufacturer), but also because purchases of painkillers were limited to two packets per transaction (one packet only in the case of codeine-containing medication), according to national guidelines [298]. 22 packets of different batches of tablets/caplets containing 200mg ibuprofen as the sole API were purchased in a similar manner, encompassing six different manufacturing sources. A packet each of other types of painkillers containing combinations of APIs, or related APIs, were also purchased as test samples (dubbed “OTC-Other”). The details of all samples are listed in the Appendix.

4.2.2 Sample scanning

The EDXRD setup B has been described previously in section 2.1.2. Raster scanning was introduced as preliminary tests found that some OTC pills displayed preferred orientation effects, occasionally producing very strong peaks. For the unpackaged scans, one pill from each batch listed in the Appendix was removed from its blister and EDXRD spectra were acquired for 5, 15, 30, 75, 150, 300, and 600s. All scans were triplicated, with the pill removed and replaced in a different orientation each time (i.e. either rotated upside down, or flipped back to front) to account for within-sample and positioning differences.

A second dataset was collected for all the above batches and for the same range of acquisition times – again in triplicate – using a second pill from each pack kept sealed within its blister. A third dataset was collected for the same within-blister pills, but this time positioned at the centre of an additional ring of cardboard – making up the dataset named “bliscard”.

4.2.3 Chemometrics

Triplicate scans were averaged before analysis. For both paracetamol and ibuprofen sample sets, a random number generator was used to select a test set of 5 samples, with the remainder used as a training set. PCA models were then constructed using the training set only in each case. Separate models were created and evaluated for each acquisition time. This process was repeated for two additional test and training set combinations (also selected randomly) to check the robustness of the results. This whole process was then repeated for the blister-packaged, then the “bliscard” datasets.

The test sets of spectra (i.e. 5 “positive” test samples per model), as well as the spectra from the “OTC-Other” set (i.e. 19 “negative” test samples for all models), were then classified using their relevant PCA model in The Unscrambler. The significance level was kept at the default value of 5% throughout this study. The raw data were used in all cases, due to the conclusion from the previous chapter that pre-treatments did not result in distinctive improvements to results.

The resulting classification tables (indicating whether each sample was classed as belonging to a particular PCA model – or not) from each scenario were used to tally the numbers of true positives and true negatives. These were in turn used to calculate sensitivities and specificities, which were plotted vs acquisition time.

4.3 Results and Discussion

4.3.1 Exploratory analysis and PCA model development

4.3.1.1 *Paracetamol*

The API weight percentages for the samples were calculated using the nominal mass of paracetamol (500mg) divided by the mass of each pill used; these were found to range between 83 and 91weight%. Thus, excipients (of which there were anywhere between three and 13 listed) made up 9 - 17weight% of the pills. There was little variation seen in their background contribution to the EDXRD spectra even where they differed between manufacturers, which is probably due to the mixture of organic and inorganic excipients (i.e. covering a broad momentum transfer range), as well as there being a low proportion of each. The spectra were all dominated by the paracetamol peaks.

Differences between sample spectra were also expected to arise from the varying thicknesses of the pills. In the results from Chapter 3, it was established that the sub-3mm-thick pressed

tablets did not suffer greatly from self-attenuation effects. The OTC paracetamol samples, on the other hand, ranged between 3.8mm and 5.2mm in thickness. Yet, it was not possible to apply any attenuation corrections in this instance, as the compositions of the pills were unknown – only the quantity of API is given in a pharmaceutical formulation, along with a list of excipients of unspecified amounts.

Triplicating the data collection process allowed checks to be made on preferred orientation effects that can be significant in the case of paracetamol, as seen previously. For example, some samples in the “unpacked” dataset exhibited the occasional strong peak (e.g. Alexander’s Paracetamol (2) shown in Figure 4.1A), but for the most part the raster scanning meant that the effect was not strongly apparent (e.g. Hedex (1) in Figure 4.1C). In addition, some of the differences between replicates may have been caused by other changes such as slight differences in pill positioning, inhomogeneity in the distribution of API within the pill, and the fact that the amount of API could vary from the stated value of 500mg by $\pm 5\%$ according to the British pharmacopoeia.

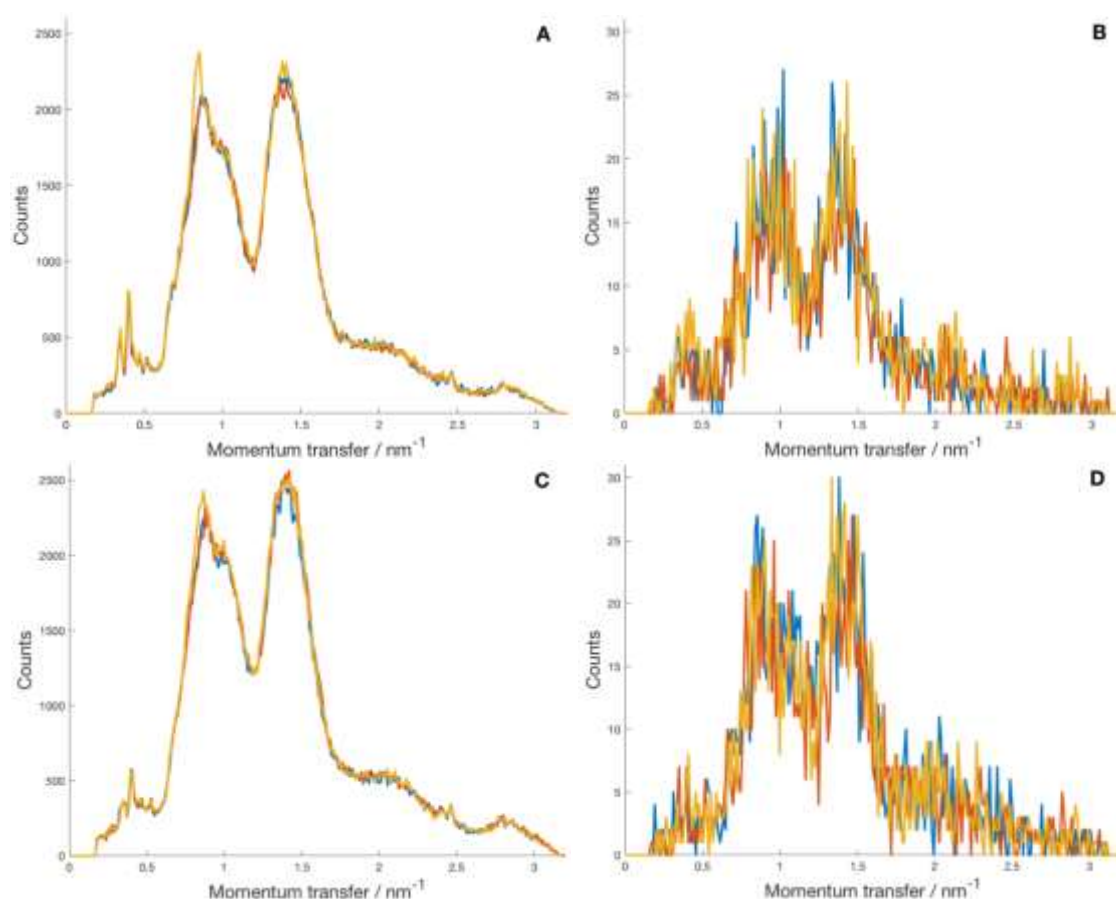


Figure 4.1 Triplicate spectra collected for unpackaged Alexander’s Paracetamol (2) (A & B) and Hedex (1) (C & D) for 600s and 5s acquisitions respectively

Figure 4.1B and D demonstrate the greater levels of noise in spectra acquired for the shortest acquisition time of 5 seconds compared to the 10-minute (600s) scan. The shape of the diffraction peaks was above the noise level however, so the use of chemometric methods was expected to draw out these key features whilst discarding the noise.

The PC2 vs PC1 scores plot from the PCA analysis on the full unpackaged dataset, using the raw data for the 600s acquisitions, is presented in Figure 4.3. PC1 and PC2 described 72.7% and 11.6% of the variance respectively. The former separated samples between tablets and caplets due to the different thicknesses between these two pill shapes; the caplets were 1.3mm thicker on average than tablets, and thus contained a greater amount of material – and hence paracetamol – in the diffracting volume. The effect was not attributed to differences in API weight percentages, which were comparable across tablets and caplets. The PC1 loadings shown in Figure 4.3 corresponded very well to the paracetamol reference diffraction pattern (generated using Mercury v.3.9 [238] and CSD-HXACAN18 [239], with peak broadening). The negative loadings on the characteristic L-lines explain why all tablets, being thinner, had a negative PC1 score; as they were less affected by attenuation, these peaks were more prominent in their spectra. The PC2 loading (not shown) highlighted a preferred orientation peak that separated out the Boots Paracetamol (1) sample – hence its high PC2 score.

In addition, the scores plot indicated that there was some spread in PC-space dependent on manufacturer (see symbols in Figure 4.2). However, as there was plenty of overlap between these sub-groups, the dataset was treated as a whole for 500mg paracetamol formulations.

For comparison, the equivalent data for the 5-second acquisition is shown in Figure 4.4. The samples appear more evenly spread here, but the tablet samples all had negative scores for PC1, and there was some evidence of grouping by manufacturer. PC1 here described only 16.6% of the between-sample variance, followed by 9.43% by PC2. Although these were very low values, the loadings plots showed that anything above that for PC1 (shown in Figure 4.5) were describing noise.

Following this initial analysis, the samples were split randomly into test and training sets, as shown in Table 7.1 (Appendix). PCA models were created for the three training datasets of raw spectra, for each acquisition time. In all cases, the removal of these five test samples did not change the conclusion that one PC was optimal to describe the dataset. The loading plots for any higher PCs described preferred orientation effects and noise, so were not used even if explained variances of the resulting models were occasionally very low (particularly for the shorter acquisition times, as seen above).

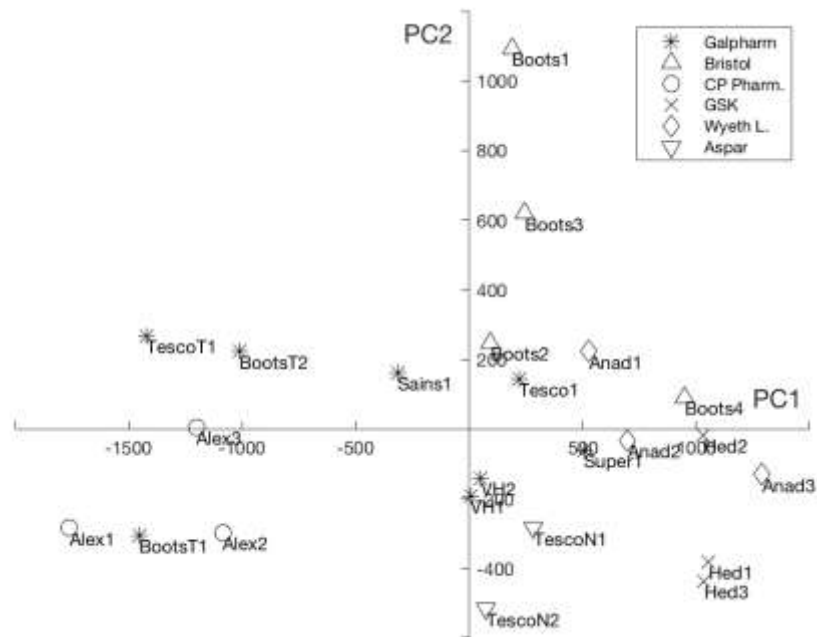


Figure 4.2 PC2 vs PC1 scores from PCA on spectra from 600s scans of unpackaged paracetamol

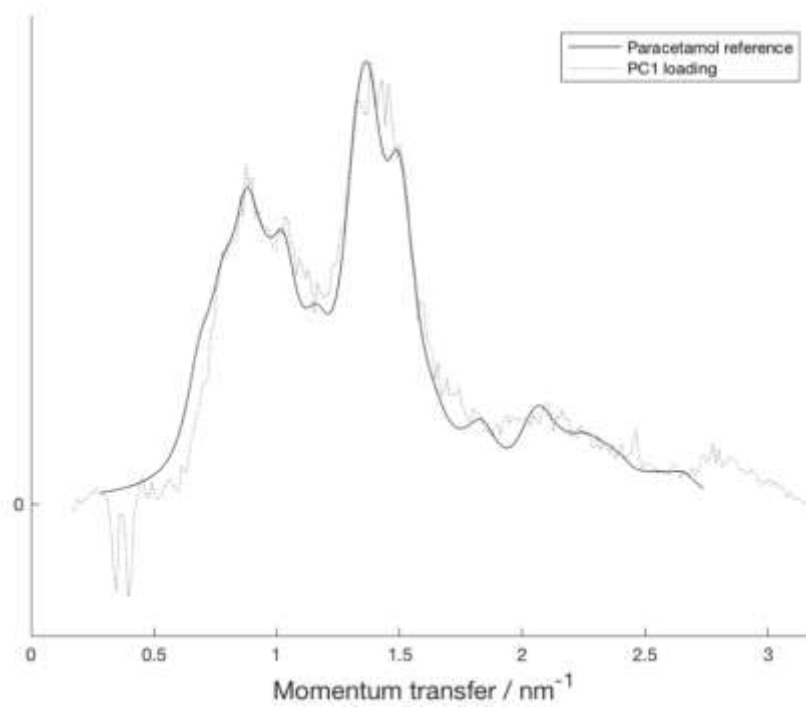


Figure 4.3 PC1 loadings from PCA on spectra from 600s scans of unpackaged paracetamol

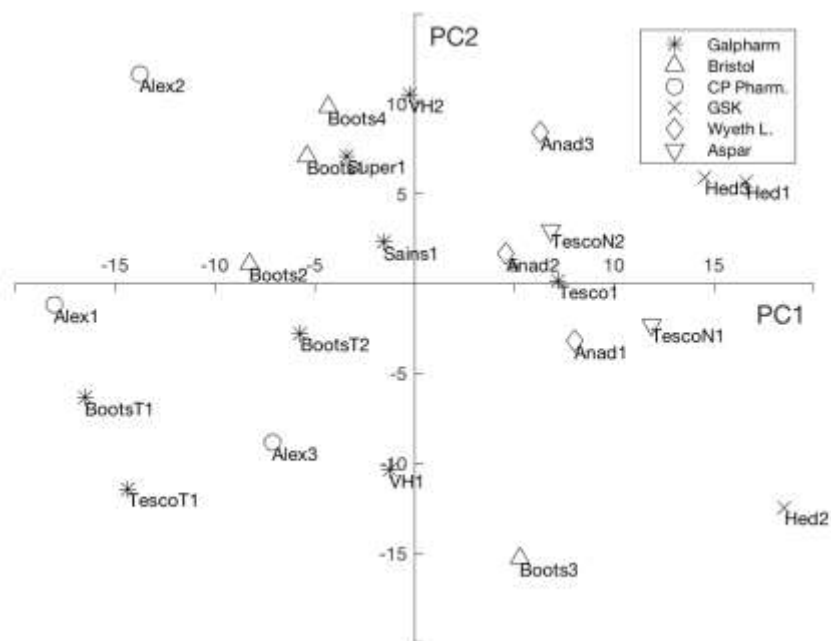


Figure 4.4 PC2 vs PC1 scores from PCA on spectra from 5s scans of unpackaged paracetamol

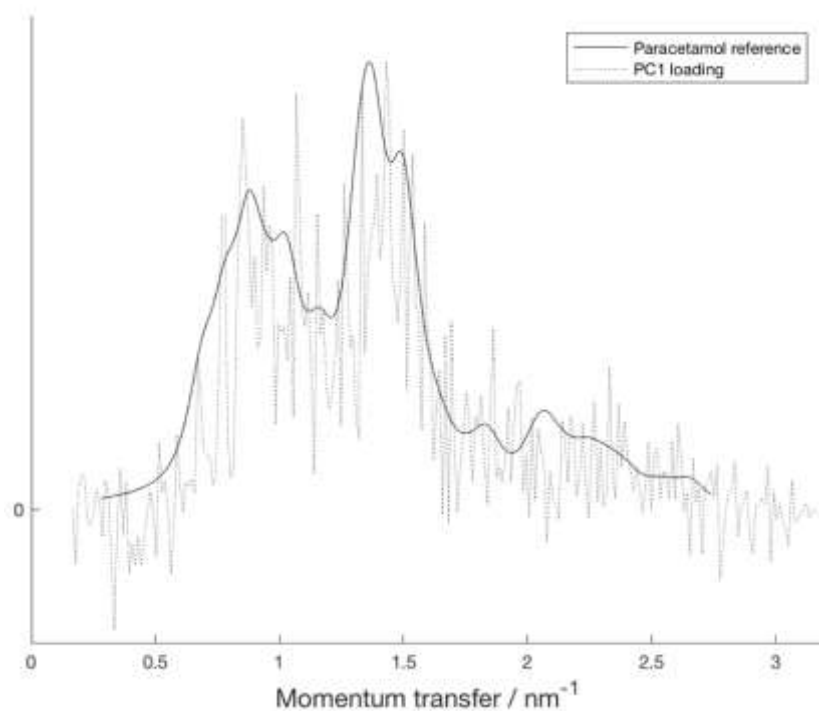


Figure 4.5 PC1 loadings from PCA on spectra from 5s scans of unpackaged paracetamol

Prior to data collection for the packaged samples, spectra were collected for a selection of blister-packaged paracetamol samples from the same manufacturer (Galpharm International Ltd) in two configurations: with the foil side, then the plastic side of the blister facing the X-ray source. PCA was performed on these spectra, and a two-sample t-test was applied to the scores for PCs 1 and 2 to check whether the blister orientation affected the EDXRD spectra. In both

cases, the null hypothesis (that both “foil” and “plastic” sets were from populations with equal means) was not rejected at a 5% significance level – and this was the case for all acquisition times used. Therefore, the difference between the two were deemed to be negligible and later scans were made without repeating separate datasets for foil and plastic faces of the blister.

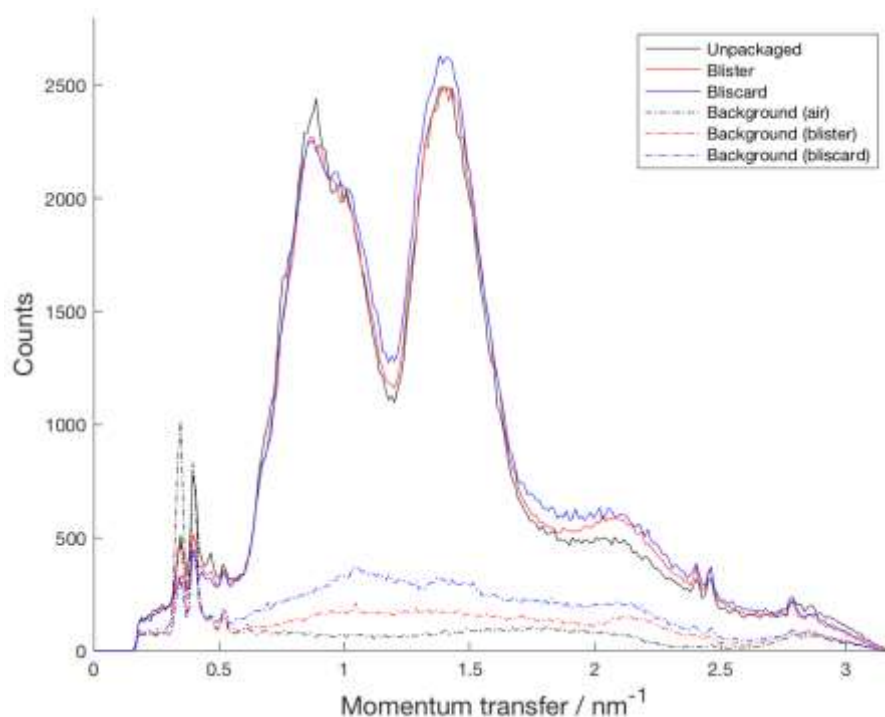


Figure 4.6 Boots Paracetamol (4) spectra with different packaging levels, plus background spectra (600s)

The spectra collected for the blister and “bliscard” datasets occasionally displayed preferred orientation effects that masked the increased scatter at higher energies and greater attenuation at lower energies. In general, however, the introduction of packaging followed the same pattern as that shown in Figure 4.6. The addition of card was notable in its greater scatter contribution compared to the blister-only case at higher momentum transfer values. However, this additional scatter combined with the greater attenuating effect from the addition of card (see Figure 3.6) meant that the diffraction peak at $\sim 0.9\text{nm}^{-1}$ was similar in intensity to that from samples with blister-packaging only.

The same PCA procedure was then applied, with scores plots for the 600s acquisitions presented in Figure 4.7 for the blister-packaged, and Figure 4.9 for the “bliscard” samples. These demonstrated similar features to the unpackaged case, with the thinner tablet samples and the thicker caplets grouping separately, and the first PC describing the majority of the variance (75.6% for blister, 82.0% for “bliscard”). Their respective PC1 loadings plots (Figure 4.8 and Figure 4.10) matched the paracetamol reference spectrum well. Thus, one PC was again chosen as the optimal number for SIMCA analysis.

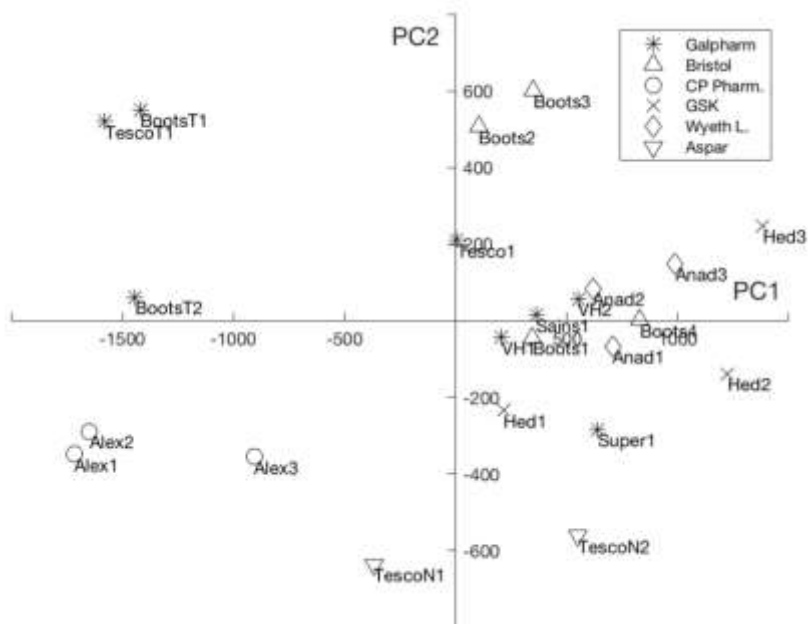


Figure 4.7 PC2 vs PC1 scores from PCA on spectra from 600s scans of blister-packaged paracetamol

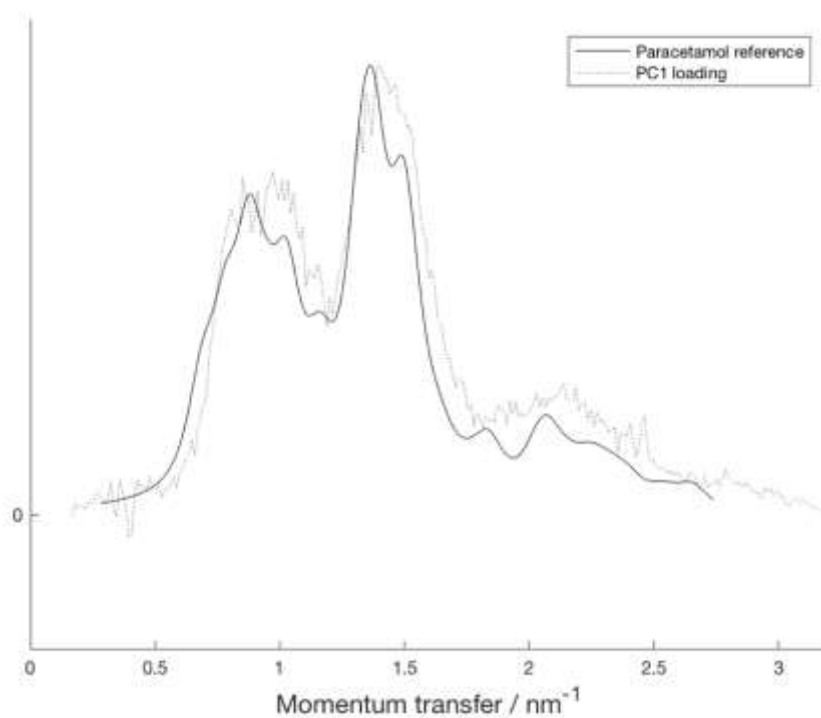


Figure 4.8 PC1 loadings from PCA on spectra from 600s scans of blister-packaged paracetamol

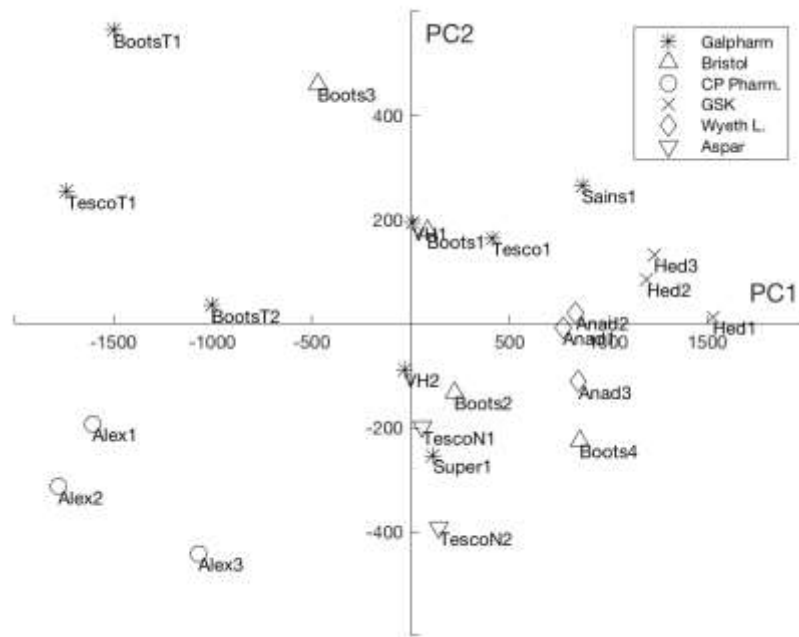


Figure 4.9 PC2 vs PC1 scores PC1 loadings from PCA on spectra from 600s scans of “bliscard” paracetamol

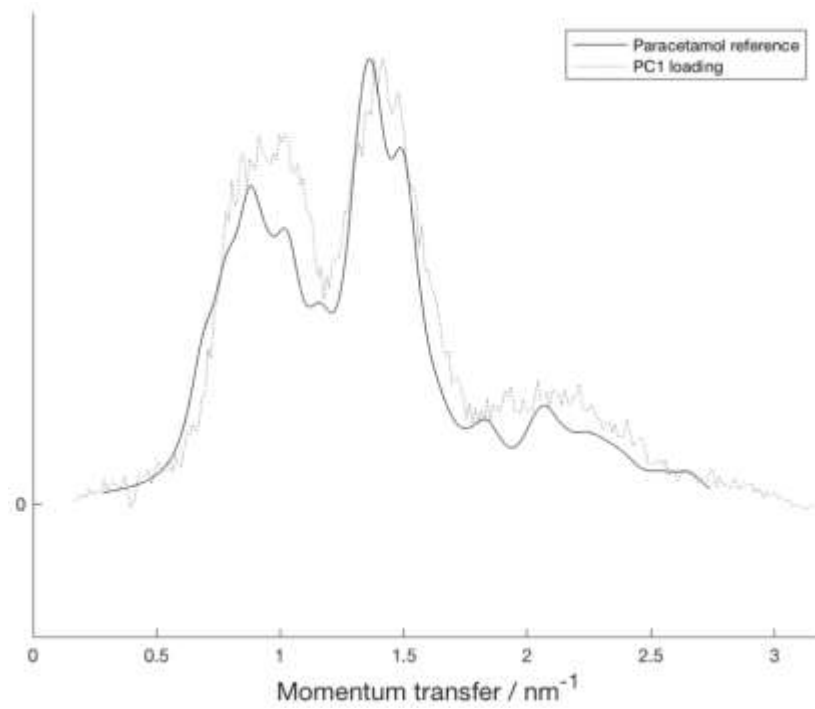


Figure 4.10 PC1 loadings from PCA on spectra from 600s scans of “bliscard” paracetamol

4.3.1.2 Ibuprofen

The API weight percentages of ibuprofen formulations were calculated as above; these had a much wider range: between 35 and 76weight%. The smaller amount of API (200mg) resulted in greater sensitivity of its weight percentage to the differences in pill sizes – pill thicknesses varied between 4.2 and 6.6mm – and the proportion of excipients was greater than in the case of paracetamol. Correspondingly, the variation seen in the latter’s background contribution to the EDXRD spectra was much greater, as demonstrated by Figure 4.11; a similar effect was documented in Rodionova *et al.*’s study of NIR spectra of amlodipine drugs which contained only 10mg of API [52]. It was also noticeable that the number and type of excipients used varied much more depending on manufacturer, plus a large proportion of pills had a hard coating, which had not been seen in the paracetamol case.

Preferred orientation effects were not observed in the vast majority of scans. Within the unpackaged spectra, discrepancies were seen in Alexander’s Ibuprofen (1) and (2), and Nurofen caplets (1) only. For the blister and “bliscard” scans, once again, Alexander’s Ibuprofen (1) and (2) both had the greatest variations between replicate scans; in addition, Nurofen tablets (1) had one small extra peak in one replicate, at 0.67nm^{-1} , and Sainsbury’s Ibuprofen (2) and Tesco Ibuprofen (1) had a stronger peak at 1.98nm^{-1} . All of these were found to correspond to diffraction peaks seen in the ibuprofen reference spectrum (generated using Mercury v.3.9 [238] and CSD-IBPRAC03 [239], with peak broadening).

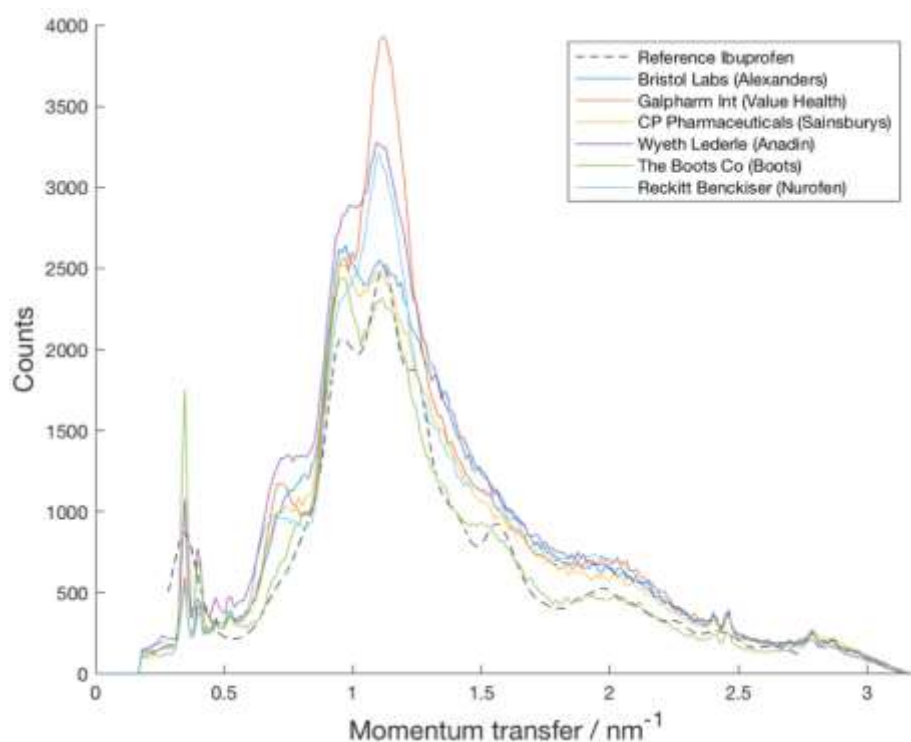


Figure 4.11 EDXRD spectra from ibuprofen manufacturers included in this study

The PC2 vs PC1 scores plot from the PCA analysis carried out on the 600s acquisitions of EDXRD spectra for the full, unpackaged, sample set is presented in Figure 4.12. It was clear from this plot, plus from inspecting the PC3 scores, that there was a greater separation based on manufacturers, as would be expected from the range of spectral shapes seen in Figure 4.11. It also highlighted that although both the new Superdrug Ibuprofen caplets and the Alexander's Ibuprofen tablets were manufactured by Bristol Laboratories Ltd, they had distinctly different spectra due to a different composition of excipients used. Pre-processing of all spectra was attempted, but did not appear to increase nor decrease the separation based on manufacturer differences.

The explained variances for PCs 1, 2 and 3 were 70.7%, 17.6%, and 6.45% respectively, and their respective loadings plots are shown in Figure 4.13. The first two PCs had loadings pointing to the high intensity of the main ibuprofen peaks in the Galpharm International-made samples (o's in the scores plot) compared to relatively low intensity of these in the spectra of the CP Pharmaceuticals-made samples (* in the scores plot) in Figure 4.12; hence the range from positive scores for the former to negative scores for the latter along these two PCs. The 3rd PC loadings in Figure 4.13 focused on the low-energy ibuprofen diffraction peak that was strongest in the Boots Ibuprofen samples (see Figure 4.11). Higher PCs were not found to describe much additional variation, nor did the loadings or residuals plots indicate that they contained useful information worth including in the model. Therefore, 3 PCs were deemed to be optimal in this case.

The samples were divided into training and test sets as above (see Table 7.2 in the Appendix), and PCA models were created for each acquisition time. In addition, due to the more distinct manufacturer differences that were observed, a PCA model comprising of those samples manufactured by CP Pharmaceuticals *only* was made for testing.

As was the case for paracetamol, the removal of five test samples to create the training sets did not change the conclusion that retaining 3 PCs was optimal to describe the unpackaged ibuprofen dataset. For the CP-only PCA model, one PC (90.5% of explained variance for 600s dataset) was considered to be sufficient for describing the major spectral features. This same procedure was applied to the blister and "bliscard" spectra, and the same conclusions were drawn regarding the number of PCs required to best describe their training datasets.

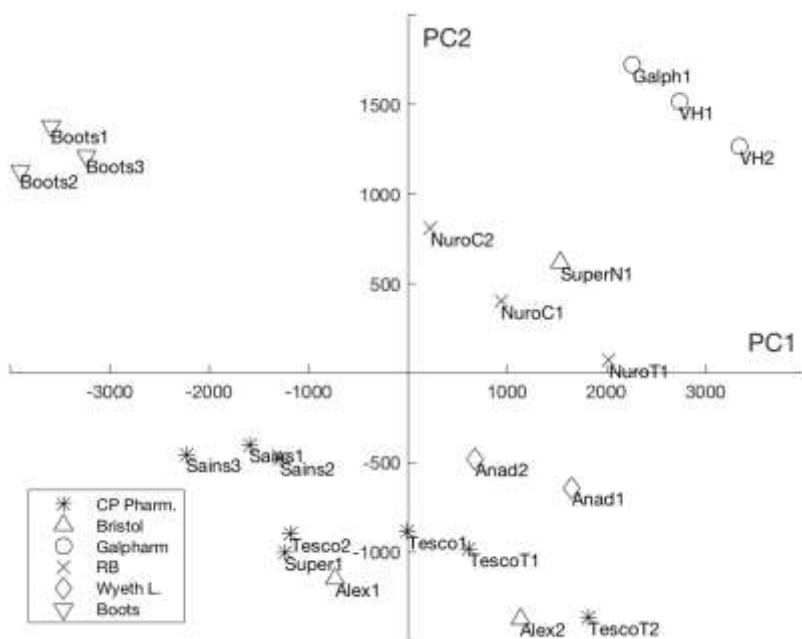


Figure 4.12 PC2 vs PC1 scores from PCA on spectra from 600s scans of unpacked ibuprofen

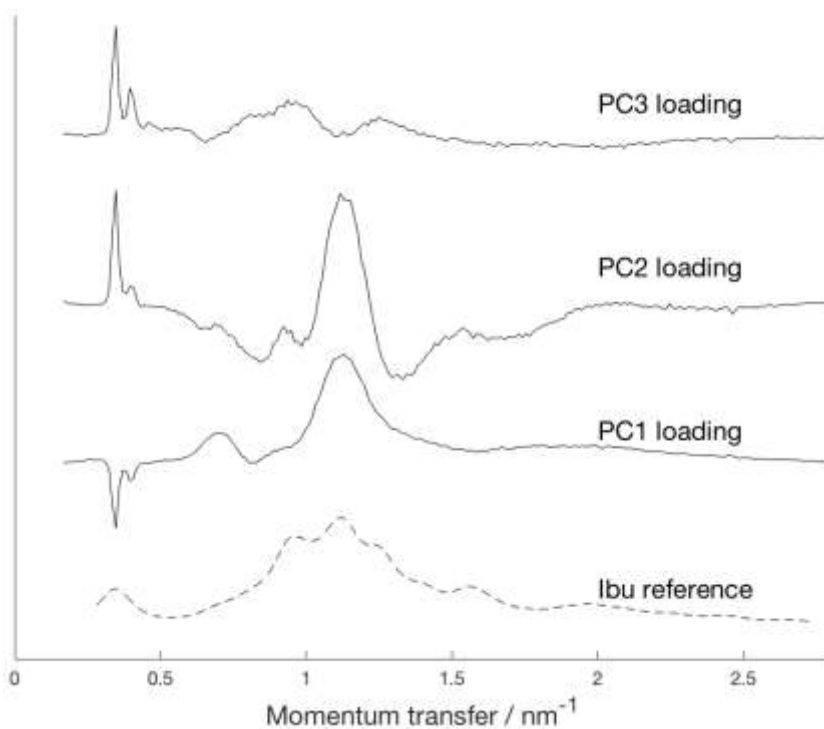


Figure 4.13 PCs 1-3 loadings from PCA on spectra from 600s scans of unpacked ibuprofen

4.3.1.3 OTC-Other

The remainder of the samples, listed in Table 7.3 (see Appendix), were used as part of the test set for SIMCA analysis, and were scanned in the same manner as all other samples. Initially, the full dataset of paracetamol, ibuprofen, and “OTC-other” spectra was used to carry out exploratory data analysis in the form of PCA. This type of unsupervised pattern recognition is

useful even when supervised pattern recognition is to be used, in order to check assumptions about the differences between groups.

The resulting PC2 vs PC1 scores plot in Figure 4.14 reassuringly divided up the paracetamol and ibuprofen samples along PC1. The PC1 loadings in Figure 4.15 demonstrated how the peaks it features correspond to some key ibuprofen peaks in the positive part, and paracetamol peaks in the negative. The sample very close to zero along the PC1 axis in Figure 4.14, labelled “NuMol”, was Nuromol: a drug containing *both* 500mg paracetamol and 200mg ibuprofen.

The scores plot also illustrated how paracetamol- and ibuprofen-related “OTC-Other” samples fell very close to the paracetamol and ibuprofen-only clusters – see for example, the position of samples “AnadEx” (Anadin Extra, containing paracetamol, aspirin and caffeine) and “NuPI” (Nurofen Plus, containing ibuprofen and codeine) in Figure 4.14. Along with Pro Plus (caffeine only), the soluble tablets were far removed from the rest due to their low API weight% (17weight% paracetamol in both cases) combined with the XRD peaks from a distinctly different set of excipients such as carbonates and citric acid. These could be considered as equivalent to grossly counterfeit samples when attempting classification by SIMCA.

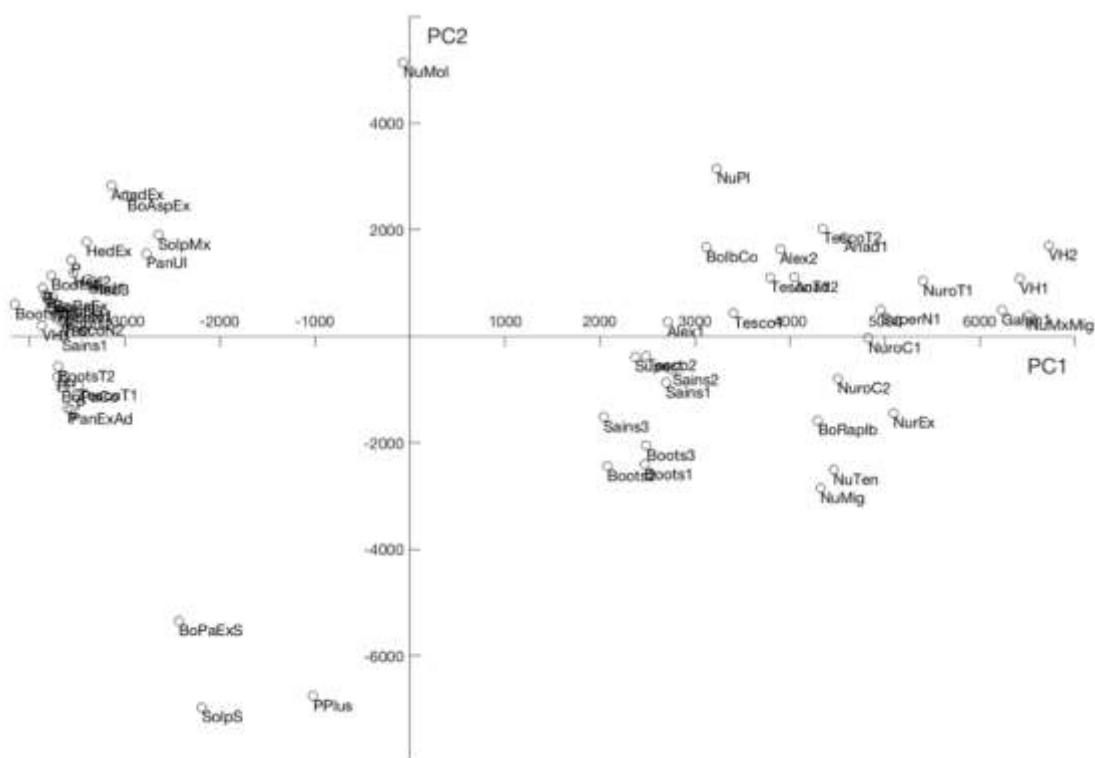


Figure 4.14 PC2 vs PC1 scores from PCA on spectra from 600s scans of all unpacked samples

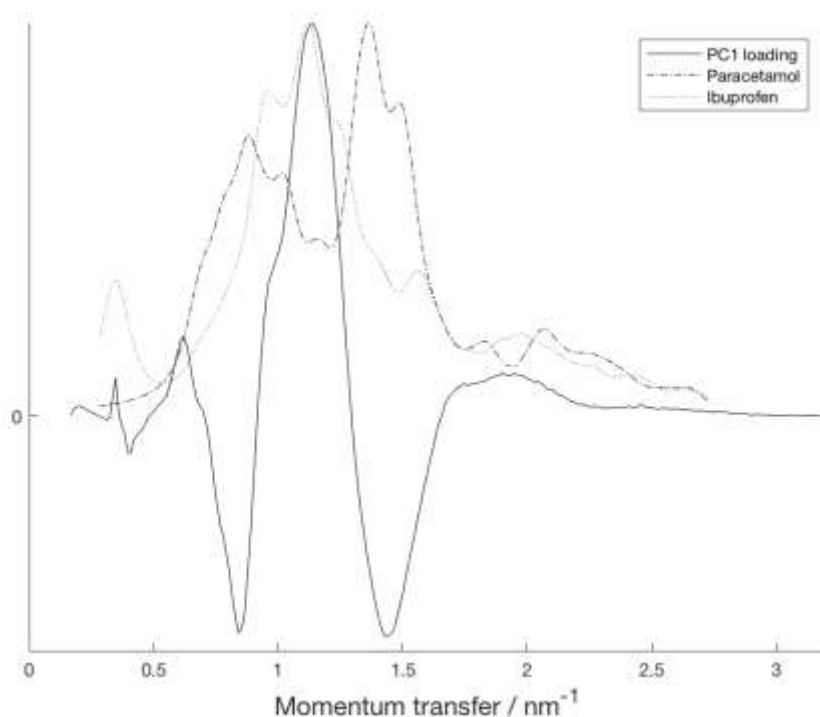


Figure 4.15 PC1 loadings from PCA on spectra from 600s scans of all unpackaged samples

4.3.2 SIMCA classification

4.3.2.1 Paracetamol

SIMCA classification was carried out using the three test sets with their respective training set PCA models, for all acquisition times and packaging levels. The resulting sensitivities and specificities of the system for any given set of parameters were plotted as graphs in Figure 4.16 and Figure 4.17 respectively.

Firstly, the plots of sensitivity in Figure 4.16 made it clear that for the most part, all five of the paracetamol 500mg test samples were correctly classified as “paracetamol”. This was regardless of the counting time, right down to 5-second acquisition times, and regardless of packaging levels. Yet at longer scanning times, some of the unpackaged samples suffered from a false negative, where the Boots Paracetamol Caplet (1) and the Alexander’s Paracetamol (1) samples were misclassified by the PCA models from training sets 1 and 2 respectively. In the former case, this may be attributed to the fact that one of the triplicate spectra displayed an odd peak at 0.79nm^{-1} that had not been seen elsewhere, and was not modelled by the training set. As for Alexander’s Paracetamol (1), one of the triplicate scans appeared to have some areas of lower intensity, possibly caused by some issues with preferred orientation, which made it stand apart from the modelled paracetamol spectrum. These effects were not repeated in the blister and “bliscard” cases, as these involved the examination of a different pill from the same batch.

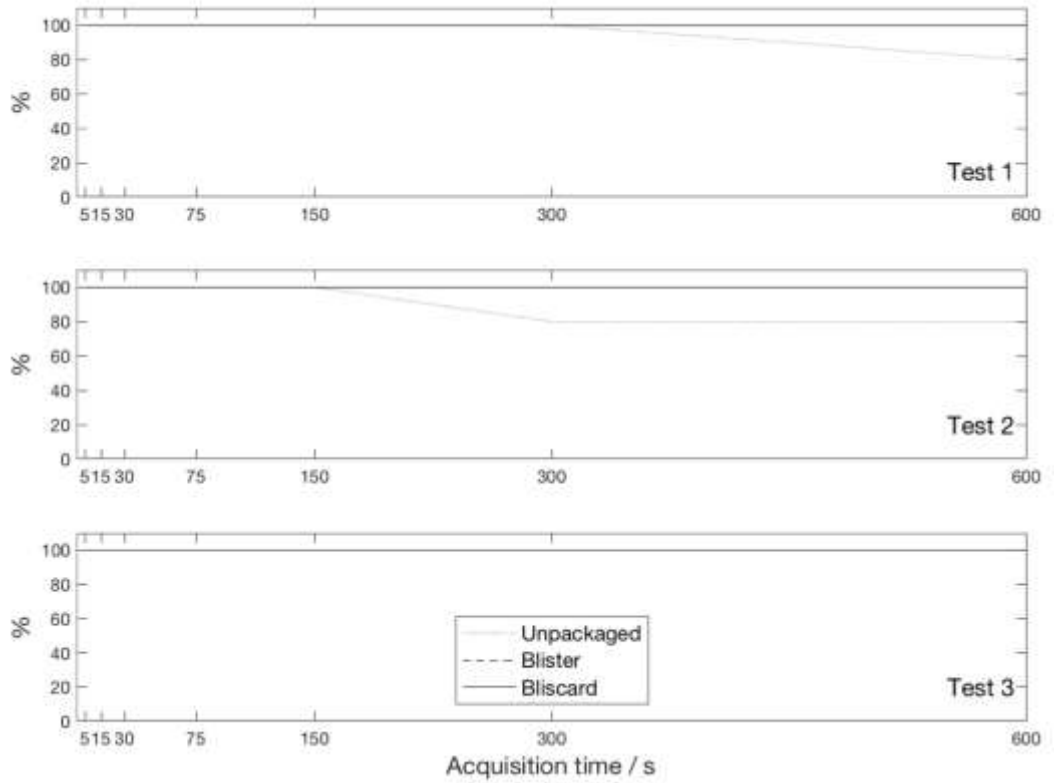


Figure 4.16 Sensitivity results from SIMCA tests on paracetamol models

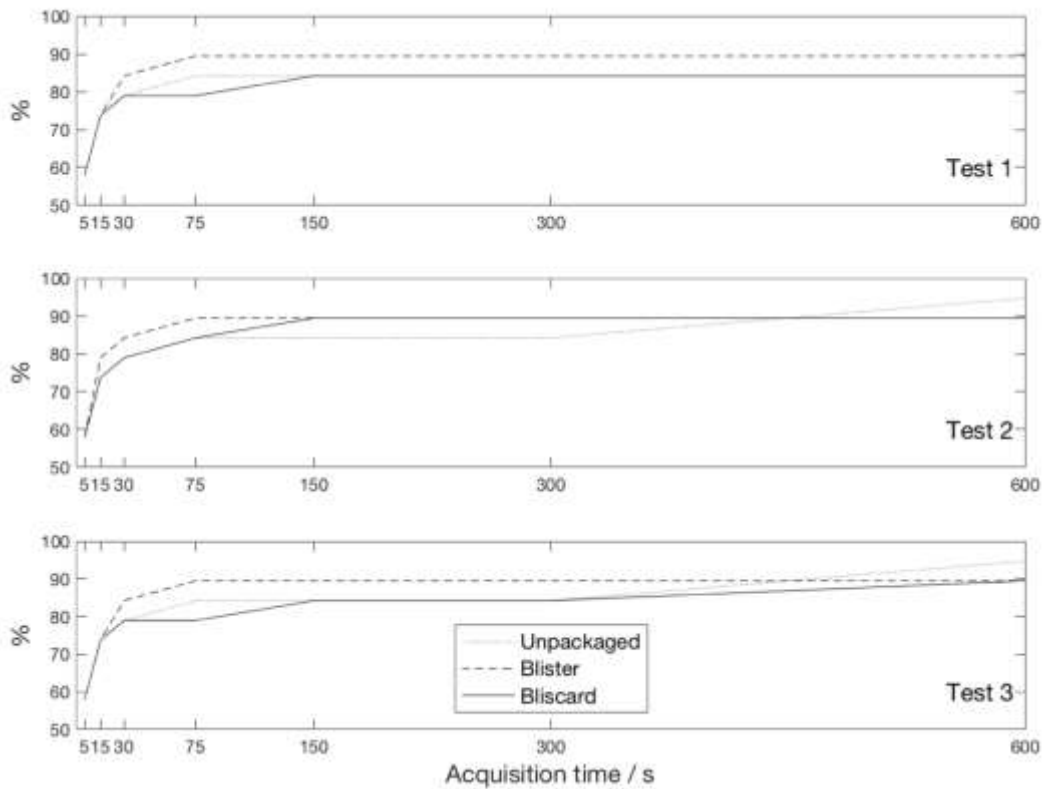


Figure 4.17 Specificity results from SIMCA tests on paracetamol models

The results on specificity in Figure 4.17 demonstrated how the different levels of difficulty in correctly rejecting the poor-quality-drug analogues were as expected. Samples that were classed as false positives are listed below, in order of highest to lowest frequency of misclassification:

- Paracetamol (500mg) + codeine (8mg) – false positive in *all* cases;
- Paracetamol (500mg) + codeine (12.8mg) – mostly from ≤ 300 s;
- Paracetamol (500mg) + caffeine (65mg) – *except* soluble versions, from ≤ 30 s;
- Paracetamol (500mg) + aspirin (300mg) + caffeine (45mg) – for ≤ 5 s.

None of the remaining “OTC-Other” samples were misclassified under any circumstance studied; note that the *soluble* paracetamol (500mg) + caffeine (65mg) tablets contained markedly different excipients and were far larger in size, resulting in distinctly different EDXRD spectra. By taking the mass of the Boots Paracetamol & Codeine tablet into account, the 8mg of codeine translated to a mere 1.4weight%. In addition, the tablets were 87weight% paracetamol – close to the values for the paracetamol-only samples used to construct the PCA models. The spectra in Figure 4.18 demonstrated how the strong paracetamol peak centred around 1.5nm^{-1} overshadowed the additional codeine diffraction contribution in this region (reference spectrum from CSD-QUBSEM [239], with peak broadening), thus making the overall spectra very similar to one another. Similarly, the 12.8mg of codeine in Panadol Ultra and Solpadeine Max translated to only 1.9weight% and were also prone to being misclassified. This was similar to the findings by Said *et al.*, where NIR spectra from the “negative control” sample Paramol, containing 500mg paracetamol and 7.46mg dihydrocodeine tartrate, were found to be difficult to separate from the 500mg-paracetamol PCA model in their classification studies [188].

Overall, although the blister-packaged case appeared to perform better than the others in test scenarios 1 and 3, the specificities were similar for all packaging levels and across the three tests, with differences in percentage usually caused by just one more or fewer false positive. It improved with longer counting times, and dropped off sharply below 30s. It was apparent from Figure 4.17 that counting times ≥ 150 s were required in the current setup to achieve a best-case sensitivity of $>84\%$ (i.e. with only the three codeine-containing samples misclassified) for all levels of packaging.

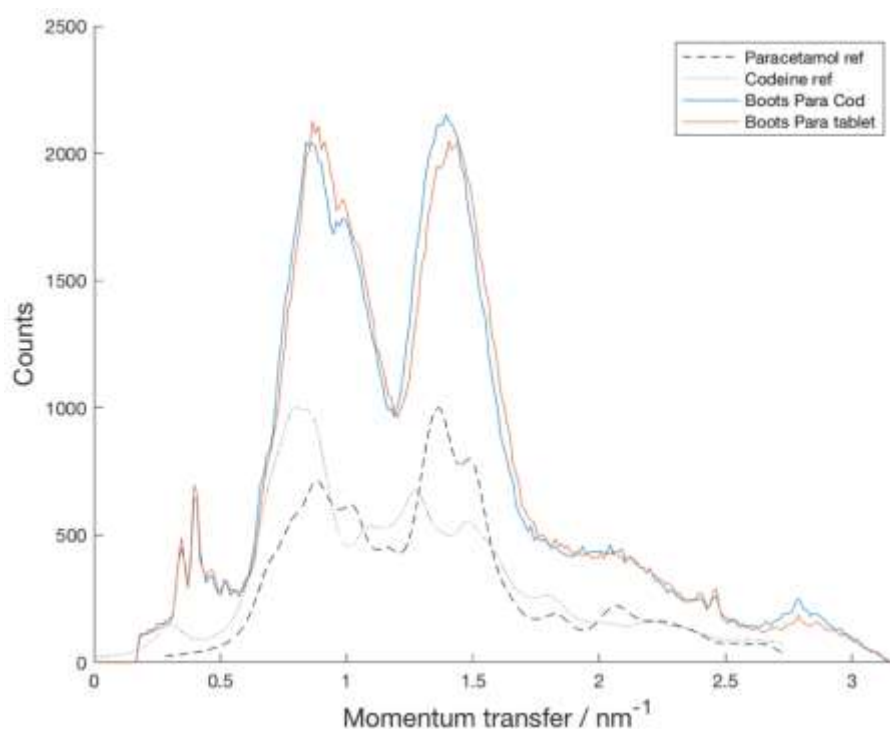


Figure 4.18 Spectra from Boots Paracetamol tablets with and without codeine (unpackaged, 600s scans) compared to reference spectra

4.3.2.2 *Ibuprofen*

SIMCA classification was carried out using the three test sets with their respective PCA models, and their sensitivities and specificities were calculated. The sensitivities were found to be 100% in all cases, so have not been presented graphically. The specificities were plotted in Figure 4.19; these were 100% for acquisition times ≥ 75 s.

These results followed the same general pattern whereby the number of false positives increased and hence the specificity decreased at lower acquisition times. The first false positives were detected at acquisition times of 30s in the unpackaged samples (in all three iterations of the model), unlike the packaged models which had specificities of 100% down to and including 30s. The misclassified samples were the two ibuprofen and codeine-containing drugs: Boots Ibuprofen & Codeine and Nurofen Plus. This discrepancy between the unpackaged and packaged result is possibly due to the reduction in counts in the low momentum transfer region in the spectra of the latter datasets, thus making them more sensitive to changes from the introduction of codeine (with its major peak at 0.8nm^{-1}) and correctly rejecting these samples. Notably, although the Boots Ibuprofen & Codeine and Nurofen Plus samples contained the same quantity and calculated weight percentage of codeine in the caplets as Panadol Ultra and Solpadeine Max discussed above, they were only misclassified in these shorter scans – in fact, an order of magnitude shorter than for the paracetamol case (30s vs 300s acquisitions). The

differences here were that the proportion of ibuprofen in these pills was less than half that of paracetamol (30weight% vs 75weight% of API), and that the ibuprofen diffraction peaks did not overlap as much with those of codeine, as shown in Figure 4.20 (compared to Figure 4.18).

The samples that gave false positives are listed below, in order of decreasing likelihood of being misclassified, and follow the expected pattern according to the difficulty of detecting such differences in API content; the remaining test samples were not misclassified:

- Ibuprofen (200mg) + codeine (12.8mg) – ≤ 30 s for unpackaged and ≤ 15 s for packaged;
- Sodium ibuprofen (256mg) and ibuprofen lysine (both 342mg and 684mg versions) – mostly from ≤ 15 s;
- Paracetamol + codeine – for some tests on 5s unpackaged and blister models;
- Paracetamol + caffeine – misclassified in 5s blister test 1 and “bliscard” test 2.

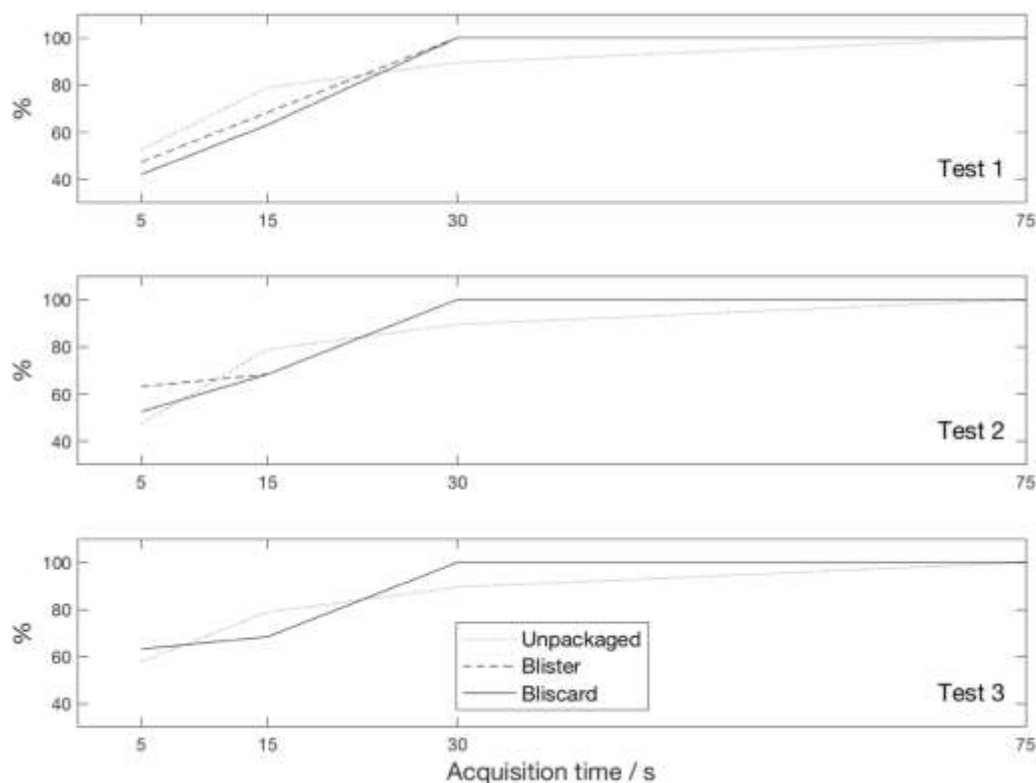


Figure 4.19 Specificity results from SIMCA tests on ibuprofen models

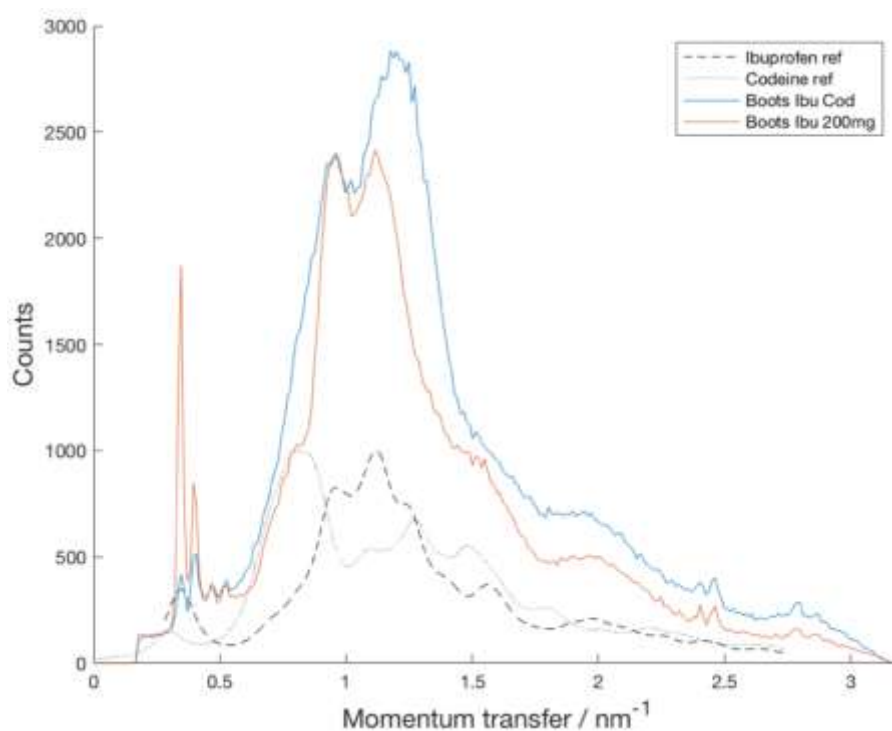


Figure 4.20 Spectra from Boots Ibuprofen caplets with and without codeine (unpacked, 600s scans) compared to reference spectra

Lastly, the results from SIMCA carried out on the PCA model made up of samples manufactured by CP Pharmaceuticals Ltd only are presented in Figure 4.21. It was found that Alexander's Ibuprofen (Bristol International Ltd) was always classified as a positive result, taken to be a true positive in this scenario, thus preventing the sensitivity from falling to zero. The similarity between Bristol International and CP Pharmaceuticals' ibuprofen sample spectra was evident in Figure 4.11; upon closer inspection of their excipients list, it was found that these were largely the same, and that Bristol International Ltd's formulation was changed in the case of the new Superdrug caplets, which therefore did *not* classify as "CP Pharmaceuticals" in the same way. Anadin Joint Pain (Wyeth Lederle S.r.l.) also gave a positive result using the packaged models at all acquisition times, and from ≤ 300 s for the unpackaged; Nurofen (Reckitt Benckiser Healthcare), was next most likely to fall within the bounds of the model (≤ 75 s). It was only when the acquisition time was reduced to 5s that all ibuprofen samples gave a true positive result in all cases – i.e. 100% sensitivity *if* the original intention was to detect ibuprofen-only samples of any manufacturer.

Instead, if all the non-"CP Pharma" samples were tested against this model with the expectation that they should *not* classify as belonging to this model (i.e. for manufacturer-specific authentication), the results presented in Figure 4.22 were obtained. The specificities never reached 100% within the < 600 s time scales that were studied due to the false positives from

Alexander's Ibuprofen samples. It then deteriorated further in the ≤ 150 s region, initially due to the increase in numbers of ibuprofen-only samples that gave a positive classification, but also due to the increase in the number of "OTC-Other" samples contributing to the false positive rate. The ibuprofen and codeine samples were misclassified for the packaged samples as well as unpackaged from ≤ 30 s – a worse result than for the earlier models where a variety of manufacturers was represented in the "ibuprofen" model. Thus, it appeared that if one manufacturer wished to authenticate their own product, the current method would not be effective due to the number of false positive results, particularly at shorter acquisition times.

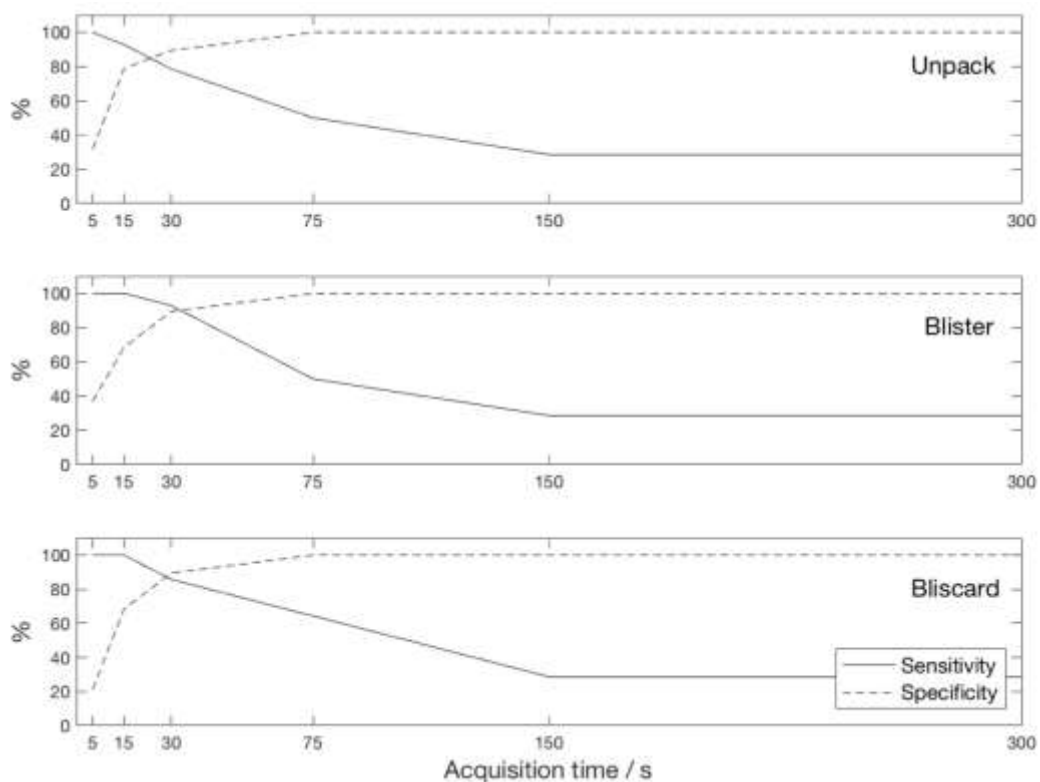


Figure 4.21 Results from SIMCA tests on CP Pharmaceuticals model

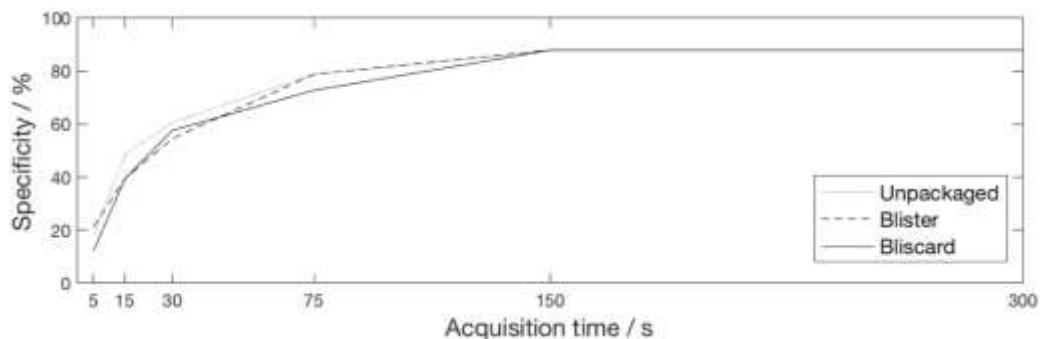


Figure 4.22 Results from SIMCA tests for manufacturer-specific authentication

Overall, the results for ibuprofen were consistent between the three tests and were stable down to shorter acquisition times than in the paracetamol experiment. The absence of strong preferred orientation effects thus appeared to have improved robustness of the models, even though there were greater between-sample variations in the spectra. By grouping manufacturers together when creating the PCA model in order to cover as much of these variations as possible (as well as, potentially, regions where other unrepresented manufacturers were likely to fall) in the PC space, SIMCA analysis gave specificities of 100% at acquisition times ≥ 75 s, regardless of packaging level.

4.4 Summary

In this chapter, SIMCA was applied to EDXRD spectra, correctly classifying paracetamol or ibuprofen-only samples, whilst rejecting samples with related or different APIs. The best results (with 100% sensitivity and maximum specificity) were achieved when using the spectra obtained for ≥ 150 s scans in the case of paracetamol (albeit misclassifying samples containing small quantities of codeine) and for ≥ 75 s scans in the case of ibuprofen. The models constructed from packaged sample spectra performed almost equally well, with differences in specificity a result of a few false positives in each case – and in some cases, the packaged models outperformed the unpackaged.

Despite differences in pill thicknesses resulting in some grouping in the paracetamol case, and the greater manufacturer differences observed for ibuprofen, this information was incorporated into the PCA models used for SIMCA and thus did not appear to have an undesirable influence on classification results.

Some of the limitations of the method were highlighted by the instances where small quantities of codeine had its peaks masked by a major paracetamol peak, resulting in a false positive result. Preferred orientation effects in test spectra were also shown to produce the occasional false negative result. It was also found that if manufacturer differences are large, as was the case for ibuprofen, it is important to ensure that an appropriate training set was used to model the API of interest for optimal classification results.

This study provided an insight into the potential of this method for checking whether the EDXRD spectrum from a medicine matches spectra from genuine samples stored as PCA models in a “library”, such that any counterfeit or substandard medicines would be detected. Although in this example the two types of API were investigated separately, in practice, SIMCA could be applied to multiple models simultaneously to check whether an unknown sample spectrum matches any of these – or none. Crucially, the presence of packaging – whether plastic, aluminium foil, or card – was not found to hamper this outcome.

Despite this, whilst these data acquisition times were relatively fast compared to more elaborate analytical methods such as chromatography and mass spectrometry, for the purposes for fast sample screening these would ideally need to be reduced further. This led to the idea of testing the newly-built *miniPixD* instrument for a series of analogous experiments that are described in the following chapter.

Chapter 5: *miniPixD* tests

5.1 Background

The results of SIMCA classification using EDXRD spectra in the previous chapter were encouraging, but in general the setup required the triplicated spectra to be collected for ≥ 150 s for optimal results. By contrast, Raman spectroscopy, which has been applied to in-field evaluation of pharmaceuticals, took 1 to 5 seconds for data collection and 30s in total including the additional time for data analysis [202]. Hence, a further reduction in the sample scanning time required for accurate classification of XRD data would be advantageous for fast screening and to bring it on a par with spectroscopic methods.

The *miniPixD* system that was described in section 2.2 was therefore tested for this purpose. Although capable of image-guided XRD, this capability was not trialled here as the aim of this experiment was to repeat the study in Chapter 4 with reduced acquisition times to see what effect this had on classification results. In addition, the use of the higher, 10% significance level was tested in an attempt to reduce the false positive rate – albeit increasing the risk of false negatives. This approach has been reported in the literature as being useful when relatively small sample sizes were used to construct the PCA models used in SIMCA analysis [262].

5.2 Methodology

5.2.1 Sample collection

For the most part, the same painkillers that were purchased for use in the previous chapter's work were re-used here, although a fresh tablet or caplet from each batch was used for both the unpackaged and the blister-packaged *miniPixD* scans. Additional samples that were purchased have been included in the tables in the Appendix; in particular, paracetamol samples manufactured by Galpharm International were targeted so as to build up a manufacturer-specific sample set. Samples that had expired since the previous experiment were not used.

5.2.2 Sample scanning & data analysis

XRD data were acquired for 60×1 s whilst continuously raster-scanning the samples; all scans were triplicated as before, and repeated for unpackaged, blister, and “bliscard” packaging levels. These data were converted from their raw .dat files into .hxt files offline using a program provided with the HEXITEC detector and by inputting the energy calibration parameters that were determined as described in section 2.2.1.. A Matlab script was written and used to load, convert into momentum transfer space, and sum these .hxt files such that they were combined into 1, 5, 15, 30, and 60s-scans for each sample.

These datasets were exported into The Unscrambler, and the triplicate spectra were averaged before analysis. Initial PCA models constructed using the full momentum transfer region ($0 - 9.98\text{nm}^{-1}$) described less of the explained variance in the first few PCs than what was observed in the previous chapter, seemingly due to additional variations between spectra in the high momentum transfer region that were unrelated to sample composition. This effect was possibly caused by the issues with system stability, resulting in variations in background over different days of use. To mitigate this effect, only the $0.04 - 2.50\text{nm}^{-1}$ region of the spectra was used for PCA analysis, as this comprised the region where diffraction peaks of interest occurred.

Three randomly-selected sets of five test samples were removed from both the paracetamol and ibuprofen sample sets before constructing PCA models with the remaining sample spectra (i.e. training sets of 22 and 19 samples respectively). The test sets of spectra for both paracetamol and ibuprofen, plus the “OTC-Other” samples, were classified using SIMCA on corresponding PCA models for both classes of medicine simultaneously. There were therefore five “positive” test samples and 21 “negative” test samples, of which 16 were “OTC-Other” and five were from the other test set. In addition, PCA models for the Galpharm paracetamol samples and CP Pharmaceuticals ibuprofen samples were created, and classification tests were carried out using all remaining samples. All classification results were recorded for both the 5% and 10% significance levels, and were used to calculate sensitivities and specificities.

5.3 Results and Discussion

5.3.1 Exploratory analysis and PCA model development

5.3.1.1 Paracetamol

The spectra collected using the *miniPixD* differed significantly in terms of background contributions compared to the previous EDXRD setup used. As mentioned in section 2.2.2, efforts were made to reduce undesirable background effects by covering the slot collimator on the X-ray source as well as introducing aluminium filtering. However, as can be seen in Figure 5.1, the “air” background remained high. However, the *difference* between background and sample spectra was clearly visible, showing the presence of paracetamol XRD peaks in this case.

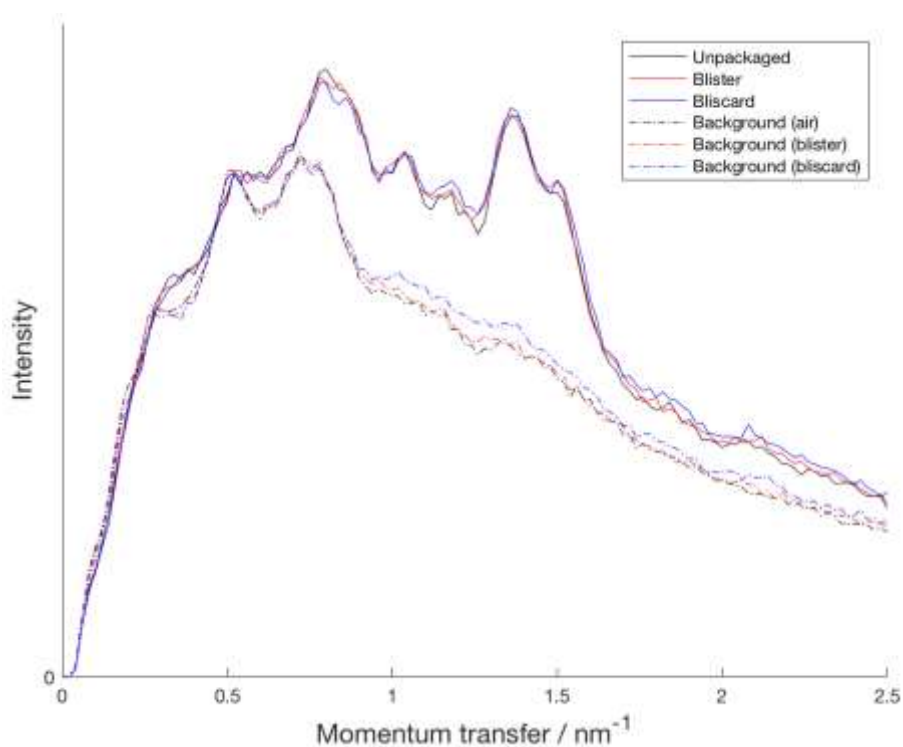


Figure 5.1 Alexander's Paracetamol (1) spectra with different packaging levels, plus backgrounds (60s)

Figure 5.2 demonstrates how the different acquisition times used affected the quality of the spectra. In all cases, the two major peaks of the paracetamol XRD profiles remained visible. The backgrounds have been subtracted in this example for illustrative purposes; background-subtractions were not carried out on the data more generally as this would be an unnecessary step when using PCA.

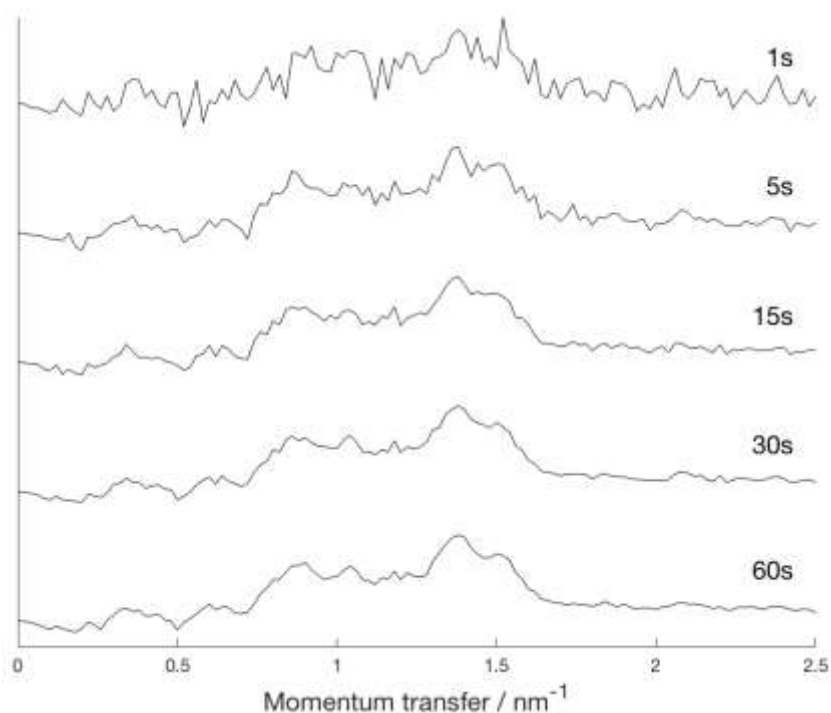


Figure 5.2 Background-subtracted unpackaged spectra from Alexander's Paracetamol (1) for all acquisition times used

The PC2 vs PC1 scores plot from PCA on the full unpackaged dataset, using the raw data for the 60s acquisitions, is presented in Figure 5.3. PC1 described 89.4% of the variance, and once again the main separation was between tablets and caplets. PC2 described only an additional 1.5% of the variance. It was noted that some of the scores for samples purchased later in the experiment, such as Boots Paracetamol Tablets (4) and Hedex (3) (labelled "BootsParaT4" and "Hedex3" in the figure) appeared to have separated out from the rest of the samples along PC2, highlighting the ongoing issue of stability of the system even though a 4-hour waiting period was applied prior to commencing sample scans on any given day. As the experiment was carried out over the course of a few months, other changes to the system and its environment may have had an effect. Regardless, the PC1 loadings plot shown in Figure 5.4 corresponded well to the paracetamol reference pattern, and some features remained visible even with the 1s acquisitions (Figure 5.6). In the latter case, the first PC only described 15.2% of the variance, but as higher PCs did not describe any further features of interest, one PC was chosen as the optimal number for use in SIMCA. This conclusion applied to all paracetamol PCA models with the five test samples removed, including those with packaging.

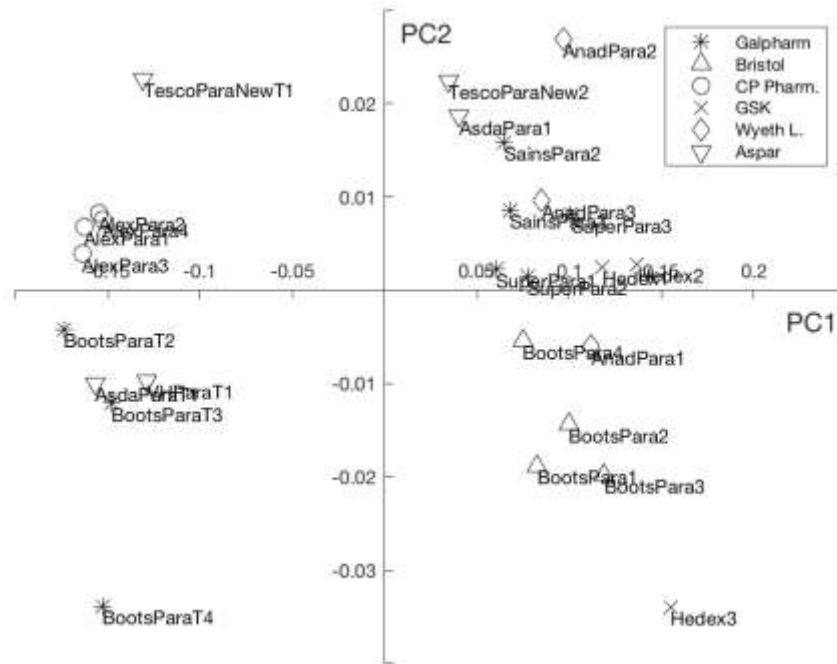


Figure 5.3 PC2 vs PC1 scores from PCA on spectra from 60s scans of unpackaged paracetamol

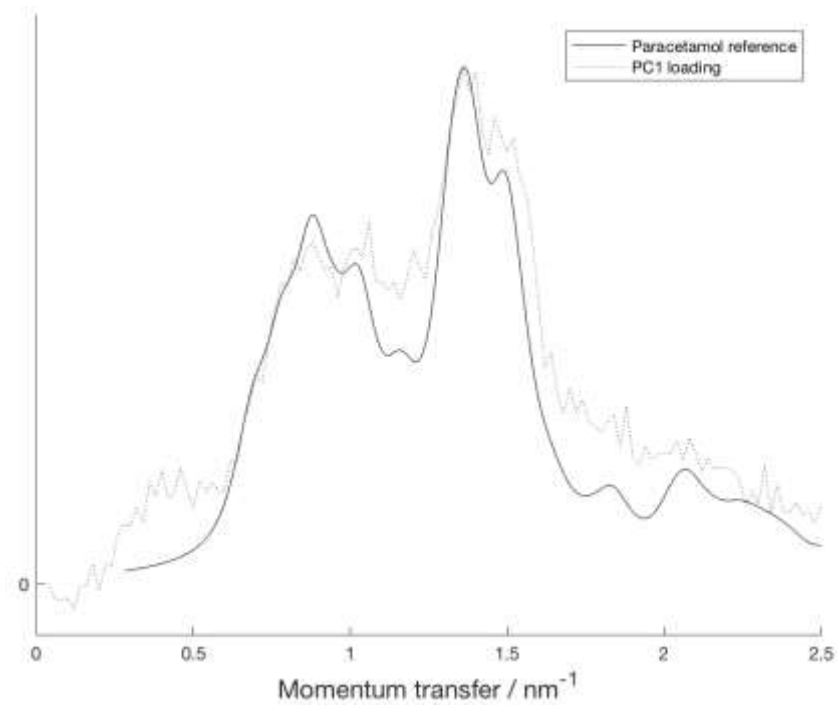


Figure 5.4 PC1 loadings from PCA on spectra from 60s scans of unpackaged paracetamol

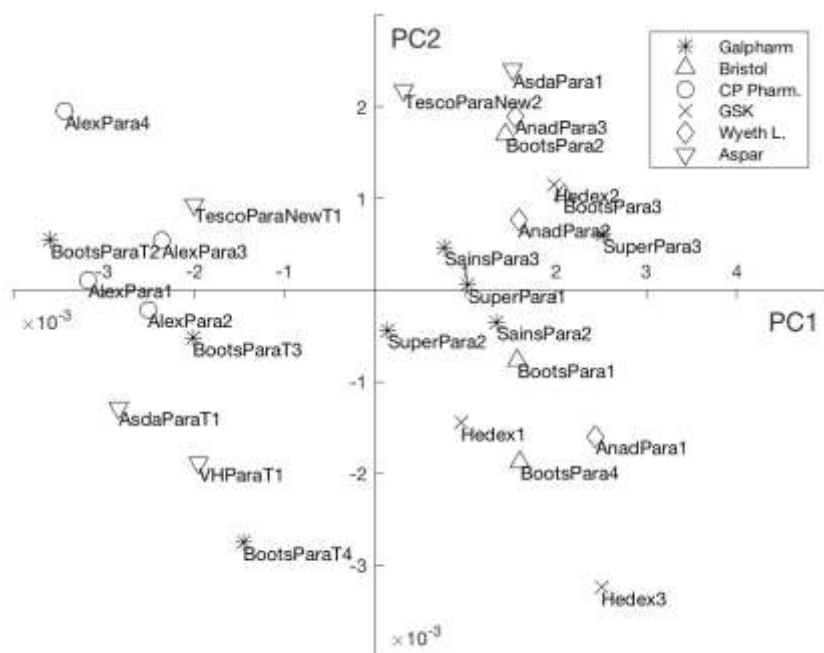


Figure 5.5 PC2 vs PC1 scores from PCA on spectra from 1s scans of unpackaged paracetamol

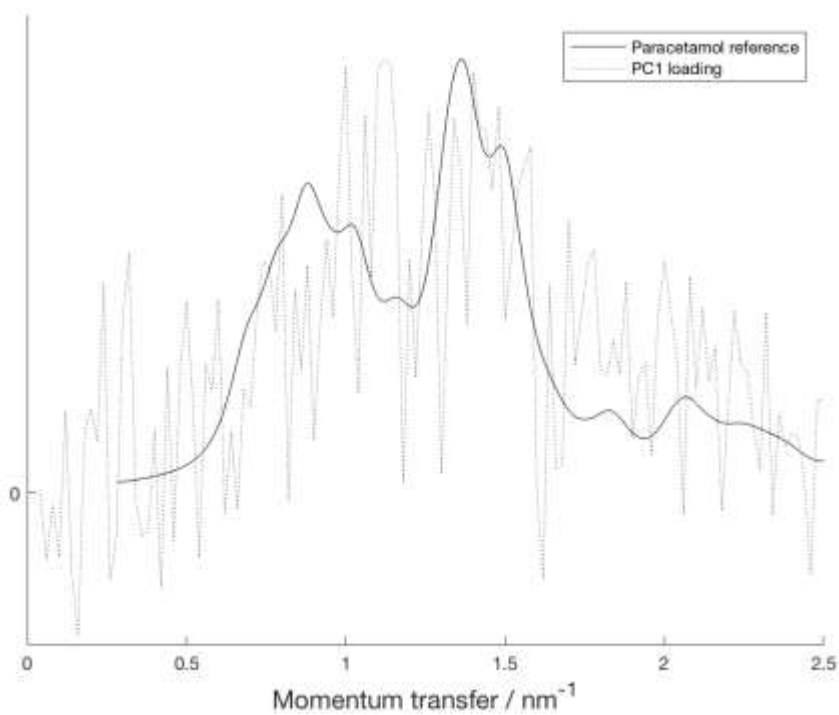


Figure 5.6 PC1 loadings from PCA on spectra from 1s scans of unpackaged paracetamol

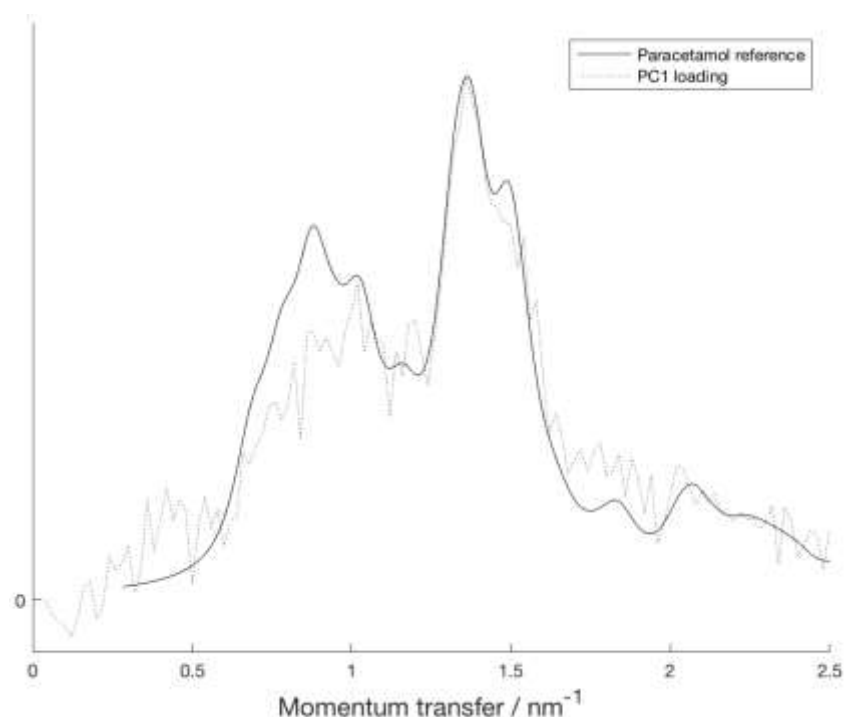


Figure 5.7 PC1 loadings plot from PCA on spectra from 60s scans of unpackaged Galpharm paracetamol samples

Although the sample set was relatively small, the eight Galpharm International-manufactured paracetamol samples were used to create an additional PCA model for testing against paracetamol from other manufacturers. The first PC described 91.7% of the variance and its loading plot, shown in Figure 5.7, demonstrated how it matched the reference spectrum's most intense peak well, but the lower peak at 0.71nm^{-1} less well.

5.3.1.2 Ibuprofen

The scores and loadings plots from PCA on the unpackaged ibuprofen samples scanned for 60s are shown in Figure 5.8 and Figure 5.9 respectively. The separations between manufacturers seemed less evident from the PC2 vs PC1 scores plot, however with the 3rd PC included in the 3D plot, these groupings became clearer. The first three PCs described 77.3%, 10.8% and 4.93% of the variance respectively, and as all three corresponding loadings plots (Figure 5.9) demonstrated features that helped describe the differing ibuprofen samples, these were retained for SIMCA analysis. Three PCs were chosen for the other ibuprofen models also, except in the case of the 1s scans. Here, the noisy spectra meant that features could not be discerned above the first PC loadings – an example is shown in Figure 5.10, from PCA on all unpackaged ibuprofen samples (explained variance 37.0%) – so only the one PC was used for modelling.

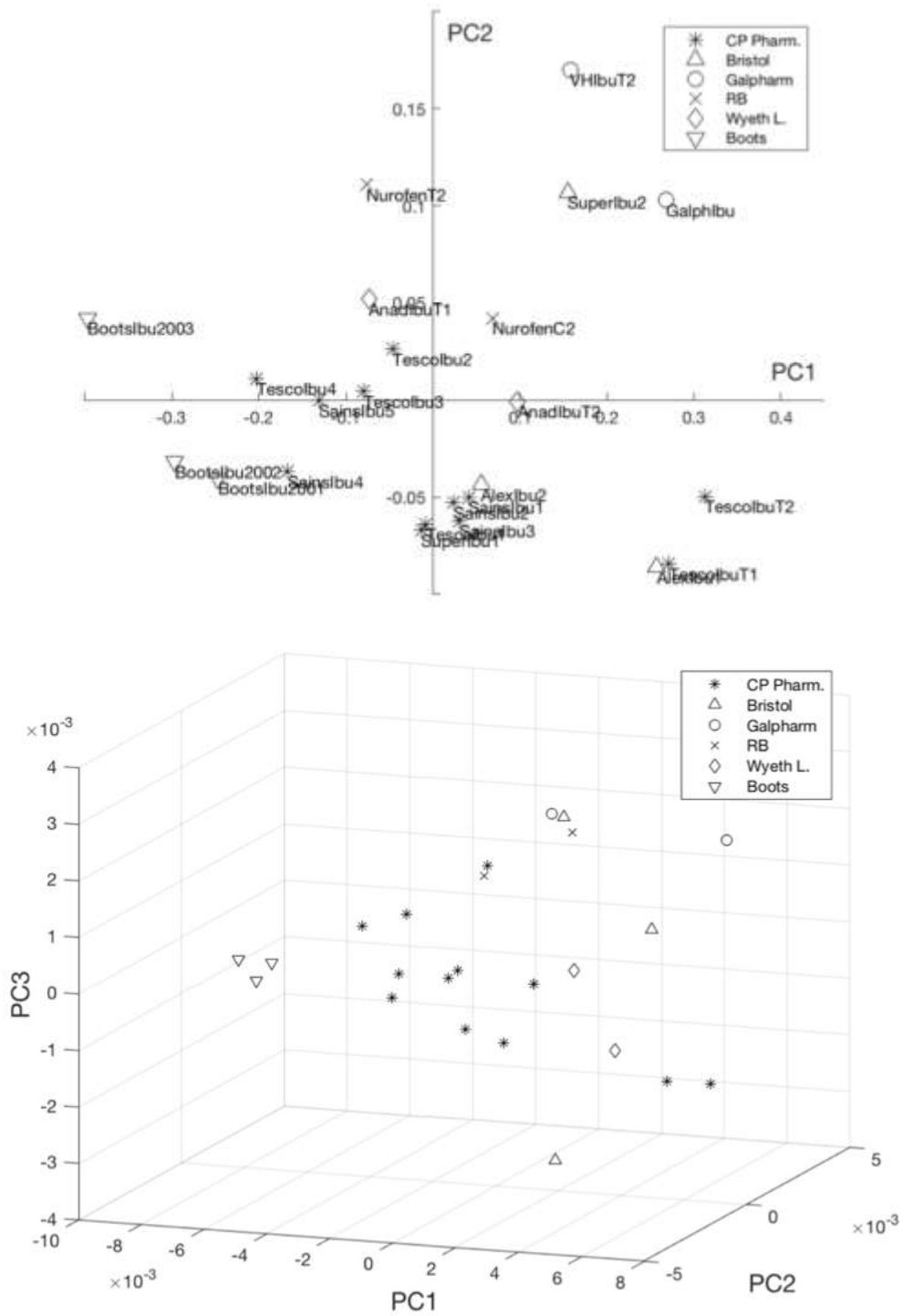


Figure 5.8 PC2 vs PC1 scores (top) and PCs 1-3 scores (bottom) from PCA on spectra from 60s scans of unpackaged ibuprofen

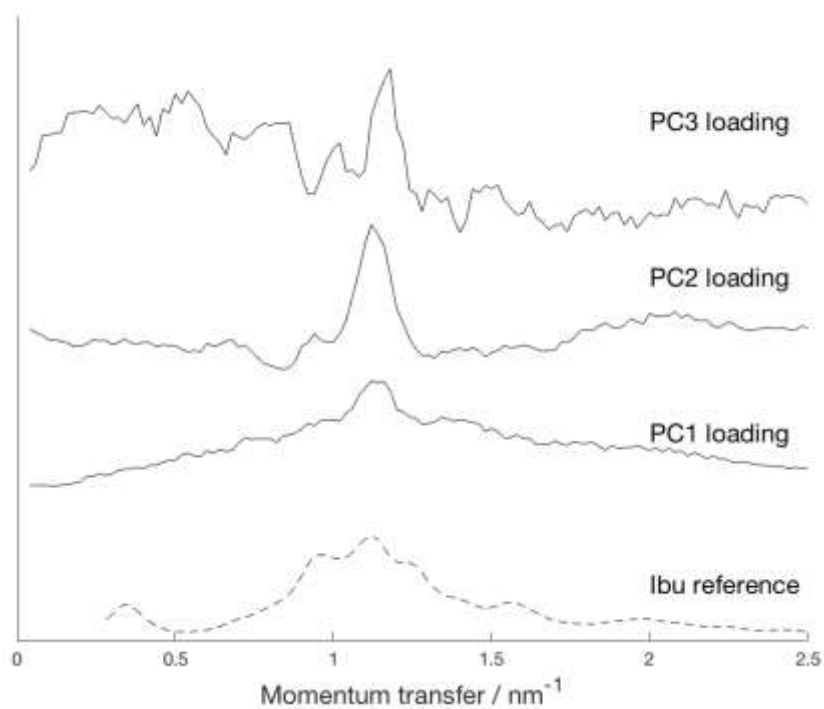


Figure 5.9 PCs 1-3 loadings from PCA on spectra from 60s scans of unpackaged ibuprofen

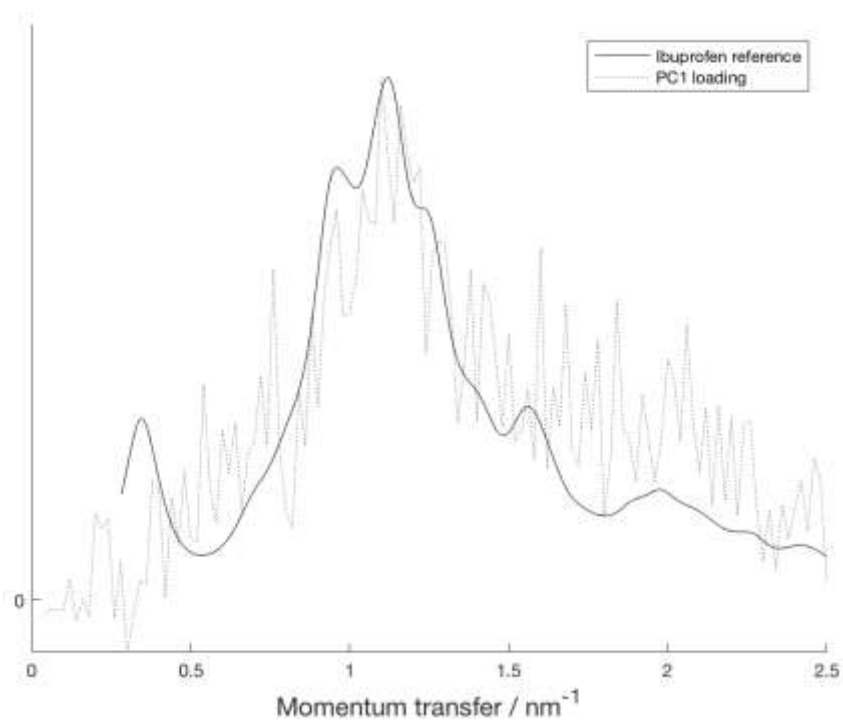


Figure 5.10 PC1 loadings from PCA on spectra from 1s scans of unpackaged ibuprofen

5.3.2 SIMCA classification

5.3.2.1 Paracetamol

SIMCA classification resulted in 100% sensitivity in all scenarios, unlike in the previous experiment where the longer acquisition times increased the chances of a preferred orientation peak becoming more prominent thus resulting in the occasional false negative. Therefore, the sensitivities were not represented graphically, but specificities were plotted as shown in Figure 5.11 for the two significance levels. The specificities were found to only significantly reduce at sub-5s acquisition times. The differences between the different packaging levels between 15-60s were caused by one or two misclassifications, and generally the unpackaged appeared to perform the best whilst “bliscard” samples had slightly lower specificities. The specificities for the ≤ 5 s scans were more clearly consistent in being highest for unpackaged and lowest for “bliscard” samples across all tests. At 5s, this ranged from 71% to 81% using the 5% significance level; and between 76% and 81% using the 10% significance level.

The maximum specificities were 86% and 95% for the 5 and 10% significance levels respectively in the unpackaged case; these fell to 81% and 86% respectively in the “bliscard” case. They did not reach 100% in any of the time periods studied, due to the misclassification of Boots Paracetamol & Codeine in *all* cases, resulting in the 95% specificity in the best-case scenario (unpackaged samples with 60s scans, using the 10% significance level). As expected, the next samples most likely to be misclassified were Panadol Ultra and Solpadeine Max – containing slightly more codeine. The higher significance level improved the overall results due to this differentiation between the 8mg and 12.8mg codeine samples.

There was a greater reduction in the number of false positives when the significance level was raised to 10% at the shortest, 1s acquisition times. As a result, the specificities were significantly higher – 63% as opposed to 40% for unpackaged samples, and 56% compared to 14% for “bliscard”. This difference in response is explained by the H_i vs S_i plots shown in Figure 5.12. The dashed lines show the positions of the H_{max} and S_{max} limits calculated by The Unscrambler for determining class membership (using the equations presented in section 2.3.3). Because the 1s scans suffered from a lower signal to noise ratio, the between-sample differences were diminished (illustrated by comparing the scores plots in Figure 5.3 and Figure 5.5) and hence the sample-to-model distances were relatively small. Differences in the threshold value therefore resulted in a sizeable change in the number of false positives. By comparison, in the 60s case the difference in specificity was solely based on the Panadol Ultra and Solpadeine Max classifications.

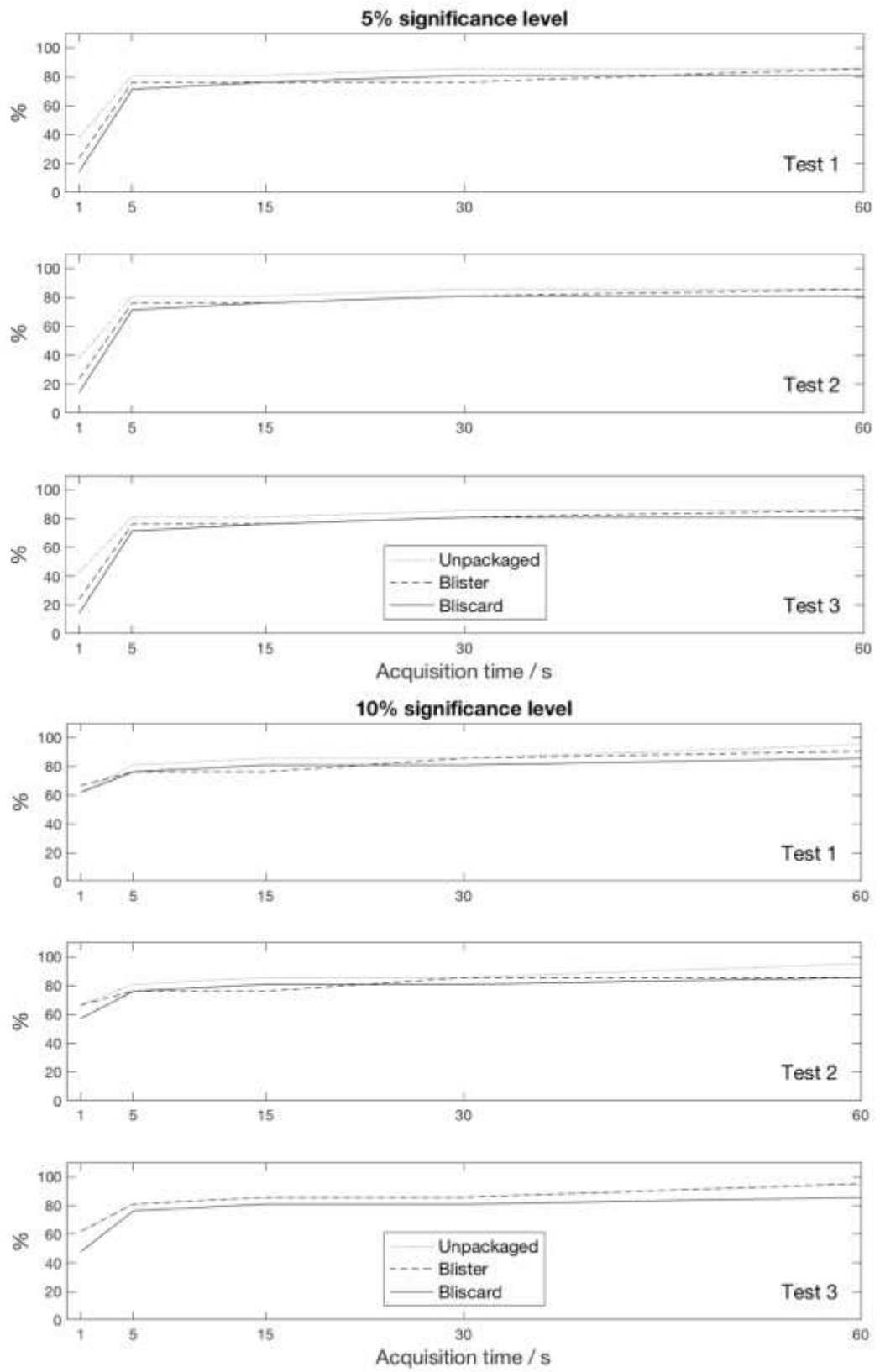


Figure 5.11 Specificity results from SIMCA tests on paracetamol models

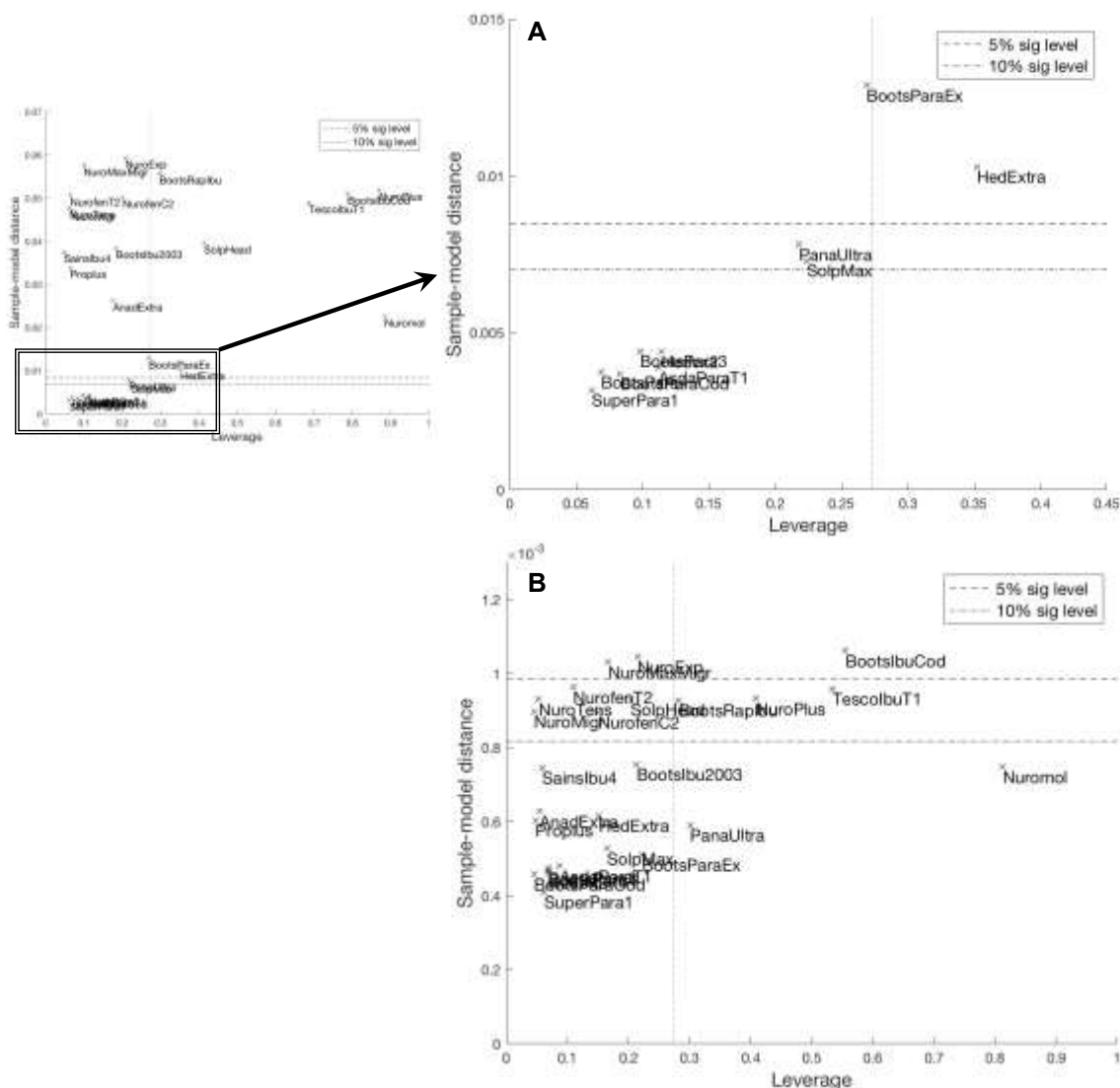


Figure 5.12 H_i vs S_i plots for unpackaged (A) 60s & (B) 1s scans (paracetamol Test 1)

The results of classifications made against the Galpharm-paracetamol manufacturer-specific PCA training model revealed that it classified *all* other paracetamol samples as “false positive” in all cases. When specificities were instead calculated based on the same 21 “negative” test samples used in Test 1 above, the results (Figure 5.13) were found to follow the same trend as for the randomly-selected training sets, with very similar performance (only ± 1 false positives, except in the 1s case where specificities fell considerably). Boots Paracetamol & Codeine remained misclassified even in the best case (unpackaged samples with 60s scans; 10% significance level), meaning that 100% specificity was not attained. These results suggested that not only were the Galpharm samples representative of all the other manufacturers tested, but that the eight samples in the training set were sufficient to model the variations seen in these paracetamol formulations.

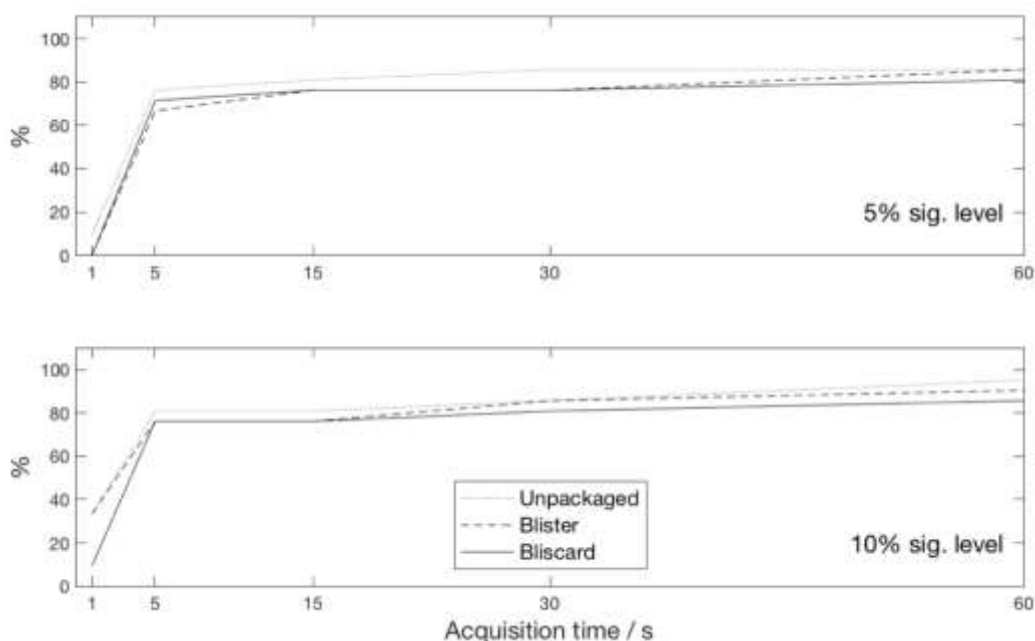


Figure 5.13 Specificity results from SIMCA tests on Galpharm paracetamol model

5.3.2.2 Ibuprofen

SIMCA classification of the ibuprofen test samples consistently gave a sensitivity of 100%. The specificities for 30 and 60s were also 100% in all instances. The other scan times for different packaging levels and tests 1-3 are shown in Figure 5.14. At the 5% significance level, for all levels of packaging, specificities fell from 100% at 30s to 67% at 5s, falling to 0% at times at 1s. The change in significance level to 10% meant that 100% specificity was achieved down to 15s scans, but with a sharp fall in performance beyond 5s once again.

The difference in performance at times <15s compared to paracetamol can be attributed to the fact that the thresholds used for classification were influenced by the number of calibration samples used to make the PCA model, and the number of PCs chosen. The greater the number of PCs used (i.e. three as opposed to one), the higher the threshold for leverage (equation (17) in section 2.3.3); and the smaller the training set (19 samples vs 22), the higher the thresholds for leverage *and* for sample-model distance (the latter due to a rise in the F_{crit} value – see equation (15)). As a result of this, in some cases the specificity fell to 0% at 1s, where distinctly different APIs were being misclassified. The H_i vs S_i plot in Figure 5.15 demonstrates how the separation between samples still exists, but these threshold values do not prevent the paracetamol samples, for example, from giving a false positive classification result.

The manufacturer-specific test performed better than for paracetamol, as expected, due to the greater differences between each manufacturers' products. The specificities did not reach 100%, however, because the Alexander's Ibuprofen, Anadin Joint Pain, and Nurofen samples were

consistently misclassified as “positive” at all scanning times. Figure 5.8 suggested that these samples, manufactured by Bristol Laboratories, Wyeth Lederle and Reckitt Benckiser respectively, had similarities in their spectra which resulted in them being loosely grouped together in the scores plot. Raising the significance level to 10% only marginally improved the sensitivity of the model by no longer misclassifying one of the Nurofen samples. On the other hand, the model performed just as well as the other ibuprofen mixed-manufacturer models when it came to classifying other “negative” test spectra from “OTC-Other” and paracetamol. If the ibuprofen test samples were discounted, 100% specificity was maintained down to 30s at the 5% significance level, and down to 15s at the 10% significance level – the same as what was observed in Figure 5.14. Therefore, although this model was not applicable for manufacturer-specific authentication (nor for ibuprofen authentication more generally, as it would conversely result in false negatives if viewed as such), it was still capable of rejecting samples containing any other APIs from classification.

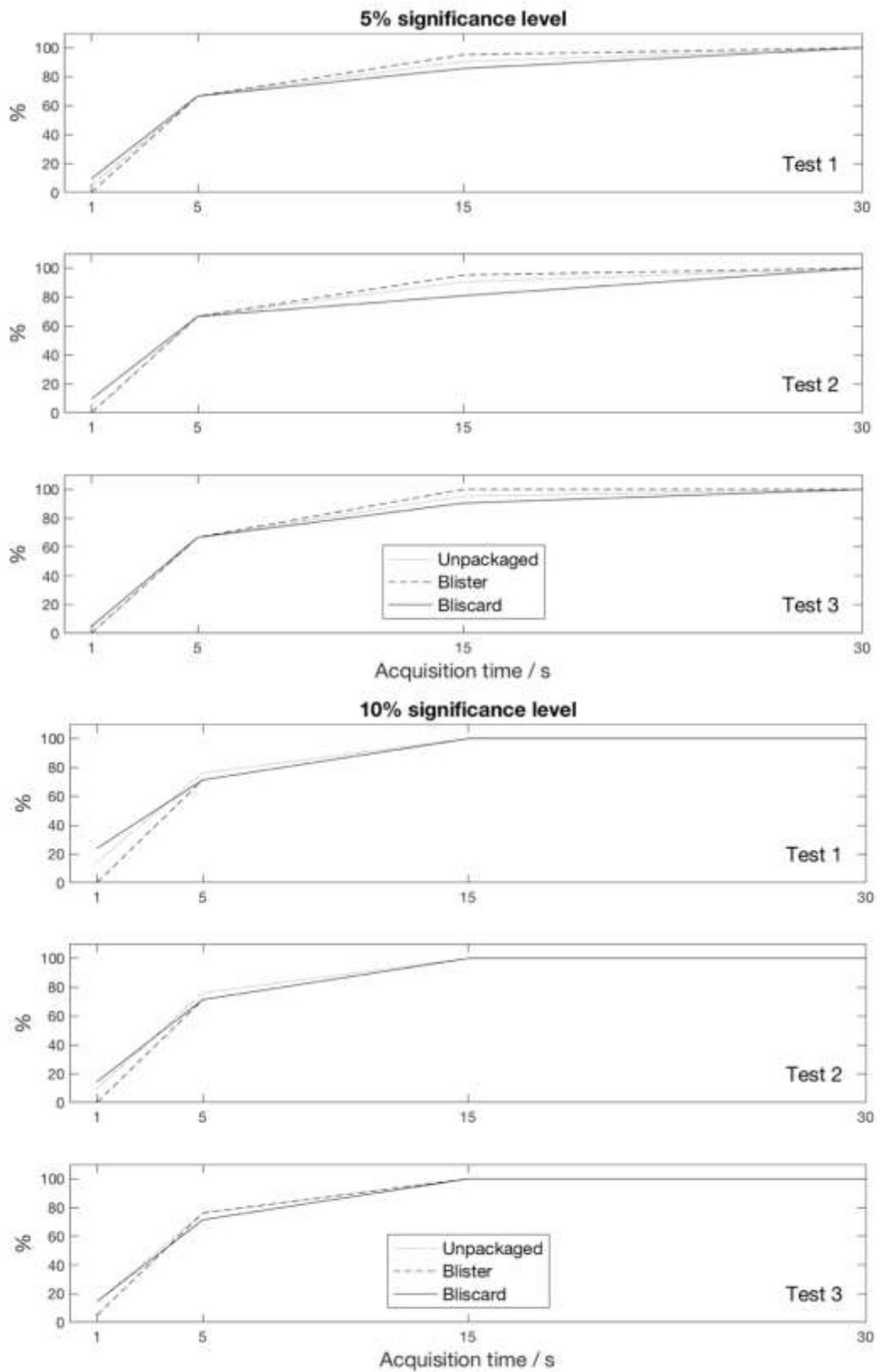


Figure 5.14 Specificity results from SIMCA tests on ibuprofen models

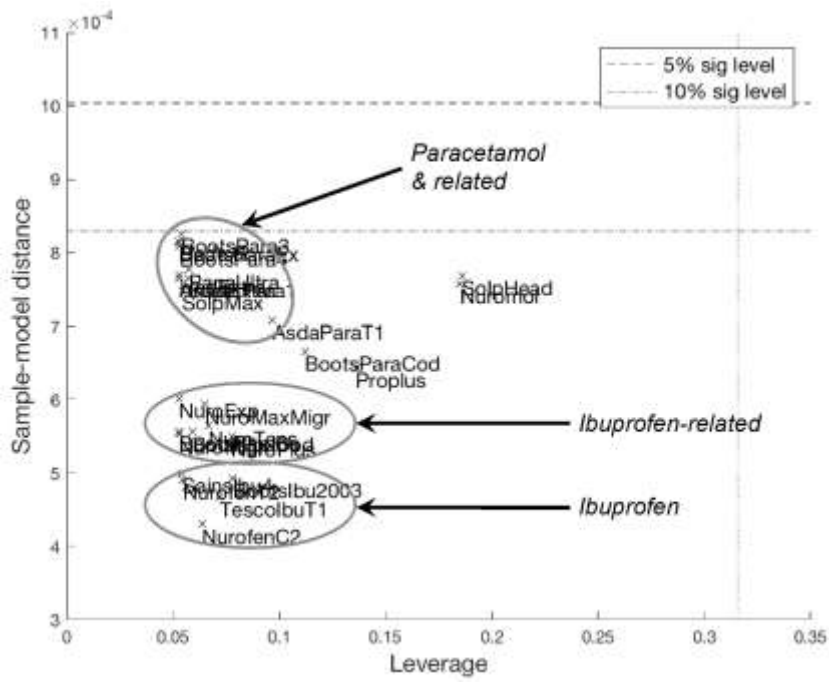


Figure 5.15 Hi vs Si plot for blister-packaged 1s scans (ibuprofen Test 1)

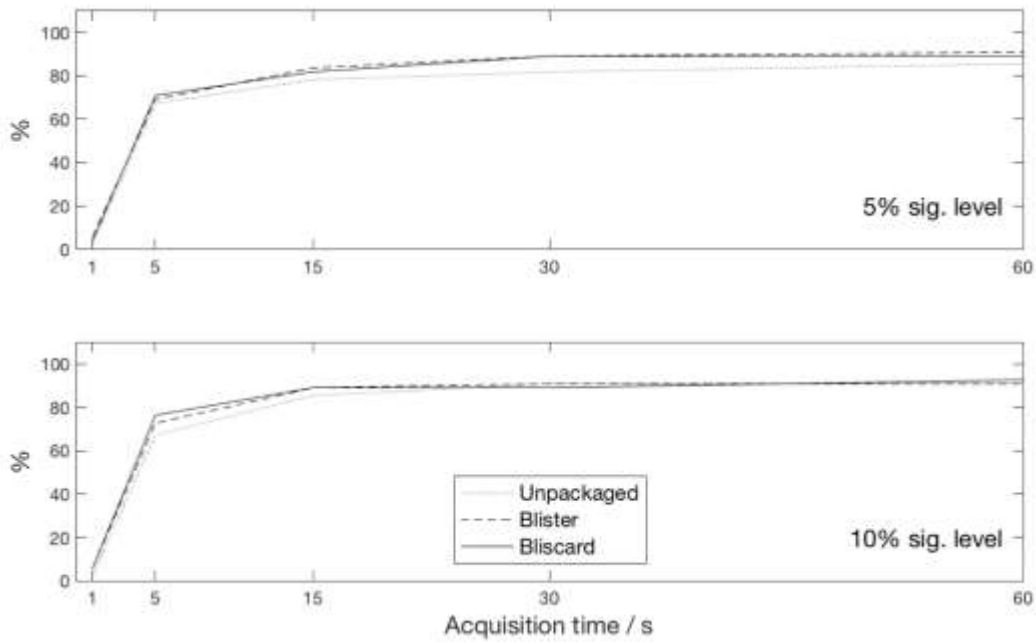


Figure 5.16 Specificity results from SIMCA tests on CP Pharmaceuticals ibuprofen model

5.4 Summary

The above experiments were carried out to test whether the data collection time required for obtaining high sensitivities and specificities from SIMCA classification of XRD spectra could be reduced by trialling the novel *miniPixD* system.

When SIMCA was applied to paracetamol models constructed using *miniPixD* spectra, the codeine-containing samples were misclassified, as observed previously in Chapter 4. The fewest false positives were recorded for the longest, 60s scans examined here. However, if a trade-off were to be made for scanning time, disregarding these particularly “difficult” samples (in terms of authentication), 15s scans were sufficient for all other test samples to be classified correctly in the unpackaged case. For the blister and “bliscard” sample spectra, 30s scans were required to maintain the specificity at >80%. Specificities from tests carried out on the ibuprofen model, on the other hand, were 100% for all packaging levels for times ≥ 15 s.

Therefore, the scanning times required for the *miniPixD* system were found to be a fifth of the optimal timings found using the EDXRD system. This reduction may have been greater were it not for a few key differences in the system setups – notably, the X-ray tube was operated at 72kV and 0.7mA for *miniPixD* vs 80kV and 2mA for EDXRD (Setup B), thus reducing the X-ray flux (for reasons explained in section 2.2.2); and the X-rays were more strictly collimated here (0.6mm-diameter pinhole vs 1.1mm in the EDXRD setup).

Nevertheless, this was an excellent result in terms of reducing the measurement time required for the detection of “counterfeit and substandard medicine” analogues to the order of tens of seconds, whilst maintaining the ability to scan through packaging layers.

Chapter 6: Conclusions and Future Work

6.1 Conclusions

The widespread problem of counterfeit and substandard medicines was discussed in the introductory chapter to this thesis. Although many analytical techniques have the potential to be applied to test suspect medicines, they all suffer from different strengths and limitations. Some of the key features that would be desirable in any technique are for it to be fast, easy to use, and portable. It was notable that the literature on the subject was lacking in studies into the application of XRD, and more specifically EDXRD. The work presented in this thesis sought to address this by assessing the practicality of applying EDXRD and the “PixD” method to the analysis of pharmaceutical medicines. In doing so, we demonstrated that:

- 1) EDXRD is suitable for quantifying pharmaceutical mixtures non-destructively;
- 2) It can be used for through-packaging (including foil) analysis of tablets and caplets;
- 3) The time required for inspection can be greatly reduced by the use of PixD.

Conclusions from each experiment that was carried out are discussed in more detail below.

6.1.1 Controlled mixture tests

PLSR calibration models were constructed using EDXRD data collected from ternary mixtures of known compositions that had been pressed into tablets. Using full cross-validation, these were found to have predictive abilities on a par with those reported in the literature for ADXRD, which was highly encouraging. Furthermore, this result was successfully replicated for tablets inside “packaging”, thereby demonstrating the potential for using this non-destructive method to assess packaged products such as medicines. Note that this differs from the usual meaning of “non-destructive” as used in the research literature, which typically refers to tablets that do not have to be crushed or dissolved for analysis, but *are* often removed from packaging (or at least from the cardboard box, if not their blister packaging). Lyndgaard *et al.* had previously achieved through-blister quantification of paracetamol using Raman spectroscopy [289], but as far as the author is aware, the quantification of paracetamol through both blister (plastic and foil) and card packaging layers has yet to be reported in the literature.

6.1.2 Intact formulation tests

SIMCA was used to authenticate a range of OTC painkiller medications when compared to PCA models constructed using EDXRD spectra of paracetamol and ibuprofen samples. The test subjects ranged from those with very similar to completely different API compositions. It was found that sensitivities and specificities of 100% were achieved for data acquisition times down to 75s in the case of the ibuprofen model; the paracetamol model had the best results at 150s, and highlighted some of the limitations of the method. These difficulties were caused by overlapping API peaks when one of these constituted a relatively small weight percentage of the mixture (as was the case with paracetamol and codeine), and preferred orientation effects. These issues are particular to each chemical and to each combination of chemicals, so it is difficult to predict at this stage how much of an influence these factors would have on this authentication method more generally.

In addition to the above, a manufacturer-specific authentication test was attempted using a PCA model constructed from EDXRD spectra of ibuprofen samples from one manufacturer only. Sensitive analytical techniques can detect when samples are from a different manufacturing site due to the different excipients and manufacturing methods used. However, although some other manufacturers' ibuprofen samples were rejected by the model when using SIMCA classification, it also gave false positive results for others.

Therefore, it was concluded that overall this method functioned best for the authentication of a certain class of medicine, e.g. paracetamol-only or ibuprofen-only. In the case of ibuprofen, the model performed best when the original PCA model covered the variations between a variety of manufacturers (which were larger than for paracetamol). It was also noted that the small "positive" test set may have influenced the sensitivity result; further testing is required to ensure that this 100% true positive rate is maintained for a larger test set.

6.1.3 *miniPixD* tests

The above SIMCA classification tests were repeated using the *miniPixD* instrument, which was found to reduce the data collection times required for best results by a factor of five – i.e. down to 15 - 30s. The ibuprofen model performed best, whereas the paracetamol case suffered from the continued misclassification of samples containing small amounts of codeine. Although specificity was improved with longer scanning times (i.e. misclassifying the 8mg codeine only instead of the 12.8mg codeine samples also), it is not known whether further increases to counting times and improved statistics would have changed this misclassification. Considering

that 600s acquisitions on the previously-used EDXRD system did not result in any improvement, this would be equivalent to >120s on the *miniPixD* instrument (presuming it is five times faster at acquiring data of the same statistical quality), which has yet to be tested. It also became apparent that the thresholds used by the SIMCA classification function in The Unscrambler may have affected the results where the test sample-to-model distances were seemingly large enough to discriminate the “negative” test samples visually (in H_i vs S_i plots), but were lower than the limits calculated by the software.

Overall, the use of the *miniPixD* permitted rapid XRD data acquisition and authenticated medicines with specificities that were largely unaffected by the introduction of layers of packaging. With further improvements to the data analysis methods and/or the instrumentation, it is expected to have great potential in the field of counterfeit and substandard medicines detection.

6.2 Future work

The work presented in this thesis consisted of a “proof of concept” study on the use of XRD for the rapid authentication of medicines. Therefore, there is much scope to explore this area further, and this section will provide some suggestions for next steps required to address some of the current limitations of the methods used.

6.2.1 Sampling medicines

The studies described in this thesis focused on two common APIs – paracetamol and ibuprofen. Firstly, it would be beneficial to extend this current work with a larger test set, in particular with greater numbers of “positive” test samples. In addition, because some of the issues (preferred orientation, for example) are very much particular to each compound or mixture, it would be necessary to validate the method with other types of pharmaceutical. The proportion of API within tablets and caplets also varies greatly between products, as some are only needed in small amounts – for example, one study had a sample set of medications containing between 1mg and 500mg of various APIs [191] – so it would be interesting to examine the effect of this. Note that as mentioned in section 4.3.1.1, the *actual* amount of API in the samples used here was unknown (due to there being a tolerated deviation from the stated amount), but this could be resolved in future by the use of HPLC. It may also be useful to extend the work regarding manufacturer-specific authentication, although previous studies on poor-quality medicines do

not always specify whether they are interested in particular manufacturers, instead focusing on detecting the presence and quantity of API, so this may not be required.

The samples that were used were selected based on their low cost and availability in local pharmacies without prescription (other studies have similarly used OTC medicines purchased locally [188,202,299]). Obtaining a wider range of medicines may be challenging due to the expense and the fact that many medicines are prescription-only. The author also encountered difficulties in obtaining “real” counterfeit and substandard samples to test; some researchers have overcome this by collaborating with police departments or regulatory authorities [191,300]. Samples of counterfeit drugs that were kindly provided by the MHRA unfortunately lacked their genuine counterparts, thus the data collected from these have not been presented here.

Furthermore, this study was limited to solid dosage forms, i.e. caplets and tablets, due to their ubiquitous nature. It would however be necessary to test any system using other dosage forms, such as capsules and oral suspensions, in order to fully assess the technique’s strengths and limitations. ADXRD analysis of capsules has previously been attempted by Phadnis *et al.*, who had to abandon this method as they found that this only gave the spectrum of the gelatin capsule itself [301]. This is something that is not expected to be a problem due to the greater penetration depth of the X-ray energies used in EDXRD and *miniPixD*.

6.2.2 Instrumentation

The *miniPixD* instrument has already demonstrated its high specificity by correctly rejecting samples containing small quantities of additional API, or related APIs, in the majority of cases. This compares well to certain other methods discussed in section 1.2.2.3 that were only capable of detecting drugs that were grossly counterfeit or substandard. It may be beneficial to use stricter collimation to improve angular resolution, thus providing better differentiation between diffraction peaks; however, higher X-ray tube currents or longer acquisition times would be needed to compensate for the corresponding decrease in X-ray flux.

The system did not necessitate any form of sample preparation such as grinding tablets into powders, which would normally be required for ADXRD analysis. The issue of preferred orientation did however dictate the need for raster scanning during data collection. It would be interesting to carry out further studies without raster scanning to see what effect this has on the sensitivity and specificity of authentication. Note that the sample stages would be included in the *miniPixD* instrument in its current form regardless, due to the line-scanning method used for X-ray imaging.

A limitation of the present study is that an idealised sample set up was used, where a single pill or blister was placed in a known position such that it sat within the X-ray beam path. The reality is that many packets of medicines contain two stacked sheets of blisters – and in addition, the patient information leaflet found inside such packets would add to the attenuation of X-rays if located in the beam path. These scenarios have yet to be investigated, but the *miniPixD* system overcomes the inability to “see” sample positions within packaging by allowing X-ray imaging and IGXRD. Some sample images of a counterfeit Viagra sample (provided by the MHRA) are presented in Figure 6.1. It will also be important to assess whether authentication is possible using XRD data collected from medicines in other forms of packaging, such as bottles. Eliasson *et al.* indicated that although blister packaging is the norm in the UK, many medicines are sold in plastic bottles in the USA [200], so such differences would need to be taken into account to facilitate wider implementation of the method.

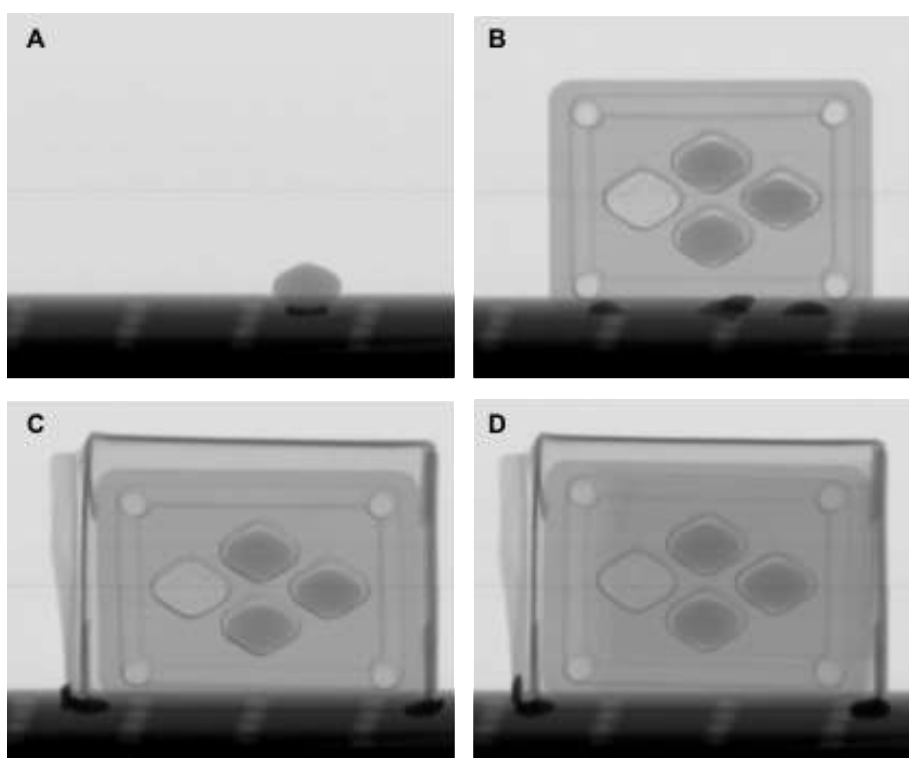


Figure 6.1 Images of counterfeit Viagra sample taken using *miniPixD*: (A) unpackaged, (B) in blister only, (C) in blister and card packet, and (D) with patient information leaflet

Another issue with positioning a sample within intact packaging is that the sample-to-detector distance used in the data analysis, which was determined prior to data collection (as described in section 2.2.1), will no longer be known accurately. This results in incorrect angles being assigned to each pixel in the HEXITEC detector, such that any diffracted X-rays that are detected are assigned incorrect momentum transfer values, as described by the case of thicker samples (an analogous situation) in Moss *et al.* [277]. In the example given, the use of a 5mm-

thick sample resulted in an uncertainty in the central pixel angle value of 5.83° [$+0.42^\circ$, -0.40°], i.e. 5.43° - 6.25° , depending on whether the diffracted X-ray originated from the front or rear of the sample. This corresponds to a range of 1.52 - 1.75nm^{-1} (instead of the expected value of 1.64nm^{-1}) for an example X-ray energy of 40keV (the broad peak in the X-ray tube spectrum is centred around this value when operated at 72kV as it was here). In other words, even a shift of $\pm 2.5\text{mm}$ in sample-to-detector distance would shift peak centres in the output spectrum by approx. $\pm 0.1\text{nm}^{-1}$, potentially affecting the ability for SIMCA analysis to recognise sample spectra as belonging to a particular PCA model. The effect of such deviations on the sensitivities and specificities of classification thus need to be examined in detail in future work. In addition, some suggestions for remedying this situation include the introduction of detector-side collimation, so that the scattering angles accessible to any particular pixel is restricted – but is technically challenging – or the use of coded aperture techniques [276].

Lastly, the stability of the system needs to be thoroughly assessed and measures put in place such that data collection is reproducible over long periods. The 4-hour “warm-up” time may otherwise be needed after the system is initially switched on, which may cause problems in its implementation. A shutter system that seals off the X-ray source’s primary collimator slot – used for imaging – would also be beneficial so that its IGXRD capability can be fully exploited when required.

6.2.3 Data analysis methods

The results from the final experiments suggested that modifications to the classification method could potentially be a route to improving the accuracy of medicines authentication without necessitating changes to the instrument per se. Restricting the significance levels further may indeed be useful for increasing the discrimination power of the models, as the potential for overlap between different PCA models used in SIMCA classification would decrease [262] – a possible issue as more medicine types are added to a database – but carries the risk of increasing the number of false negatives. Therefore, any modifications made to the classification thresholds need to be approached with caution. Some recent works by Rodionova *et al.* suggest an adaptation of the SIMCA method, called data-driven SIMCA (DD-SIMCA) which better utilises the information provided in the initial PCA analysis to create threshold values for classification [52,302], which may be of use in this situation.

Alternatively, statistical methods other than chemometrics could be applied. A few studies have used simple spectral correlation methods to classify both NIR and Raman spectra successfully, although the threshold values need to be selected carefully in each instance prior to

classification [155,188,303]. Such methods require good quality spectra such that noise does not affect these “matches”, so the XRD data collected at short scanning times would likely need some pre-treatments for these to potentially work.

In addition, it is unclear from the literature what the target rates for sensitivity and specificity should be, and whether this would differ for the detection of different “levels” of poor-quality medicines – in particular substandard medicines, which may be only very slightly different in their composition, and are by their very nature much harder to detect. Although the ideal would be to reach 100% in all cases, it would be interesting to pose the question to healthcare practitioners as to what the trade-offs would be in different contexts.

6.2.4 Implementation

Kovacs *et al.*'s review, “Technologies for Detecting Falsified and Substandard drugs in Low and Middle-Income Countries”, had ranked XRD very lowly out of the technologies that were assessed based on various parameters [158]. However, many of these points have been or can be improved based on the outcomes of this thesis, as detailed in Table 3.4. Note that “fast” here is defined as <5 minutes; and the “medium” price range is defined as US\$ 10,000-100,000.

Thus, after the proposed further studies are carried out and modifications are made, the *miniPixD* instrument – or any future incarnation of it – has the potential to be deployed for fast screening of medicines in situations where destructive, quantitative laboratory analyses are considered too time consuming or are unavailable. For example, pharmaceutical manufacturers could use this as a quick inspection tool to prevent substandard medicines from being sold to their clients. Pharmaceutical wholesalers and pharmacies could provide further checks for substandard medicines and also detect the introduction of counterfeit medicines into the supply chain (whether accidental or intentional) before these reach patients. Checks could also be made at borders and postal sorting offices, which are particularly important for tackling the large quantities of counterfeit medicines being sold through fake online pharmacies.

In more remote locations, such an instrument could be incorporated into a “mobile laboratory” for carrying out spot checks in shops, pharmacies and informal marketplaces, to flag both counterfeit and substandard medicines. For example, the Chinese regulatory authorities equipped hundreds of vans with NIR spectroscopy, TLC, and colorimetry instrumentation for this purpose; suspect drugs were then sent to centralised laboratories for further analysis [26,87].

	Reviewers' comment	Updated situation
Sample preparation needed	Yes	No
Performance	Unknown	Moderate performance; misclassifies samples with low quantities of "contaminant"
Laboratory supplies	None	None
Speed	Slow	Fast
Need electricity	Yes	Yes
Level of training required	Chemist	Would require "laboratory technician" level by use of in-built classification algorithm (as for portable spectroscopic methods)
Facility requirements	Research laboratory	Potential for use in mobile laboratory
Device price	High	Should aim to bring cost down to "medium" level (as for portable spectroscopic methods)

Table 6.1 Update to comments for "Powder X-ray diffraction" extracted from Kovacs *et al.*'s table comparing technologies for detecting counterfeit and substandard drugs [158]

A WHO report previously stated that the burden of verifying the authenticity of a product should not fall on patients [94] – but some of the technologies currently being trialled in less economically developed countries (such as scratch-off codes on packaging to be sent by SMS for verification) rely on the consumers to police the medicine supply chain. Ideally, the likelihood of poor-quality medicines reaching patient level should be negligible, and the strategic use of an analytical technique like XRD could aim to achieve this goal. However, the contents of the database do not necessarily have to be exhaustive – rather, they could be tailored to the particular situation if only a subset of medicines is of interest. More importantly, such a database would need to be updated so as to reflect any changes made to manufacturing processes over the course of time. Candolfi *et al.* previously mentioned this issue, stating that: "in general, different batches of the same formulation should match each other, which is however, not always the case in real life situations due to new feed stock of the material,

different equipment for production, etc.” [304] – highlighted by the case of Bristol Laboratories-manufactured ibuprofen in this thesis.

It is also important to note in the context of counterfeit medicines detection that these are known to have significant dose-to-dose variations, meaning that sampling just one tablet from a pack carries the risk of giving a false positive authentication result. Therefore, a better method would be to test multiple samples in practice [305]. Such issues would be addressed in any documentation and training given at the time of deploying the instrument.

Last but not least, there are many potential social issues when it comes to the implementation of any new technology, which must not be overlooked. Notably, in this particular area of pharmaceutical crime and pharmaceutical regulation, issues of the lack of awareness, non-compliance, and corruption have been cited in section 1.1.3. Therefore, any new technical countermeasures must be introduced alongside the various social countermeasures that were listed in section 1.2.1 in order to achieve the best possible results.

A final comment on counterfeit and substandard medicines

At the outset of this thesis, the problem of defining counterfeit and substandard medicines was addressed (see section 1.1.1) as it had become a point of contention for many practitioners working in this field. The WHO reported earlier this year (at their seventieth World Health Assembly on 29th May 2017) that an agreement had been reached to use the three mutually exclusive classifications detailed in Figure 6.2.

Figure 6.2 Classification of medical products to be used by the WHO global surveillance and monitoring system and the member state mechanism [306]

In addition, two key publications on the subject were launched on 29th November 2017 [306]:

- “WHO Global Surveillance and Monitoring System for substandard and falsified medical products”, highlighting causes, impacts and solutions; and
- “A study on the public health and socioeconomic impact of substandard and falsified medical products”, which includes estimates of failure rates and associated spending.

The above is an indication of the timeliness of the research presented in this thesis – the first report contains a section entitled “Improving detection technologies in the field and the laboratory”, detailing the continued efforts by the WHO and collaborators to evaluate existing and emerging drug screening technologies.

Chapter 7: Appendix

The following tables provide details on the samples that were purchased for analysis in the “Intact Formulations Tests” in Chapter 4, and the “*miniPixD* tests” in Chapter 5.

The caplets and tablets are marked in the second column of all tables by a “C” or “T” respectively. The samples used in the test sets are marked by crosses in the final columns of Table 7.1 and Table 7.2, whilst the cells with a slash through them denote those which were not used in that experiment either because they were yet to be purchased, or because they expired. In Table 7.3, the sample shaded in light grey was purchased at a later date for the *miniPixD* experiments whilst those in darker grey were not used.

Brand	T/C	No.	Manufacturer	Batch no.	Expiry	Mass / g	API %	Dimensions / mm			EDXRD			miniPixD		
								L	H	T	1	2	3	1	2	3
Alexander's	T	1	CP Pharmaceuticals Ltd.	XQ10482	Apr-18	0.562	89	12.8	12.8	3.8		x			x	
Alexander's	T	2	CP Pharmaceuticals Ltd.	XQ10500	Apr-18	0.554	90	12.8	12.8	3.8						
Alexander's	T	3	CP Pharmaceuticals Ltd.	XQ10506	Apr-18	0.566	88	12.8	12.8	3.9	x					x
Alexander's	T	4	CP Pharmaceuticals Ltd.	XQ11019	Jul-18	0.560	89	12.7	2.7	3.8	/	/	/			x
Anadin	C	1	Wyeth Lederle S.r.l.	BRL001	Apr-19	0.556	90	17.6	7.6	5.1						
Anadin	C	2	Wyeth Lederle S.r.l.	BRL004	Apr-19	0.560	89	17.6	7.6	5.2						
Anadin	C	3	Wyeth Lederle S.r.l.	BRL006	Apr-19	0.555	90	17.6	7.6	5.2	x	x	x			x
Asda	C	1	Aspar Pharmaceuticals Ltd.	160351	Feb-21	0.550	91	18.1	7.6	4.7	/	/	/			x
Asda	T	1	Aspar Pharmaceuticals Ltd.	160291	Jan-21	0.570	88	12.8	12.8	4.1	/	/	/		x	
Boots	C	1	Bristol Laboratories Ltd.	AUI162090	Oct-17	0.565	89	16.6	8.3	5.1	x					x
Boots	C	2	Bristol Laboratories Ltd.	AUI162092	Nov-17	0.560	89	16.6	8.3	5.1			x			x
Boots	C	3	Bristol Laboratories Ltd.	AUI172095	Nov-17	0.559	90	16.7	8.3	5.1			x	x		
Boots	C	4	Bristol Laboratories Ltd.	AUI165038	Jan-20	0.552	91	16.6	8.4	5.0				x		
Boots	T	1	Galpharm International Ltd.	PAK23B35	Jan-16	0.550	91	12.8	12.8	3.8		x		/	/	/
Boots	T	2	Galpharm International Ltd.	PAK3D55	Mar-18	0.561	89	12.7	12.7	3.8	x					
Boots	T	3	Galpharm International Ltd.	PAK23K51	Oct-18	0.570	88	12.7	12.7	3.9	/	/	/			
Boots	T	4	Galpharm International Ltd.	PAK24K51	Oct-18	0.550	91	12.7	12.7	3.8	/	/	/			
Hedex	C	1	GlaxoSmithKline Dungarvan Ltd.	140267	Feb-18	0.592	84	17.7	7.5	5.1		x				
Hedex	C	2	GlaxoSmithKline Dungarvan Ltd.	EG5K	Oct-18	0.596	84	17.7	7.4	5.1					x	
Hedex	C	3	GlaxoSmithKline Dungarvan Ltd.	UU5E	Oct-18	0.606	83	17.7	7.5	5.2			x			x
Sainsbury's	C	1	Galpharm International Ltd.	PAD8L24	Nov-15	0.554	90	16.6	8.3	5.0	/	/	/		/	/
Sainsbury's	C	2	Galpharm International Ltd.	PAD7K54	Oct-18	0.560	89	16.5	8.2	5.0	/	/	/		/	/
Sainsbury's	C	3	Galpharm International Ltd.	PAD14K54	Oct-18	0.560	89	16.5	8.2	5.0	/	/	/		/	/

Superdrug	C	1	Galpharm International Ltd.	PAD61I41	Aug-17	0.549	91	16.5	8.2	4.9	x			x	x
Superdrug	C	2	Galpharm International Ltd.	PAD13J45	Sep-17	0.560	89	16.6	8.3	5.0	/	/	/	/	/
Superdrug	C	3	Galpharm International Ltd.	PAD14J45	Sep-17	0.560	89	16.7	8.3	5.0	/	/	/	/	/
Tesco	C	1	Galpharm International Ltd.	PAD6L25	Nov-15	0.555	90	16.5	8.3	5.0	/	/	/	/	/
Tesco (new)	C	1	Aspar Pharmaceuticals Ltd.	150692	May-20	0.555	90	18.1	7.6	4.9		x	/	/	/
Tesco (new)	C	2	Aspar Pharmaceuticals Ltd.	150694	May-20	0.558	90	18.1	7.6	4.9	/	/	/	/	/
Tesco	T	1	Galpharm International Ltd.	PAK25A31	Dec-15	0.552	91	12.7	12.7	3.9	/	/	/	/	/
Tesco (new)	T	1	CP Pharmaceuticals Ltd.	XQ10970	Jul-18	0.560	89	12.8	12.8	3.9	/	/	/	/	x
Value Health	C	1	Galpharm International Ltd.	PAD23B31	Jan-16	0.561	89	16.6	8.3	4.9	/	/	/	x	/
Value Health	C	2	Galpharm International Ltd.	PAD44B31	Jan-16	0.558	90	16.5	8.2	4.9	/	/	/	/	/
Value Health	T	1	Aspar Pharmaceuticals Ltd.	160393	Mar-21	0.580	86	12.9	12.9	4.1	/	/	/	/	/

Table 7.1 Details of paracetamol samples

Brand	T/C	No.	Manufacturer	Batch no.	Expiry	Mass / g	API %	Dimensions / mm			EDXRD			miniPixD		
								L	H	T	0	1	2	1	2	3
Alexander's	T	1	Bristol Laboratories Ltd.	HW5004	Mar-18	0.444	45	10.8	10.8	6.0	x		x			
Alexander's	T	2	Bristol Laboratories Ltd.	HW5010	Mar-18	0.462	43	10.9	10.9	6.1						x
Anadin Joint Pain	T	1	Wyeth Lederle S.r.l.	BSS001	Feb-18	0.484	41	11.4	11.4	5.9						x
Anadin Joint Pain	T	2	Wyeth Lederle S.r.l.	BSS003	Mar-18	0.467	43	11.3	11.3	5.8						
Boots 200mg	C	1	The Boots Company PLC	14AS006A	May-17	0.270	74	13.4	6.3	4.3	x					x
Boots 200mg	C	2	The Boots Company PLC	15AS002A	Mar-18	0.264	76	13.4	6.3	4.2		x				
Boots 200mg	C	3	The Boots Company PLC	15AS004A	Apr-18	0.269	74	13.3	6.3	4.3						x

Galpharm	C	1	Galpharm International Ltd.	1504062	Mar-18	0.477	42	15.5	6.7	5.6		x					
Nurofen	C	1	Reckitt Benckiser Healthcare Int. Ltd.	BL224	Mar-17	0.450	44	14.1	7.2	5.1		x	/	/	/		
Nurofen	C	2	Reckitt Benckiser Healthcare Int. Ltd.	BR738	Aug-17	0.428	47	14.1	7.1	5.0				x			
Nurofen	T	1	Reckitt Benckiser Healthcare Int. Ltd.	BD193	Jul-16	0.426	47	10.7	10.7	5.9		x	x	/	/	/	
Nurofen	T	2	Reckitt Benckiser Healthcare Int. Ltd.	DB339	May-19	0.430	47	10.5	10.5	5.7	/	/	/		x	x	
Sainsbury's	C	1	CP Pharmaceuticals Ltd.	XP10689	Jul-17	0.389	51	14.7	6.7	5.3	x						x
Sainsbury's	C	2	CP Pharmaceuticals Ltd.	XP10666	Jun-17	0.369	54	14.5	6.7	5.2		x	x				
Sainsbury's	C	3	CP Pharmaceuticals Ltd.	XQ10971	Jul-18	0.433	46	14.7	7.0	5.8		x					x
Sainsbury's	C	4	CP Pharmaceuticals Ltd.	XS10173	Jan-20	0.400	50	14.9	7.0	5.5	/	/	/		x		
Sainsbury's	C	5	CP Pharmaceuticals Ltd.	XS10181	Jan-20	0.410	49	14.7	6.8	5.4	/	/	/				x
Superdrug	C	1	CP Pharmaceuticals Ltd.	XQ10337	Feb-18	0.424	47	14.8	7.0	5.6	x						
Superdrug (new)	C	2	Bristol Laboratories Ltd.	FCE035001	Jul-20	0.564	35	16.0	7.2	5.8							x
Tesco	C	1	CP Pharmaceuticals Ltd.	XQ10755	Jun-18	0.440	45	14.9	7.3	5.7		x					
Tesco	C	2	CP Pharmaceuticals Ltd.	XQ10942	Jul-18	0.438	46	14.7	7.1	5.7							
Tesco	C	3	CP Pharmaceuticals Ltd.	XR11471	Nov-19	0.460	43	15.0	7.1	5.6	/	/	/				
Tesco	C	4	CP Pharmaceuticals Ltd.	XS10304	Feb-20	0.460	43	14.9	7.0	5.6	/	/	/				
Tesco	T	1	CP Pharmaceuticals Ltd.	XQ10434	Mar-18	0.449	45	10.9	10.9	6.2					x		
Tesco	T	2	CP Pharmaceuticals Ltd.	XQ11067	Aug-18	0.481	42	10.8	10.8	6.6	x						x
Value Health	T	1	Galpharm International Ltd.	1400142	Apr-17	0.475	42	11.4	11.4	5.8				/	/	/	
Value Health	T	2	Galpharm International Ltd.	1400369	Mar-18	0.500	40	11.4	11.4	5.8							x

Table 7.2 Details of ibuprofen samples

Brand	T/C	Manufacturer	Batch no.	Expiry	Mass / g	API %						Dimensions / mm			
						Para	Asp	Ibu	IbuLys	Nalbu	Cod	Caff	L	H	T
Pro Plus	T	Pharmapac UK Ltd.	4D026	Mar-17	0.159							31	8.6	8.6	3.1
Boots Paracetamol Extra	C	Wrafton Laboratories Ltd.	62686A	Feb-17	0.646	77						10	17.6	7.6	5.7
Panadol Extra Advance	C	GlaxoSmithKline Dungarvan Ltd.	140157	Dec-15	0.755	66						8.6	18.1	8.4	5.7
Hedex Extra	C	GlaxoSmithKline Dungarvan Ltd.	140128	Dec-18	0.694	72						9.4	17.7	7.5	5.9
Solpadeine Headache Soluble	T	GlaxoSmithKline Dungarvan Ltd.	1410536	Oct-18	2.923	17						2.2	25.7	25.7	3.8
Boots Paracetamol Extra Soluble	T	Fannin (UK)	Y32820	Nov-16	2.950	17						2.2	23.3	23.3	4.9
Panadol Ultra	C	GlaxoSmithKline Dungarvan Ltd.	4601	Jul-18	0.667	75					1.9		16.1	8.6	5.6
Solpadeine MAX	C	GlaxoSmithKline Dungarvan Ltd.	4602	Jul-18	0.668	75					1.9		16.1	8.6	5.6
Boots Paracetamol & Codeine	T	Bristol Laboratories Ltd.	CN4136	Oct-17	0.573	87					1.4		12.8	12.8	3.8
Boots Aspirin Extra	C	Wrafton Laboratories Ltd.	60607A	Jul-16	0.635	32	47					7.1	17.6	7.2	5.9
Anadin Extra	C	Wyeth Lederle S.r.l.	3NZ031	Jun-16	0.639	31	47					7.0	17.7	7.3	5.8
Anadin Extra	C	Pfizer Consumer Manufact. Italy S.r.l.	DNZ011	Feb-20	0.640	31	47					7.0	17.6	7.2	5.8
Nuromol	C	Reckitt Benckiser Healthcare Int. Ltd.	BD061	Jul-17	0.878	57		23					19.3	8.2	7.3
Boots Ibuprofen & Codeine	C	Custom Pharmaceuticals Ltd.	82852	Oct-16	0.680			29			1.9		16.8	7.9	6.1
Nurofen Plus	C	Reckitt Benckiser Healthcare Int. Ltd.	BG612	Oct-17	0.661			30			1.9		16.2	7.2	6.8
Nurofen Express	C	Reckitt Benckiser Healthcare Int. Ltd.	BH314	Oct-16	0.487					53			14.9	8.2	5.2
Boots Rapid Ibuprofen lysine	C	Wrafton Laboratories Ltd.	64603A	Nov-17	0.452				76				14.7	7.6	5.9
Nurofen Tension Headache	C	Reckitt Benckiser Healthcare Int. Ltd.	BG563	Jul-17	0.420				81				14.7	7.7	4.9
Nurofen Migraine Pain	C	Reckitt Benckiser Healthcare Int. Ltd.	BH067	Sep-17	0.408				84				14.7	7.7	4.8
Nurofen Max. Strength Migr. Pain	C	Reckitt Benckiser Healthcare Int. Ltd.	BG847	Sep-17	0.800				86				19.2	9.0	6.6

Table 7.3 Details of 'OTC-Other' samples

Bibliography

- [1] BBC News Online, Fireball fears over fake lighters, BBC News Online. (2007).
http://news.bbc.co.uk/1/hi/scotland/tayside_and_central/6946483.stm.
- [2] UNICRI, Counterfeiting - A global spread, a global threat, Turin, 2007.
- [3] Food Standards Agency, Food Standards Scotland, Food Crime Annual Strategic Assessment: a 2016 baseline, 2016.
- [4] OECD, EUIPO, Trade in Counterfeit and Pirated Goods - Mapping the Economic Impact, OECD Publishing, Paris, 2016.
- [5] Frontier Economics, Estimating the Global Economic and Social Impacts of Counterfeiting and Piracy: A Report commissioned by Business Action to Counterfeiting and Piracy, London, 2011.
- [6] R. Cockburn, Counterfeit drug racket, ABC Radio National - The Science Show. (2006).
- [7] L. Reynolds, M. McKee, Organised crime and the efforts to combat it: a concern for public health., *Global. Health.* 6 (2010) 21.
- [8] OECD, The Economic Impact of Counterfeiting and Piracy, OECD Publishing, Paris, 2007.
- [9] UNICRI, Counterfeit Medicines and Organised Crime, Turin, 2012.
- [10] IRACM, E. Przyswa, Counterfeit medicines and criminal organisations, Paris, 2013.
- [11] UNODC, Counterfeit: Don't buy into organized crime, (n.d.). <https://www.unodc.org/counterfeit/>.
- [12] F. Clark, Rise in online pharmacies sees counterfeit drugs go global., *Lancet* (London, England). 386 (2015) 1327–8.
- [13] K. Van der Elst, N. Davis, Global Risks 2011, World Econ. Forum. (2011).
- [14] U. Kahn et al., Falsified Medicines and the Global Public's Health, London, 2012.
- [15] UNODC, The Globalization of Crime - A Transnational Organized Crime Threat Assessment, Vienna, 2010.
- [16] C. Edwards, C. Jeffray, On Tap - Organised Crime and the Illicit Trade in Tobacco, Alcohol and Pharmaceuticals in the UK, London, 2014.
- [17] K. Dégardin et al., Understanding and fighting the medicine counterfeit market, *J. Pharm. Biomed. Anal.* 87 (2014) 167–175.
- [18] R. Taylor et al., Pharmacopoeial quality of drugs supplied by Nigerian pharmacies, *Lancet.* 357 (2001) 1933–1936.
- [19] M. Park, S. Ahn, Quantitative Analysis of Sildenafil and Tadalafil in Various Fake Drugs Recently Distributed in Korea, *J. Forensic Sci.* 57 (2012) 1637–1640.
- [20] B. Venhuis et al., Recent developments in counterfeits and imitations of Viagra, Cialis and Levitra. A 2005-2006 update, Bilthoven, the Netherlands, 2007.
- [21] F.M. Fernandez et al., Poor quality drugs: grand challenges in high throughput detection, countrywide sampling, and forensics in developing countries, *Analyst.* 136 (2011) 3073–82.
- [22] S. Sengaloundeth, M. Green, Stratified random survey of the proportion of poor quality oral

artesunate sold at medicine outlets in the Lao PDR - Implications for therapeutic failure and drug, *Malar. J.* 8 (2009) 172.

- [23] H. Kaur et al., Antimalarial drug quality: methods to detect suspect drugs, *Therapy.* 7 (2010) 49–57.
- [24] A. Attaran et al., How to achieve international action on falsified and substandard medicines, *BMJ.* 345 (2012) e7381.
- [25] S.J. Fraser et al., Simultaneous qualitative and quantitative analysis of counterfeit and unregistered medicines using Raman spectroscopy, *J. Raman Spectrosc.* 44 (2013) 1172–1180.
- [26] Institute of Medicine (IOM), *Countering the Problem of Falsified and Substandard Drugs*, National Academies Press, Washington, D.C., 2013.
- [27] T. Dorlo, R. Ravinetto, Commentary: substandard medicines are the priority for neglected tropical diseases, *BMJ.* 7518 (2012) 1–2.
- [28] A. Katsnelson, Substandard drugs overshadowed by focus on fakes., *Nat. Med.* 16 (2010) 364.
- [29] R.M. Ravinetto et al., Poor-quality medical products: time to address substandards, not only counterfeits, *Trop. Med. Int. Heal.* 17 (2012) 1412–1416.
- [30] H. Kaur et al., Fake anti-malarials: start with the facts, *Malar. J.* 15 (2016) 86.
- [31] P.N. Newton et al., Counterfeit anti-infective drugs., *Lancet Infect. Dis.* 6 (2006) 602–13.
- [32] P.N. Newton et al., Guidelines for field surveys of the quality of medicines: a proposal., *PLoS Med.* 6 (2009) e52.
- [33] T. Almuzaini et al., Substandard and counterfeit medicines: a systematic review of the literature., *BMJ Open.* 3 (2013) e002923.
- [34] P.R. DeCola, Nursing and Health Policy Perspectives: We need to “get real” about counterfeit medicine, *Int. Nurs. Rev.* 57 (2010) 275–276.
- [35] World Health Organisation (WHO), *Definitions of SSFFC Medical Products*, WHO. (n.d.). <http://www.who.int/medicines/regulation/ssffc/definitions/en/> (accessed August 25, 2016).
- [36] World Health Organisation (WHO), *The Rational Use of Drugs - Report of the Conference of Experts*, Nairobi 25-29 November 1985, 1987.
- [37] SSFFC Medical Products - WHO Role, WHO. (n.d.). <http://www.who.int/medicines/regulation/ssffc/role/en/> (accessed August 25, 2016).
- [38] S. Sundar et al., A cluster of cases of severe cardiotoxicity among kala-azar patients treated with a high-osmolarity lot of sodium antimony gluconate., *Am. J. Trop. Med. Hyg.* 59 (1998) 139–43.
- [39] C. Lo, 130,000 counterfeit Panadol pills are seized, *South China Morning Post.* (2003). <http://www.scmp.com/article/426936/130000-counterfeit-panadol-pills-are-seized> (accessed August 30, 2016).
- [40] Pfizer, *Case Study: Lipitor US Recall*, (2007). <https://www.pfizer.com/files/products/LipitorUSRecall.pdf> (accessed August 30, 2016).
- [41] P.N. Newton et al., Manslaughter by fake artesunate in Asia - Will Africa be next?, *PLoS Med.* 3 (2006) e197.
- [42] C. Stothers, Counterfeit pharmaceuticals enter the parallel supply chain, *J. Intellect. Prop. Law*

- Pract. 2 (2007) 797–798.
- [43] J. Primo-Carpenter, M. McGinnis, Matrix of drug quality reports in USAID-assisted countries, Rockville, Md. United States. (2008).
- [44] M.M. Cheng, Is the Drugstore Safe? Counterfeit Diabetes Products on the Shelves, *J. Diabetes Sci. Technol.* 3 (2009) 1516–1520.
- [45] J. Cohn et al., When falsified medicines enter the supply chain: description of an incident in Kenya and lessons learned for rapid response., *J. Public Health Policy.* 34 (2013) 22–30.
- [46] The Lancet, Strengthening global action against poor quality drugs, *Lancet.* 381 (2013) 599.
- [47] IRACM, 150,000 doses of falsified Postinor 2 discovered in Nigeria, (2013).
<http://www.iracm.com/en/2013/09/150-000-doses-of-falsified-postinor-2-discovered-in-nigeria/>.
- [48] World Health Organization, Medical Product Alert No. 4/2015 - Adverse reactions caused by Falsified Diazepam in Central Africa, Geneva, 2015.
- [49] Counterfeit Norco Poses New Danger, *JAMA.* 315 (2016) 2390.
- [50] R. Cockburn, Death By Dilution, *Am. Prospect.* (2005).
- [51] T. Kelesidis et al., Counterfeit or substandard antimicrobial drugs: a review of the scientific evidence., *J. Antimicrob. Chemother.* 60 (2007) 214–36.
- [52] O.Y. Rodionova et al., Quantitative risk assessment in classification of drugs with identical API content., *J. Pharm. Biomed. Anal.* 98C (2014) 186–192.
- [53] P. Taberner et al., Mind the gaps--the epidemiology of poor-quality anti-malarials in the malarious world--analysis of the WorldWide Antimalarial Resistance Network database., *Malar. J.* 13 (2014) 139.
- [54] G.M.L. Nayyar et al., The global pandemic of falsified medicines: laboratory and field innovations and policy perspectives., *Am. J. Trop. Med. Hyg.* 92 (2015) 2–7.
- [55] G. Jackson et al., Assessing the problem of counterfeit medications in the United Kingdom., *Int. J. Clin. Pract.* 66 (2012) 241–50.
- [56] B. Baert, B. De Spiegeleer, Quality analytics of internet pharmaceuticals, *Anal. Bioanal. Chem.* 398 (2010) 125–136.
- [57] F.B. Palumbo et al., Policy implications of drug importation, *Clin. Ther.* 29 (2007) 2758–2767.
- [58] Medicines and Healthcare products Regulatory Agency (MHRA), Counterfeit Medicine Recalls and previously seen counterfeits, (2013).
<http://www.mhra.gov.uk/Safetyinformation/Generalsafetyinformationandadvice/Adviceandinformationforconsumers/counterfeitmedicinesanddevices/FalsifiedMedicineRecallsandpreviouslyseencounterfeits/index.htm> (accessed April 6, 2014).
- [59] The Economist, Fake pharmaceuticals: Bad medicine, *Econ.* (2012).
- [60] FDA, FDA Conducts Preliminary Review of Agency’s Diversion and Counterfeit Criminal Case Information, (2011). <https://wayback.archive-it.org/7993/20170113093347/http://www.fda.gov/downloads/Drugs/DrugSafety/DrugIntegrityandSupplyChainSecurity/UCM272150.pdf> (accessed September 23, 2016).

- [61] Pharmaceutical Security Institute, Counterfeit Situation - Therapeutic Categories, (n.d.).
<http://www.psi-inc.org/therapeuticCategories.cfm>.
- [62] T.P.C. Dorlo et al., A Poor-Quality Generic Drug for the Treatment of Visceral Leishmaniasis: A Case Report and Appeal, *PLoS Negl. Trop. Dis.* 6 (2012) e1544.
- [63] H. Kaur et al., Chemical and bioassay techniques to authenticate quality of the anti-leishmanial drug miltefosine., *Am. J. Trop. Med. Hyg.* 92 (2015) 31–8.
- [64] O. Onwujekwe et al., Quality of anti-malarial drugs provided by public and private healthcare providers in south-east Nigeria, *Malar. J.* 8 (2009) 22.
- [65] H. Kaur et al., A nationwide survey of the quality of antimalarials in retail outlets in Tanzania, *PLoS One.* 3 (2008) e3403.
- [66] A.C.D.Q.P.T. and the I.S. ACT Consortium Drug Quality Project Team and the IMPACT2 Study Team, Quality of Artemisinin-Containing Antimalarials in Tanzania’s Private Sector--Results from a Nationally Representative Outlet Survey., *Am. J. Trop. Med. Hyg.* 92 (2015) 75–86.
- [67] M. Antignac et al., Quality Assessment of 7 Cardiovascular Drugs in Sub-Saharan African Countries: Results of the Seven Study by Drug and Version of Drug, *Glob. Heart.* 11 (2016).
- [68] P. Taberner et al., A Repeat Random Survey of the Prevalence of Falsified and Substandard Antimalarials in the Lao PDR: A Change for the Better, *Am. J. Trop. Med. Hyg.* 92 (2015) 95–104.
- [69] O. Rada et al., Quality of Antimalarials at the Epicenter of Antimalarial Drug Resistance: Results from an Overt and Mystery Client Survey in Cambodia, *Am. J. Trop. Med. Hyg.* 92 (2015) 39–50.
- [70] N. Yoshida et al., A cross-sectional investigation of the quality of selected medicines in Cambodia in 2010, *BMC Pharmacol. Toxicol.* 15 (2014) 13.
- [71] P.N. Newton et al., Impact of poor-quality medicines in the “developing” world., *Trends Pharmacol. Sci.* 31 (2010) 99–101.
- [72] G.M.L. Nayyar et al., Poor-quality antimalarial drugs in southeast Asia and sub-Saharan Africa, *Lancet Infect. Dis.* 12 (2012) 488–496.
- [73] A. Johnston, D.W. Holt, Substandard drugs: A potential crisis for public health, *Br. J. Clin. Pharmacol.* 78 (2014) 218–243.
- [74] J.P. Renschler et al., Estimated under-five deaths associated with poor-quality antimalarials in sub-Saharan Africa., *Am. J. Trop. Med. Hyg.* 92 (2015) 119–26.
- [75] D. Pullirsch et al., Microbiological contamination in counterfeit and unapproved drugs, *BMC Pharmacol. Toxicol.* 15 (2014) 34.
- [76] R.B. Taylor et al., Drug quality, a contributor to drug resistance?, *Lancet.* 346 (1995) 122.
- [77] World Health Organization (WHO), Global plan for artemisinin resistance containment (GPARC), Geneva, 2011.
- [78] World Health Organization (WHO), Overcoming antimicrobial resistance, Geneva, 2000.
- [79] M.I. Issack, Substandard drugs, *Lancet.* 358 (2001) 1463.
- [80] A. Binagwaho et al., Combatting substandard and falsified medicines: a view from Rwanda., *PLoS Med.* 10 (2013) e1001476.

- [81] P.N. Newton et al., A link between poor quality antimalarials and malaria drug resistance?, *Expert Rev. Anti. Infect. Ther.* 14 (2016) 531–533.
- [82] Wellcome Trust, American Pharmaceutical Group, Opinion Formers' Conference on Counterfeit Medicines - Perspectives and action, London, 2009.
- [83] L.K. Basco, Molecular epidemiology of malaria in Cameroon. XIX. Quality of antimalarial drugs used for self-medication, *Am. J. Trop. Med. Hyg.* 70 (2004) 245–250.
- [84] M. Tremblay, Medicines Counterfeiting is a Complex Problem: A Review of Key Challenges Across the Supply Chain, *Curr. Drug Saf.* 8 (2013) 43–55.
- [85] Institute for International Research on Criminal Policy (IRCP), The European pharmaceutical sector and crime vulnerabilities, Maklu, 2007.
- [86] G. Orizio et al., "Save 30 % if you buy today". Online pharmacies and the enhancement of peripheral thinking in consumers y, (2010) 970–976.
- [87] R. Mukhopadhyay, The Hunt for Counterfeit Medicine, *Anal. Chem.* 79 (2007) 2622–2627.
- [88] Transparency International, Global Corruption Report 2006, London, 2006.
- [89] M. Shepherd, Beef up international cooperation on counterfeits., *Nat. Med.* 16 (2010) 366.
- [90] WHO Regional Committee for Africa, Regional Strategy on Regulation of Medical Products in the African Region, 2016-2025, Addis Ababa, 2016.
- [91] L. Syhakhang et al., Knowledge and perceptions of drug quality among drug sellers and consumers in Lao PDR, *Health Policy Plan.* 19 (2004) 391–401.
- [92] R. Cockburn et al., The global threat of counterfeit drugs: why industry and governments must communicate the dangers., *PLoS Med.* 2 (2005) e100.
- [93] P.N. Newton et al., Falsified medicines in Africa: all talk, no action., *Lancet. Glob. Heal.* 2 (2014) e509–e510.
- [94] International Medical Products Anti-Counterfeiting Taskforce (IMPACT), IMPACT Final Brochure, 2008.
- [95] W.L. Hamilton et al., Public health interventions to protect against falsified medicines: a systematic review of international, national and local policies, *Health Policy Plan.* 31 (2016) 1448–1466.
- [96] Medicines and Healthcare products Regulatory Agency (MHRA) et al., Counterfeit Medicines Advice for Healthcare Professionals, 2009.
- [97] A.A. Khan, Pakistani drug regulator "destined to be a failure," *Nature.* (2012).
- [98] F. El-Jardali et al., Interventions to combat or prevent drug counterfeiting: a systematic review., *BMJ Open.* 5 (2015) e006290.
- [99] Promoting the Quality of Medicines in Developing Countries (PQM), (n.d.).
<http://www.usp.org/global-health-programs/promoting-quality-medicines-pqmusaid> (accessed July 1, 2016).
- [100] A.M. Weiss, Buying prescription drugs on the internet: promises and pitfalls., *Cleve. Clin. J. Med.* 73 (2006) 282–8.

- [101] K.S. Lee et al., Combating Sale of Counterfeit and Falsified Medicines Online: A Losing Battle, *Front. Pharmacol.* 8 (2017) 268.
- [102] C.M.R. Casabona et al., International strategies in fighting against medicaments fraud and other similar offences. The MEDICRIME Convention, *Crime, Law Soc. Chang.* 68 (2017) 95–122.
- [103] R. Bate, A. Attaran, A counterfeit drug treaty: great idea, wrong implementation., *Lancet.* 376 (2010) 1446–8.
- [104] A. Attaran et al., Why and How to Make an International Crime of Medicine Counterfeiting, *J. Int. Crim. Justice.* 9 (2011) 325–354.
- [105] B.J. Venhuis et al., Medicrime convention: against falsified medical products, *Lancet.* 386 (2015) 855–856.
- [106] A. Attaran, Stopping Murder by Medicine: Introducing the Model Law on Medicine Crime, *Am. J. Trop. Med. Hyg.* 92 (2015) 127–132.
- [107] Interpol - Pharmaceutical Crime - Operations, (n.d.). <http://www.interpol.int/Crime-areas/Pharmaceutical-crime/Operations/> (accessed January 1, 2013).
- [108] J. Spink et al., Addressing the Risk of Product Fraud: A Case Study of the Nigerian Combating Counterfeiting and Sub-Standard Medicines Initiatives, *J. Forensic Sci. Criminol.* 4 (2016).
- [109] WHO Surveillance and Monitoring System, (n.d.). <http://www.who.int/medicines/regulation/ssffc/surveillance/en/> (accessed July 27, 2015).
- [110] T.K. Mackey et al., Counterfeit drug penetration into global legitimate medicine supply chains: a global assessment., *Am. J. Trop. Med. Hyg.* 92 (2015) 59–67.
- [111] Medicines and Healthcare products Regulatory Agency (MHRA), Falsified Medical Products Strategy 2012-2015, 2012.
- [112] J.C. Kohler et al., An examination of pharmaceutical systems in severely disrupted countries., *BMC Int. Health Hum. Rights.* 12 (2012) 34.
- [113] L. Taylor, Counterfeits: “dead rat” cinema ad hits UK TV screens, *PharmaTimes Online.* (2009).
- [114] European Alliance for Access to Safe Medicines (EAASM), Counterfeiting the Counterfeiter, Leigh-on-Sea, 2012.
- [115] FDA, Know Your Source: Protecting Patients from Unsafe Drugs, (2014). <http://www.fda.gov/Drugs/ResourcesForYou/HealthProfessionals/ucm389121.htm> (accessed January 16, 2015).
- [116] K. Dégardin et al., Forensic intelligence for medicine anti-counterfeiting., *Forensic Sci. Int.* 248 (2015) 15–32.
- [117] IMPACT Secretariat at the Italian Medicines Agency (AIFA), IMPACT - The Handbook, Rome, 2011.
- [118] K. Weigmann, Elixirs of death. International organizations are working towards a global solution to address the problem of falsified and substandard medicines, but progress has stagnated., *EMBO Rep.* 14 (2013) 597–600.
- [119] J. Brant, R. Malpani, Eye on the Ball: Medicine regulation - not IP enforcement - can best deliver

- quality medicine, Oxford, 2011.
- [120] M. Seear, Pharmaceutical quality: an urgent and unresolved issue, *Lancet Infect. Dis.* 12 (2012) 428–429.
- [121] P. Newton et al., A collaborative epidemiological investigation into the criminal fake artesunate trade in South East Asia, *PLoS Med.* 5 (2008) e32.
- [122] A. a Alfadl et al., Counterfeit drug demand: perceptions of policy makers and community pharmacists in Sudan, *Res. Social Adm. Pharm.* 9 (2012) 302–10.
- [123] E. 't Hoen, F. Pascual, Viewpoint: Counterfeit medicines and substandard medicines: Different problems requiring different solutions., *J. Public Health Policy.* 36 (2015) 384–9.
- [124] A. Patel et al., “This body does not want free medicines”: South African consumer perceptions of drug quality, *Health Policy Plan.* 25 (2010) 61–69.
- [125] WHO Technical Report Series, No. 902 - Thirty-sixth Report, Annex 9: Guidelines on packaging for pharmaceutical products, Geneva, 2002.
- [126] A.K. Deisingh, Pharmaceutical counterfeiting., *Analyst.* 130 (2005) 271–9.
- [127] M.S. Kumbhar et al., Tamper Evident Pharmaceutical Packaging - Needs and Advances, *Int. J. Pharm. Sci. Rev. Res.* 13 (2012) 141–152.
- [128] European Commission, Commission Delegated Regulation (EU) 2016/161 of 2 October 2015 supplementing Directive 2001/83/EC of the European Parliament and of the Council by laying down detailed rules for the safety features appearing on the packaging of medicinal products for human use, *Off. J. Eur. Union.* (2016).
- [129] R. Johnston, Tamper-indicating seals: practices, problems, and standards, *World Cust. Organ. Secur. Meet.* (2003).
- [130] R. Johnston, Why Pharma’s Tamper-Evident Packaging Strategies Don’t Work, *Pharm. Manuf.* (2005).
- [131] L. Cozzella et al., Drug packaging security by means of white-light speckle, *Opt. Lasers Eng.* 50 (2012) 1359–1371.
- [132] T. Blumenthal et al., Patterned direct-write and screen-printing of NIR-to-visible upconverting inks for security applications, *Nanotechnology.* 23 (2012) 185305.
- [133] M. Davison, *Pharmaceutical Anti-Counterfeiting: Combating the Real Danger from Fake Drugs*, John Wiley & Sons, Inc., Hoboken, NJ, USA, 2011.
- [134] D. Bansal et al., Anti-counterfeit technologies: a pharmaceutical industry perspective., *Sci. Pharm.* 81 (2013) 1–13.
- [135] National Electrical Manufacturers Association (NEMA), *Authentication Technologies for Brand Protection*, Rosslyn, 2009.
- [136] A. Goldhammer, *PhRMA Comments on FDA Anti-Counterfeiting Drug Initiative*, Rockville, 2006.
- [137] G. Satchwell, *A Sick Business: Counterfeit medicines and organised crime*, The Stockholm Network, London, 2004.
- [138] D. Barboza, 2,000 Arrested in China in Counterfeit Drug Crackdown, *New York Times.* (2012).

- [139] E. Lefebvre et al., Technological strategies to deal with counterfeit medicines: the European and North-American perspectives, *Int. J. Educ. Inf. Technol.* 5 (2011) 275–284.
- [140] Joint Response (EAEPC/EFPIA/GIRP/PGEU), Coding & Serialisation - Delegated Act on the Detailed Rules for a Unique Identifier for Medicinal Products for Human use, and its Verification, 2012.
- [141] N. Basta, 2015 Product Security Report, *Pharm. Commer.* (2015).
- [142] P. Taylor, It's official: DSCSA enforcement will be delayed one year, *Secur. Ind.* (2017).
<https://www.securindustry.com/pharmaceuticals/it-s-official-dscsa-enforcement-will-be-delayed-one-year/s40/a4956/> (accessed December 9, 2017).
- [143] P. Taylor, Pharma serialization snapshot: China, *Secur. Ind.* (2016).
<https://www.securindustry.com/pharmaceuticals/pharma-serialization-snapshot-china/s40/a2911/> (accessed December 9, 2017).
- [144] P. Ekblom, Gearing up against crime: A dynamic framework to help designers keep up with the adaptive criminal in a changing world, *Int. J. Risk Secur. Crime.* (1997).
- [145] F. Fernandez, Prevalence and detection of counterfeit pharmaceuticals: a mini review, *Ind. Eng. Chem. Res.* 47 (2008) 585–590.
- [146] B. a Liang, Fade to black: importation and counterfeit drugs., *Am. J. Law Med.* 32 (2006) 279–323.
- [147] A.L.W. Po, Too much, too little, or none at all: Dealing with substandard and fake drugs, *Lancet.* 357 (2001) 1904.
- [148] R. Martino, M. Malet-Martino, Counterfeit drugs: analytical techniques for their identification, *Anal. Bioanal. Chem.* 398 (2010) 77–92.
- [149] The Partnership for Safe Medicines, *Consumer Resources*, (n.d.).
<https://www.safemedicines.org/wp-content/uploads/2008/12/PSM-Consumer-Resources.pdf>.
- [150] M.D. Green et al., Use of refractometry and colorimetry as field methods to rapidly assess antimalarial drug quality, *J. Pharm. Biomed. Anal.* 43 (2007) 105–110.
- [151] A. Rodomonte, M. Gaudiano, Counterfeit drugs detection by measurement of tablets and secondary packaging colour, *J. Pharm. Biomed. Anal.* 53 (2010) 215–220.
- [152] J.L. Baxter et al., Hydrodynamics-induced variability in the USP apparatus II dissolution test, *Int. J. Pharm.* 292 (2005) 17–28.
- [153] L. Höllein et al., Routine quality control of medicines in developing countries: Analytical challenges, regulatory infrastructures and the prevalence of counterfeit medicines in Tanzania, *TrAC Trends Anal. Chem.* 76 (2016) 60–70.
- [154] J. Sabartova et al., Survey of the quality of selected antimalarial medicines circulating in six countries of sub-Saharan Africa, Geneva, 2011.
- [155] M.D. Green et al., Integration of Novel Low-Cost Colorimetric, Laser Photometric, and Visual Fluorescent Techniques for Rapid Identification of Falsified Medicines in Resource-Poor Areas: Application to Artemether-Lumefantrine, *Am. J. Trop. Med. Hyg.* 92 (2015) 8–16.
- [156] N. Ranieri et al., Evaluation of a new handheld instrument for the detection of counterfeit

- artesunate by visual fluorescence comparison., *Am. J. Trop. Med. Hyg.* 91 (2014) 920–4.
- [157] US Food and Drug Administration (FDA), US Department of Health & Human Services, FDA Facts: FDA's Counterfeit Detection Device CD-3, 2013.
- [158] S. Kovacs et al., Technologies for detecting falsified and substandard drugs in low and middle-income countries., *PLoS One.* 9 (2014) e90601.
- [159] J.S. Batson et al., Assessment of the effectiveness of the CD3+ tool to detect counterfeit and substandard anti-malarials, *Malar. J.* 15 (2016) 119.
- [160] P. Yager et al., Microfluidic diagnostic technologies for global public health, *Nature.* 442 (2006) 412–418.
- [161] World Changing Ideas 2013, *Sci. Am.* (2013). <http://www.scientificamerican.com/report/world-changing-ideas-2013/> (accessed April 6, 2014).
- [162] N.T. Ho et al., Rapid and Specific Drug Quality Testing Assay for Artemisinin and Its Derivatives Using a Luminescent Reaction and Novel Microfluidic Technology, *Am. J. Trop. Med. Hyg.* 92 (2015) 24–30.
- [163] E. Deconinck et al., Chromatography in the detection and characterization of illegal pharmaceutical preparations., *J. Chromatogr. Sci.* 51 (2013) 791–806.
- [164] L. Hoellein, U. Holzgrabe, Development of simplified HPLC methods for the detection of counterfeit antimalarials in resource-restraint environments., *J. Pharm. Biomed. Anal.* 98C (2014) 434–445.
- [165] H. Yu et al., Characterization of drug authenticity using thin-layer chromatography imaging with a mobile phone., *J. Pharm. Biomed. Anal.* 125 (2016) 85–93.
- [166] M. Lalani et al., Substandard Antimalarials Available in Afghanistan: A Case for Assessing the Quality of Drugs in Resource Poor Settings, *Am. J. Trop. Med. Hyg.* 92 (2015) 51–58.
- [167] I. Fadeyi et al., Quality of the Antibiotics--Amoxicillin and Co-Trimoxazole from Ghana, Nigeria, and the United Kingdom, *Am. J. Trop. Med. Hyg.* 92 (2015) 87–94.
- [168] S. Phanouvong, Y. Dijiba, The quality of antimalarial medicines in eastern Thailand: a case study along the Thai-Cambodian border., *Southeast Asian J. Trop. Med. Public Health.* (2013).
- [169] B.J. Visser et al., Assessing the quality of anti-malarial drugs from Gabonese pharmacies using the MiniLab®: a field study., *Malar. J.* 14 (2015) 273.
- [170] J.-R. Ioset, H. Kaur, Simple field assays to check quality of current artemisinin-based antimalarial combination formulations., *PLoS One.* 4 (2009) e7270.
- [171] M.T. Koesdjojo et al., Low-cost, high-speed identification of counterfeit antimalarial drugs on paper., *Talanta.* 130 (2014) 122–7.
- [172] A.A. Weaver, M. Lieberman, Paper test cards for presumptive testing of very low quality antimalarial medications., *Am. J. Trop. Med. Hyg.* 92 (2015) 17–23.
- [173] A.A. Weaver et al., Paper analytical devices for fast field screening of beta lactam antibiotics and antituberculosis pharmaceuticals., *Anal. Chem.* 85 (2013) 6453–60.
- [174] N. Amin et al., Capillary electrophoresis for the assay of fixed-dose combination tablets of

- artesunate and amodiaquine, *Malar. J.* 11 (2012) 149.
- [175] R. Marini et al., Reliable low-cost capillary electrophoresis device for drug quality control and counterfeit medicines, *J. Pharm. Biomed. Anal.* 53 (2010) 1278–87.
- [176] National University of Rwanda in Butare - Pharmelp, (2015). <http://pharmelp.ch/project-in-rwanda-2015-2> (accessed July 7, 2016).
- [177] M.D. Likar et al., Rapid identification and absence of drug tests for AG-013736 in 1mg Axitinib tablets by ion mobility spectrometry and DART™ mass spectrometry, 2011.
- [178] R.M. O'Donnell et al., Pharmaceutical applications of ion mobility spectrometry, *TrAC Trends Anal. Chem.* 27 (2008) 44–53.
- [179] J.D. Dunn et al., Using a portable ion mobility spectrometer to screen dietary supplements for sibutramine, *J. Pharm. Biomed. Anal.* 54 (2011) 469–474.
- [180] R. Santamaria-Fernandez et al., Detection of counterfeit antiviral drug Heptodin™ and classification of counterfeits using isotope amount ratio measurements by multicollector inductively coupled plasma mass spectrometry (MC-ICPMS) and isotope ratio mass spectrometry (IRMS), *Sci. Justice.* 49 (2009) 102–106.
- [181] R. Bate et al., Pilot study comparing technologies to test for substandard drugs in field settings, *African J. Pharm. Pharmacol.* 3 (2009) 165–170.
- [182] P. Sacré et al., Comparison and combination of spectroscopic techniques for the detection of counterfeit medicines, *J. Pharm. Biomed. Anal.* 53 (2010) 445–453.
- [183] D. Custers et al., ATR-FTIR spectroscopy and chemometrics: An interesting tool to discriminate and characterize counterfeit medicines., *J. Pharm. Biomed. Anal.* 112 (2014) 181–189.
- [184] M.J. Anzanello et al., A framework for selecting analytical techniques in profiling authentic and counterfeit Viagra and Cialis., *Forensic Sci. Int.* 235 (2014) 1–7.
- [185] Y. Roggo et al., A review of near infrared spectroscopy and chemometrics in pharmaceutical technologies., *J. Pharm. Biomed. Anal.* 44 (2007) 683–700.
- [186] S.H.F. Scafi, C. Pasquini, Identification of counterfeit drugs using near-infrared spectroscopy, *Analyst.* 126 (2001) 2218–2224.
- [187] I. Storme-Paris et al., Challenging near infrared spectroscopy discriminating ability for counterfeit pharmaceuticals detection, *Anal. Chim. Acta.* 658 (2010) 163–174.
- [188] M. Said et al., Near-infrared spectroscopy (NIRS) and chemometric analysis of Malaysian and UK paracetamol tablets: A spectral database study, *Int. J. Pharm.* 415 (2011) 102–109.
- [189] A. Guillemain et al., Performance of NIR handheld spectrometers for the detection of counterfeit tablets, *Talanta.* 165 (2017) 632–640.
- [190] B.K. Wilson et al., A New Handheld Device for the Detection of Falsified Medicines: Demonstration on Falsified Artemisinin-Based Therapies from the Field, *Am. J. Trop. Med. Hyg.* (2017) 16–0904.
- [191] S. Assi et al., Identification of counterfeit medicines from the Internet and the World market using near-infrared spectroscopy, *Anal. Methods.* 3 (2011) 2231.

- [192] J. Cruz, M. Blanco, Content uniformity studies in tablets by NIR-CI, *J. Pharm. Biomed. Anal.* 56 (2011) 408–412.
- [193] C. Ricci et al., Characterization of genuine and fake artesunate anti-malarial tablets using Fourier transform infrared imaging and spatially offset Raman spectroscopy through blister packs., *Anal. Bioanal. Chem.* 389 (2007) 1525–32.
- [194] M.B. Lopes et al., Investigation into classification/sourcing of suspect counterfeit HeptodinTM tablets by near infrared chemical imaging, *Anal. Chim. Acta.* 633 (2009) 149–155.
- [195] S. Wilczyński et al., The use of hyperspectral imaging in the VNIR (400–1000nm) and SWIR range (1000–2500nm) for detecting counterfeit drugs with identical API composition, *Talanta.* 160 (2016) 1–8.
- [196] M.B. Lopes et al., Quantification of components in non-homogenous pharmaceutical tablets using near infrared reflectance imaging, *J. Near Infrared Spectrosc.* 18 (2010) 333–340.
- [197] G.P. Sabin et al., Characterization of sildenafil citrate tablets of different sources by near infrared chemical imaging and chemometric tools, 2013.
- [198] D.E. Braun et al., Simultaneous quantitative analysis of ternary mixtures of D-mannitol polymorphs by FT-Raman spectroscopy and multivariate calibration models., *Int. J. Pharm.* 385 (2010) 29–36.
- [199] S. Neuberger, C. Neusüß, Determination of counterfeit medicines by Raman spectroscopy: Systematic study based on a large set of model tablets., *J. Pharm. Biomed. Anal.* 112 (2015) 70–78.
- [200] C. Eliasson, P. Matousek, Noninvasive authentication of pharmaceutical products through packaging using spatially offset Raman spectroscopy, *Anal. Chem.* 79 (2007) 1696–1701.
- [201] C. Ricci et al., Assessment of hand-held Raman instrumentation for in situ screening for potentially counterfeit artesunate antimalarial tablets by FT-Raman spectroscopy and direct ionization mass spectrometry., *Anal. Chim. Acta.* 623 (2008) 178–86.
- [202] M. Hajjou et al., Assessment of the performance of a handheld Raman device for potential use as a screening tool in evaluating medicines quality, *J. Pharm. Biomed. Anal.* 74 (2013) 47–55.
- [203] S. Assi, Raw material identification using dual laser handheld Raman spectroscopy, *Eur. Pharm. Rev.* 18 (2013) 25–31.
- [204] Cobalt Light Systems - Spatially Offset Raman Spectroscopy, (n.d.).
<https://www.coballight.com/technology/sors> (accessed May 8, 2013).
- [205] U. Holzgrabe, M. Malet-Martino, Analytical challenges in drug counterfeiting and falsification – The NMR approach, *J. Pharm. Biomed. Anal.* 55 (2011) 679–687.
- [206] G. Pagès et al., Evaluation of a benchtop cryogen-free low-field ¹H NMR spectrometer for the analysis of sexual enhancement and weight loss dietary supplements adulterated with pharmaceutical substances, *Anal. Chem.* 86 (2014) 11897–11904.
- [207] G. Kyriakidou et al., Batch-specific discrimination using nuclear quadrupole resonance spectroscopy., *Anal. Chem.* 87 (2015) 3806–11.
- [208] C. Chen et al., Authentication of Medicines Using Nuclear Quadrupole Resonance Spectroscopy,

IEEE/ACM Trans. Comput. Biol. Bioinforma. 13 (2016) 417–430.

- [209] Conphirmer, (n.d.). <http://www.conphirmer.com/> (accessed August 12, 2013).
- [210] J. Barras et al., Nitrogen-14 Nuclear Quadrupole Resonance Spectroscopy: A Promising Analytical Methodology for Medicines Authentication and Counterfeit Antimalarial Analysis, *Anal. Chem.* 85 (2013) 2746–2753.
- [211] J. Barras et al., The Emerging Field of Medicines Authentication by Nuclear Quadrupole Resonance Spectroscopy, *Appl. Magn. Reson.* 43 (2012) 511–529.
- [212] S.A. Speakman, Basics of X-ray powder diffraction, Cent. Mater. Sci. Eng. MIT. (2011). [http://prism.mit.edu/xray/Basics of X-Ray Powder Diffraction.pdf](http://prism.mit.edu/xray/Basics%20of%20X-Ray%20Powder%20Diffraction.pdf) (accessed April 13, 2015).
- [213] H. Brittain, X-ray diffraction III: pharmaceutical applications, *Spectroscopy*. 16 (2001) 14–18.
- [214] R. V Haware et al., Data fusion of Fourier transform infrared spectra and powder X-ray diffraction patterns for pharmaceutical mixtures., *J. Pharm. Biomed. Anal.* 56 (2011) 944–9.
- [215] Z. Németh et al., Quantitative determination of famotidine polymorphs: X-ray powder diffractometric and Raman spectrometric study., *J. Pharm. Biomed. Anal.* 49 (2009) 338–46.
- [216] S. Yamamura, Y. Momose, Quantitative analysis of crystalline pharmaceuticals in powders and tablets by a pattern-fitting procedure using X-ray powder diffraction data, *Int. J. Pharm.* 212 (2001) 203–212.
- [217] E. Fukuoka et al., Evaluation of crystallite orientation in tablets by X-ray diffraction methods., *Chem. Pharm. Bull. (Tokyo)*. 35 (1987) 1564–1570.
- [218] B.D. Cullity, *Elements of X-ray Diffraction*, Addison-Wesley Publishing Company Inc., Reading, MA, 1956.
- [219] R. Jenkins, R.L. Snyder, *Introduction to X-ray Powder Diffractometry*, John Wiley & Sons, Inc., Hoboken, NJ, USA, 1996.
- [220] V.J. Hurst et al., Accurate quantification of quartz and other phases by powder X-ray diffractometry, *Anal. Chim. Acta.* 337 (1997) 233–252.
- [221] J.K. Cockcroft et al., Powder Diffraction, *Adv. Certif. Powder Diffr. Web.* (n.d.). <http://pd.chem.ucl.ac.uk/pdnn/diff2/kinemat2.htm> (accessed April 6, 2014).
- [222] International Centre for Diffraction Data (ICDD), Tutorial - How to Analyze Drugs Using X-ray Diffraction, (n.d.). [http://www.icdd.com/knowledge/tutorials/pdf/How to Analyze Drugs.pdf](http://www.icdd.com/knowledge/tutorials/pdf/How%20to%20Analyze%20Drugs.pdf) (accessed April 6, 2014).
- [223] J. Lu, S. Rohani, Polymorphism and crystallization of active pharmaceutical ingredients (APIs), *Curr. Med. Chem.* 16 (2009) 884–905.
- [224] K. Nagapudi, J. Jona, Amorphous Active Pharmaceutical Ingredients in Preclinical Studies: Preparation, Characterization, and Formulation, *Curr. Bioact. Compd.* 4 (2008) 213–224.
- [225] J.K. Cockcroft et al., Instrument X-ray Optics: Reflection Geometry, *Adv. Certif. Powder Diffr. Web.* (n.d.). <http://pd.chem.ucl.ac.uk/pdnn/inst1/optics1.htm> (accessed April 6, 2014).
- [226] I. Ivanisevic et al., Uses of X-Ray Powder Diffraction In the Pharmaceutical Industry, in: *Pharm. Sci. Encycl.*, John Wiley & Sons, Inc., Hoboken, NJ, USA, 2010.

- [227] N.V.Y. Scarlett et al., Outcomes of the International Union of Crystallography Commission on Powder Diffraction Round Robin on Quantitative Phase Analysis: samples 2, 3, 4, synthetic bauxite, natural granodiorite and pharmaceuticals, *J. Appl. Crystallogr.* 35 (2002) 383–400.
- [228] W.E.I. Dong et al., PHARMACEUTICAL TECHNOLOGY A Quick Method for the Quantitative Analysis of Mixtures . 1 . Powder X-Ray Diffraction, 97 (2008) 2260–2276.
- [229] J.N. O'Dwyer, J.R. Tickner, Quantitative mineral phase analysis of dry powders using energy-dispersive X-ray diffraction., *Appl. Radiat. Isot.* 66 (2008) 1359–62.
- [230] National Institute of Standards and Technology (NIST), NIST X-Ray Form Factor, Attenuation and Scattering Tables, (n.d.). <https://physics.nist.gov/PhysRefData/FFast/html/form.html> (accessed November 20, 2017).
- [231] National Institute of Standards and Technology (NIST), NIST XCOM Database, (n.d.). <https://physics.nist.gov/PhysRefData/Xcom/html/xcom1.html> (accessed December 2, 2017).
- [232] N. Chieng et al., An overview of recent studies on the analysis of pharmaceutical polymorphs., *J. Pharm. Biomed. Anal.* 55 (2011) 618–44.
- [233] N. Chieng et al., Quantitative solid-state analysis of three solid forms of ranitidine hydrochloride in ternary mixtures using Raman spectroscopy and X-ray powder diffraction., *J. Pharm. Biomed. Anal.* 49 (2009) 18–25.
- [234] G.A. Stephenson et al., Characterization of the solid state: quantitative issues, *Adv. Drug Deliv. Rev.* 48 (2001) 67–90.
- [235] C. Theodorakou, M.J. Farquharson, The classification of secondary colorectal liver cancer in human biopsy samples using angular dispersive x-ray diffraction and multivariate analysis., *Phys. Med. Biol.* 54 (2009) 4945–57.
- [236] T. Mitsui et al., Determination of the Blend Composition Ratio of Cocaine to Hydrogencarbonate by X-Ray Diffraction Using Multivariate Analysis, *Anal. Sci.* 7 (1991) 941–945.
- [237] G.L. Perlovich et al., Polymorphism of paracetamol, *J. Therm. Anal. Calorim.* 89 (2007) 767–774.
- [238] C.F. Macrae et al., Mercury CSD 2.0 – new features for the visualization and investigation of crystal structures, *J. Appl. Crystallogr.* 41 (2008) 466–470.
- [239] C.R. Groom et al., The Cambridge Structural Database, *Acta Crystallogr. Sect. B Struct. Sci. Cryst. Eng. Mater.* 72 (2016) 171–179.
- [240] J.K. Maurin et al., The usefulness of simple X-ray powder diffraction analysis for counterfeit control--the Viagra example., *J. Pharm. Biomed. Anal.* 43 (2007) 1514–8.
- [241] D. Blake, A Historical Perspective of the Development of the CheMin Mineralogical Instrument for the Mars Science Laboratory Mission, *Geochemical Soc.* (2010).
- [242] P. Sarrazin et al., Vibrating sample holder for XRD analysis with minimal sample preparation, *Jt. Comm. Powder Diffr. Stand. Int. Cent. Diffr. Data.* 48 (2005) 156–164.
- [243] D. Blake et al., Characterization and Calibration of the CheMin Mineralogical Instrument on Mars Science Laboratory, *Space Sci. Rev.* 170 (2012) 341–399.
- [244] M. Wilkinson, Beyond terra firma, *Chem. World.* (2010) 50–53.

- [245] D.F. Blake et al., The use of Field-Portable pXRD for the Rapid Identification of Counterfeit Pharmaceutical Products and Subsequent Excipient Identification and Quantification, (2010). <http://www.icdd.com/ppxrd/09/presentations/2010-ppxrd-Blake.pdf> (accessed December 3, 2017).
- [246] M.D. Moore et al., Evaluation of chemometric algorithms in quantitative X-ray powder diffraction (XRPD) of intact multi-component consolidated samples., *J. Pharm. Biomed. Anal.* 49 (2009) 619–26.
- [247] M. Varasteh et al., Quantitative determination of polymorphic impurity by X-ray powder diffractometry in an OROS formulation., *Int. J. Pharm.* 366 (2009) 74–81.
- [248] Y. Otsuka et al., Quantification of Pharmaceutical Compounds Based on Powder X-Ray Diffraction with Chemometrics, *Chem. Pharm. Bull. (Tokyo)*. 64 (2016) 1129–1135.
- [249] K. Nikowitz et al., Multivariate calibration of the degree of crystallinity in intact pellets by X-ray powder diffraction, *Int. J. Pharm.* 502 (2016) 107–116.
- [250] M. Suda et al., An accurate quantitative analysis of polymorphic content by chemometric X-ray powder diffraction., *Anal. Sci.* 24 (2008) 451–7.
- [251] D.M. Croker et al., A comparative study of the use of powder X-ray diffraction, Raman and near infrared spectroscopy for quantification of binary polymorphic mixtures of piracetam., *J. Pharm. Biomed. Anal.* 63 (2012) 80–6.
- [252] F. Been et al., Profiling of counterfeit medicines by vibrational spectroscopy., *Forensic Sci. Int.* 211 (2011) 83–100.
- [253] E. Deconinck et al., Chemometrics and chromatographic fingerprints to discriminate and classify counterfeit medicines containing PDE-5 inhibitors, *Talanta*. 100 (2012) 123–133.
- [254] B. Krakowska et al., Chemometrics and the identification of counterfeit medicines – A review, *J. Pharm. Biomed. Anal.* 127 (2016) 112–122.
- [255] F. Tian et al., Influence of sample characteristics on quantification of carbamazepine hydrate formation by X-ray powder diffraction and Raman spectroscopy., *Eur. J. Pharm. Biopharm.* 66 (2007) 466–74.
- [256] A. Siddiqui et al., Chemometric methods for the quantification of crystalline tacrolimus in solid dispersion by powder X-ray diffractometry., *J. Pharm. Sci.* 103 (2014) 2819–28.
- [257] Z. Rahman et al., Comparison of X-ray powder diffraction and solid-state nuclear magnetic resonance in estimating crystalline fraction of tacrolimus in sustained-release amorphous solid dispersion and development of discriminating dissolution method, *J. Pharm. Sci.* 104 (2015) 1777–1786.
- [258] R. Caliandro et al., Multivariate analysis of quaternary carbamazepine-saccharin mixtures by X-ray diffraction and infrared spectroscopy, *J. Pharm. Biomed. Anal.* 78–79 (2013) 269–279.
- [259] K. Varmuza, P. Filzmoser, *Introduction to multivariate statistical analysis in chemometrics*, CRC press, Boca Raton, FL, 2009.
- [260] S.M. Clark, Thirty Years of Energy-Dispersive Powder Diffraction, *Crystallogr. Rev.* 8 (2002) 57–92.
- [261] I.L. Spain, D.R. Black, Energy dispersive x-ray diffraction in the diamond anvil, high-pressure

- apparatus: Comparison of synchrotron and conventional x-ray sources, *Rev. Sci. Instrum.* 56 (1985) 1461–1463.
- [262] E.A. Ryan, M.J. Farquharson, Breast tissue classification using x-ray scattering measurements and multivariate data analysis, *Phys. Med. Biol.* 52 (2007) 6679–96.
- [263] J. Bordas et al., Small-angle scattering experiments on biological materials using synchrotron radiation, *Nature.* 262 (1976) 541–545.
- [264] J. Bordas et al., Small-angle scattering and diffraction experiments in biology and physics employing synchrotron radiation and energy-dispersive techniques, *J. Appl. Crystallogr.* 11 (1978) 434–441.
- [265] R. Luggar, M. Farquharson, Multivariate analysis of statistically poor EDXRD spectra for the detection of concealed explosives, *X-Ray Spectrom.* 27 (1998) 87–94.
- [266] E. Cook et al., Energy dispersive X-ray diffraction as a means to identify illicit materials: A preliminary optimisation study, *Appl. Radiat. Isot.* 65 (2007) 959–967.
- [267] I. Drakos et al., Multivariate analysis of energy dispersive X-ray diffraction data for the detection of illicit drugs in border control, *Crime Sci.* 6 (2017) 1.
- [268] A.J. Dicken et al., Energy-dispersive X-ray diffraction using an annular beam, *Opt. Express.* 23 (2015) 13443.
- [269] B. Kämpfe et al., Energy Dispersive X-Ray Diffraction, Part. Part. Syst. Charact. 22 (2005) 391–396.
- [270] A. Mendoza Cuevas et al., Energy dispersive X-ray diffraction and fluorescence portable system for cultural heritage applications, *X-Ray Spectrom.* 44 (2015) 105–115.
- [271] J.K. Cockcroft et al., Mode (5): Energy-dispersive, *Adv. Certif. Powder Diffr. Web.* (n.d.). <http://pd.chem.ucl.ac.uk/pdnn/inst2/endis.htm> (accessed April 6, 2014).
- [272] C.M. Dozier, N. Anibou, An innovative EDXRD verification probe, *Powder Diffr.* 24 (2009) 102–106.
- [273] D. O’Flynn et al., Explosive detection using pixellated X-ray diffraction (PixD), *J. Instrum.* 8 (2013) P03007–P03007.
- [274] P. Seller et al., Pixellated Cd(Zn)Te high-energy X-ray instrument, *J. Instrum.* 6 (2011) C12009–C12009.
- [275] D. O’Flynn et al., Materials identification using a small-scale pixellated x-ray diffraction system, *J. Phys. D. Appl. Phys.* 49 (2016) 175304.
- [276] R. Moss et al., miniPixD: a compact sample analysis system which combines X-ray imaging and diffraction, *J. Instrum.* 12 (2017) P02001–P02001.
- [277] R.M. Moss et al., Correlation of X-ray diffraction signatures of breast tissue and their histopathological classification, *Sci. Rep.* 7 (2017) 12998.
- [278] R.D. Luggar et al., Determination of the geometric blurring of an energy dispersive X-ray diffraction (EDXRD) system and its use in the simulation of experimentally derived diffraction profiles, *Nucl. Instruments Methods Phys. Res. Sect. A Accel. Spectrometers, Detect. Assoc. Equip.* 383 (1996) 610–618.

- [279] M.C. Veale et al., Characterization of M- π -n CdTe pixel detectors coupled to HEXITEC readout chip, *J. Instrum.* 7 (2012) C01035–C01035.
- [280] CAMO ASA, *The Unscrambler User Manual*, 1998.
- [281] K.R. Beebe et al., *Chemometrics : a practical guide*, Wiley, 1998.
- [282] J.-B. Sirven et al., Feasibility study of rock identification at the surface of Mars by remote laser-induced breakdown spectroscopy and three chemometric methods, *J. Anal. At. Spectrom.* 22 (2007) 1471.
- [283] K.H. Esbensen et al., *Multivariate Data Analysis: In Practice : an Introduction to Multivariate Data Analysis and Experimental Design*, CAMO Software, 2002.
- [284] Åsmund Rinnan et al., Review of the most common pre-processing techniques for near-infrared spectra, *TrAC Trends Anal. Chem.* 28 (2009) 1201–1222.
- [285] J. Huang et al., RAMAN: Practical Considerations in Data Pre-treatment for NIR and Raman Spectroscopy, *Am. Pharm. Rev.* 13 (2010) 116.
- [286] J. Engel et al., Breaking with trends in pre-processing?, *TrAC Trends Anal. Chem.* 50 (2013) 96–106.
- [287] S. Assi et al., On the quantification of ciprofloxacin in proprietary Ciproxin tablets and generic ciprofloxacin tablets using handheld Raman spectroscopy, *J. Raman Spectrosc.* 43 (2012) 1049–1057.
- [288] J. Griffen et al., Comprehensive quantification of tablets with multiple active pharmaceutical ingredients using transmission Raman spectroscopy--a proof of concept study., *J. Pharm. Biomed. Anal.* 115 (2015) 277–82.
- [289] L.B. Lyndgaard et al., Quantification of paracetamol through tablet blister packages by Raman spectroscopy and multivariate curve resolution-alternating least squares, *Chemom. Intell. Lab. Syst.* 125 (2013) 58–66.
- [290] M. Tiwari et al., Quantification of olanzapine polymorphs using powder X-ray diffraction technique., *J. Pharm. Biomed. Anal.* 43 (2007) 865–72.
- [291] D. Beckers et al., X-ray detection in packaging, US 7756248 B2, 2010.
- [292] R. Pilchik, Pharmaceutical blister packaging, Part I. Rationale and materials, *Pharm. Technol.* 24 (2000) 68–78.
- [293] D. Robinson, Inhomogeneity correction and the analytic anisotropic algorithm, *J. Appl. Clin. Med. Phys.* 9 (2008) 112–122.
- [294] D. Twede et al., *Cartons, Crates and Corrugated Board, Second Edition: Handbook of Paper and Wood Packaging Technology*, 2nd ed., DEStech Publications, Inc., Lancaster, Pennsylvania, USA, 2015.
- [295] CAMO, *The Unscrambler Appendices: Method References*, (n.d.).
[http://www.camo.com/TheUnscrambler/Appendices/The Unscrambler Method References.pdf](http://www.camo.com/TheUnscrambler/Appendices/The%20Unscrambler%20Method%20References.pdf)
 (accessed December 8, 2014).
- [296] Ł. Komsta, J.K. Maurin, Recognition of active ingredients in tablets by chemometric processing of X-ray diffractometric data., *Talanta.* 82 (2010) 850–3.
- [297] R.G. Brereton, *Applied Chemometrics for Scientists*, John Wiley & Sons, Ltd, Chichester, UK, 2007.

- [298] The Blue Guide: Advertising and Promotion of Medicines in the UK, London, 2014.
- [299] E. Deconinck, P.Y. Sacré, Classification trees based on infrared spectroscopic data to discriminate between genuine and counterfeit medicines, *J. Pharm. Biomed. Anal.* 57 (2012) 68–75.
- [300] T.M.C. Pereira et al., Viagra® and Cialis® blister packaging fingerprinting using Fourier transform infrared spectroscopy (FTIR) allied with chemometric methods, *Anal. Methods.* 6 (2014) 2722.
- [301] N. V Phadnis et al., Identification of drugs in pharmaceutical dosage forms by X-ray powder diffractometry., *J. Pharm. Biomed. Anal.* 15 (1997) 929–43.
- [302] O.Y. Rodionova et al., Discriminant analysis is an inappropriate method of authentication, *TrAC Trends Anal. Chem.* 78 (2016) 17–22.
- [303] L. Li et al., Identification of anisodamine tablets by Raman and near-infrared spectroscopy with chemometrics., *Spectrochim. Acta. A. Mol. Biomol. Spectrosc.* 127 (2014) 91–7.
- [304] A. Candolfi et al., Comparison of classification approaches applied to NIR-spectra of clinical study lots, *J. Pharm. Biomed. Anal.* 16 (1998) 1329–1347.
- [305] B.J. Venhuis et al., Dose-to-dose variations with single packages of counterfeit medicines and adulterated dietary supplements as a potential source of false negatives and inaccurate health risk assessments., *J. Pharm. Biomed. Anal.* 89 (2014) 158–65.
- [306] World Health Organisation (WHO), Substandard and Falsified (SF) Medical Products, (2017). <http://www.who.int/medicines/regulation/ssffc/en/> (accessed December 12, 2017).